

Arthritis & Rheumatology

An Official Journal of the American College of Rheumatology
www.arthritisrheum.org and wileyonlinelibrary.com

Editor

Daniel H. Solomon, MD, MPH, *Boston*

Deputy Editors

Richard J. Bucala, MD, PhD, *New Haven*

Mariana J. Kaplan, MD, *Bethesda*

Peter A. Nigrovic, MD, *Boston*

Co-Editors

Karen H. Costenbader, MD, MPH, *Boston*

David T. Felson, MD, MPH, *Boston*

Richard F. Loeser Jr., MD, *Chapel Hill*

Journal Publications Committee

Chair - Betty Tsao, PhD, *Charleston*

Member - ARP Liaison

Cynthia Crowson, PhD, *Stewartville*

Members

Faria Latif Sami, MD, *Birmingham*

Elana Bernstein, MD, MSc, *New York*

Daniel B. Horton, MD, MSCE, *New Brunswick*

Suraj Rajasimhan, PharmD

Krati Chauhan, MD, PhD, *Burlington*

Himanshu Vashistha, PhD, MBA, *Great Neck*

Editorial Staff

Susan Case, *Vice President, Strategic Marketing,*

Communications and Publishing, Maryland

Maggie Parry, *Director, Quality and Production, Georgia*

Brian T. Robinson, *Director, Digital Content, Pennsylvania*

Chris Reynolds, *Product Manager, Georgia*

Christy Austin, *Publishing Coordinator, Washington*

Laura Bolte, *Managing Editor, North Carolina*

Associate Editors

Marta Alarcón-Riquelme, MD, PhD, *Granada*

Neil Basu, MD, PhD, *Glasgow*

Edward M. Behrens, MD, *Philadelphia*

Bryce Binstadt, MD, PhD, *Minneapolis*

Nunzio Bottini, MD, PhD, *San Diego*

John Carrino, MD, MPH, *New York*

Andrew Cope, MD, PhD, *London*

Adam P. Croft, MBChB, PhD, MRCP,
Birmingham

Nicola Dalbeth, MD, FRACP, *Auckland*

Chad Deal, MD, *Cleveland*

Brian M. Feldman, MD, FRCPC, MSc, *Toronto*

Richard A. Furie, MD, *Great Neck*

J. Michelle Kahlenberg, MD, PhD,
Ann Arbor

Yvonne Lee, MD, MMSc, *Chicago*

Katherine Liao, MD, MPH, *Boston*

Bing Lu, MD, DrPH, *Boston*

Stephen P. Messier, PhD,

Winston-Salem

Rachel E. Miller, PhD, *Chicago*

Janet E. Pope, MD, MPH, *FRCPC,*

London, Ontario

Lisa G. Rider, MD, *Bethesda*

Christopher T. Ritchlin, MD, MPH,
Rochester

William Robinson, MD, PhD, *Stanford*

Carla R. Scanzello, MD, PhD,

Philadelphia

Georg Schett, MD, *Erlangen*

Ami A. Shah, MD, MHS, *Baltimore*

Sakae Tanaka, MD, PhD, *Tokyo*

Maria Trojanowska, PhD, *Boston*

Edith M. Williams, PhD, MS, *Rochester*

Advisory Editors

Ayaz Aghayev, MD, *Boston*

Joshua F. Baker, MD, MSCE,
Philadelphia

Bonnie Bermas, MD, *Dallas*

Jamie Collins, PhD, *Boston*

Kristen Demoruelle, MD, PhD, *Denver*

Christopher Denton, PhD, FRCP, *London*

Anisha Dua, MD, MPH, *Chicago*

John FitzGerald, MD, *Los Angeles*

Lauren Henderson, MD, MMSc, *Boston*

Monique Hinchcliff, MD, MS, *New Haven*

Hui-Chen Hsu, PhD, *Birmingham*

Mohit Kapoor, PhD, *Toronto*

Seoyoung Kim, MD, ScD, MSCE, *Boston*

Vasileios Kytтарis, MD, *Boston*

Carl D. Langefeld, PhD, *Winston-Salem*

Christian Lood, PhD, *Seattle*

Dennis McGonagle, FRCPI, PhD, *Leeds*

Julie Paik, MD, MHS, *Baltimore*

Amr Sawalha, MD, *Pittsburgh*

Julie Zikherman, MD, *San Francisco*

AMERICAN COLLEGE OF RHEUMATOLOGY

Carol Langford, MD, MHS, *Cleveland*, **President**

William Harvey, MD, MSc, *Boston*, **President-Elect**

Anne Bass, MD, *New York*, **Treasurer**

Angus Worthing, MD, *Washington, DC*, **Secretary**

Steven Echard, IOM, CAE, *Atlanta*, **Executive Vice-President**

© 2025 American College of Rheumatology. All rights reserved, including rights for text and data mining and training of artificial technologies or similar technologies. No part of this publication may be reproduced, stored or transmitted in any form or by any means without the prior permission in writing from the copyright holder. Authorization to copy items for internal and personal use is granted by the copyright holder for libraries and other users registered with their local Reproduction Rights Organization (RRO), e.g. Copyright Clearance Center (CCC), 222 Rosewood Drive, Danvers, MA 01923, USA (www.copyright.com), provided the appropriate fee is paid directly to the RRO. This consent does not extend to other kinds of copying or use such as copying for general distribution, for advertising or promotional purposes, for creating new collective works, for resale, or for artificial intelligence tools or technologies. Special requests should be addressed to: permissions@wiley.com.

Access Policy: Subject to restrictions on certain backfiles, access to the online version of this issue is available to all registered Wiley Online Library users 12 months after publication. Subscribers and eligible users at subscribing institutions have immediate access in accordance with the relevant subscription type. Please go to online@wiley.com for details.

The views and recommendations expressed in articles, letters, and other communications published in Arthritis & Rheumatology are those of the authors and do not necessarily reflect the opinions of the editors, publisher, or American College of Rheumatology. The publisher and the American College of Rheumatology do not investigate the information contained in the classified advertisements in this journal and assume no responsibility concerning them. Further, the publisher and the American College of Rheumatology do not guarantee, warrant, or endorse any product or service advertised in this journal.

Cover design: Todd Machen

© This journal is printed on acid-free paper.

Arthritis & Rheumatology

An Official Journal of the American College of Rheumatology
www.arthritisrheum.org and wileyonlinelibrary.com

VOLUME 77 • May 2025 • NO. 5

In This Issue	A15
Journal Club	A16
Clinical Connections	A17
Special Articles	
In Memoriam: J. Claude Bennett, MD, 1933–2024 <i>S. Louis Bridges Jr, Kenneth G. Saag, and William J. Koopman</i>	497
Editorial: Living With Sjögren Disease: Prospects for Disease-Modifying Therapies <i>E. William St. Clair</i>	499
Editorial: Modic Changes and Tumor Necrosis Factor Inhibition: Is the Door Shut? <i>Jennifer S. Hanberg, Joerg Ermann, and Jeffrey N. Katz</i>	503
Expert Perspectives on Clinical Challenges: Expert Perspective: Diagnostic Approach to Differentiating Juvenile Dermatomyositis From Muscular Dystrophy <i>Jacqueline A. Madison, Sean P. Ferris, Marianne Kerski, Grace Hile, Sophia Matossian, Cara Komisar, Peter J. Strouse, Elizabeth Ames, Erin Neil Knierbein, and Jessica L. Turnier</i>	506
Notes from the Field: Do We Need Distinct Pediatric Classification Criteria for Rheumatic Diseases That Affect Both Children and Adults? <i>Coziana Ciurtin, Marija Jelusic, and Seza Ozen</i>	521
Rheumatoid Arthritis	
Substitution of Glutamic Acid at Position 71 of DR β 1*04:01 and Collagen-Specific Tolerance Without Alloreactivity <i>Vibha Jha, Brian M. Freed, Elizabeth R. Sunderhaus, Jessica E. Lee, Edward B. Prage, Manjula Miglani, Edward F. Rosloniec, Jennifer L. Matsuda, Marilyne G. Coulombe, Amy S. McKee, and Christina L. Roark</i>	526
Spondyloarthritis	
Development of Extramusculoskeletal Manifestations in Upadacitinib-Treated Patients With Psoriatic Arthritis or Axial Spondyloarthritis <i>Denis Poddubnyy, Bhumik Parikh, Dirk Elewaut, Victoria Navarro-Compán, Stefan Siebert, Michael Paley, Derek Coombs, Ivan Lagunes, Ana Biljan, Priscila Nakasato, Peter Wung, and Ennio Lubrano</i>	536
Systemic Lupus Erythematosus	
Role of STING Deficiency in Amelioration of Mouse Models of Lupus and Atherosclerosis <i>Yudong Liu, Carmelo Carmona-Rivera, Nickie L. Seto, Christopher B. Oliveira, Eduardo Patino-Martinez, Yvonne Baumer, Tiffany M. Powell-Wiley, Nehal Mehta, Sarfaraz Hasni, Xuan Zhang, and Mariana J. Kaplan</i>	547
Sjögren's Syndrome	
Safety and Efficacy of Ianalumab in Patients With Sjögren's Disease: 52-Week Results From a Randomized, Placebo-Controlled, Phase 2b Dose-Ranging Study <i>Thomas Dörner, Simon J. Bowman, Robert Fox, Xavier Mariette, Athena Papas, Thomas Grader-Beck, Benjamin A. Fisher, Filipe Barcelos, Salvatore De Vita, Hendrik Schulze-Koops, Robert J. Moots, Guido Junge, Janice Woznicki, Monika Sopala, Alexandre Avrameas, Wen-Lin Luo, and Wolfgang Hueber</i>	560
Systemic Sclerosis	
Autologous Nonmyeloablative Hematopoietic Stem Cell Transplantation for Diffuse Cutaneous Systemic Sclerosis: Identifying Disease Risk Factors for Toxicity and Long-Term Outcomes in a Prospective, Single-Arm Trial <i>George E. Georges, Dinesh Khanna, Mark H. Wener, Matthew G. Mei, Maureen D. Mayes, Robert W. Simms, Vaishali Santhorawala, Chitra Hosing, Suzanne Kafaja, Attaphol Pawarode, Leona A. Holmberg, Jason Kolfenbach, Daniel E. Furst, Keith M. Sullivan, Suiyuan Huang, Ted Gooley, and Richard A. Nash</i>	571

Autoinflammatory Disease

Characterization of Genetic Landscape and Novel Inflammatory Biomarkers in Patients With Adult-Onset Still Disease

Joanne Topping, Leon Chang, Fatima Nadat, James A. Poulter, Alice Ibbotson, Samuel Lara-Reyna, Christopher M. Watson, Clive Carter, Linda P. Pournara, Jan Zernicke, Rebecca L. Ross, Catherine Cargo, Paul A. Lyons, Kenneth G. C. Smith, Francesco Del Galdo, Jürgen Rech, Bruno Fautrel, Eugen Feist, Michael F. McDermott, and Sinisa Savic, on behalf of the ImmunAID Consortium 582

Pediatric Rheumatology

Clinical, Immunologic, and Genetic Characteristics in Patients With Syndrome of Undifferentiated Recurrent Fevers

Marci Macaraeg, Elizabeth Baker, Elizabeth Handorf, Michael Matt, Elizabeth K. Baker, Hermine Brunner, Alexei A. Grom, Michael Henrickson, Jennifer Huggins, Wenying Zhang, Pui Lee, Rebecca Marsh, and Grant S. Schulert 596

Evaluating Renal Disease in Pediatric-Onset Antineutrophil Cytoplasmic Antibody–Associated Vasculitis: Disease Course, Outcomes, and Predictors of Outcome

Kirandeep K. Toor, Audrea Chen, David A. Cabral, Cherry Mammen, Else S. Bosman, Ye Shen, Jeffrey N. Bone, Damien Noone, Eslam Al-Abadi, Susanne Benseler, Roberta Berard, Marek Bohm, Sirirat Charuvanij, Kathryn Cook, Paul Dancey, Samundeeswari Deepak, Ciaran Duffy, Barbara Eberhard, Melissa Elder, Dirk Foell, Dana Gerstbacher, Merav Heshin-Bekenstein, Adam Huber, Karen E. James, Susan Kim, Marisa Klein-Gitelman, Neil Martin, Flora McErlane, L. Nandini Moorthy, Charlotte Myrup, Phil Riley, Susan Shenoi, Vidya Sivaraman, Tamara Tanner, Stacey Tarvin, Linda Wagner-Weiner, Rae S. M. Yeung, Kelly L. Brown, and Kimberly A. Morishita, on behalf of the PedVas Investigators Network 606

Low Back Pain

Efficacy of a Tumor Necrosis Factor Inhibitor in Chronic Low-Back Pain With Modic Type 1 Changes: A Randomized Controlled Trial

Elisabeth Gjefsen, Lars C. Bråten, Erica Ponzi, Magnhild H. Dagestad, Gunn H. Marchand, Thomas Kadar, Gunnstein Bakland, Anne J. Haugen, Fredrik Granviken, Tonje W. Flørenes, Nils Vetti, Lars Grøvle, Aksel T. Nilsen, Astrid Lunestad, Thor E. Holmgard, Morten Valberg, Nils Bolstad, Ansgar Espeland, Jens I. Brox, Guro L. Goll, Kjersti Storheim, and John-Anker Zwart 615

Letter

An Investigation of the Relationship Between Weight Management and Gout: Insights from the THIN Database Study and Recommendations for Improvement. Comment on the Article by Wei et al

Ling Zhang, Jun Li, and Yaling Li 624

Reply

Jie Wei, Yilun Wang, Chao Zeng, Guanghua Lei, and Yuqing Zhang 625

Correspondence to the Risk of Lung Cancer in Rheumatoid Arthritis and Rheumatoid Arthritis–Associated Interstitial Lung Disease: Comment on the Article by Brooks et al

Tsai Yi Hung, Chen Dong, Brian Shiian Chen, and James Cheng Chung Wei 625

Environmental Risk Factors Should not be Overlooked: Comment on the Article by Brooks et al

Andreea Lazarut-Nistor and David G. Hutchinson 626

Reply

Bryant R. England, Rebecca T. Brooks, and Ted R. Mikuls 627

The Effect of Air Pollution and Genetic Susceptibility on Systemic Lupus Erythematosus: Comment on the Article by Xing et al

Na Wang, Hu Chen, and Shugang Liu 627

Cover image: The image on the cover (from Liu et al; pages 547–559) shows immunofluorescence analysis of aortic sections from ApoE^{−/−}–Sting1^{−/−} mice fed a high-fat diet, indicating a significant reduction in CD68+macrophages (green) and α-smooth muscle actin (red) in the arteries of mice that lack STING. These observations suggest that STING plays a key role in enhancing vascular inflammation and promoting atherogenesis.

In this Issue

Highlights from this issue of *A&R* | By Lara C. Pullen, PhD

Tumor Necrosis Factor Inhibitor Fails to Improve Chronic Low-Back Pain

p. 615 In this issue, Gjefsen et al (p. 615) report the results from the first study to investigate the efficacy of intravenous tumor necrosis factor inhibitors as a treatment for chronic low-back pain (LBP) with type 1 Modic changes (MCs). Results from the BackToBasic study indicated that, when it came to reducing pain-related disability over 5 months, infliximab did not demonstrate superiority over placebo. The investigators found that the incidence of reported moderate adverse events (AEs) was higher in the group that received infliximab. However, severe AEs and the overall number of AEs

were similar between the treatment groups.

The randomized, triple-blind study included 128 patients and utilized validated outcome measures. Patients were aged 18-65 years with a mean age of 43 years and had moderate to severe chronic low-back pain and MCs. The majority (65.6%) of patients were female. The mean Oswestry Disability Index (ODI) score (\pm standard deviation) at baseline was 33.5 ± 10.8 . The researchers evaluated a dose regimen for infliximab consistent with the approved dose for ankylosing spondylitis. They included all patients who received at least one dose of the allocated infusion in their primary analyses. The

team reported monthly data over 5 months but acknowledged that they could not be sure they had chosen the optimal time to evaluate the treatment effect.

Patients had an average ODI score change (\pm SD) over 5 months of $-7.0 (\pm 9.7)$ in the group that received infliximab and $-6.4 (\pm 10.4)$ in the group that received placebo. The difference in ODI score change between the two groups from baseline to 5 months was 1.3 ODI points. The prespecified secondary outcomes, including LBP intensity, disability, and health-related quality of life, showed no superiority of infliximab at 5 months.

Insights into Renal Disease in Pediatric-Onset ANCA-Associated Vasculitis

p. 606 While kidney biopsies currently play an important role in aiding prognostication at around the time of diagnosis (TOD) of chronic kidney disease (CKD), previous studies have demonstrated that adult patients with CKD stages 4 and 5 and lower “baseline” estimated glomerular filtration rate (eGFR) are at a higher risk for kidney failure and need renal replacement therapy. In this issue, Toor et al (p. 606) report that although most pediatric-onset, antineutrophil cytoplasmic antibody (ANCA)-associated vasculitis (AAV) patients achieve inactive renal disease by 12 months, almost half have evidence of damage. Their study is the most extensive to date of renal outcomes in pediatric AAV and indicates that renal function at diagnosis strongly predicts renal function at 12 months.

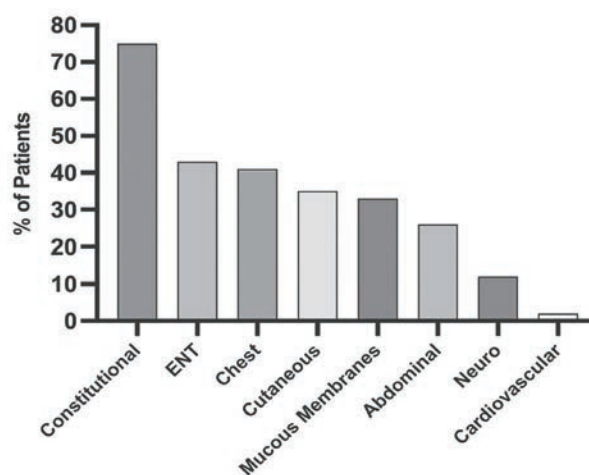


Figure 1. Percentage of pediatric onset AAV cases (y-axis) with organ-specific system involvement (x-axis) at the time of diagnosis.

Most patients in the study were female and White and were diagnosed with granulomatosis with polyangiitis. The median age

at diagnosis was 13.8 years. Patients generally received standard therapy with either cyclophosphamide or rituximab, combined with glucocorticoids in varied regimens. The researchers used eGFR instead of measured GFR to estimate renal function in the context of real-world registry data collection.

While most pediatric patients presented with very high renal disease activity at diagnosis, most achieved inactive renal disease 12-24 months after diagnosis. Nevertheless, the study demonstrated a high rate of significant renal disease in pediatric AAV. The investigators identified an eGFR cut point threshold of 38 mL/min/1.73m², below which patients exhibited a higher likelihood of having significant renal dysfunction by 12 months.

Development of Extramusculoskeletal Manifestations in Patients Treated with Upadacitinib

An analysis of the Swedish Population Patient Register revealed an association between uveitis flares and radiographic axial spondyloarthritis (r-axSpA) diagnosis. This

p. 536

may be because patients with r-axSpA have a higher tendency for recurrence of uveitis compared with those who have psoriatic arthritis (PsA) or the general population. **In this issue, Poddubnyy et al (p. 536)** report the results from a post hoc analysis designed to assess the impact of upadacitinib on the development of extramusculoskeletal manifestations (EMMs)

from the SpA SELECT clinical trials. They found that for patients with SpA, treatment with upadacitinib 15 mg was associated with a reduction in the development of EMMs.

The investigators analyzed adverse events of relevant EMMs as reported by the investigators of the SELECT trials. The authors note in their discussion that they did not evaluate the development of psoriasis in PsA as they considered it a core manifestation of the disease. Most patients did not have a baseline history of EMMs. The researchers found that the development of EMMs in patients treated with upadacitinib 15 mg was generally low

across PsA, r-axSpA, and nonradiographic axSpA (nr-axSpA).

Overall, having a history of uveitis appeared to predispose patients with r-axSpA to future uveitis events regardless of treatment. The team also found that, across PsA, r-axSpA, and nr-axSpA, patients, especially those with r-axSpA, experienced less uveitis when treated with upadacitinib than when treated with placebo. Moreover, for patients with PsA, rates of uveitis were similar when treated with upadacitinib 15 mg or adalimumab. New onset or flares of inflammatory bowel disease were low across PsA, r-axSpA, and nr-axSpA.

Journal Club

A monthly feature designed to facilitate discussion on research methods in rheumatology.

Characterization of Genetic Landscape and Novel Inflammatory Biomarkers in Patients with Adult-Onset Still Disease

Topping et al, *Arthritis Rheumatol.* 2025;77:582–595.

Adult-onset Still disease (AOSD) is a systemic autoinflammatory disorder of unknown etiology, typically presenting with prolonged intermittent fevers, arthralgias, and evanescent rash. The authors aimed to uncover the underlying pathological mechanisms of AOSD and identify potential therapeutic targets through a combination of next-generation sequencing and assays for inflammatory biomarkers. This study included a total of 106 cases of AOSD, 30 of which were refractory to treatment.

Whole exome sequencing was performed to investigate rare, potentially pathogenic germline and somatic variants across virtual gene panels associated with inflammation, clonal hematopoiesis of indeterminate potential, and type I interferonopathies. Differences in transcriptome profile were investigated using bulk RNA sequencing; inflammatory cytokines and interferon scores were measured from sera using multi-analyte flow assays; and *NLRP3* inflammasome activation was assessed using a novel in-house flow cytometry assay.

Using these methods, Topping et al identified an increase in rare germline variants associated with monogenic autoinflammatory disease, which suggests an underlying genetic predisposition to AOSD. Furthermore, 23.3% of AOSD cases (vs. 6.1% of healthy controls) had a combination of both germline and somatic

variants within their virtual gene panels, showing a potential role for somatic variants in AOSD disease pathogenesis. Transcriptome profiling showed potential to predict phenotype severity, showing strong positive correlation with Still Activity Score, a composite clinical score for AOSD. Numerous inflammatory cytokines were significantly elevated in AOSD cases, in addition to *NLRP3* inflammasome activation, showing the assays' potential utility in researching other inflammatory conditions.

Questions

1. What would be the best approach to identifying genes of interest from whole exome data, outside of targeted gene panels?
2. How might we conduct somatic variant analysis in tissues of interest, in the absence of patient-matched, normal tissue samples?
3. What other conditions would you expect to share similar inflammatory biomarker profiles to AOSD?
4. What challenges may be present in the assay design for a specific inflammasome?

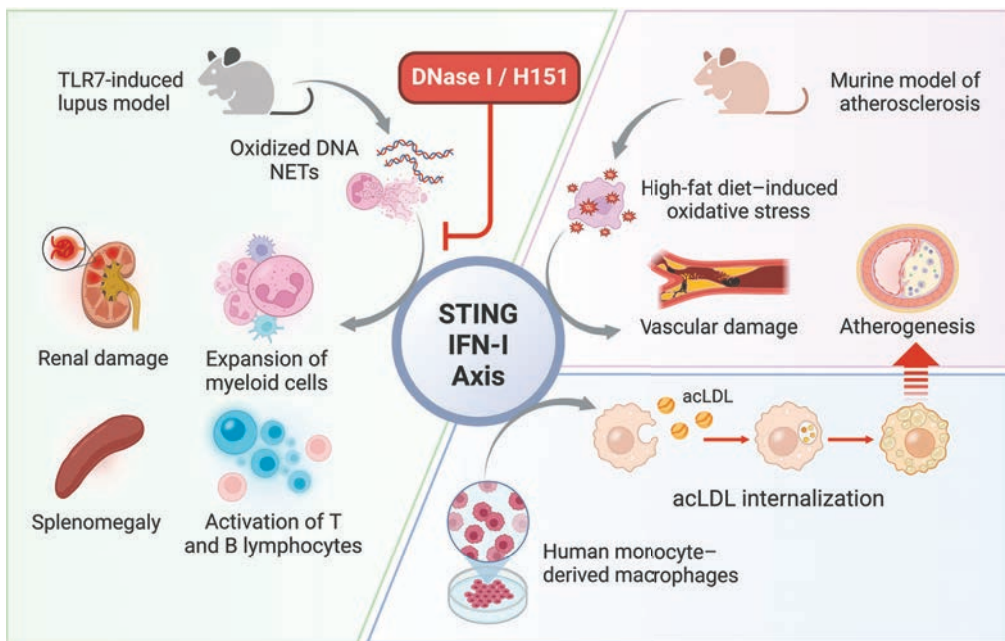
Clinical Connections

Role of STING Deficiency in Amelioration of Lupus and Atherosclerosis

Liu et al, *Arthritis Rheumatol.* 2025;77:547–559

CORRESPONDENCE

Mariana J. Kaplan, MD: mariana.kaplan@nih.gov



KEY POINTS

- STING-driven IFN responses and proinflammatory signals promote immune dysregulation and tissue damage in TLR7-driven autoimmunity.
- STING deficiency protects against vascular damage and reduces atherosclerosis burden.
- IFN signaling promotes macrophage uptake of acetylated LDL that promotes plaque formation.
- Targeting STING may have therapeutic potential in SLE and related autoimmune disorders.

SUMMARY

Abnormal activation of pathways that detect nucleic acids has been linked to autoimmune diseases such as systemic lupus erythematosus (SLE). SLE is a systemic autoimmune condition marked by immune reactions against nucleic acids, overactivation of the type I interferon (IFN-I) pathway, and an increased risk of cardiovascular disease, including atherosclerosis. Liu et al demonstrated that the stimulator of IFN genes (STING), a sensor that detects nucleic acids inside cells, plays a key role in worsening autoimmunity, vascular damage, and atherosclerosis.

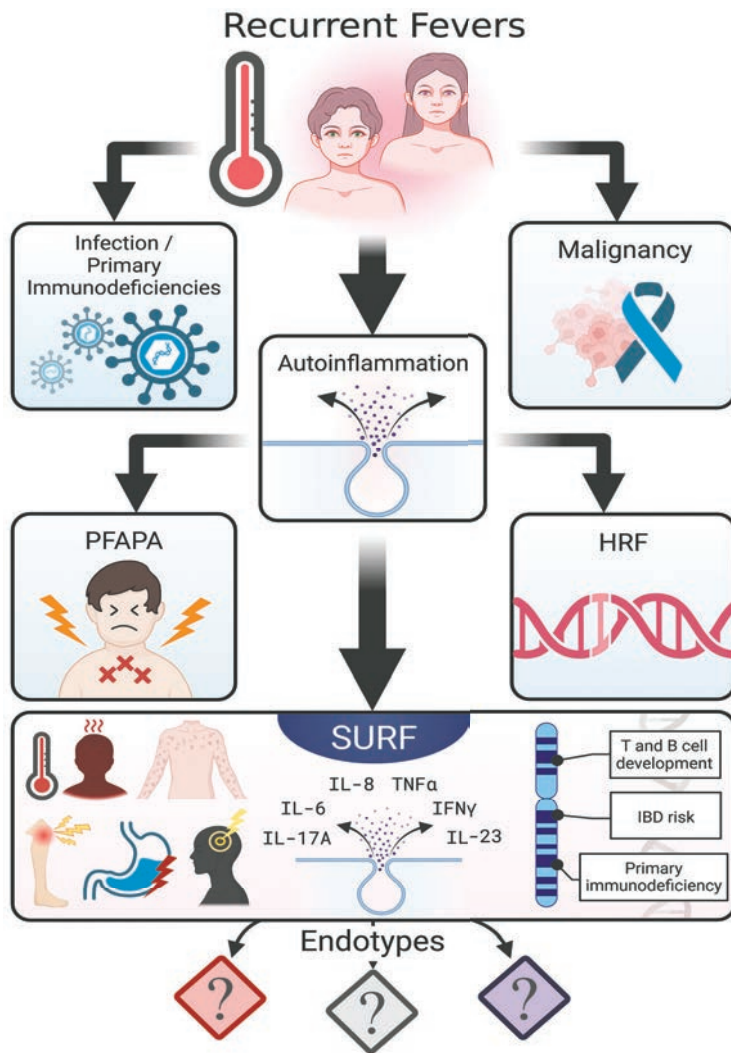
In a mouse model of TLR7-driven lupus, the absence of STING reduced disease severity, including decreasing spleen size, less immune complex deposition and damage in the kidneys, less expansion of myeloid cells, and lower activation of T and B lymphocytes. DNA release, particularly in its oxidized form, and increased formation of neutrophil extracellular traps can activate the STING-mediated pathways in lupus pathology. Blocking STING activity with the inhibitor H-151 or degrading extracellular DNA with DNase I protected lupus-prone mice, leading to lower IFN-I activity. In atherosclerosis, STING activation also worsens vascular inflammation and promotes plaque formation. A high-fat diet increases oxidative stress in blood vessels, triggering STING-driven IFN-I signaling. This signaling enhances macrophage uptake of modified low-density lipoproteins (acetylated LDL), accelerating plaque buildup. In patients with SLE, increased DNA oxidation is linked to disease severity, kidney dysfunction, and vascular inflammation. These findings suggest that STING contributes to immune dysregulation and vascular damage in SLE, highlighting it as a potential therapeutic target.

Characteristics of Patients With Syndrome of Undifferentiated Recurrent Fevers

Macaraeg et al, *Arthritis Rheumatol.* 2025;77:596–605

CORRESPONDENCE

Grant S. Schulert, MD, PhD: Grant.schulert@cchmc.org



SUMMARY

Recurrent fevers are a common presentation to pediatric rheumatology, and a significant burden to affected children and their families. Children with recurrent fevers but without a confirmed molecular diagnosis, and not fulfilling criteria for periodic fever, adenitis, pharyngitis, and aphthous stomatitis syndrome (PFAPA), are termed Syndrome of Undifferentiated Recurrent Fevers (SURF). While there is growing recognition that SURF is a distinct clinical entity, little is known regarding the clinical, immunologic, and genetic diversity of patients with SURF, and there is no consensus on best treatment practices.

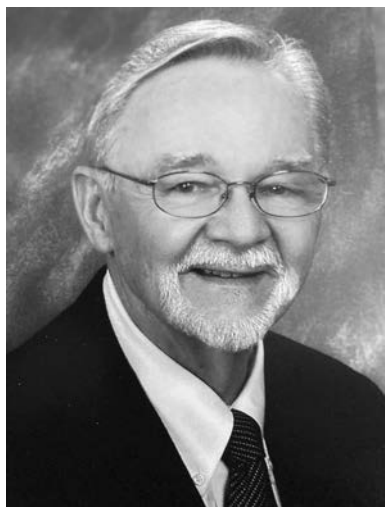
In a large, single-center cohort of SURF patients, Macaraeg et al found that, while clinically heterogeneous, SURF patients were more likely to experience rash and arthralgias while having distinctly less pharyngitis and adenopathy compared to PFAPA. They also found a subset of SURF patients with more systemic inflammation and higher prevalence of rash and need for biologic use compared to other patients. SURF patients frequently demonstrated a variety of rare, potentially deleterious genetic variants in genes important for B cell development; immunodeficiencies; and inflammatory bowel disease (IBD) risk. Although many SURF patients responded to treatments typically used for PFAPA, others required anti-IL-1 biologic therapy, with high response rates. Taken together, this work supports that while SURF is distinct from PFAPA and hereditary fever syndromes (HRFs), it remains a diagnosis of exclusion and likely encompasses multiple distinct and recognizable disease groups/endotypes.

KEY POINTS

- SURF is distinct from PFAPA and HRFs, and patients and fever episodes within SURF are heterogeneous.
- A subset of SURF patients have higher levels of IFN γ , IL-12p70, and IL-23, with rash and increased biologic use.
- Variants of unknown clinical significance commonly found in SURF patients include genes implicated in T and B cell development, immunodeficiencies, and IBD risk.

IN MEMORIAM

J. Claude Bennett, MD, 1933–2024



J. Claude Bennett, MD, died on August 11, 2024, in Birmingham, Alabama, at the age of 90. Dr Bennett served as President of the American Rheumatism Association (now the American College of Rheumatology) from 1981 to 1982 and was Editor in Chief of *Arthritis & Rheumatism* (now *Arthritis & Rheumatology*) from 1975 to 1980. A native of Birmingham, Alabama, Bennett received his undergraduate degree from Howard College (now Samford University) and, in 1958, an MD degree from Harvard Medical School. After additional training at Harvard and the National Institutes of Health (NIH), he began a postdoctoral fellowship at the California Institute of Technology in 1960, only 7 years after the structure of DNA had been reported by Watson and Crick. At that time, it was thought that each protein in the human body was encoded by a specific gene (the one gene–one protein hypothesis). However, the human genome was not large enough to encode millions of different antibodies, thus presenting a paradox.

Bennett and his mentor Dr William Dreyer were among the first scientists to propose the presence of sets of immunoglobulin gene segments that were rearranged differently as a mechanism of antibody diversity (*Proc Natl Acad Sci U S A* 1965;54(3):864). This manuscript generated significant interest and was highlighted on the front page of the *New York Times* (Sullivan W. “Key to antibody origin may be near.” November 29, 1965).

In 1965, Dr Bennett joined the faculty of the University of Alabama at Birmingham (UAB) School of Medicine where he studied rheumatoid factor and inflammatory and autoimmune mechanisms in rheumatoid arthritis. From 1977 to 1982, he was Director of the UAB Division of Clinical Immunology and Rheumatology and held the rare distinction of concomitantly serving as Chair of the UAB Department of Microbiology, directing research programs in immunology, bacteriology, and virology. In 1977, Bennett became the inaugural Director of the NIH-funded UAB Multipurpose Arthritis Center, the forerunner of many subsequent National Institute of Arthritis and Musculoskeletal and Skin Diseases–funded program grants.

In 1982, based on his extraordinary success in developing rheumatology patient care, education, and research, Dr Bennett was named Chair of the UAB Department of Medicine. His sphere of influence and commitment to excellence was thus applied to the field of internal medicine, in which he continued to exhibit exceptional leadership and service. He was President of the Association of American Physicians, President of the Association of Professors of Medicine, and Chair of the American Board of Internal Medicine. In 1986, he was elected a member of the Institute of Medicine (now the National Academy of Medicine). He served as editor of three editions of the *Cecil Textbook of Medicine*. Dr Bennett was actively involved in the expansion and promotion of the field of rheumatology and basic research throughout his career. His scientific and clinical background led him to become a strong and consistent advocate for the integration of a didactic scientific curriculum into the clinical training programs.

In 1992, Dr Bennett received the John Phillips Memorial Award in Clinical Medicine from the American College of Physicians for his lifetime of innovative and impactful work in clinical medicine. He was the recipient of the Kober Medal from the Association of American Physicians and was named a Master of the American College of Physicians and a Master of the American College of Rheumatology. The Association of Professors of Medicine bestowed on him the Robert H. Williams Distinguished Chair of Medicine Award for outstanding contributions to academic internal medicine in education, research, patient care, and faculty development. Bennett was appointed the fourth President of UAB in 1993. After many additional contributions to the

University, he retired from UAB in 1996 and became President and Chief Operating Officer of BioCryst Pharmaceuticals, Inc. He continued to apply his intellect and creativity by providing scientific input into drug design and clinical development programs.

Despite his many honors and accomplishments, Claude remained humble, thoughtful, and caring—all characteristics of how he led his life both at work and at home. These qualities endeared him to his family, friends, and colleagues. He took a very active interest in promoting the careers of trainees and colleagues by quickly recognizing their talents and supporting their efforts to succeed. His vision and leadership contributed greatly to the development of the field of rheumatology and to medicine overall. He was a most respected teacher and mentor to UAB medical students, graduate students, residents, and fellows.


Despite offers of leadership positions at several prestigious medical centers over the years, he remained at UAB for the entirety of his 31-year career in academic medicine. After his long and distinguished career, Dr Bennett resided in Birmingham with his wife Frances. In addition to his brilliance and remarkable accomplishments, Claude was kind and generous. He was a beloved father and grandfather, had a great appreciation for the arts and good food, and was always quick to share an

optimistic comment. He left an indelible mark on the care of patients with rheumatic diseases, on the development of new therapeutic approaches based on scientific research, and on the careers of his many trainees and colleagues. He will be greatly missed.

ACKNOWLEDGMENTS

There is overlap of the content in this article with an article recently published by one of the authors (SLB) describing Dr Bennett's accomplishments (Bridges SL Jr, Gay S., J. Claude Bennett, MD: scholar, physician, and leader. *Rheum Dis Clin North Am* 2024;50 (1):57–63).

Author disclosures are available at <https://onlinelibrary.wiley.com/doi/10.1002/art.43056>.

S. Louis Bridges, Jr, MD, PhD 
bridgesl@hss.edu
Hospital for Special Surgery
and Weill Cornell Medicine
New York, New York
Kenneth G. Saag, MD, MSc
William J. Koopman, MD
University of Alabama at Birmingham

EDITORIAL

Living With Sjögren Disease: Prospects for Disease-Modifying Therapies

E. William St. Clair

Living with Sjögren disease (SjD), or Sjögren syndrome or simply Sjögren, is mostly about learning to cope with physical tiredness, dryness, and joint pain. It is predominantly these symptoms that drive the reduced quality of life in this disease.¹ SjD may also lead to systemic disease activity in about one-third of patients by affecting extraglandular tissues and organs, including the joints, lungs, kidneys, skin, and nervous system. In 5% to 10% of cases, the disease course in SjD may be further complicated by the development of non-Hodgkin lymphoma, a poor prognostic factor. This clinical heterogeneity has created major challenges in evaluating the clinical efficacy of new therapies for SjD. Moreover, distinct profiles of symptom severity in SjD have been linked to different biomarkers,² implying that precision medicine strategies may ultimately prove to be the best approach.

SjD lacks a licensed disease-modifying drug in its arsenal. Investigative efforts to date have mostly focused on targeted approaches. In SjD, the salivary gland tissue is characterized by a chronic inflammatory response. This pathophysiology is orchestrated by T and B cells, macrophages, dendritic cells, and activated epithelial cells, which in turn drive the production of proinflammatory cytokines, such as interferons and BAFF, as well as stimulate the secretion of chemokines and other soluble mediators. B cells have garnered the most recent attention as therapeutic targets and for good reason. They are revved up on overdrive in SjD, producing excessive amounts of Ig and autoantibodies and forming ectopic germinal centers in glandular and lymphoid tissues where autoreactive clones may escape tolerance checkpoints. In this issue of *Arthritis & Rheumatology*, Dörner et al are in lockstep with this plan of attack as they describe the second part of a randomized, placebo-controlled, phase 2b dose-ranging study of ianalumab in patients with SjD.³

Ianalumab, a monoclonal antibody to the BAFF receptor (BAFF-R), acts both to block the BAFF-R and deplete BAFF-R-expressing B cells via antibody-dependent cellular cytotoxicity, distinguishing it from belimumab, a monoclonal antibody against

soluble BAFF, the natural ligand for the BAFF-R. The BAFF/BAFF-R pathway stands at the intersection between innate and adaptive immunity and plays a critical role in B cell maturation, germinal center formation, and B cell survival. The ianalumab study participants met the 2002 American European Consensus Group classification criteria,⁴ had a positive test result for anti-SSA/Ro, and had moderate-to-high systemic disease activity as defined by a EULAR Sjögren's Syndrome Disease Activity Index [ESSDAI] score ≥ 6 . The first part of the trial was reported previously,⁵ in which eligible participants were randomly allocated in a 1:1:1:1 ratio to receive ianalumab at a 5-, 50-, or 300-mg dose or placebo by the subcutaneous route every 4 weeks for 24 weeks. The 24-week primary end point, a dose-response model of the change in ESSDAI score, was met with statistical significance. The ESSDAI score decreased in all of the dosage groups, with the greatest change in the ianalumab 300-mg group. The 300-mg group had a mean (SD) decrease in ESSDAI score from 13.1 (6.7) to 4.9 (3.9), with a least-squares mean-adjusted difference from placebo of 1.92 (95% confidence interval–4.15 to 0.32). Although the change in ESSDAI score easily exceeded the threshold of a three-point decrease corresponding to minimal clinically important improvement,⁶ the placebo group also showed a mean (SD) decrease in ESSDAI from 13.0 (7.1) to 7.0 (5.1). Clinical trials of other investigational agents using the ESSDAI as a primary end point have produced placebo responses of this magnitude. In this study, treatment with ianalumab, however, failed to improve symptoms of dryness, fatigue, and joint pain, as measured by the EULAR Sjögren's Syndrome Patient Reported Index (ESSPRI).⁷

In the trial's second part, participants in the 300-mg group were rerandomized at week 24 to receive either 300 mg of ianalumab every 4 weeks or placebo, whereas the participants initially allocated to the placebo group were switched to 150 mg of ianalumab every 4 weeks; participants in the 5-mg and 50-mg groups entered safety follow-up.³ The clinical efficacy in the 300-mg dose

E. William St. Clair, MD: Duke University, Durham, North Carolina.
Author disclosures are available at <https://onlinelibrary.wiley.com/doi/10.1002/art.43060>.

Address correspondence via email to E. Williams St. Clair, MD, at stcla003@mc.duke.edu.

Submitted for publication October 12, 2024; accepted in revised form November 6, 2024.

group was sustained through week 52, a reassuring finding. Although the safety profile revealed no alarming safety signals, more infections were observed in the ionalumab groups than the placebo group and included eight serious adverse events of infection. A larger phase 3 trial that is underway will expand our understanding of ionalumab's safety and clinical efficacy.

The ESSDAI and the ESSPRI have been widely used as primary and secondary end points in clinical trials of investigational therapies for SjD. They have been the reference standards for measuring systemic disease activity and patients' symptoms, respectively. The ESSDAI includes 12 domains: constitutional, lymphadenopathy, glandular, articular, cutaneous, pulmonary, renal, muscular, peripheral nervous system, central nervous system, hematologic, and biologic.⁸ The individual domains have a range of scores (1–3) and are weighted (1–7) according to severity. Eligibility in most recent clinical trials requires participants to have moderate-to-high disease activity, as defined by an ESSDAI score of ≥ 5 . Only about 15% of the SjD population meet these criteria,⁹ excluding the vast majority of patients from clinical trials who mostly have dryness, fatigue, and joint pain.

Some of the domains in the ESSDAI are relatively easy to evaluate in the clinic (eg, constitutional, glandular), whereas others depend exclusively on objective measures (eg, renal), and yet others require sophisticated testing (eg, pulmonary: lung function tests and chest computed tomography scan). The scoring system is complicated in practice and requires faithful adherence to the precise definitions for each of the domains while excluding long-lasting features that do not reflect active disease. Investigator training is essential to make certain the ESSDAI is scored properly. Sponsors typically use medical monitors who meticulously check the investigator's scores to ensure accuracy and consistency. In trials, the most frequently scored domains are constitutional, articular, glandular, lymphadenopathy, hematologic, and biologic.¹⁰ Some of the domains are relatively insensitive to change (peripheral nervous system, central nervous system, and pulmonary), whereas others are rarely scored (muscular). The poorly performing domains are often excluded from the ESSDAI score that determines trial eligibility (eg, ESSDAI ≥ 5) to ensure a participant's responsiveness to therapy. The exclusion of these poorly performing domains in the calculation of the qualifying ESSDAI score enriches the study population with more potential responders and increases the probability of detecting a clinical effect of the study drug. Echoing the results of the phase 2 ionalumab trial, studies have found that a treatment-related decrease in the ESSDAI score does not necessarily lead to a corresponding improvement in patients' symptoms.

The ESSPRI was designed as a clinical outcome for SjD to evaluate the symptoms of fatigue, dryness, and pain. It is scored using three visual analog scales. There are concerns the ESSPRI score does not reliably reflect the patient experience, and therefore other patient-reported outcomes, such as symptom diaries, fatigue scales, and Patient-Reported Outcomes Measurement

Information System health measures, must be included as secondary end points to capture the full range and depth of symptoms. Thus far, investigational drugs tested in SjD have not consistently reduced symptoms of fatigue, dryness, and pain or favorably impacted objective measures of ocular dryness and hyposalivation. It is possible that glandular dysfunction may be difficult to reverse in established disease of relatively long duration.

Investigators and pharmaceutical sponsors have been in a quandary of late owing to the failure of several biologics to show clinical efficacy in SjD, despite initial promising results and a strong scientific rationale. Nevertheless, the SjD pipeline has a bright outlook (see Table 1). In addition to ionalumab's burgeoning fortunes, dazodalibep, a nonantibody fusion protein CD40 ligand antagonist¹¹; iscalimab, a CD40 monoclonal antibody¹²; telitacept, a recombinant transmembrane activator, calcium modulator, and cyclophilin ligand interactor-Fc fusion protein¹³; and remibrutinib, an oral BTK inhibitor¹⁴ have each been studied in phase 2 trials and have led to significant improvement in systemic disease activity, as measured by the ESSDAI score. However, only treatment with dazodalibep was associated with a significant reduction in the ESSPRI score,¹¹ although this finding must be viewed with caution owing to a small sample size. Notably, this improvement in ESSPRI was observed in a distinct SjD subgroup with a predominance of symptoms (ESSPRI ≥ 5) and low systemic disease activity (ESSDAI < 5). Reinvigorated by these positive trials, the SjD pipeline has been blossoming with activity. Leading the pack in phase 3 trials are ionalumab, dazodalibep, telitacept, and deucravacitinib, although other agents in phase 2 studies are following close behind. Many more are charting their course in phase 1 studies.

There has been a growing appreciation that drug discovery in SjD would benefit from the use of composite end points to capture the full disease spectrum. To this end, expert groups have developed and validated two composite end points, namely the Composite of Relevant Endpoints for Sjögren's Syndrome (CRESS)¹⁵ and the Sjögren's Tool for Assessing Response (STAR).¹⁶ They are similar in concept and consist of core sets with five domains encompassing systemic activity (assessed by the ClinESSDAI, the ESSDAI minus the biologic domain), patient-reported outcomes, lacrimal gland function, salivary gland function, and a biologic profile. Analyses from previously completed trials suggests the use of these composite outcomes may reduce the placebo response and thereby more readily differentiate response rates among treatment arms. These composite end points encapsulate a global disease outcome and provide an opportunity to achieve a treatment response by either a reduction in systemic disease activity or an improvement in symptoms of fatigue, dryness, and pain. The use of a composite measure, such as CRESS or STAR, as a primary clinical end point enables the selection of study participants with a diverse range of clinical phenotypes, namely those with moderate-to-high systemic disease

Table 1. Phase 2 and 3 clinical trials of investigational therapies for Sjögren's syndrome*

Drug	Target	Sponsor	Phase	Scientific rationale based on mechanism of action
Ianalumab	Mab to BAFF-R	Novartis	3	BAFF-R is critically involved in B cell maturation; up-regulated BAFF in salivary gland tissue and serum
Dazodalibep	Non-antibody CD40 ligand antagonist	Amgen	3	CD40L-CD40 pathway essential for ectopic germinal center formation and Ig-class switching; CD40 and CD40L upregulated in salivary gland tissue
Deucravacitinib	Oral TYK2 inhibitor	Bristol-Myers Squibb	3	Tyk2 signaling involved in type 1 interferon production
Telitacicept	TACI-Fc fusion protein	RemeGen	3	Blockade of APRIL and BAFF in a preclinical animal model of SjD reduced inflammatory foci and IgG and IgM in the salivary gland
HZN-1116/AMG329	FLT3 ligand Mab	Amgen	2	Flt-3 ligand important in B lymphocyte development and lymphoid malignancies; elevated Flt-3L serum levels in SjD
Anifrolumab	Type 1 interferon receptor Mab	University Medical Center Groningen	2	Type 1 interferon signature in salivary gland and blood
Abiprubart	CD40 Mab	Kiniska Pharmaceuticals	2	CD40-CD40L signaling central to B cell development (see above)
RSLV-132	RNase-Fc fusion Protein	Resolve Therapeutics	2	Destroy pathogenic RNA-containing immune complexes
Nipocalimab	FcRN Mab	Janssen	2	Reduce disease-causing autoantibodies

* BAFF-R = B cell activating factor-receptor; TYK2 = tyrosine kinase 2; TACI = transmembrane activator and calcium modulator and cyclophilin ligand interactor; APRIL=a proliferation-inducing ligand; FLT3 = Fms-related receptor tyrosine kinase 3; FcRN = neonatal Fc receptor; Mab = monoclonal antibody.

activity, as well as those with a heavy symptom burden and an ESSDAI score <5. This approach would allow a greater proportion of patients with SjD to participate in clinical trials and increases the generalizability of the results. These advances in clinical trial design along with the rich pipeline of new therapies for SjD are a sign of real progress and an exciting prospect for patients and rheumatologists who are urgently in need of effective therapeutic options.

AUTHOR CONTRIBUTIONS

Dr St. Clair drafted the article, revised it critically for important intellectual content, and approved the final version to be published.

REFERENCES

- Lendrem D, Mitchell S, McMeekin P, et al; UK primary Sjögren's Syndrome Registry. Health-related utility values of patients with primary Sjögren's syndrome and its predictors. *Ann Rheum Dis* 2014; 73(7):1362–1368.
- Berry JS, Tam J, Casement J, et al. Examining the biological pathways underlying clinical heterogeneity in Sjogren's syndrome: proteomic and network analysis. *Ann Rheum Dis* 2024;83(1):88–95.
- Dörner T, Bowman SJ, Fox R, et al. Safety and efficacy of ivalumab in patients with Sjögren's disease: 52-week results from a randomized, placebo-controlled, phase 2b dose-ranging study. *Arthritis Rheumatol* 2025;77(5):560–570.
- Vitali C, Bombardieri S, Jonsson R, et al. Classification criteria for Sjogren's syndrome: a revised version of the European criteria proposed by the American-European Consensus Group. *Ann Rheum Dis* 2002;61(6):554–558.
- Bowman SJ, Fox R, Dörner T, et al. Safety and efficacy of subcutaneous ivalumab (VAY736) in patients with primary Sjögren's syndrome: a randomised, double-blind, placebo-controlled, phase 2b dose-finding trial. *Lancet* 2022;399(10320):161–171.
- Seror R, Bootsma H, Saraux A, et al; EULAR Sjögren's Task Force. Defining disease activity states and clinically meaningful improvement in primary Sjögren's syndrome with EULAR primary Sjögren's syndrome disease activity (ESSDAI) and patient-reported indexes (ESSPRI). *Ann Rheum Dis* 2016;75(2):382–389.
- Seror R, Ravaud P, Mariette X, et al; EULAR Sjögren's Task Force. EULAR Sjogren's Syndrome Patient Reported Index (ESSPRI): development of a consensus patient index for primary Sjogren's syndrome. *Ann Rheum Dis* 2011;70(6):968–972.
- Seror R, Ravaud P, Bowman SJ, et al; EULAR Sjögren's Task Force. EULAR Sjogren's syndrome disease activity index: development of a consensus systemic disease activity index for primary Sjogren's syndrome. *Ann Rheum Dis* 2010;69(6):1103–1109.
- Oni C, Mitchell S, James K, et al; UK Primary Sjögren's Syndrome Registry. Eligibility for clinical trials in primary Sjögren's syndrome: lessons from the UK Primary Sjögren's Syndrome Registry. *Rheumatology (Oxford)* 2016;55(3):544–552.
- de Wolff L, Arends S, Pontarini E, et al. Development and performance of the Clinical Trials ESSDAI (ClinTrialsESSDAI), consisting of frequently active clinical domains, in two randomised controlled trials in primary Sjogren's syndrome. *Clin Exp Rheumatol* 2021;39(6 suppl 133):100–106.
- St Clair EW, Baer AN, Ng WF, et al. CD40 ligand antagonist dazodalibep in Sjögren's disease: a randomized, double-blinded, placebo-controlled, phase 2 trial. *Nat Med* 2024;30(6):1583–1592.
- Fisher BA, Mariette X, Papas A, et al; TWINSS study group. Safety and efficacy of subcutaneous ivalumab (CFZ533) in two distinct populations of patients with Sjögren's disease (TWINSS): week 24 results of a randomised, double-blind, placebo-controlled, phase 2b dose-ranging study. *Lancet* 2024;404(10452):540–553.

13. Xu D, Fang J, Zhang S, et al. Efficacy and safety of telitacicept in primary Sjögren's syndrome: a randomized, double-blind, placebo-controlled, phase 2 trial. *Rheumatology (Oxford)* 2024;63(3):698–705.
14. Dörner T, Kaul M, Szántó A, et al. Efficacy and safety of remibrutinib, a selective potent oral BTK inhibitor, in Sjögren's syndrome: results from a randomised, double-blind, placebo-controlled phase 2 trial. *Ann Rheum Dis* 2024;83(3):360–371.
15. Arends S, de Wolff L, van Nimwegen JF, et al. Composite of Relevant Endpoints for Sjögren's Syndrome (CRESS): development and validation of a novel outcome measure. *Lancet Rheumatol* 2021; 3(8):e553–e562.
16. Seror R, Baron G, Camus M, et al; NECESSITY WP5 - STAR development working group; NECESSITY WP5- STAR development working group. Development and preliminary validation of the Sjögren's Tool for Assessing Response (STAR): a consensual composite score for assessing treatment effect in primary Sjögren's syndrome. *Ann Rheum Dis* 2022;81(7): 979–989.

EDITORIAL

Modic Changes and Tumor Necrosis Factor Inhibition: Is the Door Shut?

Jennifer S. Hanberg,¹  Joerg Ermann,²  and Jeffrey N. Katz² 

First described in 1988, Modic changes are magnetic resonance imaging (MRI) findings in the lumbar spine that are present in approximately 43% of patients with back pain and are thought to reflect pathobiological states characterized by combinations of inflammation, bone turnover, and fibrosis.^{1–3} Three subtypes of Modic changes are delineated by their characteristic appearance on MRI, but multiple types may coexist in any individual patient, and lesions may progress between types over time. Type 1 changes are hypointense on T1-weighted sequences and hyperintense on T2-weighted sequences, type 2 changes are hyperintense on T1-weighted sequences and hyper- or isointense on T2-weighted sequences, and type 3 changes are hypointense on both T1- and T2-weighted images.^{1,2} Similar MRI changes have been described in other locations and other diseases, where they have received different names. For example, in axial spondyloarthritis, bone marrow lesions that are hypointense on T1-weighted sequences and hyperintense on T2-weighted (equivalent to Modic type 1 changes) are called bone marrow edema and are considered to represent active inflammatory lesions.⁴

Histopathological studies of Modic changes have been sparse.² Type 1 Modic changes may reflect an active bone turnover state accompanied by increased pain signaling and nerve fiber density in the vertebra.⁵ As a result, type 1 changes represent a clinically important target for potential intervention.⁵ Controversy has surrounded the primary stimulus that leads to Modic changes and the optimal management for patients who exhibit these findings. Some evidence has supported a potential role for an infectious catalyst,⁶ but trials of antibiotics have yielded mixed results.⁷ Many researchers believe that Modic changes begin with an increased load on the vertebra initializing a sequence of endplate damage, disc herniation into the endplate, a repair response to the herniation, and changes in tissue-level

cytokine expression, including an upregulation of inflammatory mediators that include tumor necrosis factor (TNF).⁵

Several key findings have led to the hypothesis that Modic type 1 changes are largely inflammatory in nature and may respond to anti-inflammatory treatment, including TNF inhibitors. TNF-immunoreactive cells are more densely populated in endplates with type 1 Modic changes compared with type 2 Modic changes,⁵ C-reactive protein levels are higher in patients with type 1 compared to patients with type 2 Modic changes and low back pain,⁸ and response to intradiscal steroid injection was found to be superior in patients with type 1 Modic changes compared to patients with type 2 Modic changes.⁹ A trial of infliximab for treating patients with disc herniation-induced sciatica suggested a signal for symptomatic benefit in a subgroup of patients who had Modic changes at the level of the herniation.¹⁰ Because individualized treatment for symptomatic degenerative disc disease remains an important and elusive target, there has therefore been significant interest in the therapeutic potential for anti-inflammatory treatment for patients with type 1 Modic changes.

The results of the BackToBasic randomized controlled trial, which was designed to address this hypothesis, are reported by Gjeffen et al in this issue of *Arthritis and Rheumatology*.¹¹ The trial's protocol was published previously.¹² The study recruited 129 adult participants with chronic low back pain and Modic type 1 changes in the lumbar spine between 2018 and 2022. The trial specified minimum scores for either pain or disability as additional inclusion criteria. Patients with specific spinal diagnoses such as axial spondyloarthritis were excluded. Participants were randomized to four masked intravenous infusions over 14 weeks of either infliximab 5 mg/kg or placebo. The primary outcome was change in the Oswestry Disability Index (ODI) from baseline to five months, with secondary outcomes including a change in low back pain intensity and additional measures of disability and health-related quality of life. The ODI, a validated and frequently used self-report

Supported by the National Institute of Arthritis and Musculoskeletal and Skin Diseases/NIH (grants T32-AR-007530 and P30-AR-072577).

¹Jennifer S. Hanberg, MD: Brigham and Women's Hospital, Boston, Massachusetts; ²Joerg Ermann, MD, Jeffrey N. Katz, MD, MSc: Brigham and Women's Hospital and Harvard Medical School, Boston, Massachusetts.

Author disclosures are available at <https://onlinelibrary.wiley.com/doi/10.1002/art.43068>.

Address correspondence via email to Jennifer S. Hanberg, MD, at jhanberg@mgb.org.

Submitted for publication November 14, 2024; accepted in revised form November 18, 2024.

measure, consists of 10 questions about potential pain-related functional limitations, each scored from 0 to 5, and the final score is reported as a percentage from 0 to 100.¹³

The BackToBasic trial was powered to detect a 10-point difference in ODI change scores between the infliximab and placebo groups, a relatively large difference that is comparable to the SD of the ODI in the study sample. While both groups improved over five months, the trial result was negative with respect to the primary outcome, with an estimated between-group difference of 1.3 points at five months on the ODI (95% confidence interval [CI], -2.1 to 4.6). Indeed, in Figure 2¹¹, we see that the difference between groups at 5 months was small. In exploratory analyses, the investigators identified that the difference in ODI between the trial arms widened at 9 months to an estimated difference of 4.2 (95% CI, 0.8–7.6) ODI points. This is a modest difference (about 40% of an SD) and smaller than most proposed minimal clinically important differences for the ODI (5 to 17 points on an absolute scale).¹⁴ The authors have appropriately reported the primary outcome without undue speculation regarding the nine-month finding. However, on broader visual inspection of Figure 2¹¹, we observe that the difference between the treatment and placebo groups narrowed at five months compared with prior months and again widened at nine months, suggesting the null primary result may be partly attributable to chance.

In addition to the patient-reported outcomes reported in this manuscript, repeat imaging data, as described in the BackToBasic protocol, would be of interest. Bone marrow edema in axial spondyloarthritis improves with TNF inhibition,¹⁵ demonstrating that the lack of improvement in type 1 Modic changes in the BackToBasic trial would provide additional evidence against the role of anti-TNF therapies in this subset of patients with low back pain.

These considerations aside, the very small net improvement in ODI at five months because of treatment with infliximab in the BackToBasic trial may not be surprising, given the important pathobiological differences between axial spondyloarthritis (in which bone marrow edema at similar locations is seen and for which infliximab is quite effective¹⁶) and degenerative disc disease. In the former, immune cell activity and inflammation are primary actors in the production of back pain, stiffness, and disability, and TNF inhibitors and other immunomodulators result in dramatic clinical improvement for many patients.¹⁷ By contrast, in degenerative disc disease, inflammation is thought to be a downstream effect of a primary mechanical disturbance, which itself may provide a nociceptive stimulus.¹⁸ Treating the downstream inflammatory component of the disorder may not reverse the pathologic mechanical processes that ultimately drive pain and disability. Furthermore, low back pain in the context of degenerative disc disease is frequently multifactorial, resulting from structural factors (including increased load and damage to richly innervated bone, nerve injury and impingement, and ligamentous strain), inflammation arising from these structural

factors, and pain centralization.¹⁸ A treatment strategy that addresses each of these mechanisms successfully would be exceptional among medical therapeutics; thus, it is not surprising that the infliximab treatment effect was modest in this trial.

Prior research has yielded mixed results regarding the role for systemic immunomodulation in osteoarthritis (OA) and degenerative disc disease. Methotrexate was recently shown to reduce pain in randomized controlled trials with individuals with hand OA (with synovitis on MRI)¹⁹ and individuals with knee OA (without the requirement for synovitis on imaging).²⁰ A secondary analysis of a large randomized controlled trial found that treatment with the anti-interleukin-1 beta antibody canakinumab was associated with reduced hazard for individuals with hip and knee replacement, regardless of history of inflammatory arthritis or gout.²¹ However, TNF inhibition in particular has not shown efficacy with respect to clinical outcomes for individuals with hand OA.²²

Overall, the results of the BackToBasic trial advance the discussion regarding the distinction between primary versus secondary inflammation in individuals with musculoskeletal disease, in particular helping to address the question of whether treatments that are successful in the former will be equally effective in the latter. Based on the results from this well-executed study, we can conclude that TNF inhibition is unlikely to have a clinically important effect on clinical outcomes in individuals with low back pain with Modic changes. However, it is difficult to shut the door tightly on the use of targeted anti-inflammatory therapies for individuals with degenerative disc disease. For example, the between-group difference of 0.4 SD at nine months in an exploratory analysis raises the question of whether potent immunomodulatory therapy may exert a delayed effect on pain and function. This observation should be addressed in another trial. Further studies are also needed to better understand the processes driving type 1 Modic changes at the cellular and molecular level. Although the role for targeted immunomodulation in secondary inflammatory pathology (including degenerative low back pain with Modic changes) requires further study, we suggest that expectations for such treatment should remain guarded because of the primary role of other mechanical processes.

AUTHOR CONTRIBUTIONS

All authors were involved in drafting the article or revising it critically for important intellectual content, and all authors approved the final version to be published.




REFERENCES

1. Modic MT, Steinberg PM, Ross JS, et al. Degenerative disk disease: assessment of changes in vertebral body marrow with MR imaging. *Radiology* 1988;166(1 Pt 1):193–199.
2. Dudli S, Fields AJ, Samartzis D, et al. Pathobiology of Modic changes. *Eur Spine J* 2016;25(11):3723–3734.
3. Jensen TS, Karppinen J, Sorensen JS, et al. Vertebral endplate signal changes (Modic change): a systematic literature review of prevalence

- and association with non-specific low back pain. *Eur Spine J* 2008; 17(11):1407–1422.
4. Maksymowych WP, Lambert RG, Østergaard M, et al. MRI lesions in the sacroiliac joints of patients with spondyloarthritis: an update of definitions and validation by the ASAS MRI working group. *Ann Rheum Dis* 2019;78(11):1550–1558.
 5. Ohtori S, Inoue G, Ito T, et al. Tumor necrosis factor-immunoreactive cells and PGP 9.5-immunoreactive nerve fibers in vertebral endplates of patients with discogenic low back pain and Modic type 1 or type 2 changes on MRI. *Spine (Phila Pa 1976)* 2006;31(9):1026–1031.
 6. Jha SC, Sairyo K. The role of *Propionibacterium acnes* in and Modic type 1 changes: a literature review. *J Med Invest* 2020;67(1.2):21–26.
 7. Wong AYL, Mallow GM, Pinto SM, et al. The efficacy and safety of oral antibiotic treatment in patients with chronic low back pain and Modic changes: a systematic review and meta-analysis. *JOR Spine* 2024; 7(1):e1281.
 8. Rannou F, Ouanes W, Boutron I, et al. High-sensitivity C-reactive protein in chronic low back pain with vertebral end-plate Modic signal changes. *Arthritis Rheum* 2007;57(7):1311–1315.
 9. Fayad F, Lefevre-Colau MM, Rannou F, et al. Relation of inflammatory Modic changes to intradiscal steroid injection outcome in chronic low back pain. *Eur Spine J* 2007;16(7):925–931.
 10. Korhonen T, Karppinen J, Paimela L, et al. The treatment of disc-herniation-induced sciatica with infliximab: one-year follow-up results of FIRST II, a randomized controlled trial. *Spine (Phila Pa 1976)* 2006;31(24):2759–2766.
 11. Gjesfens E, Bråten LC, Ponzi E, et al. Efficacy of a tumor necrosis factor inhibitor in chronic low-back pain with Modic type 1 changes: a randomized controlled trial. *Arthritis Rheumatol* 2025;77(5): 615–623.
 12. Gjesfens E, Bråten LCH, Goll GL, et al. The effect of infliximab in patients with chronic low back pain and Modic changes (the Back-ToBasic study): study protocol of a randomized, double blind, placebo-controlled, multicenter trial. *BMC Musculoskelet Disord* 2020;21(1):698.
 13. Fairbank JC, Pynsent PB. The Oswestry Disability index. *Spine (Phila Pa 1976)* 2000;25(22):2940–2952; discussion 2952.
 14. Schwind J, Learman K, O'Halloran B, Showalter C, Cook C. Different minimally important clinical difference (MCID) scores lead to different clinical prediction rules for the Oswestry disability index for the same sample of patients. *J Man Manip Ther* 2013;21(2):71–78.
 15. Krabbe S, Sørensen IJ, Jensen B, et al. Inflammatory and structural changes in vertebral bodies and posterior elements of the spine in axial spondyloarthritis: construct validity, responsiveness and discriminatory ability of the anatomy-based CANDEN scoring system in a randomised placebo-controlled trial. *RMD Open* 2018;4(1): e000624.
 16. Ramiro S, Nikiphorou E, Sepiano A, et al. ASAS-EULAR recommendations for the management of axial spondyloarthritis: 2022 update. *Ann Rheum Dis* 2023;82(1):19–34.
 17. Danve A, Deodhar A. Treatment of axial spondyloarthritis: an update. *Nat Rev Rheumatol* 2022;18(4):205–216.
 18. Li W, Gong Y, Liu J, et al. Peripheral and central pathological mechanisms of chronic low back pain: a narrative review. *J Pain Res* 2021; 14:1483–1494.
 19. Wang Y, Jones G, Keen HI, et al. Methotrexate to treat hand osteoarthritis with synovitis (METHODS): an Australian, multisite, parallel-group, double-blind, randomised, placebo-controlled trial. *Lancet* 2023;402(10414):1764–1772.
 20. Kingsbury SR, Tharmanathan P, Keding A, et al. Pain Reduction with oral methotrexate in knee osteoarthritis : a randomized, placebo-controlled clinical trial. *Ann Intern Med* 2024;177(9):1145–1156.
 21. Schieker M, Conaghan PG, Mindeholm L, et al. Effects of interleukin-1 β inhibition on incident hip and knee replacement: exploratory analyses from a randomized, double-blind, placebo-controlled trial. *Ann Intern Med* 2020;173(7):509–515.
 22. Estee MM, Cicuttini FM, Page MJ, et al. Efficacy of tumor necrosis factor inhibitors in hand osteoarthritis: a systematic review and meta-analysis of randomized controlled trials. *Osteoarthritis Cartil Open* 2023;5(4):100404.

EXPERT PERSPECTIVES ON CLINICAL CHALLENGES

Expert Perspective: Diagnostic Approach to Differentiating Juvenile Dermatomyositis From Muscular Dystrophy

Jacqueline A. Madison, Sean P. Ferris,  Marianne Kerski,  Grace Hile, Sophia Matossian, Cara Komisar, Peter J. Strouse, Elizabeth Ames, Erin Neil Knierbein, and Jessica L. Turnier 

Introduction

A 4-year-old boy had 2 months of persistent fatigue, leg pain, inability to keep up with peers, and difficulty going up stairs. He exhibited an uncoordinated gait and inability to squat or rise from the ground but no joint swelling, tenderness, or rashes. His creatine kinase (CK) level was 1,681 units/L (upper limit of normal 257 units/L). He was referred to the Pediatric Neurology department to consider a muscular dystrophy (MD) diagnosis. Genetic testing for neuromuscular disorders revealed two variants of unknown significance. A magnetic resonance imaging (MRI) scan of the left pelvis and thigh demonstrated patchy T2 hyperintensity and enhancement with mild diffusion restriction and no atrophy or fatty replacement. His weakness progressed, and 6 months after symptom onset he was referred to the Pediatric Rheumatology department. Examination revealed a faint bilateral heliotrope rash and marked drop out, dilation, and hemorrhage of nailfold capillaries. His CK level remained elevated at 618 units/L, as did the aspartate aminotransferase, aldolase, lactate dehydrogenase, von Willebrand factor antigen, and neopterin levels. Muscle biopsy showed perifascicular atrophy, increased major histocompatibility complex class I (MHC-I) and myxovirus resistance A (MxA) expression, complement deposition in capillaries, and acute myopathic changes, including degeneration/regeneration, consistent with juvenile dermatomyositis (JDM). Myositis-specific antibody testing was positive for anti-nuclear matrix protein 2 (NXP2). The patient was initiated on intravenous and oral corticosteroids, subcutaneous methotrexate, intravenous Ig, and physical therapy, leading to a recovery of muscle strength nearly 1 year after symptom onset.

Dr Turnier's work was supported by the National Institute of Arthritis and Musculoskeletal and Skin Diseases, NIH (K23 career development grant K23-AR-080789); a Cure JM grant; a Childhood Arthritis and Rheumatology Research Alliance Large grant; and a Chan Zuckerberg Initiative Award for Patient-Partnered Collaborations for Single-Cell Analysis of Rare Inflammatory Pediatric Diseases.

Jacqueline A. Madison, MD, Sean P. Ferris, MD, PhD, Marianne Kerski, MD, Grace Hile, MD, Sophia Matossian, MScR, Cara Komisar, DPT, Peter J. Strouse,

Background

Despite different disease pathogenesis, pediatric patients with MD and JDM can present very similarly, especially if there is no prominent rash typical of JDM. Reaching a confirmed diagnosis can be difficult. The time to diagnosis is often prolonged, with an average delay to diagnosis of 6 months in JDM^{1,2} and 2 years in Duchenne MD (DMD).^{3,4} In this article, we focus on a diagnostic approach to differentiate JDM from MD. We recommend a more standardized use of nailfold capillaroscopy (NFC), myositis-specific autoantibody (MSA) testing, and muscle biopsy to aid in more quickly achieving diagnostic certainty.

The term juvenile myositis (JM) or juvenile idiopathic inflammatory myopathy (IIM) describes a group of rare, multisystem autoimmune diseases in children that predominantly affect the muscles and variably affect other organ systems, including the skin, lungs, gastrointestinal tract, and heart. JDM is the most common form of JM, affecting approximately 85% of children with myositis.⁵ Although JDM traditionally presents with characteristic rashes, including Gottron papules and heliotrope rash,^{6–8} the pathognomonic rash can be subtle or even absent at presentation.⁹ Children with JDM can also display heterogeneous disease phenotypes and even, at times, present first with other organ manifestations, such as interstitial lung disease (ILD). Although the discovery of MSAs has aided greatly in increased recognition of specific JDM phenotypes,¹⁰ other rarer forms of JM are less studied, often lack characteristic skin manifestations, and hence can still be difficult to classify and diagnose.⁸

The current classification criteria used for JM are the 2017 European League Against Rheumatism/American College of Rheumatology classification criteria for adult and juvenile IIM.⁶ These criteria are composed of a weighted point system for

MD, Elizabeth Ames, MD, PhD, Erin Neil Knierbein, DO, Jessica L. Turnier, MD: University of Michigan Medical School, Ann Arbor.

Author disclosures and graphical abstract are available at <https://onlinelibrary.wiley.com/doi/10.1002/art.43057>.

Address correspondence via email to Jessica L. Turnier, MD, at turnierj@med.umich.edu.

Submitted for publication April 10, 2024; accepted in revised form October 15, 2024.

clinical variables, including age at onset, patterns of muscle weakness, skin manifestations, laboratory test findings, and muscle biopsy features⁶; the resultant score leads to a predictive probability of whether or not the patient has IIM. With characteristic rash and muscle findings, one can fairly confidently reach a diagnosis of juvenile IIM; indeed, 97% of patients with JDM were correctly classified without a muscle biopsy. Without a rash, however, biopsy is usually required to fulfill the points for definite IIM. The criteria were developed to include juvenile IIM and so may be used in pediatric patients. For juvenile IIM, though, the criteria only distinguish between (1) JDM and (2) JM other than JDM, because there were too few pediatric patients in the latter category to further delineate their JM classification subgroup. This classification system is an update from the 1975 Bohan and Peter diagnostic criteria¹¹ and allows more flexibility in JDM classification for patients with variable phenotypes and who have not had muscle biopsy or electromyography performed.

The myositis community is currently working to update the IIM classification criteria to include further differentiation of IIM subtypes in children, such as antisynthetase syndrome and immune-mediated necrotizing myopathy (IMNM), and to include additional clinical variables with diagnostic utility. An international survey of JDM specialists in 2006 identified additional findings that could be helpful in diagnosis and included muscle MRI and ultrasound scans, NFC abnormalities, calcinosis, and dysphonia.¹² The 2012 Single Hub and Access point for Rheumatology in Europe (SHARE) initiative, an evidence-based guideline out of Europe, also developed 33 diagnostic recommendations for JDM and provided strength-of-evidence support for each, including a recommendation that muscle biopsy be performed in patients with JDM who are atypical or lacking classic rash, which was a recommendation based on expert opinion, as were the majority of recommendations.¹³

The most well-known forms of MD are dystrophinopathies, including DMD and Becker MD (BMD). However, there is increasing recognition with more widescale genetic testing that there are more than 40 different genes associated with an MD phenotype.¹⁴ These diseases are all genetic and progressive and have some typical findings on muscle biopsy.¹⁴

Similar to MD, the diagnostic categories of other noninflammatory myopathies in children are also diverse groups of diseases with variable phenotypes. Noninflammatory myopathies important to consider include congenital and metabolic myopathies.¹⁵ Other causes of weakness that are not of primary muscle origin must also be considered, such as infection, malignancy, thyroid disease, and other toxic/metabolic causes, including medication side effects. To better evaluate children with a presenting symptom of proximal muscle weakness, we worked with a multidisciplinary team, including experts in rheumatology, neurology, genetics, dermatology, pathology, radiology, and physical therapy, to develop guidance on diagnostic tools to aid in the work-up of pediatric patients with myopathy, with a specific focus on

differentiating between JDM and MD and the ultimate goal of shortening the time to diagnosis to improve patient outcomes.

Approach

Clinical history. The history is the first step in discerning between JDM and MD, and subtle differences in disease presentation can be important first clues to heighten suspicion for JDM compared with MD. Figure 1 provides an algorithm for diagnostic work-up based on our expert opinion while also drawing from recommendations of previously published guidelines and classification schemes.^{6,11–13} Table 1 highlights key differences between JDM and MD and provides additional context to accompany the Figure 1 algorithm. The expected time course for the development of weakness can provide the first branch point in making a diagnosis. In MD, the presentation is usually chronic with gradual disease progression; whereas, in JDM, the time course can be variable from chronic to more rapid in onset. JDM presentation can also be severe and fulminant, more often involving hospitalization when compared with MD.⁴ In JDM, there may also be a trigger noted before disease onset, especially infection or an environmental factor such as exposure to increased UV light.^{16,17} Although we do not expect definite disease triggers in MD, occasionally a worsening of disease can occur with illnesses, weight gain, linear growth, and some medications, particularly with anesthesia.¹⁸ In MD, the developmental delay of gross motor skills is expected. In some forms of MD, motor delay can start very early, even with decreased movement in utero. Dysphonia and dysphagia are rarer in MD and, if present, may occur later, whereas in JDM, they can be seen at presentation.

The associated extramuscular symptoms can be different in JDM compared with MD. Patients with JDM are more likely to report associated skin changes, although subtle rashes may go unnoticed. Some patients with JDM also have constitutional symptoms like fatigue, weight loss, or fever,⁹ which are uncommonly reported in MD or other noninflammatory myopathies.⁴ JDM, as a vasculopathy, may involve multiple other organ systems, which may manifest as symptoms of dyspnea, abdominal pain, and hematochezia. Additional symptoms of Raynaud phenomenon, sclerodactyly, arthritis, and mucositis can raise suspicion for overlap myositis. Some features of clinical history may also suggest other types of noninflammatory myopathy in children. Global developmental delay and abnormal facies, for example, would immediately raise suspicion for an underlying genetic syndrome and should lead to earlier genetic testing. Exercise intolerance and intermittent symptoms, including episodes of rhabdomyolysis, might point to a metabolic myopathy, which would necessitate a prompt, focused laboratory work-up.

In JDM, family history of autoimmune disease is variable, but it can be supportive of a diagnosis if present.⁴ Family history of

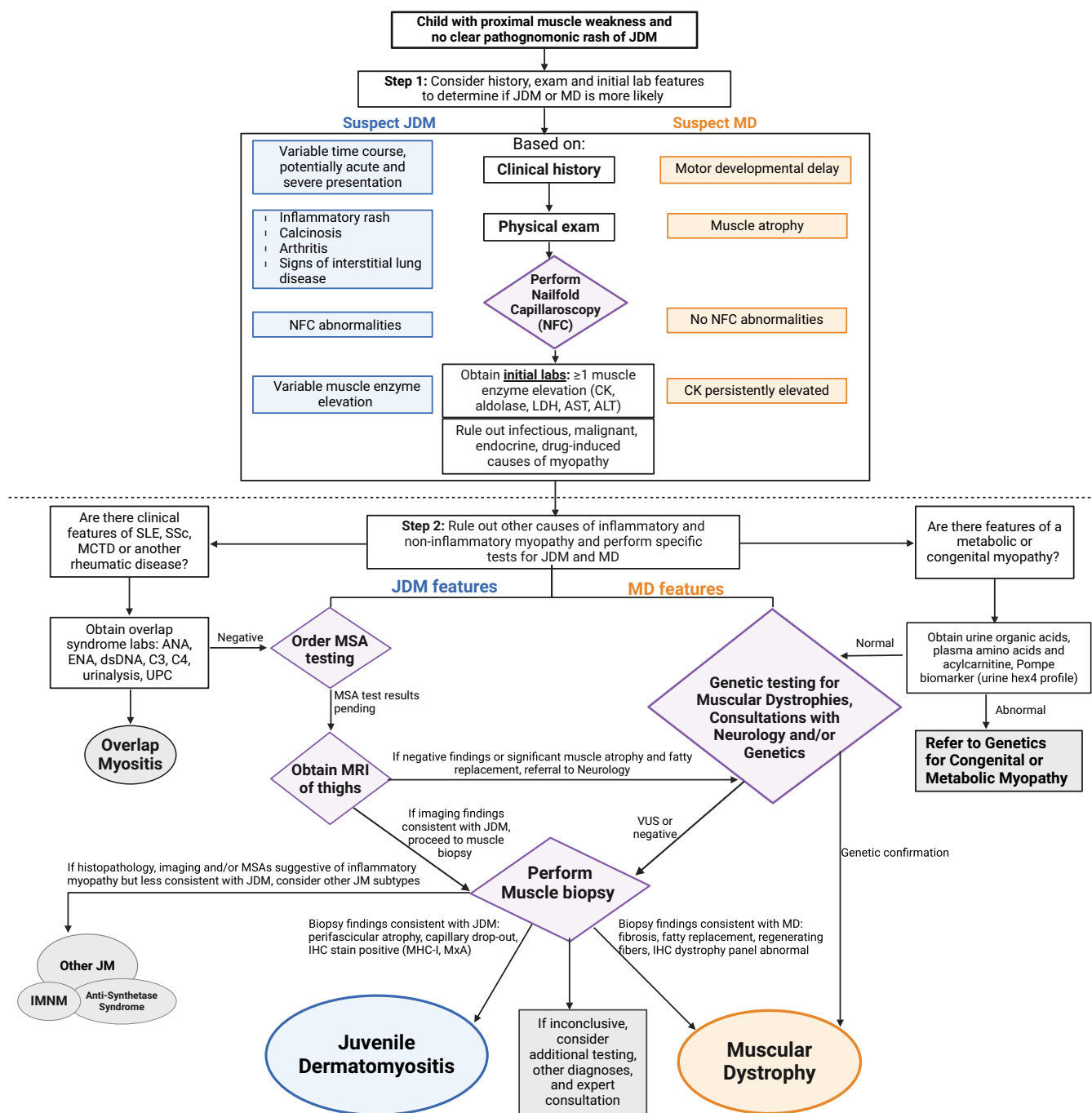


Figure 1. A proposed diagnostic algorithm of the approach to the medical examination of a child presenting with proximal muscle weakness and no clear pathognomonic rash of JDM with the goal of differentiating between JDM and MD and ruling out other diagnoses. Throughout the algorithm, purple diamonds indicate highlighted diagnostic tools which, in our expert opinion, may be especially helpful in differentiating diagnostic possibilities. In the first step, clinical history, physical examination, and initial laboratory features more consistent with JDM or MD are in the laterally placed colored boxes. ALT, alanine transaminase; ANA, antinuclear antibody; AST, aspartate transaminase; CK, creatine kinase; dsDNA, double-stranded DNA; ENA, extractable nuclear antigen; IHC, immunohistochemistry; IMNM, immune-mediated necrotizing myopathy; JDM, juvenile dermatomyositis; JM, juvenile myositis; LDH, lactate dehydrogenase; MCTD, mixed connective tissue disease; MD, muscular dystrophy; MHC-I, major histocompatibility complex class I; MRI, magnetic resonance imaging; MSA, myositis-specific autoantibody; MxA, myxovirus resistance A; NFC, nailfold capillaroscopy; SLE, systemic lupus erythematosus; SSc, systemic scleroderma; UPC, urine protein creatinine; VUS, variant of unknown significance.

MD is supportive, but de novo mutations do occur (for example, one-third of DMD is from de novo variants), so a lack of family history does not rule out MD.¹⁹

Physical and musculoskeletal examination. The physical examination is a critical part of clinical assessment in a child with reported muscle weakness to establish the

Table 1. Comparison of diagnostic features between JDM and MD*

Feature	JDM	MD
History	<ul style="list-style-type: none"> Variable time course in disease presentation May have trigger to disease onset, including association with infection or environmental exposure, such as UV light Symptom presentation may be more acute and severe, resulting in hospitalization Rash, even if subtle, and redness at nailbeds Constitutional symptoms (fatigue, weight loss, and fever) Other system involvement: dyspnea and GI (abdominal pain and hematochezia) Strong family history of rheumatic disease 	<ul style="list-style-type: none"> Motor developmental delay Chronic, gradual progression of disease course Family history of MD Possibly acute worsening with anesthesia Rarely decreased movement in utero
Examination	<ul style="list-style-type: none"> Weakness of proximal muscles, trunk/core, and neck Dysphonia and dysphagia Rash: heliotrope, Gottron papules or sign, calcinosis, subcutaneous edema, ulcerations, and other; may be subtle Abnormal nailfold capillaroscopy (dropout, hemorrhage, dilation, and abnormal morphology) Other: lung crackles as a sign of ILD and abdominal tenderness as a sign of GI involvement Sometimes range of motion deficit and concurrent arthritis 	<ul style="list-style-type: none"> Weakness of proximal muscles and particular distinguishing muscle groups: pectorals, periscapular, biceps, and facial muscles Muscle atrophy Dysphonia and dysphagia rare and later
Laboratory tests	<ul style="list-style-type: none"> MSAs MAAs Muscle enzymes elevated to variable degree (CK, aldolase, LDH, AST, and ALT) vWF Ag and neopterin elevated 	<ul style="list-style-type: none"> CK persistently elevated in most cases Genetic testing for MDs via neuromuscular panel or WES
Imaging	<ul style="list-style-type: none"> MRI with patchy or diffuse symmetric muscle edema in proximal musculature and subcutaneous edema 	<ul style="list-style-type: none"> MRI with muscle atrophy and fatty replacement of muscle
Histopathology	<ul style="list-style-type: none"> Perifascicular atrophy and/or perifascicular basophilic fibers Lymphocytic inflammation (perivascular/perimysial and/or endomysial) Immunohistochemical staining: MHC-I positivity, MxA positivity, C5b9 (perifascicular capillary positivity and dilation), CD31 (capillary drop out), CD3, and CD20 	<ul style="list-style-type: none"> Fibrosis Fatty replacement Regenerating muscle fibers (individual or group) Diffuse variation of myofiber size and fiber hypertrophy Abnormalities seen on dystrophy immunohistochemical panel for DMD, BMD, dystrophins, and others
Other testing	<ul style="list-style-type: none"> EMG notable for complex repetitive discharge Work-up for ILD: PFTs and chest CT scan Cardiac work-up: EKG and echocardiogram 	<ul style="list-style-type: none"> Work-up for cardiomyopathy: EKG and echocardiogram

* The distinguishing features are in bold. ALT, alanine transaminase; AST, aspartate transaminase; BMD, Becker muscular dystrophy; CK, creatine kinase; CT, computed tomography; DMD, Duchenne muscular dystrophy; EKG, electrocardiogram; EMG, electromyography; GI, gastrointestinal; ILD, interstitial lung disease; JDM, juvenile dermatomyositis; LDH, lactate dehydrogenase; MAA, myositis-associated autoantibody; MD, muscular dystrophy; MHC-I, major histocompatibility complex class I; MRI, magnetic resonance imaging; MSA, myositis-specific autoantibody; MxA, myxovirus resistance A; PFT, pulmonary function test; vWF Ag, von Willebrand factor antigen; WES, whole-exome sequencing.

(1) presence, severity, and pattern of weakness and (2) presence of other organ involvement and/or inflammation, such as in the skin or lungs, which might aid in the differential diagnosis. The initial musculoskeletal evaluation should include an assessment of strength, range of motion, joint mobility, gait, flexibility, balance, and functional mobility (ie, skipping, jumping, and squatting). In JDM, initial muscle weakness appears in the quadriceps, biceps, neck flexor, and abdominal muscles.²⁰ Joint range of motion can be limited secondary to both muscle and joint inflammation; this is more frequently observed in the elbows, wrists, fingers, knees, and ankles.²¹ Patients with JDM typically present with functional mobility deficits, including difficulty with tasks such as supine to sit, sit to stand, reaching overhead, lifting head from supine, and stair negotiation.²²

Standardized muscle assessments have been tested and validated in the evaluation of muscle disease for JDM and should

be performed whenever possible.^{23–25} We standardly perform Manual Muscle Testing (MMT-8) and the Childhood Myositis Assessment Scale (CMAS) at initial evaluation and then follow the scores over time to assess response to therapy and guide changes in treatment plan. The MMT-8 evaluates a set of eight muscles tested unilaterally or bilaterally in addition to axial (neck flexor) testing (the highest score is 80 [unilateral] or 150 [bilateral]). Our case report patient's MMT-8 score at diagnosis was 95 of 150. The CMAS is a 14-item observational, performance-based instrument with a maximum total score of 52 that was developed to evaluate muscle strength, physical function, and endurance and has been validated for those aged 4–18 years.²³

It is difficult to differentiate between JDM and MD with the musculoskeletal examination alone, because both diseases can present with a similar pattern of proximal muscle weakness (Table 1). In our experience, JDM can present with more

weakness in the upper body, primarily the neck and shoulder flexors, compared with DMD. Patients with DMD can present with interscapular weakness, leading to scapular winging, a unique finding.²⁶ Joint mobility is not typically impacted in the early stages of DMD, but muscle length restrictions of the gastrocnemius-soleus complex and tensor fasciae latae are often observed.²⁶ A typical gait pattern in DMD consists of increased lateral sway, toe walking, and increased lumbar lordosis.²⁶ Muscle atrophy is another feature seen on examination more commonly, but not exclusively, in patients with MD compared with JDM.⁴

Skin examination. In JDM, there are well-described dermatologic manifestations, but in practice, skin findings can be variable, ranging from pathognomonic to nonspecific, sometimes subtle findings.^{6–8} Skin findings may precede, accompany, or postdate muscle involvement.²⁷ Pathognomonic cutaneous findings include Gottron papules, also known as atrophic dermal papules of dermatomyositis, which appear as erythematous, scaly papules on the extensor surfaces of the metacarpophalangeal joints classically, although they can also appear on other joints and are specific to JDM. Rash can also present as Gottron sign, less discrete, erythematous, scaly plaques on the extensor surfaces of joints. Heliotrope rash is manifested by a violaceous periorbital erythema accompanied by edema and sometimes scale. Patients with JDM can have severe skin manifestations, including calcinosis and cutaneous vasculopathy.²⁸ Without characteristic skin findings, more diagnostic tests may be required to firmly establish a diagnosis.⁶ It is also important to note that some forms of JM, in particular IMNM, may lack skin manifestations and are at particular risk of being misdiagnosed as MD. There are no commonly reported skin findings in MD.

NFC. NFC is a noninvasive technique that allows for detailed examination of microcirculation changes that may occur with myositis or other autoimmune diseases. The gold standard for NFC assessment is video capillaroscopy^{29,30}; however, the use of more traditional instruments, such as the dermatoscope and ophthalmoscope, are still useful in capturing NFC abnormalities seen in JDM.

In NFC assessment, the EULAR study group on microcirculation in rheumatic diseases has developed recommendations for standardized NFC parameters to collect, and “normal” NFCs appear like “teeth-on-a-comb” and are characterized by regular density (more than eight end-row capillary loops per millimeter), a capillary diameter of <20 μ m measured from the apex, and normal morphology or lack of abnormal morphology, such as branched or ramified capillaries^{30,31} (Figure 2A). The most common abnormal nailfold findings in JDM include decreased density (“dropout,” less than eight end-row loops per millimeter), dilated capillaries (>20 μ m diameter), hemorrhage, and branched or “bushy” capillaries^{31,32} (Figure 2D–G). In a recent AI-based study,

a deep neural network model achieved a high accuracy of differentiating NFC images in JDM versus controls with a sensitivity of 0.85 and a specificity of 0.90, providing further evidence that NFC has the potential to aid in diagnosis.³³ In 2023, Melsens et al evaluated NFC findings across different pediatric rheumatic diseases and identified abnormal capillary morphology to be distinctive to JDM and mixed connective tissue disease, even compared with lupus and systemic sclerosis in children.³¹ Even within IIM, disorganization of capillaries, avascularity, and giant capillaries (>50 μ m diameter) have been demonstrated as characteristic of DM and overlap myositis but are typically absent in antisynthetase syndrome and IMNM.^{32,34}

The severity of NFC changes in JDM can also be a potential indicator of disease stage and activity. Fewer end-row loops have been shown to associate with a longer duration of untreated disease and higher disease activity scores for skin at diagnosis.^{35–37} 37 NFC density has also been associated with muscle disease activity, with higher modified disease activity scores and lower CMAS scores associating with decreased NFC density.³⁸ A study analyzing NFC changes in 140 treatment-naïve patients with JDM also identified decreased NFC density in anti-transcription intermediary factor 1 γ (TIF1 γ)-positive JDM and increased NFC hemorrhage in patients with dysphagia.³⁶

In our patient’s case, classic JDM NFC findings were seen at diagnosis and aided in diagnostic certainty, including NFC dropout, dilation, nonconvex tips, and overall disorganization (Figure 2B). After 4 months receiving immunosuppressive therapy, our patient demonstrated remarkable capillary regeneration, an absence of dilated or giant capillaries, and a “straightening out” of previously abnormal loops (Figure 2C). These findings are consistent with recent literature that immunosuppressive treatment seems to reduce NFC abnormalities.³²

In patients with clinical myopathy for whom there is diagnostic uncertainty or lack of pathognomonic JDM rash, the presence of NFC abnormalities can be one of the first more rapid indicators of an inflammatory myopathy. We recommend that NFC be performed at initial assessment in a child with proximal muscle weakness (Figure 1) to guide additional diagnostic work-up. There have not been studies to evaluate the utility of NFC in MD; although there is no suspicion of abnormal findings, this should be confirmed by rigorous testing.

Initial laboratory evaluation

Serum muscle enzymes are frequently elevated in JDM to a variable degree^{2,39,40} (Table 1 and Figure 1); however, different muscle enzymes may be elevated in individual patients, and normal muscle enzymes do not rule out a diagnosis of JDM or another JM subtype. Although patients with MD usually have a more persistent elevation in muscle enzymes, specifically CK, throughout the early disease course, the level of muscle enzyme elevation is generally not helpful in differentiating JDM from MD.⁴

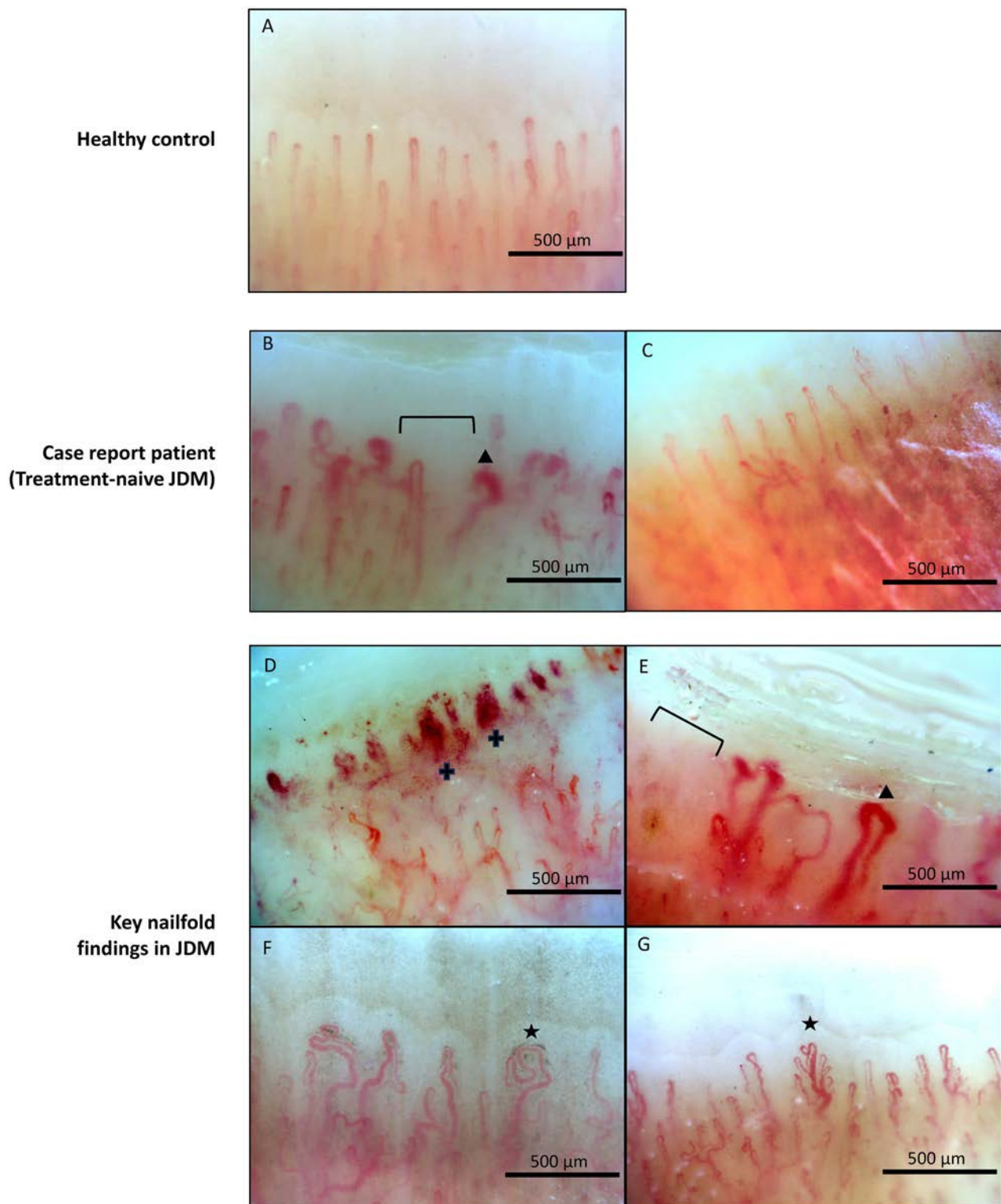


Figure 2. Nailfold video capillaroscopy findings from a (A) healthy control, (B) the case study patient with JDM at treatment-naive visit, and (C) 4 months after treatment initiation and (D–G) examples of key nailfold findings in JDM. (A) A healthy control patient; note the teeth-on-a-comb appearance, regular spacing and organization, no hemorrhage, no dropout (>8 end-row loops/mm), and lack of dilation ($<20\mu\text{m}$ diameter measured from the apex). (B) Case study patient with JDM at treatment-naive visit. Note the nailfold capillary drop out (bracket), dilation (triangle), and overall disorganization. (C) Case study patient with JDM 4 months after treatment initiation. The image shows the recovery of normal density, no dilation, and regular spacing. (D) Example of microhemorrhage (plus sign) and decreased density in treatment-naive patient with JDM. (E) Example of dilation (triangle) and dropout (bracket) in treatment-naive JDM. (F) Example of abnormal morphology (star) in JDM, defined by a nonconvex tip. (G) Example of abnormal morphology (star) with branched, “bushy” capillary in JDM. JDM, juvenile dermatomyositis.

We suggest a broad initial laboratory work-up to rule out other causes of myopathy and then a narrowing in on focused testing based on the most likely diagnosis, as highlighted in our proposed algorithm in Figure 1. Levels of neopterin and von Willebrand factor antigen are additional biomarkers that have been found to correlate with JDM disease activity; their levels in MD have not been established.^{41–43} For a patient with suspected metabolic myopathy, additional laboratory evaluation is critical to aid in the identification of metabolic causes, such as fatty acid oxidation disorders, mitochondrial disorders, and glycogen storage diseases, such as Pompe disease. Initial laboratory testing should also include an acylcarnitine profile to identify specific patterns indicative of impaired fatty acid oxidation. Urine organic acid analysis is invaluable for diagnosing mitochondrial disorders because it can detect characteristic organic aciduria resulting from impaired mitochondrial metabolism. Additionally, screening for Pompe disease biomarkers, specifically the enzyme acid alpha-glucosidase activity in blood and measurement of urine hexose tetrasaccharide levels are crucial.⁴⁴ These tests, when used

collectively, can provide a comprehensive overview of the metabolic pathways involved and guide the differential diagnosis toward specific metabolic myopathies.⁴⁵

MSAs. Approximately 40% to 70% of patients with JDM will test positive for an MSA.^{46–50} Testing for MSAs, autoantibodies against several intracellular proteins, is indicated in the initial work-up of JDM (Figure 1 and Table 1), because MSA subtyping can aid in clinical phenotyping and prognostication⁵¹ (Table 2). The gold standard for MSA detection is immunoprecipitation, although in recent years, several commercially available immunoassays have been developed and are performed by line blot or enzyme-linked immunosorbent assay.⁵² These tests may have low sensitivity for identifying key MSAs commonly seen in JDM, including TIF1 γ , and high rates of false positives.⁵³ The timing of sampling may impact MSA results, because certain MSA titers have been shown to decrease in response to treatment.⁵⁴ There are some additional potential issues associated with MSA testing, including a lack of uniformity of results from different laboratories

Table 2. MSAs and MAAs in children*

	Diagnosis	Features ^{48–51}	Frequency in pediatrics, ^{48,49} %
MSA			40–70
TIF1 γ (anti-p155/140)	JDM	Severe skin manifestations, photosensitivity, skin ulcerations, lipodystrophy, and chronic disease course. No increased risk of malignancy as seen in adults	18–36
NXP2 (anti-MJ)	JDM	Severe muscle involvement with dysphagia and dysphonia and increased risk of calcinosis	15–23
MDA5	JDM	ILD including rapidly progressive in Asia; mild muscle disease; arthritis and ulcerations	7–8 in US, 38–54 in Japan
Mi-2	JDM	High CK and severe histologic features on muscle biopsy yet benign clinical course; classic JDM rash; responds well to standard therapies	3–5
SAE	JDM	Amyopathic disease initially with later muscle involvement	1
Jo-1	Antisynthetase syndrome	Myositis, arthritis, Raynaud phenomenon, mechanic's hands, and ILD	<5
PL-12			
OJ			
EJ			
PL-7			
KS			
Zo	IMNM	Severe muscle disease with high CK and significant weakness; refractory to therapy; no skin manifestations; possible cardiac involvement	1
Ha			
SRP	IMNM	Severe muscle disease with high CK and significant weakness; often lacks skin manifestations; refractory to therapy	1
HMGCR	IMNM	Severe muscle disease with high CK and significant weakness; often lacks skin manifestations; refractory to therapy	1
MAA			16–20
PM/Scl	Overlap myositis	PM/Scl overlap; increased risk of ILD, arthritis, Raynaud phenomenon, and mechanic's hands	3–5
Ro52	Overlap myositis	Frequently associated with MSAs, especially antisynthetase antibodies; increased risk of ILD	6
U1RNP	Overlap myositis	Overlap myositis with SLE and scleroderma	5–15

* The associated disease, clinical features, and frequency of MSAs and MAAs in pediatric patients with myositis. CK, creatine kinase; EJ, glycyl-tRNA synthetase; Ha, tyrosyl-tRNA synthetase; HMGCR, 3-hydroxy-3-methylglutaryl CoA reductase; ILD, interstitial lung disease; IMNM, immune-mediated necrotizing myopathy; JDM, juvenile dermatomyositis; Jo-1, histidyl-tRNA synthetase; KS, asparaginyl-tRNA synthetase; MAA, myositis-associated autoantibody; MDA5, melanoma differentiation associated protein 5; MSA, myositis-specific autoantibody; NXP2, nuclear matrix protein 2; OJ, isoleucyl-tRNA synthetase; PL-12, alanyl-tRNA synthetase; PL-7, threonyl-tRNA synthetase; PM, polymyositis; SAE, small ubiquitin-like modifier activating enzyme; Scl, scleroderma; SLE, systemic lupus erythematosus; SRP, signal recognition particle; TIF1 γ , transcription intermediary factor 1 γ ; U1RNP, U1 ribonucleoprotein; Zo, phenylalanyl-tRNA synthetase.

and delays of weeks in receiving results during a critical time in which other testing and even treatment may need to be pursued. The absence of an MSA does not rule out JDM—approximately one-third of children with JDM will not test positive for an MSA,⁴⁷ but the presence of an MSA was one of the most important features in distinguishing JM from MD in a series of 48 cases.⁴

The most prevalent MSAs in children with JDM are TIF1 γ and NXP2, which differs from the MSA distribution reported in adults with dermatomyositis.⁵⁵ Table 2 describes the clinical phenotypes observed in JDM and other patients with JM with specific MSAs.^{46–49,54–56} A subset of patients with JM (16%–20%) can have myositis-associated autoantibodies (MAAs), including anti-Ro52, anti-U1RNP, and anti-PM/Scl. These patients may have clinical phenotypes of overlap symptoms with scleroderma and systemic lupus erythematosus or they may have predominant myositis.^{46,47} The presence of MAAs in patients with JM has been associated with an increased risk of refractory disease and death.⁵⁷

Genetic testing. The role of genetic testing for patients with suspected MD or metabolic myopathies has become increasingly common because of decreasing costs, improved availability, and simultaneous evaluation of numerous genetic conditions.^{58–60} Generally, when a child presents with neuromuscular symptoms and no other health concerns, starting with a panel focused on neuromuscular conditions is reasonable. Choosing from evaluable panels should be based on the number of genes and the inclusion of medically actionable disorders, such as Pompe disease and DMD. When a child has multiple health problems or features of MD accompanied by intellectual disability, however, then whole-exome sequencing becomes the preferred method of testing.^{61,62} The presence of intellectual disability or developmental regression in addition to myopathy concerns should prompt a referral to medical genetics for comprehensive evaluation.

Although genetic testing can confirm a genetic diagnosis, it may also identify variants of uncertain significance (VUS).⁶³ These VUSs can pose challenges, but it is important to consider the mode of inheritance. If a VUS is identified in a gene associated with an autosomal recessive condition, it likely indicates carrier status and is not diagnostic. When in doubt, it is advisable to discuss these results with a geneticist or genetic counselor. Because genetic testing is more widely available and comprehensive, it is typically the next step after clinical history and examination for suspected MD; but, if additional testing is needed, muscle biopsy and MRI scans can also assist with diagnosis.^{64–66}

Imaging

MRI scans are highly sensitive at identifying edema and fatty degeneration in myopathies. The pattern of muscle involvement on MRI may suggest a particular type of myopathy when the diagnosis remains uncertain and may narrow the differential

diagnosis^{67–69} (Figure 1 and Table 1). MRI can be helpful even in clinically apparent cases of JDM, such as those with characteristic rash, to define the extent of muscular inflammation and determine the presence of muscle damage. Patients with JDM with either skin-predominant disease or longer disease duration may have evidence of muscle inflammation on MRI scans despite normal muscle enzyme levels.^{70,71} Finally, MRI scans can guide the clinician in selecting a muscle with active inflammation for biopsy.^{72,73}

A standard MR protocol is to scan the pelvis and both thighs using axial T1-weighted images, axial T2-weighted images with fat saturation or mDixon technique and coronal STIR images. Postgadolinium-based intravenous contrast T1-weighted images and diffusion-weighted images will show abnormality in the same distribution as the T2-weighted and STIR images and thus are not usually additive and can be omitted. This allows for a relatively short imaging time and alleviates the need for sedation or general anesthesia in most patients.

Differential diagnosis in a case of suspected myopathy is narrowed based on the degree of muscle edema and pattern of muscle involvement: symmetry, portions of proximal muscle involvement, and involvement of distal and axial muscles (Figure 3). High signal intensity on T2-weighted imaging (Figure 3A) and STIR (Figure 3C) is indicative of edema consistent with active inflammation in JDM, as seen in our case report patient. Although muscle edema is seen in other clinical settings, including the early stages of MD, a high degree of muscle edema is suggestive of an inflammatory myopathy.⁶⁷ T1-weighted images (Figure 3E) demonstrate muscle atrophy and fatty infiltration, which predominates in MD but is also seen secondary to chronic inflammation and steroid use. In a patient with JDM, MRI scans show high-intensity edema in skeletal muscle especially along the fascia, which is diffuse, symmetric, and inclusive of proximal musculature. Subcutaneous inflammation and calcinosis may also be apparent.^{67,74}

Muscle biopsy and histopathology

In a child without a clear diagnosis of JDM or MD after thorough history, examination, laboratory tests, imaging, and possibly genetic testing, it is important to obtain a muscle biopsy (Figure 1). There has been a trend toward a reduced frequency of obtaining muscle biopsies, especially when pathognomonic rash is present; however, it can be a critical step to differentiate JDM from other types of childhood myopathies and may provide prognostic information.^{50,75,76} Considering continued advances in genetic testing for MD and other congenital myopathies, many practitioners will order genetic testing before or in lieu of muscle biopsy. However, one recent retrospective study highlighted that the diagnostic yield of genetic testing was higher when performed after muscle biopsy.⁷⁷ Also of note, the development of the recently approved genetic therapy for DMD was dependent on demonstrating the



Figure 3. (A–C) Magnetic resonance imaging scan of the case report patient: a boy aged 4 years with juvenile dermatomyositis. (A) Axial T2-weighted spectral attenuated inversion recovery image of the midthigh shows diffuse increased signal within muscles of the thigh consistent with edema/inflammation. There is relative sparing of the distal RF muscle. (B) Axial T1 image of the midthigh shows normal muscle signal without fatty infiltration. (C) Coronal STIR image also shows diffuse increased signal within muscles of the thigh consistent with edema/inflammation. (D–F) Magnetic resonance imaging scan of a boy aged 12 years with noninflammatory myopathy. (D) Axial T2-weighted modified Dixon image of the midthigh with fat signal nulled shows normal signal with no areas of high signal to suggest edema/inflammation. (E) Axial T1-weighted image of the midthigh shows feathery high signal in muscle consistent with fatty infiltration; the VM, SM, and long-head of the B muscles are most affected with relative sparing of the VL, ST, G, and S muscles. (F) Coronal STIR image also shows normal muscle signal. B, biceps; G, gracilis; RF, rectus femoris; S, sartorius; SM, semimembranosus; ST, semitendinosus; VL, vastus lateralis; VM, vastus medialis.

presence of the microdystrophin protein in muscle biopsy samples from treated patients.⁷⁸

Histopathologic differentiation of JDM vs MD

JDM hematoxylin and eosin. JDM histopathologic features on muscle biopsy include perivascular inflammation, perifascicular atrophy, muscle fiber degeneration/regeneration, endothelial cell swelling, narrowing and obliteration of the vessel lumens, inflammatory cells within vessel walls (microvasculitis), and capillary dropout⁷⁵ (Table 1). In patients with perifascicular atrophy, basophilia of the atrophic fibers is most common. Other less common findings include muscle infarction (well-demarcated regional muscle fiber necrosis), endomysial or perimysial fibrosis, sarcoplasmic vacuolation, and internal myonuclei.⁷⁵ In our case report patient, we noted perifascicular atrophy and perifascicular basophilic fibers (Figure 4A). Although routine histologic analysis has been reported to appear normal in up to 20% of patients,⁹ additional immunohistochemical and/or electron microscopic analysis may reveal abnormalities.⁷⁵ More recently, distinct pathologic patterns have been described in patients with JDM with

different MSAs.⁷⁹ Specifically, muscle biopsies from patients with high-titer anti-Mi-2 antibodies showed prominent perifascicular myofiber necrosis, whereas myofiber necrosis was limited in patients with anti-NXP2 antibodies. Patients with anti-MDA5 antibodies showed near-normal muscle histology.⁷⁹

JDM immunohistochemistry. It is important to complement standard hematoxylin and eosin staining with immunostaining for proteins commonly dysregulated in JDM. JDM muscle biopsies often demonstrate increased sarcolemmal expression of MHC-I in muscle fibers, capillary deposition of complement (C5b9 by immunohistochemistry or multiple complement components by direct immunofluorescence⁷⁶), sarcoplasmic MxA expression⁸⁰ (Figure 4C, E, and G), or sarcoplasmic CD56 expression.⁷⁵ Complement deposition can occur in capillaries or small intramuscular arteries,⁷⁶ and variation in pattern based on MSA has been described, such as prominent capillary C5b9 deposition with anti-NXP2 and anti-TIF1 γ autoantibodies and limited capillary C5b9 deposition with anti-Mi-2 and anti-MDA5 autoantibodies.^{79,81} Increased C5b9 muscle fiber sarcolemmal staining was reported in patients with anti-Mi-2 antibodies.⁸¹

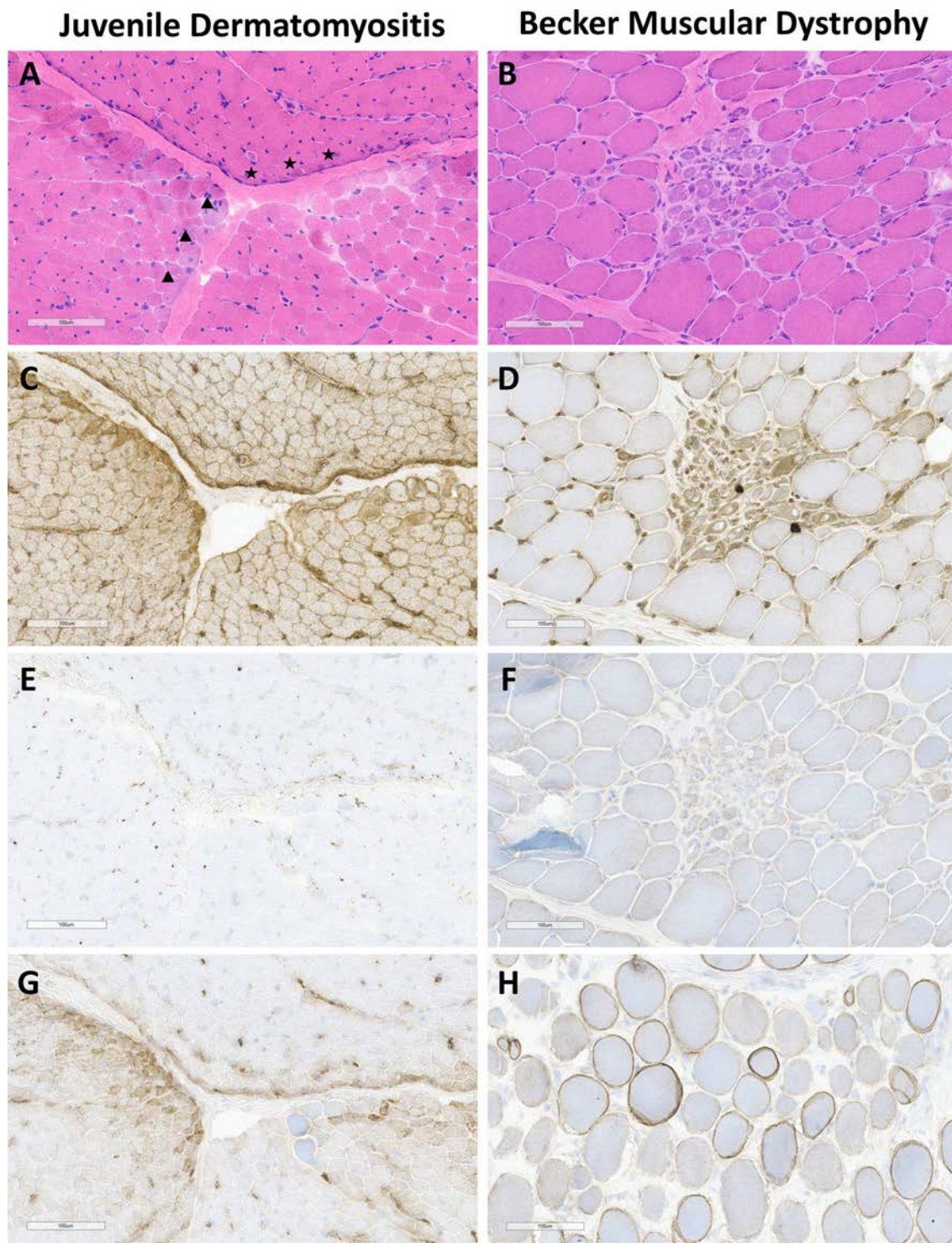


Figure 4. Muscle biopsy histopathology findings from the case of JDM described in the clinical scenario (A, C, E, and G) and a case of Becker MD in a 7-year-old boy confirmed with genetic testing (B, D, F, and H). (A) JDM hematoxylin and eosin: notable characteristics include perifascicular atrophy (subtle in this case), and perifascicular basophilic fibers. (B) MD hematoxylin and eosin: grouped atrophic, rounded, and basophilic fibers in the center of the image surrounded by abnormally large fibers. Patchy endomysial fibrosis is also present. (C) JDM Major Histocompatibility Complex class I: diffuse sarcolemmal staining with perifascicular accentuation. (D) MD Major Histocompatibility Complex class I: essentially negative for sarcolemmal staining and shows sarcoplasmic staining only in grouped atrophic fibers. (E) JDM C5b9: positive for capillary staining in areas of perifascicular atrophy and perifascicular basophilic fibers. (F) MD C5b9: negative for capillary staining. (G) JDM: positive for perifascicular sarcoplasmic myxovirus resistance A staining. (H) Dystrophin (C-terminal) staining in MD showing an abnormal mosaic pattern, which is the most common pattern seen in patients with Becker MD. Myxovirus resistance A staining not performed for the patient with MD; expected to be negative and similar in appearance to slide F. JDM, juvenile dermatomyositis; MD, muscular dystrophy.

Neonatal myosin can also be increased. Vascular markers (CD31 or CD34) can be used to evaluate for capillary dropout, which can also be seen in JDM muscle biopsies. Lymphocyte markers (CD3, CD4, CD8, and CD20) can be used to evaluate for and characterize perivascular lymphocytic inflammation. CD68 or CD163 stains can be used to evaluate for macrophage infiltration.⁷⁵ In histologically ambiguous cases, electron microscopic analysis can be performed to evaluate for tubuloreticular inclusions in endothelial cells, a highly specific finding for JDM in muscle biopsies.⁸²

MD histopathology. Muscle biopsy can distinguish MD from JDM by identifying “dystrophic changes,” which include marked fiber size variation, internal nuclei, necrotic fibers, associated inflammation, and endomysial fibrosis⁸³ (Figure 4B). Compared with JDM, the range of histologic findings that can be seen in MD and related disorders is extremely broad and varied,⁷⁷ and classical “dystrophic” findings may only be seen in a minor subset of muscle biopsies^{77,84} (Figure 4B). Other abnormal findings can include fiber type predominance, atrophy of specific fiber types, neurogenic changes, chronic myopathic changes, inflammatory changes, or evidence of mitochondrial or metabolic disease.⁷⁷ There may also be no pathologic abnormalities seen, or the findings may be mild and challenging to differentiate from within the range of normal. To evaluate for MD, a panel of immunohistochemistry stains specific to proteins encoded by genes disrupted in various MDs (limb-girdle MDs, DMD, BMD, sarcoglycanopathies, dystrophinopathies, dysferlinopathies, calpainopathies, collagen 6A-related myopathies, and merosin-negative congenital muscular atrophy) can be performed as a screening tool.⁸⁴ As an example of an abnormal and diagnostic staining pattern in a muscle biopsy, we demonstrate the presence of abnormal mosaic dystrophin staining in a case of BMD (Figure 4H). Certain MD subtypes can demonstrate significant inflammation, complicating the differentiation from JM. One study suggested that the pattern of inflammation may be different in inflammatory versus noninflammatory myopathy, with inflammatory myopathy most often demonstrating “inflammatory clusters” (groups of ≥ 20 inflammatory cells), rather than smaller groups and scattered inflammatory cells in dysferlinopathy, calpainopathy, or BMD.⁸⁵

Histopathologic features of other JM subtypes. As opposed to the classical finding of perifascicular atrophy in JDM muscle biopsies, perifascicular necrosis is the most common histopathologic feature in antisynthetase syndrome-associated myositis.^{86–88} Lymphocytic and histiocytic inflammation is common, often most prominently in perimysial areas.⁸⁸ A pattern of edematous, fragmented, and cellular perimysial tissue is commonly seen, often with increased perimysial alkaline phosphatase staining.⁸⁷ MHC-I staining is often diffusely positive (similarly to many other IIMs), with MHC-II staining more specifically highlighting a perifascicular pattern in antisynthetase syndrome.⁸⁷

The key features of muscle biopsies from patients with IMNM are variable amounts of scattered necrotic and/or regenerating muscle fibers and a concurrent limited amount of lymphocytic inflammation (“pauci-immune”).^{89–91} In fact, approximately 80% of muscle biopsies from patients with IMNM do not show significant lymphocytic infiltrates.⁸⁶ Other features of muscle biopsies from patients with IMNM may include (1) variable sarcolemmal MHC-I expression,^{89,92,93} (2) sarcolemmal complement deposition, and (3) endomysial fibrosis.⁹² Of note, this combination of features can overlap with muscle biopsy findings from patients with MD.⁹⁰ Most patients with IMNM will show a characteristic fine punctate sarcoplasmic p62 staining pattern in scattered fibers not reported in MD,^{94,95} although it is sometimes positive in other IIMs.⁹⁶

Other testing

Screening for other organ involvement is not only important for informing prognosis and treatment decisions, but it may also help differentiate JDM from noninflammatory myopathy (Table 1). One of the most serious extramuscular complications in several types of JM is ILD, which in JDM can develop chronically or be rapidly progressive. At JDM diagnosis, pulmonary function tests (PFTs) are recommended to screen for lung disease.¹³ PFTs may reveal a restrictive pattern with decreased total lung capacity or decreased diffusing capacity for carbon monoxide. A restrictive pattern on PFTs should be followed up with a high-resolution chest computed tomography scan to assess for imaging evidence of ILD. Subgroups most at risk for ILD include anti-MDA5 patients; those with overlap syndromes with particular MAAs, specifically anti-Ro52; and those in antisynthetase syndrome.⁵⁵ Baseline echocardiogram and electrocardiogram are also recommended for all patients with JDM at diagnosis. Acute symptomatic cardiac complications, such as congestive heart failure, arrhythmias, and pericardial disease, are rare, although patients have been shown to have increased rates of asymptomatic diastolic and systolic function of unclear significance with long-term follow-up.¹³ For any symptoms of dysphagia or dysphonia, swallow evaluation with speech and language pathology and video fluoroscopic swallow study should be performed.¹³ If any of these complications are present early, they might raise suspicion for JDM or another JM subtype.

Cardiac or pulmonary complications may occur in MD as the disease progresses and are usually the cause of death.^{97,98} Cardiac complications include potentially life-threatening arrhythmias and the development of hypertrophic or dilated cardiomyopathy.⁹⁸ Respiratory failure is secondary to progressive weakness of respiratory muscles, leading to hypoventilation as well as difficulties managing secretions. Patients with MD require regular monitoring of heart and lung function with echocardiogram, electrocardiogram, 24-hour Holter monitor, PFTs, and sleep study.

In our practice, electromyography or nerve conduction studies are generally performed primarily to rule out other diagnoses, for instance if there is a specific question of nerve or neuromuscular junction versus muscular origin of weakness. The needle studies are not very well tolerated, and the results can be very similar between JM and MD, although there may be an increase in complex repetitive discharge in JM as a distinguishing feature.⁴

Conclusions

A child presenting with proximal muscle weakness has a broad differential diagnosis, which requires a thoughtful, detailed work-up to arrive at a specific diagnosis. In our case report patient, diagnosis was delayed by 6 months because of an initial presumed diagnosis of MD. When genetic testing did not reveal a clear cause of myopathy, the diagnosis was reconsidered. To more quickly differentiate between JDM and MD, which can present very similarly, and improve time to diagnosis and treatment, we have presented a proposed diagnostic work-up algorithm to aid in clinical assessment and decision-making when a child presents with weakness and no definite rash of JDM (Figure 1). We highlight a few key decision points that can aid in more quickly arriving at a definitive diagnosis of JDM: (1) NFC, (2) MSA testing, and (3) muscle biopsy.

NFC is a fast, noninvasive imaging tool that can be paired with initial diagnostic examination to reveal clues as to whether a patient has an underlying systemic inflammatory process or vasculopathy. Next, if there is a high index of suspicion for JDM based on clinical features, MSA testing can be ordered with the initial laboratory tests. If positive, MSAs facilitate diagnostic clarity and assist in clinical phenotyping to further direct urgency of screening for other major organ involvement. Finally, obtaining a pretreatment muscle biopsy can provide invaluable insight into tissue-specific changes to differentiate an inflammatory from non-inflammatory myopathy and can also provide prognostic information. Moreover, muscle biopsies can be stored, with anticipated later application of novel technologies to guide personalized medical care, such as single-cell RNA-sequencing. In looking to the future in JDM diagnosis, we anticipate not only advances in the utility of NFC, MSA testing, and biopsy but also the development of novel biomarker signatures to guide care based on precision medicine.

ACKNOWLEDGMENTS

We thank the patients with JM and their families and the JM patient and family advisory committee at the University of Michigan for sharing their experiences, which inspired us to write this manuscript. We thank Dr. Rebecca Fuhlbrigge for assisting with development of the case report summary. We thank Dr. Nicholas McClellan for assisting with taking NFC images.

AUTHOR CONTRIBUTIONS

All authors contributed to at least one of the following manuscript preparation roles: conceptualization AND/OR methodology, software, investigation, formal analysis, data curation, visualization, and validation AND drafting or reviewing/editing the final draft. As corresponding author, Dr Turnier confirms that all authors have provided the final approval of the version to be published and takes responsibility for the affirmations regarding article submission (eg, not under consideration by another journal), the integrity of the data presented, and the statements regarding compliance with institutional review board/Declaration of Helsinki requirements.

REFERENCES

1. Namsrai T, Parkinson A, Chalmers A, et al. Diagnostic delay of myositis: an integrated systematic review. *Orphanet J Rare Dis* 2022; 17(1):420.
2. Mathiesen PR, Zak M, Herlin T, et al. Clinical features and outcome in a Danish cohort of juvenile dermatomyositis patients. *Clin Exp Rheumatol* 2010;28(5):782–789.
3. Thomas S, Conway KM, Fapo O, et al; Muscular Dystrophy Surveillance, Tracking, and Research Network (MD STARnet). Time to diagnosis of Duchenne muscular dystrophy remains unchanged: findings from the Muscular Dystrophy Surveillance, Tracking, and Research Network, 2000–2015. *Muscle Nerve* 2022;66(2):193–197.
4. Mamyrova G, Katz JD, Jones RV, et al; Childhood Myositis Heterogeneity Collaborative Study Group. Clinical and laboratory features distinguishing juvenile polymyositis and muscular dystrophy. *Arthritis Care Res (Hoboken)* 2013;65(12):1969–1975.
5. Pachman LM. Chapter 42: Juvenile dermatomyositis and other inflammatory myopathies in children. In: Darras BT, Royden Jones H Jr, Ryan MR, et al. *Neuromuscular Disorders of Infancy, Childhood, and Adolescence: A Clinician's Approach*. 2nd ed. Elsevier, Inc; 2014:834–881.
6. Lundberg IE, Tjälmlund A, Bottai M, et al; International Myositis Classification Criteria Project Consortium, the Euromyositis Register, and the Juvenile Dermatomyositis Cohort Biomarker Study and Repository (UK and Ireland). 2017 European League Against Rheumatism/American College of Rheumatology classification criteria for adult and juvenile idiopathic inflammatory myopathies and their major subgroups. *Arthritis Rheumatol* 2017;69(12):2271–2282.
7. Huber AM. Juvenile idiopathic inflammatory myopathies. *Pediatr Clin North Am* 2018;65(4):739–756.
8. Feldman BM, Rider LG, Reed AM, et al. Juvenile dermatomyositis and other idiopathic inflammatory myopathies of childhood. *Lancet* 2008; 371(9631):2201–2212.
9. Pachman LM, Hayford JR, Chung A, et al. Juvenile dermatomyositis at diagnosis: clinical characteristics of 79 children. *J Rheumatol* 1998;25(6):1198–1204.
10. Rider LG, Shah M, Mamyrova G, et al; Childhood Myositis Heterogeneity Collaborative Study Group. The myositis autoantibody phenotypes of the juvenile idiopathic inflammatory myopathies. *Medicine (Baltimore)* 2013;92(4):223–243.
11. Bohan A, Peter JB. Polymyositis and dermatomyositis (first of two parts). *N Engl J Med* 1975;292(7):344–347.
12. Brown VE, Pilkington CA, Feldman BM, et al; Network for Juvenile Dermatomyositis; Paediatric Rheumatology European Society (PReS). An international consensus survey of the diagnostic criteria for juvenile dermatomyositis (JDM). *Rheumatology (Oxford)* 2006; 45(8):990–993.
13. Bellutti Enders F, Bader-Meunier B, Baildam E, et al. Consensus-based recommendations for the management of juvenile dermatomyositis. *Ann Rheum Dis* 2017;76(2):329–340.

14. Mercuri E, Bönnemann CG, Muntoni F. Muscular dystrophies. *Lancet* 2019;394(10213):2025–2038.
15. Bönnemann CG, Wang CH, Quijano-Roy S, et al; Members of International Standard of Care Committee for Congenital Muscular Dystrophies. Diagnostic approach to the congenital muscular dystrophies. *Neuromuscul Disord* 2014;24(4):289–311.
16. Rider LG, Wu L, Mamyrova G, et al; Childhood Myositis Heterogeneity Collaborative Study Group. Environmental factors preceding illness onset differ in phenotypes of the juvenile idiopathic inflammatory myopathies. *Rheumatology (Oxford)* 2010;49(12):2381–2390.
17. Pachman LM, Lipton R, Ramsey-Goldman R, et al. History of infection before the onset of juvenile dermatomyositis: results from the National Institute of Arthritis and Musculoskeletal and Skin Diseases Research Registry. *Arthritis Rheum* 2005;53(2):166–172.
18. Bamaga AK, Riazi S, Amburgey K, et al. Neuromuscular conditions associated with malignant hyperthermia in paediatric patients: a 25-year retrospective study. *Neuromuscul Disord* 2016;26(3):201–206.
19. Grimm T, Kress W, Meng G, et al. Risk assessment and genetic counseling in families with Duchenne muscular dystrophy. *Acta Myol* 2012;31(3):179–183.
20. Quartier P, Gherardi RK. Juvenile dermatomyositis. *Handb Clin Neurol* 2013;113:1457–1463.
21. Tse S, Lubelsky S, Gordon M, et al. The arthritis of inflammatory childhood myositis syndromes. *J Rheumatol* 2001;28(1):192–197.
22. Wu JQ, Lu MP, Reed AM. Juvenile dermatomyositis: advances in clinical presentation, myositis-specific antibodies and treatment. *World J Pediatr* 2020;16(1):31–43.
23. Lovell DJ, Lindsley CB, Rennebohm RM, et al; The Juvenile Dermatomyositis Disease Activity Collaborative Study Group. Development of validated disease activity and damage indices for the juvenile idiopathic inflammatory myopathies. II. The Childhood Myositis Assessment Scale (CMAS): a quantitative tool for the evaluation of muscle function. *Arthritis Rheum* 1999;42(10):2213–2219.
24. Rider LG, Koziol D, Giannini EH, et al. Validation of manual muscle testing and a subset of eight muscles for adult and juvenile idiopathic inflammatory myopathies. *Arthritis Care Res (Hoboken)* 2010;62(4):465–472.
25. Huber AM, Feldman BM, Rennebohm RM, et al; Juvenile Dermatomyositis Disease Activity Collaborative Study Group. Validation and clinical significance of the Childhood Myositis Assessment Scale for assessment of muscle function in the juvenile idiopathic inflammatory myopathies. *Arthritis Rheum* 2004;50(5):1595–1603.
26. Case LE, Apkon SD, Eagle M, et al. Rehabilitation management of the patient with Duchenne muscular dystrophy. *Pediatrics* 2018;142(suppl 2):S17–S33.
27. Gerami P, Walling HW, Lewis J, et al. A systematic review of juvenile-onset clinically amyopathic dermatomyositis. *Br J Dermatol* 2007;157(4):637–644.
28. Robinson AB, Reed AM. Clinical features, pathogenesis and treatment of juvenile and adult dermatomyositis. *Nat Rev Rheumatol* 2011;7(11):664–675.
29. Karbalaie A, Emrani Z, Fatemi A, et al. Practical issues in assessing nailfold capillaroscopic images: a summary. *Clin Rheumatol* 2019;38(9):2343–2354.
30. Smith V, Herrick AL, Ingegnoli F, et al; EULAR Study Group on Microcirculation in Rheumatic Diseases and the Scleroderma Clinical Trials Consortium Group on Capillaroscopy. Standardisation of nailfold capillaroscopy for the assessment of patients with Raynaud's phenomenon and systemic sclerosis. *Autoimmun Rev* 2020;19(3):102458.
31. Melsens K, Cutolo M, Schonenberg-Meinema D, et al; EULAR Study Group on Microcirculation in Rheumatic Diseases. Standardized nailfold capillaroscopy in children with rheumatic diseases: a world-wide study. *Rheumatology (Oxford)* 2023;62(4):1605–1615.
32. Piette Y, Reynaert V, Vanhaecke A, et al. Standardised interpretation of capillaroscopy in autoimmune idiopathic inflammatory myopathies: a structured review on behalf of the EULAR Study Group on Microcirculation in Rheumatic Diseases. *Autoimmun Rev* 2022;21(6):103087.
33. Kassani PH, Ehwerhemuepha L, Martin-King C, et al. Artificial intelligence for nailfold capillaroscopy analyses - a proof of concept application in juvenile dermatomyositis. *Pediatr Res* 2024;95(4):981–987.
34. Soubrier C, Segulier J, Di Costanzo MP, et al. Nailfold videocapillaroscopy alterations in dermatomyositis, antisynthetase syndrome, overlap myositis, and immune-mediated necrotizing myopathy. *Clin Rheumatol* 2019;38(12):3451–3458.
35. Ostrowski RA, Sullivan CL, Seshadri R, et al. Association of normal nailfold end row loop numbers with a shorter duration of untreated disease in children with juvenile dermatomyositis. *Arthritis Rheum* 2010;62(5):1533–1538.
36. Pachman LM, Morgan G, Klein-Gitelman MS, et al. Nailfold capillary density in 140 untreated children with juvenile dermatomyositis: an indicator of disease activity. *Pediatr Rheumatol Online J* 2023;21(1):118.
37. Smith RL, Sundberg J, Shamiyah E, et al. Skin involvement in juvenile dermatomyositis is associated with loss of end row nailfold capillary loops. *J Rheumatol* 2004;31(8):1644–1649.
38. Schmeling H, Stephens S, Goia C, et al. Nailfold capillary density is importantly associated over time with muscle and skin disease activity in juvenile dermatomyositis. *Rheumatology (Oxford)* 2011;50(5):885–893.
39. Robinson AB, Hoeltzel MF, Wahezi DM, et al; Juvenile Myositis CARRA Subgroup, for the CARRA Registry Investigators. Clinical characteristics of children with juvenile dermatomyositis: the Childhood Arthritis and Rheumatology Research Alliance Registry. *Arthritis Care Res (Hoboken)* 2014;66(3):404–410.
40. Okong'o LO, Esser M, Wilmschurst J, et al. Characteristics and outcome of children with juvenile dermatomyositis in Cape Town: a cross-sectional study. *Pediatr Rheumatol Online J* 2016;14(1):60.
41. De Benedetti F, De Amici M, Aramini L, et al. Correlation of serum neopterin concentrations with disease activity in juvenile dermatomyositis. *Arch Dis Child* 1993;69(2):232–235.
42. Khojah A, Morgan G, Pachman LM. Clues to disease activity in juvenile dermatomyositis: neopterin and other biomarkers. *Diagnostics (Basel)* 2021;12(1):8.
43. Gibbs E, Khojah A, Morgan G, et al. The von Willebrand factor antigen reflects the juvenile dermatomyositis disease activity score. *Biomedicines* 2023;11(2):552.
44. Kishnani PS, Steiner RD, Bali D, et al. Pompe disease diagnosis and management guideline. *Genet Med* 2006;8(5):267–288.
45. van Adel BA, Tamopolsky MA. Metabolic myopathies: update 2009. *J Clin Neuromuscul Dis* 2009;10(3):97–121.
46. Pachman LM, Khojah AM. Advances in juvenile dermatomyositis: myositis specific antibodies aid in understanding disease heterogeneity. *J Pediatr* 2018;195:16–27.
47. Tansley SL. Antibodies in juvenile-onset myositis. *Curr Opin Rheumatol* 2016;28(6):645–650.
48. Rider LG, Shah M, Mamyrova G, et al; Childhood Myositis Heterogeneity Collaborative Study Group. The myositis autoantibody phenotypes of the juvenile idiopathic inflammatory myopathies. *Medicine (Baltimore)* 2013;92(4):223–243.
49. Betteridge Z, McHugh N. Myositis-specific autoantibodies: an important tool to support diagnosis of myositis. *J Intern Med* 2016;280(1):8–23.
50. Deakin CT, Yasin SA, Simou S, et al; UK Juvenile Dermatomyositis Research Group. Muscle biopsy findings in combination with

- myositis-specific autoantibodies aid prediction of outcomes in juvenile dermatomyositis. *Arthritis Rheumatol* 2016;68(11):2806–2816.
51. Damoiseaux J, Mammen AL, Piette Y, et al; ENMC 256th Workshop Study Group. 256th ENMC international workshop: myositis specific and associated autoantibodies (MSA-ab): Amsterdam, The Netherlands, 8–10 October 2021. *Neuromuscul Disord* 2022;32(7):594–608.
 52. Tansley SL, Snowball J, Pauling JD, et al; International Myositis Assessment and Clinical Studies (IMACS) Group Myositis Autoantibody Scientific Interest Group. The promise, perceptions, and pitfalls of immunoassays for autoantibody testing in myositis. *Arthritis Res Ther* 2020;22(1):117.
 53. Tansley SL, Li D, Betteridge ZE, et al. The reliability of immunoassays to detect autoantibodies in patients with myositis is dependent on autoantibody specificity. *Rheumatology (Oxford)* 2020;59(8):2109–2114.
 54. Tansley SL, Betteridge ZE, McHugh NJ. The diagnostic utility of autoantibodies in adult and juvenile myositis. *Curr Opin Rheumatol* 2013;25(6):772–777.
 55. Betteridge ZE, Gunawardena H, McHugh NJ. Novel autoantibodies and clinical phenotypes in adult and juvenile myositis. *Arthritis Res Ther* 2011;13(2):209.
 56. Tansley SL, Simou S, Shaddick G, et al. Autoantibodies in juvenile-onset myositis: their diagnostic value and associated clinical phenotype in a large UK cohort. *J Autoimmun* 2017;84:55–64.
 57. Sherman MA, Noroozi Farhadi P, Pak K, et al; Childhood Myositis Heterogeneity Collaborative Study Group. Myositis-associated autoantibodies in patients with juvenile myositis are associated with refractory disease and mortality. *Arthritis Rheumatol* 2024;76(6):963–972.
 58. Wright CF, Fitzgerald TW, Jones WD, et al; DDD study. Genetic diagnosis of developmental disorders in the DDD study: a scalable analysis of genome-wide research data. *Lancet* 2015;385(9975):1305–1314.
 59. Ballesta-Martínez MJ, Pérez-Fernández V, López-González V, et al. Validation of clinical exome sequencing in the diagnostic procedure of patients with intellectual disability in clinical practice. *Orphanet J Rare Dis* 2023;18(1):201.
 60. Retterer K, Juusola J, Cho MT, et al. Clinical application of whole-exome sequencing across clinical indications. *Genet Med* 2016;18(7):696–704.
 61. Moreno-De-Luca A, Millan F, Pesacrete DR, et al. Molecular diagnostic yield of exome sequencing in patients with cerebral palsy. *JAMA* 2021;325(5):467–475.
 62. Waldrop MA, Pastore M, Schrader R, et al. Diagnostic utility of whole exome sequencing in the neuromuscular clinic. *Neuropediatrics* 2019;50(2):96–102.
 63. Kalia SS, Adelman K, Bale SJ, et al. Recommendations for reporting of secondary findings in clinical exome and genome sequencing, 2016 update (ACMG SF v2.0): a policy statement of the American College of Medical Genetics and Genomics. *Genet Med* 2017;19(2):249–255.
 64. Kang PB, Morrison L, Iannaccone ST, et al; Guideline Development Subcommittee of the American Academy of Neurology and the Practice Issues Review Panel of the American Association of Neuromuscular & Electrodiagnostic Medicine. Evidence-based guideline summary: evaluation, diagnosis, and management of congenital muscular dystrophy: report of the Guideline Development Subcommittee of the American Academy of Neurology and the Practice Issues Review Panel of the American Association of Neuromuscular & Electrodiagnostic Medicine. *Neurology* 2015;84(13):1369–1378.
 65. Narayanaswami P, Weiss M, Selcen D, et al; Guideline Development Subcommittee of the American Academy of Neurology; Practice Issues Review Panel of the American Association of Neuromuscular & Electrodiagnostic Medicine. Evidence-based guideline summary: diagnosis and treatment of limb-girdle and distal dystrophies: report of the guideline development subcommittee of the American Academy of Neurology and the practice issues review panel of the American Association of Neuromuscular & Electrodiagnostic Medicine. *Neurology* 2014;83(16):1453–1463.
 66. Nicolau S, Milone M, Liewluck T. Guidelines for genetic testing of muscle and neuromuscular junction disorders. *Muscle Nerve* 2021;64(3):255–269.
 67. Caetano AP, Alves P. Advanced MRI patterns of muscle disease in inherited and acquired myopathies: what the radiologist should know. *Semin Musculoskelet Radiol* 2019;23(3):e82–e106.
 68. Carlier RY, Quijano-Roy S. Myoimaging in congenital myopathies. *Semin Pediatr Neurol* 2019;29:30–43.
 69. Aivazoglou LU, Guimarães JB, Link TM, et al. MR imaging of inherited myopathies: a review and proposal of imaging algorithms. *Eur Radiol* 2021;31(11):8498–8512.
 70. Abdul-Aziz R, Yu CY, Adler B, et al. Muscle MRI at the time of questionable disease flares in juvenile dermatomyositis (JDM). *Pediatr Rheumatol Online J* 2017;15(1):25.
 71. Oberle EJ, Bayer ML, Chiu YE, et al. How often are pediatric patients with clinically amyopathic dermatomyositis truly amyopathic? *Pediatr Dermatol* 2017;34(1):50–57.
 72. Degardin A, Morillon D, Lacour A, et al. Morphologic imaging in muscular dystrophies and inflammatory myopathies. *Skeletal Radiol* 2010;39(12):1219–1227.
 73. Peters SA, Köhler C, Schara U, et al. Muscular magnetic resonance imaging for evaluation of myopathies in children. Article in German. *Klin Padiatr* 2008;220(1):37–46.
 74. Venturelli N, Tordjman M, Ammar A, et al. Contribution of muscle MRI for diagnosis of myopathy. *Rev Neurol (Paris)* 2023;179(1-2):61–80.
 75. Wedderburn LR, Varsani H, Li CK, et al; UK Juvenile Dermatomyositis Research Group. International consensus on a proposed score system for muscle biopsy evaluation in patients with juvenile dermatomyositis: a tool for potential use in clinical trials. *Arthritis Rheum* 2007;57(7):1192–1201.
 76. Wargula JC, Lovell DJ, Passo MH, et al. What more can we learn from muscle histopathology in children with dermatomyositis/polymyositis? *Clin Exp Rheumatol* 2006;24(3):333–343.
 77. Yang K, Iannaccone S, Burkhalter LS, et al. Role of nerve and muscle biopsies in pediatric patients in the era of genetic testing. *J Surg Res* 2019;243:27–32.
 78. Hoy SM. Delandistrogene moxeparvec: first approval. *Drugs* 2023;83(14):1323–1329.
 79. Nguyen M, Do V, Yell PC, et al. Distinct tissue injury patterns in juvenile dermatomyositis auto-antibody subgroups. *Acta Neuropathol Commun* 2020;8(1):125.
 80. Uruha A, Nishikawa A, Tsuburaya RS, et al. Sarcoplasmic Mx1 expression: a valuable marker of dermatomyositis. *Neurology* 2017;88(5):493–500.
 81. Yasin SA, Schutz PW, Deakin CT, et al; UK Juvenile Dermatomyositis Research Group (UK and Ireland). Histological heterogeneity in a large clinical cohort of juvenile idiopathic inflammatory myopathy: analysis by myositis autoantibody and pathological features. *Neuropathol Appl Neurobiol* 2019;45(5):495–512.
 82. Oshima Y, Becker LE, Armstrong DL. An electron microscopic study of childhood dermatomyositis. *Acta Neuropathol* 1979;47(3):189–196.
 83. Sethuraman C. Muscle biopsies in children - a broad overview and recent updates: where does the future lie? *Diagn Histopathol (Oxf)* 2023;29(12):511–520.
 84. Tsao CY. Muscle disease. *Pediatr Rev* 2014;35(2):49–61.
 85. Becker N, Moore SA, Jones KA. The inflammatory pathology of dysferlinopathy is distinct from calpainopathy, Becker muscular

- dystrophy, and inflammatory myopathies. *Acta Neuropathol Commun* 2022;10(1):17.
86. Allenbach Y, Benveniste O, Goebel HH, et al. Integrated classification of inflammatory myopathies. *Neuropathol Appl Neurobiol* 2017;43(1):62–81.
 87. Tanboon J, Inoue M, Hirakawa S, et al. Muscle pathology of anti-synthetase syndrome according to antibody subtypes. *Brain Pathol* 2023;33(4):e13155.
 88. Mescam-Mancini L, Allenbach Y, Hervier B, et al. Anti-Jo-1 antibody-positive patients show a characteristic necrotizing perifascicular myositis. *Brain* 2015;138(Pt 9):2485–2492.
 89. Day JA, Limaye V. Immune-mediated necrotizing myopathy: a critical review of current concepts. *Semin Arthritis Rheum* 2019;49(3):420–429.
 90. Wang CH, Liang WC. Pediatric immune-mediated necrotizing myopathy. *Front Neurol* 2023;14:1123380.
 91. Allenbach Y, Benveniste O, Stenzel W, et al. Immune-mediated necrotizing myopathy: clinical features and pathogenesis. *Nat Rev Rheumatol* 2020;16(12):689–701.
 92. Allenbach Y, Mammen AL, Benveniste O, et al; Immune-Mediated Necrotizing Myopathies Working Group; Immune-Mediated Necrotizing Myopathies Working Group. 224th ENMC International Workshop: clinico-sero-pathological classification of immune-mediated necrotizing myopathies Zandvoort, The Netherlands, 14–16 October 2016. *Neuromuscul Disord* 2018;28(1):87–99.
 93. Alshehri A, Choksi R, Bucelli R, et al. Myopathy with anti-HMGCR antibodies: perimysium and myofiber pathology. *Neurol Neuroimmunol Neuroinflamm* 2015;2(4):e124.
 94. Fischer N, Preuß C, Radke J, et al. Sequestosome-1 (p62) expression reveals chaperone-assisted selective autophagy in immune-mediated necrotizing myopathies. *Brain Pathol* 2020;30(2):261–271.
 95. Girolamo F, Lia A, Annese T, et al. Autophagy markers LC3 and p62 accumulate in immune-mediated necrotizing myopathy. *Muscle Nerve* 2019;60(3):315–327.
 96. Milisenda JC, Pinal-Fernandez I, Lloyd TE, et al. Accumulation of autophagosome cargo protein p62 is common in idiopathic inflammatory myopathies. *Clin Exp Rheumatol* 2021;39(2):351–356.
 97. Wahlgren L, Kroksmark AK, Tulinius M, et al. One in five patients with Duchenne muscular dystrophy dies from other causes than cardiac or respiratory failure. *Eur J Epidemiol* 2022;37(2):147–156.
 98. Nigro G, Comi LI, Politano L, et al. The incidence and evolution of cardiomyopathy in Duchenne muscular dystrophy. *Int J Cardiol* 1990;26(3):271–277.

NOTES FROM THE FIELD

Do We Need Distinct Pediatric Classification Criteria for Rheumatic Diseases That Affect Both Children and Adults?

Coziana Ciurtin,¹  Marija Jelusic,² and Seza Ozen³ 

Introduction

Rheumatic diseases (RMDs) represent a diverse group of conditions that can affect individuals of any age. Although pediatric and adult rheumatologists develop specialized expertise in the recognition, diagnosis, and management of these diseases, individuals diagnosed with RMDs at distinct stages in their life face age and developmentally distinct challenges, which necessitate a comprehensive approach to health care. This approach must encompass coordinated and integrated care, including effective transition protocols for adolescents, as well as access to high-quality research at every stage in life. Developmental factors play a key role in shaping the immune system, resulting in age-related differences in disease risk, outcomes, and treatment responses, emphasizing the necessity for age-tailored approaches in both research and clinical care. This is particularly crucial because genetic predispositions, environmental influences, and socioeconomic conditions can heavily impact RMD presentation and outcomes.

The need for improved evidence-based health care in rheumatology requires high-quality, multicenter studies with suitable geographic and ethnic representation across the lifespan. Accurate classification criteria help identify homogeneous disease populations, which is vital for advancing the understanding of the disease pathogenesis and for the development and testing of tailored therapeutic strategies. Moreover, adequate classification criteria can enhance the identification of disease subtypes with different outcomes and treatment responses, paving the way for more individualized management approaches.

Although there are similarities in the presentation and management of RMDs between distinct age groups such as children and adults or younger and older adults, significant differences in pathogenesis, clinical phenotype, disease progression, and outcomes often necessitate age-specific classification criteria. However, this distinction has only been made for children rather than adults with certain RMDs, using an arbitrary age cut-

off of 16 or 18 years. Two main strategies have been employed in the classification of pediatric RMDs: one involves adapting adult classification criteria for use in pediatric populations with similar disease phenotypes, whereas the other focuses on developing and validating criteria specifically tailored to children.

A harmonized classification across the lifespan has practical implications. Clinicians recognize that epidemiologic differences between RMDs affecting children and adults should not significantly impact the performance of shared classification criteria across the lifespan. However, epidemiologic differences could be underpinned by unique genetic traits and immune characteristics of children compared to adults, reflected in distinct disease susceptibility as well as more severe trajectories for RMDs that emerge in childhood, aspects that may not be optimally addressed by a harmonized classification and research approach across the lifespan.

Conversely, there are phenotypical similarities between children and adults that span arbitrary age boundaries, which should support the use of similar classification criteria, as well as differences in clinical phenotype and pathogenesis between younger and older individuals affected by the same disease, which may not be reflected in the existent adult classification criteria. These age-related variations can be attributed to factors beyond genetics or immune system maturation and aging, including alterations in the microbiome and environmental exposures that contribute to age-dependent RMD patterns, all relevant for the selection of homogeneous disease populations for research purposes.

Because various approaches to classify RMDs in pediatric and adult rheumatology exist, we aim to evaluate their relevance and limitations and propose, wherever possible, to promote classification criteria that reflect shared clinical presentation and pathogenic mechanisms across age-corresponding RMD phenotypes while also accounting for developmental and immunologic factors that may influence disease trajectories, when relevant.

¹Coziana Ciurtin, MD, FRCP, PhD: Centre for Adolescent Rheumatology, University College London, London, United Kingdom; ²Marija Jelusic, MD, MSc, PhD: University Hospital Center Zagreb, University of Zagreb School of Medicine, Zagreb, Croatia; ³Seza Ozen, MD, PhD: Hacettepe University Faculty of Medicine, Ankara, Türkiye.

Author disclosures are available at <https://onlinelibrary.wiley.com/doi/10.1002/art.43058>.

Address correspondence via email to Coziana Ciurtin, MD, FRCP, at c.ciurtin@ucl.ac.uk.

Submitted for publication August 23, 2024; accepted in revised form November 6, 2024.

Classification of chronic inflammatory arthritis across the lifespan

Using the same classification criteria for children and adults with RMDs could harmonize research across age groups and facilitate the inclusion of both pediatric and adult populations in clinical trials. This approach could potentially expedite the approval and availability of new therapeutic options. However, standardizing the classification of RMDs is highly dependent on the particularities of the diagnostic label used in children compared with adults, which may reflect more or less heterogeneous disease phenotypes. For example, rheumatoid arthritis (RA) reflects a relatively homogeneous inflammatory arthritis phenotype in adults, whereas juvenile idiopathic arthritis (JIA) is an umbrella diagnosis in children, encompassing several subtypes of childhood arthritis characterized by heterogeneous pathogenesis and clinical presentation.

The International League of Associations for Rheumatology (ILAR) criteria,¹ commonly used for classifying JIA, have several limitations. These include arbitrary age and joint count cut-offs as well as mutually exclusive features that can complicate the classification for individuals who exhibit overlapping signs and symptoms. Moreover, the ILAR classification criteria do not address the genetic or molecular similarities among different JIA subtypes,² which can impact the adequate treatment selection and accurate risk-stratification of individuals with JIA. The ILAR subgroup of nonsystemic JIA that shares clear genetic and pathogenic mechanisms with their adult corresponding phenotype is the seropositive poly-JIA group, which often affects adolescent girls and resembles seropositive RA. The pathogenesis of early onset forms of chronic arthritis observed in young patients is less well-defined.

The Paediatric Rheumatology International Trials Organisation (PRINTO) proposed a novel classification system for JIA, categorizing the condition into four distinct subtypes.³ This classification introduces the age cut-off of 18 years, in alignment with the World Health Organization definition of childhood age-span, as well as an additional category for early-onset JIA with positive antinuclear antibodies, which the ILAR criteria¹ do not cover. The PRINTO criteria³ also suggest renaming enthesitis-related arthritis as enthesitis- or spondylitis-related JIA, recognizing its pathogenic similarities with ankylosing spondylitis. However, the exclusion of juvenile psoriatic arthritis (JPsA) from the PRINTO criteria poses challenges, especially because there are therapies specifically licensed for JPsA.⁴

A study exploring the overlap between the ILAR and PRINTO criteria in a large UK cohort found that nearly 70% of young people with JIA could not be classified into any of the named PRINTO categories.⁵ This significant discrepancy highlights the limitations of current JIA classification systems and underscores the need for further refinement and validation across diverse populations. Although anti-citrullinated peptide antibodies are important for

diagnosing and predicting outcomes in RA, and despite its genetic and phenotypic similarities to seropositive polyarticular JIA, these antibodies are not included in either the ILAR or PRINTO JIA classification criteria.

The recent decision by the Paediatric Rheumatology European Society (PReS) and the EULAR to recognize systemic JIA and adult-onset Still disease as manifestations of the same condition, now termed Still disease, is a noteworthy development.⁶ This consensus is based on shared pathogenic mechanisms, clinical presentations, and treatment strategies, underscoring the importance of a unified approach to disease classification.

Classification of systemic connective tissue diseases, vasculitides, and autoinflammatory conditions across the lifespan

These RMDs share the same pathogenesis and have rather consistent features throughout the lifespan. Systemic lupus erythematosus (SLE), with the exception of monogenic lupus, is characterized by the same type of organ and systems involvement in children and adults, with recognized differences in the prevalence of certain manifestations: a higher proportion of individuals with childhood-onset SLE (cSLE) experience systemic manifestations, lupus nephritis, and central nervous system involvement compared to adults with SLE according to various cohort studies. These differences may reflect the increased genetic burden in children as well as challenges in accessing adult SLE treatment worldwide and poorer compliance to medication in adolescence as potential factors.

Distinct classification criteria for cSLE have not been deemed necessary. Differences in presentation and severity of cSLE were adequately captured at the disease onset by the adult criteria because they are not underpinned by differences in pathogenesis between cSLE and adult-onset SLE. The American College of Rheumatology (ACR)⁷ and the Systemic Lupus International Collaborating Clinics criteria,⁸ commonly used to support SLE diagnosis, have been validated in both adult and pediatric populations, with recent updates improving their applicability across age groups.⁹ The ACR and EULAR proposed novel classification criteria in 2019, subsequently validated in adult SLE populations, were found to have satisfactory performance in cSLE as well.¹⁰

Childhood inflammatory myositis, scleroderma and Sjögren disease may be regarded within the spectrum of adult disease because of similarities in pathogenesis between children and adults. The new harmonized classification criteria for inflammatory myopathies proposed by EULAR and ACR were derived and validated in both adult and juvenile cohorts.¹¹ However, these criteria have limitations, particularly related to the exclusion of

features like calcinosis and certain myositis-specific autoantibodies, which are more prevalent in children.

The provisional classification criteria for juvenile systemic sclerosis, proposed by PReS, ACR, and EULAR, overlap with the revised adult criteria, but also include additional features relevant to children.¹² The proposal to develop distinct criteria for juvenile systemic sclerosis that incorporate specific features such as digital ulcers and periungual capillary abnormalities is driven by the aim to improve their relevance for research, diagnostic, and management of systemic sclerosis in children.¹²

Childhood-onset Sjögren disease is particularly challenging because it is rare and lacks validated classification criteria. Although diagnostic algorithms and scoring systems have been proposed to support diagnosis and classification, these are not yet widely adopted.¹³ The 2016 EULAR/ACR criteria for adult Sjögren disease¹⁴ do not classify many pediatric cases, often because children exhibit less dryness, the cardinal clinical feature in adults.¹⁵

Vasculitides present additional classification challenges because of the restriction of certain types of vasculitides to certain age groups. These diseases vary significantly in prevalence and presentation between children and adults and need to be approached in a distinct manner. For instance, giant cell arteritis does not occur in children, whereas Kawasaki disease is virtually exclusively encountered in pediatric populations; therefore, exploring classification criteria across the life course is less relevant for these two conditions. For other types of vasculitides affecting individuals of all ages, the main differences are in relation to the prevalence of various manifestations rather than disease pathogenesis. The EULAR/PRINTO/PReS-endorsed Ankara 2008 criteria for childhood vasculitides, validated and widely used, provide a basis for accurate classification.¹⁶ Distinct pediatric classification criteria were proposed for IgA vasculitis (Henoch–Schoenlein purpura), granulomatosis with polyangiitis (GPA), Takayasu Arteritis, and polyarteritis nodosa. However, recent ACR/EULAR adult classification criteria developed from the Diagnosis and Classification of Vasculitis Study (DCVAS) registry

Table 1. Challenges in optimizing the classification of RMDs across the lifespan and future research needs*

Challenges for optimizing classification criteria across the life course	Examples of RMDs for which these challenges are relevant	Future research needs
Lack of correspondence between the diagnostic labels used in children and adults with inflammatory arthritis with similar pathogenesis and clinical presentation	JIA vs adult inflammatory arthritides	Expert consensus studies to review the available literature data to propose and refine the nomenclature used for distinct subcategories of inflammatory arthritis to reflect similarities across pediatric and adult phenotypes
Scarcity of high-quality studies with geographic representation across the lifespan to define homogeneous RMD clinical phenotypes in children and adults	Lack of studies in JIA in adulthood to enable phenotype correlations with adult inflammatory arthritides; lack of initiatives or studies in SLE, inflammatory myositis, scleroderma, antiphospholipid syndrome, and rare types of vasculitides across the lifespan; recent progress has been achieved in harmonizing the longitudinal data collection across geographically diverse cohorts in some conditions (SLE, myositis, autoinflammatory diseases) but not across the life course	More collaborative, high-quality, prospective clinical studies with long-term follow-up, involving pediatric and adult rheumatologists, and patient populations across the lifespan to define shared clinical phenotypes as well as epidemiologic differences at disease presentation to support future development or refinement of classification criteria; initiation of harmonized national registries linked together across various geographic areas, capturing data and samples from individuals with RMDs across the lifespan
Scarcity of high-quality studies focused on defining the pathogenesis of RMDs affecting both children and adults	There are almost no studies exploring in parallel the pathogenesis of similar RMDs in children vs adults	High-quality studies across the lifespan including genetic, molecular, or tissue diagnosis to define commonalities and differences in the disease pathogenesis in children vs adults, and their clinical correlates; linked-in pediatric and adult RMD-specific registries
Use of existent classification criteria across the lifespan without being validated in both children and adults	Particularly relevant for rare RMDs, such as antiphospholipid syndrome, some vasculitides, IgG4-RD, etc, but also for inflammatory arthritides, which are classified completely differently in children vs adults	High-quality studies to cross-validate the existent classification criteria in both children and adult cohorts, to evaluate whether there is any need to revise the available criteria
Timely incorporation of advances in medical technologies and discoveries in classification criteria for RMDs across the lifespan	Inclusion of imaging as classification item for Sjögren disease (salivary gland ultrasound) or myositis (magnetic resonance imaging for assessment of muscle inflammation)	Periodic refinement and testing of existent classification criteria to reflect advances in diagnostic tests or incorporate new emerging phenotypes

* IgG4-RD, IgG4-related disease; JIA, juvenile idiopathic arthritis; SLE, systemic lupus erythematosus; RMDs, rheumatic diseases.

highlight the ongoing evolution of classification systems for adult vasculitides.¹⁷ Interestingly, both the Ankara 2008 and the DCVAS-derived ACR/EULAR adult criteria had a similar performance in children with GPA,¹⁸ suggesting potential for harmonization across the lifespan.

Autoinflammatory diseases primarily manifest in childhood and are characterized by recurrent systemic inflammation due to innate immune system dysfunction. The Eurofever initiative has been instrumental in gathering data on autoinflammatory diseases in children, leading to the proposal of shared classification criteria endorsed by both pediatric and adult experts. This collaborative approach underscores the potential for unified criteria that can be applied across age groups, as well as the expansion of large-scale research initiatives, including clinical trials, facilitating improved disease recognition across the life span, high-quality research, and progress toward tailored therapies.¹⁹

One size does not fit all: the value of expertise sharing and future research needs

Classification criteria should be derived through methodologically sound studies applied to age, sex and gender, and ethnically diverse cohorts with certain RMDs as well as corresponding disease mimickers. Although shared classification criteria across children and adults with similar RMDs would be advantageous in terms of harmonizing research across the lifespan and would support transition of care and access to treatments, the impact of age at onset on RMD manifestations, reflecting both the genetic burden and exposome influences on disease pathogenesis, as well as differences in clinical presentation early compared to later in life, likely determine their performance and clinical usage.

In addition to harmonizing research in RMDs, shared classification criteria could support innovative management strategies, if the disease is similar in children when compared with both younger and older adults. The British Society of Rheumatology endorses evidence and consensus-based recommendations for management of various RMDs, coproduced by pediatric and adult rheumatologists allowing an across the life course perspective. For conditions with similar pathogenesis, proposing new childhood-specific classification criteria may not be entirely appropriate, but this has to be balanced against differences in clinical presentation between children and adults with impact on identifying homogeneous disease groups.

Even if a need for better classification criteria is identified, these criteria can only be derived from optimally designed prospective longitudinal cohorts with control groups, including key disease mimickers, robust methodologic approaches, and adequate RMD population representation. This will require collaborative work across pediatric, transition, and adult care specialists, and critical input from patient-experts of all ages. We identified several challenges for optimizing classification criteria for RMDs

across the lifespan and proposed future research strategies, which we included in Table 1.

Conclusions

Classification criteria will require periodic review to incorporate advances in medical technologies and discoveries, as well as changes in research priorities to facilitate early disease classification and timely management interventions, for the overall aim to improve disease outcome and preserve quality of life at any age. We advocate for good performance classification criteria, reflecting shared pathogenic mechanism across age-distinct RMD phenotypes, which should be feasible and easy to implement. This will facilitate adequate dissemination of knowledge related to various disease processes, as well as innovation in RMD management, ultimately aiming to support wider and fairer access to research for diverse populations of all ages.

AUTHOR CONTRIBUTIONS


All authors were involved in drafting the article or revising it critically for important intellectual content, and all authors approved the final version to be published.

REFERENCES

- Petty RE, Southwood TR, Manners P, et al. International League of Associations for Rheumatology classification of juvenile idiopathic arthritis: second revision, Edmonton, 2001. *J. Rheumatol* 2004;31:390–392.
- Nigrovic PA, Colbert RA, Holers VM, et al. Biological classification of childhood arthritis: roadmap to a molecular nomenclature. *Nat Rev Rheumatol* 2021;17(5):257–269.
- Martini A, Ravelli A, Avcin T, et al; Pediatric Rheumatology International Trials Organization (PRINTO). Toward new classification criteria for juvenile idiopathic arthritis: first steps, Pediatric Rheumatology International Trials Organization international consensus. *J Rheumatol* 2019;46(2):190–197.
- Lokhandwala S, Townsend J, Ciurtin C. Existing and emerging targeted therapies in juvenile psoriatic arthritis: challenges and unmet needs. *Paediatr Drugs* 2024;26(3):217–228.
- Shoop-Worrall SJW, Macintyre VG, Ciurtin C, et al; Childhood Arthritis Prospective Study (CAPS) Principal Investigators. Overlap of International League of Associations for Rheumatology and preliminary Pediatric Rheumatology International Trials Organization classification criteria for nonsystemic juvenile idiopathic arthritis in an established UK multicentre inception cohort. *Arthritis Care Res (Hoboken)* 2024; 76(6):831–840.
- Fautrel B, Mitrovic S, De Matteis A, et al. EULAR/PReS recommendations for the diagnosis and management of Still's disease, comprising systemic juvenile idiopathic arthritis and adult-onset Still's disease. *Ann Rheum Dis* 2024;83(12):1614–1627.
- Hochberg MC. Updating the American College of Rheumatology revised criteria for the classification of systemic lupus erythematosus. *Arthritis Rheum* 1997;40:1725
- Petri M, Orbai AM, Alarcón GS, et al. Derivation and validation of the Systemic Lupus International Collaborating Clinics classification criteria for systemic lupus erythematosus. *Arthritis Rheum*. 2012;64(8):2677–86. doi:10.1002/art.34473.

9. Sag E, Tartaglione A, Batu ED, et al. Performance of the new SLICC classification criteria in childhood systemic lupus erythematosus: a multicentre study. *Clin Exp Rheumatol* 2014;32(3):440–444.
10. Aljaberi N, Nguyen K, Strahle C, et al. Performance of the new 2019 European League Against Rheumatism/American College of Rheumatology classification criteria for systemic lupus erythematosus in children and young adults. *Arthritis Care Res (Hoboken)* 2021;73(4): 580–585.
11. Bottai M, Tjärnlund A, Santoni G, et al; International Myositis Classification Criteria Project consortium, the Euromyositis register and the Juvenile Dermatomyositis Cohort Biomarker Study and Repository (JDRG) (UK and Ireland). EULAR/ACR classification criteria for adult and juvenile idiopathic inflammatory myopathies and their major subgroups: a methodology report. *RMD Open* 2017;3(2):e000507.
12. Zulian F, Woo P, Athreya BH, et al. The Pediatric Rheumatology European Society/American College of Rheumatology/European League against Rheumatism provisional classification criteria for juvenile systemic sclerosis. *Arthritis Rheum* 2007;57(2):203–212.
13. Ciurtin C, Jury EC. A new tool for stratifying children with suspected Sjögren's disease. *Lancet Rheumatol* 2024;6(5):e255–e256.
14. Shiboski CH, Shiboski SC, Seror R, et al; International Sjögren's Syndrome Criteria Working Group. 2016 American College of Rheumatology/European League Against Rheumatism Classification Criteria for Primary Sjögren's Syndrome: a consensus and data-driven methodology involving three international patient cohorts. *Arthritis Rheumatol* 2017;69(1):35–45. doi:10.1002/art.39859.
15. Basiaga ML, Stern SM, Mehta JJ, et al; Childhood Arthritis and Rheumatology Research Alliance and the International Childhood Sjögren Syndrome Workgroup. Childhood Sjögren syndrome: features of an international cohort and application of the 2016 ACR/EULAR classification criteria. *Rheumatology (Oxford)* 2021;60(7):3144–3155.
16. Ozen S, Ruperto N, Dillon MJ, et al. EULAR/PReS endorsed consensus criteria for the classification of childhood vasculitides. *Ann Rheum Dis* 2006;65(7):936–941.
17. Grayson PC, Ponte C, Suppiah R, et al; DCVAS Study Group. 2022 American College of Rheumatology/European Alliance of Associations for Rheumatology classification criteria for eosinophilic granulomatosis with polyangiitis. *Ann Rheum Dis* 2022;81(3):309–314.
18. Kaya Akca U, Batu ED, Jelusic M, et al. Comparison of EULAR/PRINTO/PReS Ankara 2008 and 2022 ACR/EULAR classification criteria for granulomatosis with polyangiitis in children. *Rheumatology (Oxford)* 2024;63(SI2):SI122–SI128.
19. Gattorno M, Hofer M, Federici S, et al; Eurofever Registry and the Paediatric Rheumatology International Trials Organisation (PRINTO). Classification criteria for autoinflammatory recurrent fevers. *Ann Rheum Dis* 2019;78(8):1025–1032.

Substitution of Glutamic Acid at Position 71 of *DRB1**04:01 and Collagen-Specific Tolerance Without Alloreactivity

Vibha Jha,¹ Brian M. Freed,¹ Elizabeth R. Sunderhaus,¹ Jessica E. Lee,¹ Edward B. Prage,¹ Manjula Miglani,¹ Edward F. Rosloniec,² Jennifer L. Matsuda,³ Marilyne G. Coulombe,¹ Amy S. McKee,¹ and Christina L. Roark¹ 

Objective. The *DRB1* locus is strongly associated with both susceptibility and resistance to rheumatoid arthritis (RA). *DRB1* alleles encoding the VKA or VRA epitope in positions 11, 71, and 74 confer the highest risk of developing RA, whereas the allele encoding VEA is protective. We therefore investigated the feasibility of creating antigen-specific tolerance without inducing alloreactivity by replacing lysine with glutamic acid at position 71 in *DRB1**04:01.

Methods. Individual *DRB1* alleles and the *DRB1**04:01^{K71E} allele were cloned into T2 cell lines to measure binding of biotinylated peptides. Transgenic animals expressing *DRB1**04:01, *DRB1**01:01, or *DRB1**04:01^{K71E} were injected with collagen to measure T cell proliferation. Skin and bone marrow transplants between *DRB1**04:01^{K71E} and *DRB1**04:01 mice were performed to determine if the single amino acid change at position 71 would be recognized as foreign. *DRB1**04:01 mice transplanted with *DRB1**04:01^{K71E} bone marrow were injected with collagen to test if resistance to collagen sensitization could be transferred.

Results. Replacing lysine (K) at position 71 in *DRB1**04:01 with glutamic acid (E) blocked collagen peptide binding and rendered the *DRB1**04:01^{K71E} mice resistant to collagen sensitization. Skin and bone marrow transplants from *DRB1**04:01^{K71E} mice were not rejected by *DRB1**04:01 mice, suggesting the single E⁷¹ difference was not recognized as allogeneic. Bone marrow from *DRB1**04:01^{K71E} mice adoptively transferred antigen-specific tolerance to collagen to *DRB1**04:01 mice.

Conclusion. These studies demonstrate that editing a single amino acid in *DRB1**04:01 blocks collagen peptide binding without inducing alloreactivity and could therefore represent a gene therapy approach to induce antigen-specific passive tolerance.

INTRODUCTION

Rheumatoid arthritis (RA) is a chronic autoimmune disease with a strong genetic link to the HLA *DRB1* locus.¹ Susceptibility to RA is highly associated with a small subset of *DRB1* alleles (*DRB1**01:01, *04:01, *04:04, *04:05, and *10:01), whereas resistance is associated with a different subset (*DRB1**03:01, *04:02, and *07:01).² A large genome-wide association study demonstrated that three amino acid positions (11, 71, and 74) in the *DRB1* peptide-binding groove account for most of the association of *DRB1* with RA.³ These three positions comprise

16 unique *DRB1* epitopes. Alleles with the VKA (V¹¹K⁷¹A⁷⁴) or VRA epitopes have the strongest associations with disease susceptibility, severity of joint disease, and risk of cardiovascular mortality.^{4–6} In contrast, the VEA epitope is found only in *DRB1**04:02 (and other extremely rare alleles) and is associated with resistance to RA and protection from bone erosions.⁴ Although *DRB1**04:01 and *DRB1**04:02 differ at four positions, the VKA/VEA dichotomy at position 71 presents a unique opportunity to examine the role of a single amino acid in RA susceptibility and resistance. We therefore introduced the K71E substitution into *DRB1**04:01 and assessed its effects on peptide binding

Supported in part by the Department of Veterans Affairs (Merit Review grant to Dr Rosloniec).

¹Vibha Jha, PhD, Brian M. Freed, PhD, Elizabeth R. Sunderhaus, PhD, Jessica E. Lee, BS, Edward B. Prage, PhD, Manjula Miglani, PhD, Marilyne G. Coulombe, PhD, Amy S. McKee, PhD, Christina L. Roark, PhD: University of Colorado, Anschutz Medical Campus, Aurora, Colorado; ²Edward F. Rosloniec, PhD: Lt. Col. Luke Weathers, Jr. Veterans Affairs Medical Center and University of Tennessee Health Science Center, Memphis, Tennessee; ³Jennifer L. Matsuda, PhD: National Jewish Health, Denver, Colorado.

Drs Jha and Freed contributed equally to this work.

Additional supplementary information cited in this article can be found online in the Supporting Information section (<https://acrjournals.onlinelibrary.wiley.com/doi/10.1002/art.43067>).

Author disclosures are available at <https://onlinelibrary.wiley.com/doi/10.1002/art.43067>.

Address correspondence via email to Christina L. Roark, PhD, at christina.roark@cuanschutz.edu.

Submitted for publication December 1, 2023; accepted in revised form November 22, 2024.

in vitro and then used transgenic mice expressing either the *DRB1**04:01 (VKA) or *DRB1**04:01^{K71E} (VEA) alleles to assess their ability to respond to collagen in vivo.

MATERIALS AND METHODS

Reagents and antibodies. Dulbecco's phosphate buffered saline (DPBS; 14190-144) and IMDM-GlutaMAX media (31980-030) were both from Life Technologies. 100 mM sodium pyruvate (11360070) and 100X thio-streptomycin/penicillin (10378016) and fetal bovine serum (FBS, 10438-026) were from Gibco, RBC Lysis Buffer was from Invitrogen (4300-54) and formaldehyde 10% solution was from Polysciences Inc (04018). The RNeasy Kit was from Qiagen (74106). Cells were stained in DPBS containing 2% FBS for flow cytometry. Cells were cultured in Iscove's Complete T cell Media (ICTM; IMDM-GlutaMAX supplemented with 10% FBS +1% thio-streptomycin + 1mM sodium pyruvate). For bone marrow transplant experiments, Baytril water was prepared in-house with enrofloxacin powder (Apexbio Technology, B1742) in autoclaved water.

For flow cytometry, we used Fixable Viability Dye eFluor™ 780 (Invitrogen, 65-0865-18), phycoerythrin (PE)-labeled streptavidin (One Lambda, LT-SAPE), PE anti-mouse CD19 clone ID3 (ThermoFisher, 12-0193-81), eFluor 450 anti-mouse CD11c clone NF418 (ThermoFisher, 48-0114-80), APC anti-HLA-DRα clone LN3 (Invitrogen 17-9956-42), StarBright Violet 440 anti-HLA-DP/DQ/DR clone WR18 (BioRad, MCA477), mouse CD16/CD32 Fc block, clone 2.4G2 (Tonbo Bioscience, 700161U500), from BD Biosciences, BUV 395 anti-mouse CD25 clone PC61 (564034) and BUV 395 anti-mouse CD8 clone 53-6.7 (563786), and from BioLegend, PE-Cy7 anti-mouse CD3 clone 17A2 (100219), PE anti-mouse CD8 clone QA17A07 (155008), AF488 anti-mouse CD4 clone GK1.5 (100423), PE-Cy7 anti-mouse F4/80 clone BM8 (124114), and BV711 anti-mouse CD3 clone 17A2 (100241). Bovine type 2 collagen protein (CN276) was from Elastin Products Inc., BD Difco *M. tuberculosis* lyophilized powder (DF0639-60-6) and BD Difco Incomplete Freund's adjuvant (DF3114338) were both purchased from Fisher Scientific. Influenza A virus H3N2 hemagglutinin protein was purchased from Sino Biological.

Peptides. Type 2 collagen²⁵⁸⁻²⁷² (PGIAGFKGEQGPKE), native and citrullinated vimentin⁶⁶⁻⁷⁸ (SAVRLRSSVPGVR and SAVRLC*i*SSVPGVR), native and citrullinated α-enolase¹¹⁻²⁵ IFDSRGNPTVEVDLF and IFDSC*i*GNPTVEVDLF, and control HA³⁰⁶⁻³¹⁸ (PKYVKQNTLKLAT) peptides were synthesized with a biotinylated polyethylene-3 linker on the N-terminus to more than 98% purity with trifluoroacetic acid removal by GenScript.

Mice. Mice were housed, bred, genotyped, and treated in the Office of Laboratory Animal Resources vivarium in accordance with Institutional Animal Care and Use Committee-approved

protocol standards at the University of Colorado Anschutz Medical Campus. The *DRB1**04:01 and *DRB1**01:01 transgenic mouse strains, both on the B6.129S2-*H2^{dIAb1-Ea}*/J background⁷ were created by Dr Edward Rosloniec.^{8,9}

To create the *DRB1**04:01^{K71E} mice, genomic constructs containing the chimeric *DRB1**04:05/I-E^dβ and chimeric *DRA1**01:01/I-E^dα (provided by Dr Yasuharu Nishimura), were used.¹⁰ Markerless recombination was used to introduce two mutations in exon 2 of *DRB1**04:05 to modify this construct to express *DRB1**04:01^{K71E} (Mouse Genetics Core Facility, National Jewish Health). The *DRA1**01:01 and *DRB1**04:01^{K71E} constructs were confirmed to contain the correct sequence (Mouse Genetics Core Facility, National Jewish Health).

To create the transgenic mice, the constructs were linearized and quantified for microinjection and then coinjected using pronuclear injections into B6N (Taconic, B6NTac) zygotes, which were transferred to pseudopregnant recipient mice. Mouse genotypes from pup tail biopsies were determined using real time polymerase chain reaction (PCR) with specific probes designed for each gene (Transnetix). A single founder was identified that expressed both the *DRA1**01:01 and *DRB1**04:01^{K71E} genes. Blood was harvested and RNA extracted to generate complementary DNA (cDNA), from which the correct sequence of each transgene was confirmed (data available upon request). Expression of HLA-*DR* on B cells isolated from blood was confirmed in the *DRB1**04:01^{K71E} founder by flow cytometry (Supplemental Figure 1). The *DRB1**04:01^{K71E} mice were backcrossed onto the B6.129S2-*H2^{dIAb1-Ea}*/J mouse strain and were genotyped by PCR (Transnetix) to generate the *DRB1**04:01^{K71E} line.

*DRB1**04:01^{K71E} mice have a normal hematopoietic profile with white blood cells, red blood cells (RBCs), platelets, lymphocytes, monocytes, granulocytes, neutrophils, eosinophils, basophils, hematocrit, mean corpuscular volume, red cell distribution width, hemoglobin, mean corpuscular hemoglobin, and mean platelet volume all within the normal reference ranges (data available upon request). The frequencies of B and T cells were comparable between HLA transgenic lines and the B cells expressed human but not mouse major histocompatibility complex (MHC) class 2 molecules (Supplemental Figure 1 and data not shown). The mice are healthy with a normal lifespan and can be maintained as a homozygous transgenic mouse line. Approximately equal numbers of age-matched (6 to 12 weeks old) male and female mice were used for all in vivo experiments (collagen sensitization, skin transplants, and bone marrow transplants) later described.

Skin transplant mouse model. Recipient mice were anesthetized and shaved, and graft beds were prepared by surgical removal of the skin behind the forelimb and lateral to the midline of each mouse. Donor skin grafts (approximately 1 cm²) were then placed on the graft bed. Tissue adhesives, Bacitracin/Neomycin/Polymyxin Ointment (Medique, 19-090-832), and petroleum jelly-infused gauze were used to stabilize the graft.¹¹

Supplemental heat was administered during surgery, and mice were monitored until normal activity was achieved. Recipient mice received subcutaneous injections of the analgesics Buprenorphine (Wedgewood Pharmacy, originally ZooPharm) at 1 mg/kg and Carprofen (Zoetis, SFU#026357) at 5 mg/kg prior to surgery, with Carprofen administered at the same dose every day for up to 7 days posttransplant. Mice were checked daily, and grafts were checked for engraftment/rejection. Rejected allografts and engrafted skin were tested for donor and recipient genes by PCR (Transnetyx) upon graft rejection or study endpoints.

Bone marrow transplant mouse model. Recipient mice were treated with Baytril water starting 48 hours pretransplant through 4 weeks posttransplant. Mice were given a partially myeloablative regimen consisting of two irradiation cycles of 3 Gy each, four hours apart. Twenty-four hours later, mice were transplanted with 5×10^6 donor bone marrow cells suspended in DPBS by retro-orbital injection.

Generation of *DRB1*-expressing T2 cells. T2 parent cells (ATCC, CRL-1992) expressing *DRA1* (previously generated¹²) were transfected with *DRB1* plasmids packaged in retroviruses. cDNA sequences were manufactured as gBlocks (Integrated DNA Technologies), which were cloned into a MSCV-IRES-GFP retroviral plasmid. Plasmids were transfected into Phoenix 293T (provided by Dr Andrew Fontenot) and packaged into retroviral vectors as previously described.^{13,14} The retrovirus was used to transduce T2 cells resulting in individual lines, each expressing *DRA1* and a single *DRB1* variant. Cells were stained and sorted for high expression of HLA-DR α and GFP expression (FACSaria, BD Biosciences). After the sort, RNA was isolated from each cell line (Qiagen RNeasy, 74106) and the *DRB1* sequences verified by Sanger sequencing (Quintara Biosciences). Cells lines were thawed and then expanded and maintained in ICTM (IMDM-GlutaMAX supplemented with 10% FBS +1% thio-streptomycin + 1mM sodium pyruvate).

***DRB1* peptide-binding assay.** Peptide binding to *DR β 1* alleles and variants was performed as previously described.¹² Briefly, T2 parent cells (controls) or T2 cells cotransfected with *DRA1* and *DRB1* were cultured overnight in 100 μ l ICTM containing 2×10^5 cells and 100 μ M biotinylated peptide. The cells were then stained with Fixable Viability Dye (FVD) eFluor™ 780 and fixed with 1% formaldehyde in DPBS to prevent loss of peptide from the cell surface. PE-labeled streptavidin was used to detect the biotinylated peptides by flow cytometry as described in Supplemental Figure 2. Peptide binding was expressed as PE mean fluorescence intensity (MFI) or as the fold increase in binding, calculated as the mean PE fluorescence intensity (MFI) detected on *DRB1*-transfected T2 cells divided by the MFI detected on untransfected T2 cells.

Tissue processing. Lymph nodes and spleens were homogenized manually using 3 mL syringe plungers and filtered through 70 μ m (lymph nodes) or 100 μ m (spleen) filters into single cell suspensions. RBCs in splenocyte suspension were lysed using RBC lysis buffer and filtered through 70 μ m filters to obtain a single cell suspension to be used for staining. Blood and tissue samples were snap frozen in liquid nitrogen, homogenized and genomic DNA was extracted using the QIAamp DNA mini kit for blood and tissue (Qiagen, 51106). For bone marrow transplants, femurs were harvested from donors, cut at each end, and bone marrow cells were pelleted by centrifugation. RBCs were lysed, and nucleated cells were washed and resuspended in DPBS.

Lymphocyte characterization of transgenic mice.

Lymph nodes and spleens were harvested from all three transgenic mice and processed as described (Tissue Processing). Cells were then stained with fluorochrome conjugated-anti-CD3, anti-CD19, anti-CD4, anti-CD8, anti-F4/80, anti-CD11c, and anti-DR- α . They were also stained with fixable viability dye. They were fixed and acquired on the LSR-II flow cytometer to obtain frequencies of various lymphocyte lineages.

CD4⁺ T cell antigen-specific recall assay. Lymph node cells from collagen-injected or HA-injected mice were cultured ex vivo in ICTM media \pm 15 μ g/mL collagen²⁵⁸⁻²⁷² or HA peptide³⁰⁶⁻³¹⁸ for 24 hours. Five μ M/mL 5'ethynyl-2'-deoxyuridine (EdU) was added to the cultures for an additional 16 hours. Cells were washed and stained with fluorochrome conjugated-anti-CD3, anti-CD4, anti-CD8, and anti-CD25 antibodies and FVD-eFluor™-780 followed by incubation with the Click-iT EdU Plus Pacific Blue detection reagent in accordance with manufacturer instructions (Click-iT plus EdU PB flow kit 50, Life Technologies, C10636). The frequency of CD4⁺ T cells that were EdU⁺ (proliferating) in response to peptide were analyzed to assess antigen-specific responses generated in vivo and the percentage of CD4⁺ cells that were positive for the activation marker CD25 was assessed. Because CD25 is expressed on regulatory T cells, some samples were stained for CD3, CD4, CD25, and FoxP3 using the anti-mouse FoxP3 staining kit (Thermo Fisher Scientific, 72-5775-40 with anti-FoxP3 clone FJK-16s) to confirm that the frequency of FoxP3+CD25+ cells was similar in immunized *DRB1**04:01 and *DRB1**04:01^{K71E} mice and did not increase with ex vivo peptide stimulation (Supplemental Figure 3).

Digital partition polymerase chain reaction (PCR).

Qiagen Genomic Services optimized the primers and probes used on the QIAcuity One instrument to quantify *DRB1**04:01 and *DRB1**04:01^{K71E} copies present in genomic DNA extracted from blood, bone marrow, spleen, or lungs. Positive and negative partitions were quantified and used to calculate copies of *DRB1**04:01 or *DRB1**04:01^{K71E} per ng of template DNA in each sample.

Statistical analysis. Flow cytometry data were acquired on the BD LSRII (RRID:SCR_002159) for Supplemental Figure 1 and on the BD FACSCanto II (RRID:SCR_018056) for all other data using FACSDiva Software version 9.1 (BD Biosciences). Data were analyzed using FlowJo version 10.8.1 (Tree Star, RRID:SCR_008520). Digital PCR data were collected and analyzed using the QIAcuity System Software Suite version 1.2 from Qiagen (9245362). Statistical analysis was performed using GraphPad Prism software version 9.1.3 (GraphPad, RRID:SCR_002798). Unpaired, two-tailed *t*-tests were performed for normally distributed data as described in the figure legends. Peptide binding on all RA-resistant alleles (*n* = 15 data points) or susceptible alleles (*n* = 40 data points) were compared, and medians were compared using a Mann-Whitney test for nonparametric data.

Study design. No statistical methods were used to predetermine the sample sizes. For mouse experiments, sample sizes were chosen to ensure equal numbers of age-matched male and female participants, with at least three mice per genotype in a single experiment. For T2 cell experiments, sample sizes were chosen to ensure at least three independently transfected T2 cells were analyzed per *DRB1* allele. No data were excluded. All data for replicates are shown in the manuscript. All data presented in the figures represent at least two replicates except for the data shown in Figure 3B, which were performed with a greater number of mice (*n* = 8) per genotype. For animal studies, mice were age-matched and sex-matched. For each genotype, both sexes were represented, and mice derived from different breeding pairs were used. Investigators were not blinded to group allocation during data collection or analysis of data, as mouse ages and genotype were determined prior to experiments.

RESULTS

Glutamic acid in position 71 and collagen peptide binding. In order to elucidate the role of position 71 in antigen presentation, we measured the binding of three RA-associated peptides to various susceptible and resistant *DRB1* alleles. We have previously shown that the binding profiles of collagen²⁵⁸⁻²⁷² to *DRB1**04:01 and *DRB1**01:01 on transfected T2 cells correlates with the ability of these cell lines to stimulate *DRB1*-restricted, collagen-specific T cell clones,^{12,15} indicating that the binding represents immunologically cognate interactions. Binding of collagen²⁵⁸⁻²⁷², citrullinated vimentin⁶⁶⁻⁷⁸, citrullinated α -enolase¹¹⁻²⁵, or influenza hemagglutinin (HA³⁰⁶⁻³¹⁸) to *DRB1**01:01/*DRB1**04:01, *01:01, and *04:02 alleles expressed on MHC Class II-deficient T2 cells were measured as shown in Figure 1. These peptides were chosen because patients with RA develop antibody responses to citrullinated vimentin and α -enolase several years prior to the development of clinical RA,¹⁶ and the appearance of CD4⁺ T cells reactive against type II

collagen generally coincides with the onset of clinical symptoms of joint disease.¹⁷⁻¹⁹ Type II collagen is also arthritogenic in animal models, causing infiltration of inflammatory cells into the joint.^{8,20} The immunodominant peptide of collagen is identical in bovine, chick, human, and rats and induces crossreactive immune responses to mouse type II collagen, which differs by a single E to D substitution in position 266.²¹ Furthermore, the sequence from 258-272 is the only collagen peptide that induces a T cell response in *DRB1**04:01 transgenic mice.⁸ We observed a direct correlation between the susceptibility to RA (as determined by Raychaudhuri et al)³ and the degree of binding of these three arthritogenic peptides. Citrullinated peptides and collagen²⁵⁸⁻²⁷² bound much more strongly to the RA-susceptible *DRB1**04:01 (VKA) than to either the weakly susceptible *DRB1**01:01 (LRA) or the resistant *DRB1**04:02 (VEA) (Figure 1).

To determine if this phenomenon was generally applicable to all susceptible and resistant alleles, peptide binding was measured on a spectrum of RA-susceptible and resistant epitopes. As a group, RA-susceptible alleles containing VKA (*DRB1**04:01), VRA (*DRB1**04:04, *04:05, *04:08, and *10:01), LRA (*DRB1**01:01 and *01:02), and PRA (*DRB1**16:01) epitopes exhibited 10-fold greater binding of citrullinated vimentin⁶⁶⁻⁷⁸ ($P = 4.9 \times 10^{-9}$) and 8-fold greater binding of citrullinated α -enolase¹¹⁻²⁵ ($P = 2.1 \times 10^{-6}$) compared with alleles with resistant epitopes. *DRB1**04:03 (VRE), which is not associated with susceptibility to RA, exhibited a lack of binding of citrullinated peptides similar to the resistant *DRB1**04:02 (VEA). However, as shown in Figure 2A, the binding of collagen²⁵⁸⁻²⁷² was most strongly associated with the VKA allele (*DRB1**04:01) and was absent with the VEA allele (*DRB1**04:02). These two alleles differ by four amino acids at positions 67, 70, 71, and 86, three of which are found in pocket 4. However, introducing the VEA epitope into *DRB1**04:01 by substituting just the glutamic acid at position 71 (*DRB1**04:01^{K71E}) eliminated binding of collagen²⁵⁸⁻²⁷² (Figure 2A, $P = 0.0047$) but did not interfere with the binding of citrullinated vimentin⁶⁶⁻⁷⁸, citrullinated α -enolase¹¹⁻²⁵, or HA³⁰⁶⁻³¹⁸. The acidic amino acid in position 266 of collagen²⁵⁸⁻²⁷² binds strongly to the basic K amino acid in position 71 in pocket 4 of *DRB1**04:01 (VKA) and is ionically repulsed by the glutamic acid (E) in *DRB1**04:01^{K71E} (VEA). As proof, mutating the collagen peptide from E to R at position 266 restored its binding to *DRB1**04:01^{K71E} and eliminated its binding to *DRB1**04:01 (Figure 2B). The K71E substitution did not affect binding of the citrullinated peptides or HA³⁰⁶⁻³¹⁸ because these peptides have neutral amino acids that are accommodated in pocket 4 regardless of charge. However, the presence of a basic amino acid in position 71 did not, by itself, promote collagen²⁵⁸⁻²⁷² binding, as evidenced by the lack of binding to *DRB1**03:01 (SKR), *DRB1**07:01 (GRQ), and *DRB1**14:01 (SRE). Nevertheless, these experiments demonstrate that a single amino acid substitution in an RA-susceptible allele can eliminate the binding of an arthritogenic peptide in an antigen-specific manner.

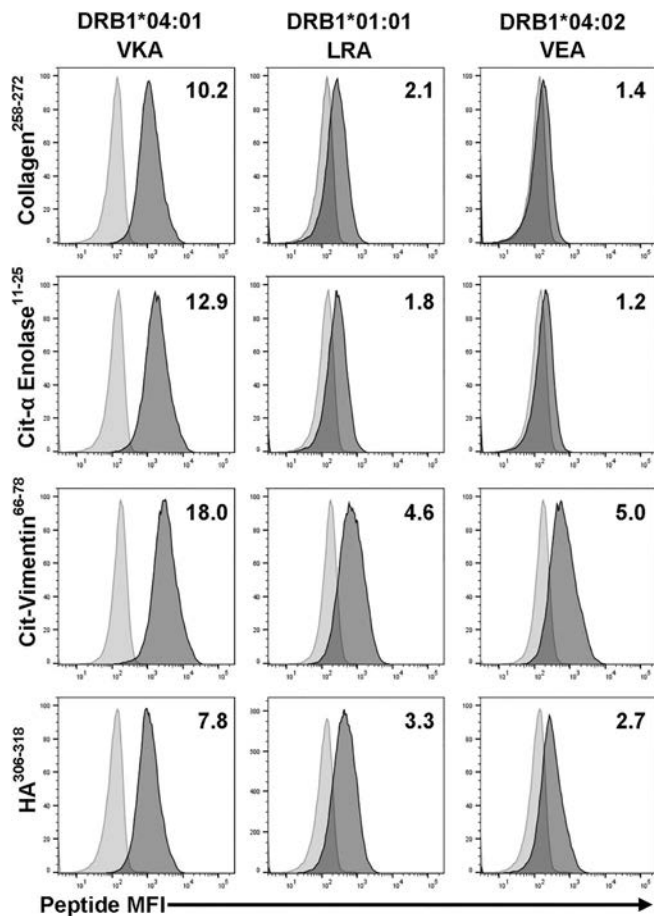


Figure 1. Peptide binding of RA-associated peptides to transfected T2 cells. Histograms show MFI of peptide binding to T2 cells expressing the indicated alleles (dark histograms) compared with untransfected T2 controls (light histograms). The data are expressed as the mean fold increase of peptide binding to *DRB1*-transfected cells over binding to T2 controls (VKA, $n = 12$; LRA and VEA, $n = 3$). Background MFI for each peptide on untransfected T2 controls ranged from 114 to 149. HA, hemagglutinin; MFI, mean fluorescence intensity; RA, rheumatoid arthritis.

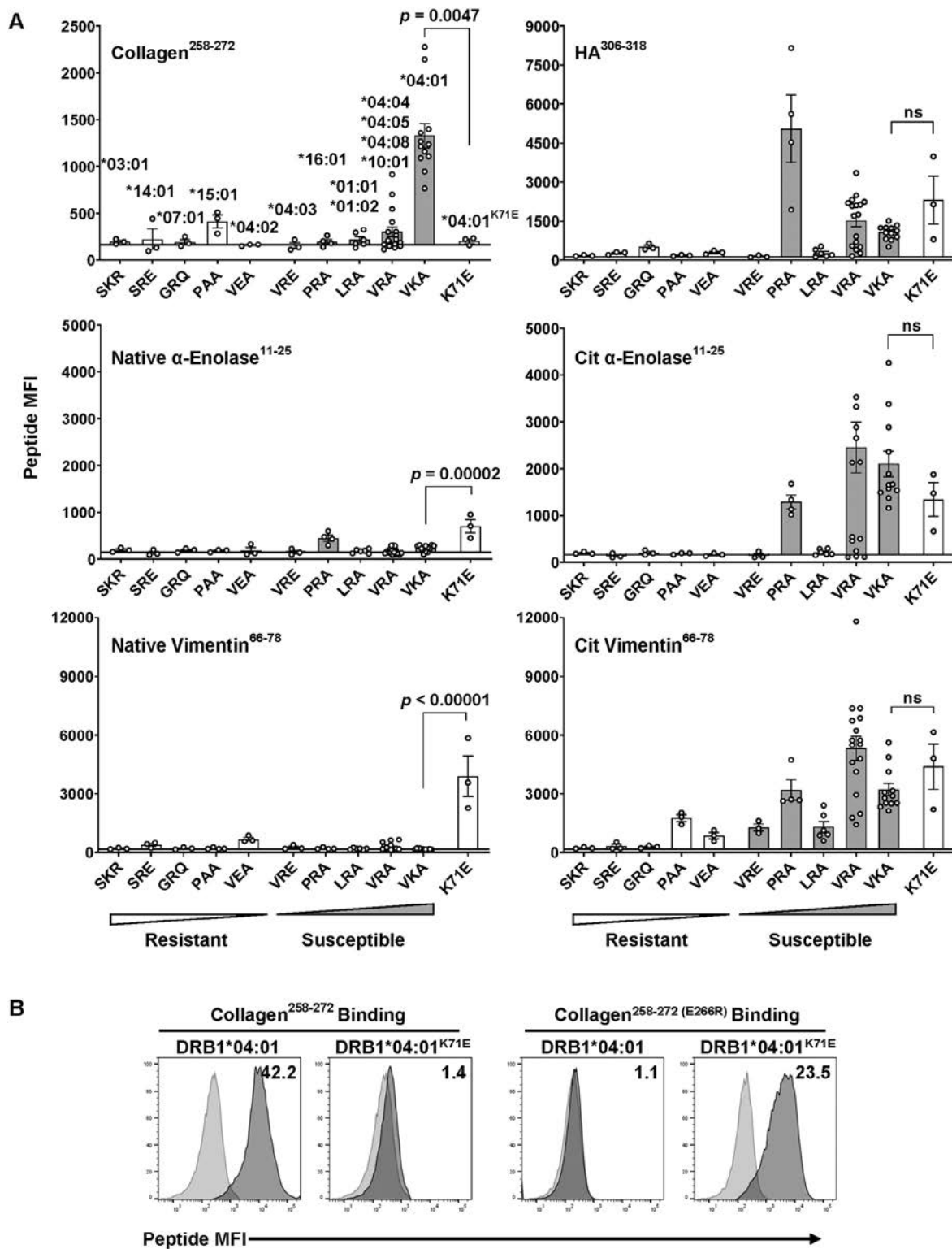
***DRB1*04:01*^{K71E} mice resistant to collagen sensitization.** To test the VKA/VEA dichotomy in vivo, we used three lines of HLA transgenic mice expressing *DRB1*04:01* (VKA), *DRB1*01:01* (LRA), or *DRB1*04:01*^{K71E} (VEA) on the same B6 murine MHC class II-knockout background. Type II collagen, or HA as a control, were emulsified in Complete Freund's adjuvant (CFA) and injected intradermally into the transgenic mice on days 0 and 21.²⁰ On day 56, lymph node cells were harvested and restimulated in vitro with collagen²⁵⁸⁻²⁷² or HA³⁰⁶⁻³¹⁸ to assess peptide-specific CD4⁺ T cell responses. CD4⁺ T cells from *DRB1*04:01* mice exhibited a strong proliferative response to collagen²⁵⁸⁻²⁷² (Figure 3A). *DRB1*01:01* (LRA) mice exhibited a weak CD4⁺ T cell proliferative response to collagen²⁵⁸⁻²⁷², which correlates with its reduced ability to bind collagen²⁵⁸⁻²⁷² in vitro (Figure 2A) and a weaker association with RA compared with *DRB1*04:01*.³ Commensurate with the in vitro peptide-binding

studies, *DRB1*04:01*^{K71E} mice did not exhibit an in vivo T cell response to collagen²⁵⁸⁻²⁷² ($P = 0.00002$) (Figure 3A). *DRB1*04:01*^{K71E} mice retained a normal response to HA³⁰⁶⁻³¹⁸ (Figure 3B), consistent with a lack of effect of K71E on peptide binding because of the neutral amino acid (asparagine) binding in pocket 4 of the *DRB1* molecule. These data demonstrate conclusively that it is possible to create antigen-specific passive tolerance by altering a single amino acid in an HLA molecule.

The *DRB1*04:01*^{K71E} allele in *DRB1*04:01* mice. The fact that *DRB1*04:01*^{K71E} mice are resistant to collagen sensitization suggests that it might be possible to treat RA with a single amino acid change via HLA gene editing. Position 71 is located in the peptide-binding groove but does not come into direct contact with the T cell receptor.²² Nevertheless, the K71E edit could theoretically alter the peptide repertoire and lead to acute or chronic rejection,²³ thereby reducing its therapeutic potential.

In order to determine if this single amino acid difference could be recognized as an alloantigen, we performed skin and bone marrow transplants between *DRB1*04:01*^{K71E} donor mice and *DRB1*04:01* recipients. The skin contains long-lived Langerhans cells that present the donor *DRB1* allele in the transplanted skin.²⁴ Skin grafts were assessed for acute rejection at 10 to 15 days posttransplant and for chronic rejection on day 70. *DRB1*04:01* and *DRB1*01:01* donor skin grafts were used as negative and positive controls, respectively. None of the autologous *DRB1*04:01* skin grafts were rejected, and all the *DRB1*01:01* skin allografts were rejected acutely by day 15. In contrast, the *DRB1*04:01*^{K71E} allografts all survived up to day 70 with no evidence of rejection (Figure 4A). Skin punch biopsies taken from *DRB1*04:01*^{K71E} grafts on day 70 were genotyped and demonstrated the presence of both *DRB1*04:01* and *DRB1*04:01*^{K71E} (data not shown), indicating that *DRB1*04:01* recipients do not recognize the K71E substitution as allogeneic. Similarly, bone marrow from *DRB1*04:01*^{K71E} donor mice engrafted and survived in *DRB1*04:01* recipients without the need for complete myeloablation (Figure 4B). Low-dose irradiation conditioning was used to allow *DRB1*04:01* recipient mice to develop mixed chimerism, thereby permitting assessment of allorecognition between *DRB1*04:01* and *DRB1*04:01*^{K71E}. Digital partition PCR was performed to confirm donor engraftment and showed the presence of mixed chimerism in the blood by day 28. On day 56, bone marrow, blood, and spleen of *DRB1*04:01* recipient mice exhibited 80% to 90% *DRB1*04:01*^{K71E} chimerism, whereas lung tissue retained predominantly the *DRB1*04:01* phenotype. These data confirm that the single K71E substitution is not recognized as an alloantigen in *DRB1*04:01* recipients.

Resistance to collagen sensitization can be adoptively transferred to *DRB1*04:01* mice by *DRB1*04:01*^{K71E} bone marrow. To test the ability of *DRB1*04:01*^{K71E} hematopoietic stem cells to adoptively transfer



collagen-specific passive tolerance, *DRB1*04:01* recipient mice were conditioned with the same low-dose irradiation regimen used in Figure 4B, and then transplanted with either autologous *DRB1*04:01* or allogeneic *DRB1*04:01*^{K71E} bone marrow. After 28 days, mice were injected with collagen/CFA, and on day 56, CD4⁺ T cells were restimulated in vitro with collagen peptide as described in Figure 3. Collagen-specific CD4⁺ T cell proliferative responses were reduced by 81% ($P = 0.008$) in mice transplanted with *DRB1*04:01*^{K71E} bone marrow compared with control mice who received autologous bone marrow (Figure 5).

DISCUSSION

Genetic susceptibility and resistance to RA and several other autoimmune diseases (eg, type 1 diabetes, multiple sclerosis,

ankylosing spondylitis, and celiac disease) is strongly linked to the HLA locus,²⁵ but the mechanisms on how these molecules influence the process is still under investigation. Here we demonstrate that a single *DRβ1* amino acid position that is strongly associated with RA susceptibility and resistance can, in fact, be edited from the susceptible to the resistant phenotype with a predictable effect on peptide binding and T cell activation. A similar phenomenon has been shown in the nonobese diabetic mouse model of type 1 diabetes, which is associated with residue 57 of the mouse MHC class II molecule, I-A^{g7}.^{26–28} HLA susceptibility to RA has long been attributed to the “shared epitope” in the *DRβ1* molecule,² but the exact nature of this association has never been clear. With the advent of high-resolution mapping in large patient populations, the amino acids in *DRβ1* that are critical to both RA susceptibility and disease severity have been conclusively

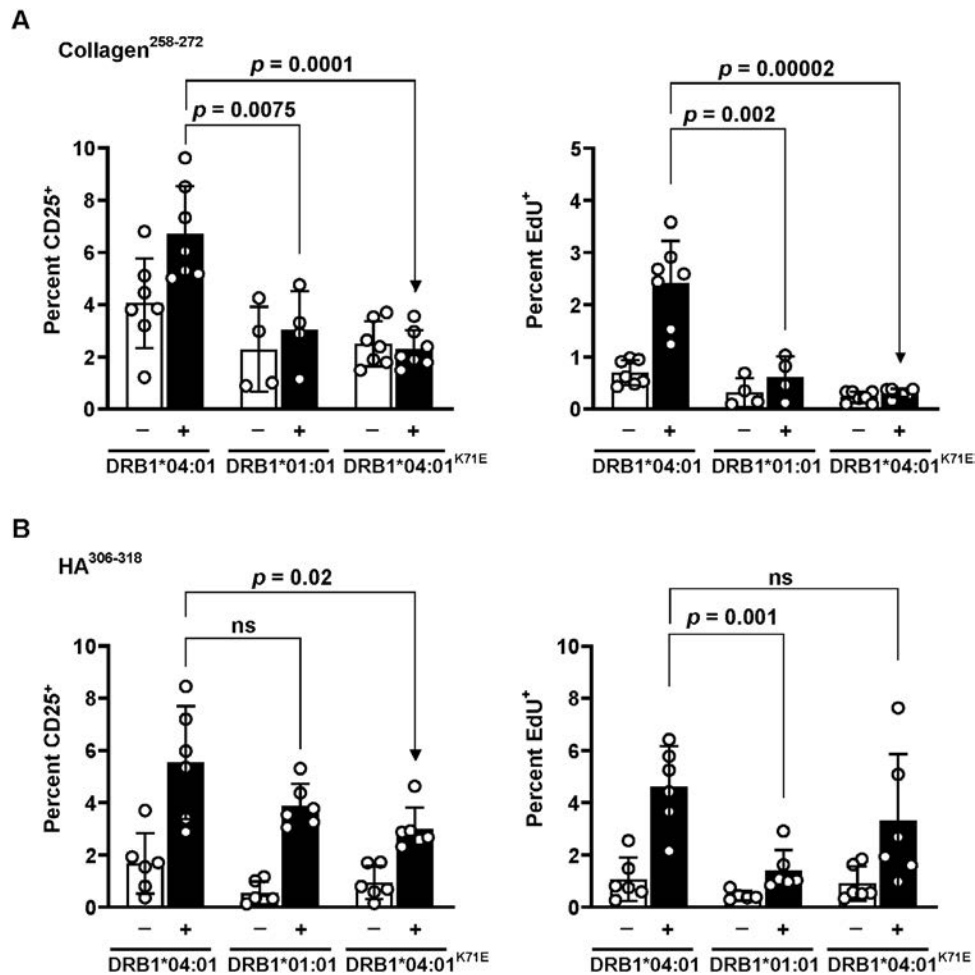


Figure 3. *DRB1*04:01*^{K71E} (VEA) transgenic mice are resistant to collagen sensitization. *DRB1*04:01* (VKA, $n = 7$), *DRB1*01:01* (LRA, $n = 4$) and *DRB1*04:01*^{K71E} (VEA, $n = 6$) transgenic animals were injected with (A) whole collagen or (B) whole hemagglutinin. The percentage of lymph node CD4⁺ T cells expressing the activation marker CD25 (left panels) or that proliferated in vitro (as detected by EdU incorporation, right panels) with (+) or without (–) the relevant peptide is shown. Dots on graphs are values from individual mice; bars indicate mean values and error bars indicate SD. An unpaired, two-tailed t -test was used to compare (A) collagen-specific activation and proliferation in *DRB1*04:01* and *DRB1*01:01* mice ($t = 4.169$, $df = 9$) and *DRB1*04:01* and *DRB1*04:01*^{K71E} mice ($t = 6.952$, $df = 12$) and (B) HA-specific activation and proliferation in *DRB1*04:01* and *DRB1*01:01* mice ($t = 4.517$, $df = 10$) and *DRB1*04:01* and *DRB1*04:01*^{K71E} ($t = 1.063$, $df = 10$). EdU, 5'-ethynyl-2'-deoxyuridine; HA, hemagglutinin; ns, not significant.

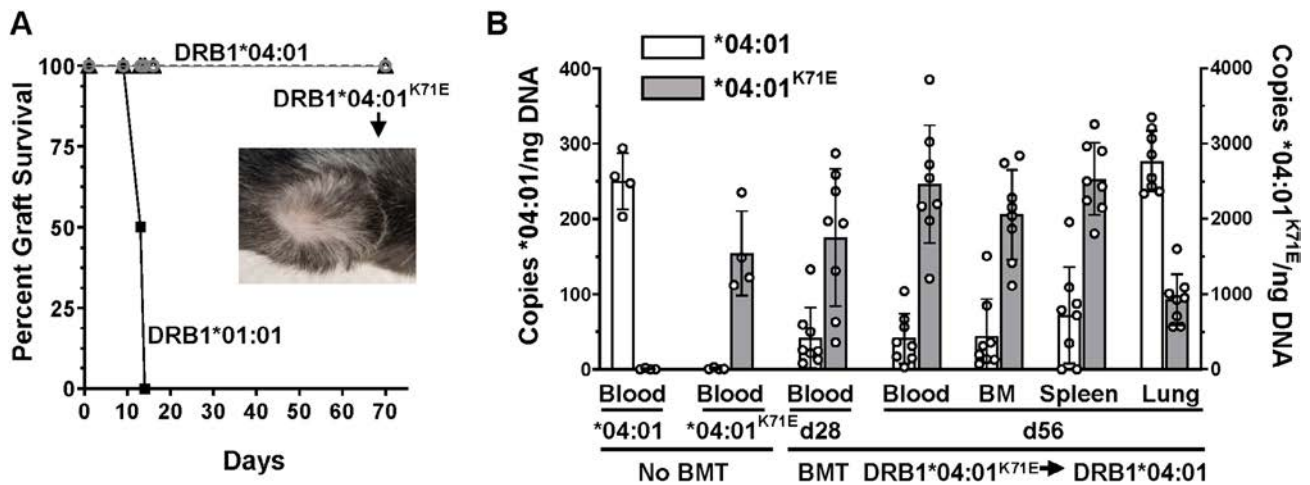


Figure 4. *DRB1*04:01^{K71E}* is not rejected by *DRB1*04:01* recipients. (A) Percent graft survival is shown for *DRB1*04:01* recipient mice that were transplanted with skin from *DRB1*04:01*, *DRB1*01:01*, or *DRB1*04:01^{K71E}* mice ($n = 3$ mice/group). Image shows a *DRB1*04:01^{K71E}* skin graft at day 70. (B) Digital partition PCR data are expressed as copies per ng DNA of each allele in untreated control mice (No BMT, $n = 4$) and in BMT mice ($n = 8$) d28 or d56 posttransplant. Dots indicate values from individual mice, bars indicate mean values and error bars indicate SD. BMT, bone marrow transplanted; d, day; PCR, polymerase chain reaction.

mapped to positions 11, 71, and 74.³ VKA, and the structurally similar VRA, are consistently associated with both susceptibility to RA and severity of the ensuing disease.^{3,4} LRA (found in *DRB1*01:01*) has a weaker association with RA and joint erosions,⁴ and this correlates with its reduced capacity to bind collagen and citrullinated peptides. In contrast, the VEA epitope is not associated with RA, suggesting that the K to E dichotomy at position 71 may play a definitive role in disease susceptibility and severity.⁴

In agreement with previous findings by Ting et al,²⁹ RA-susceptible alleles, but not RA-resistant alleles, exhibited a strong preference for the citrullinated forms of vimentin and

α -enolase compared with the native forms of these peptides (Figure 2A). This phenomenon may be due, in part, to the fact that a basic amino acid in pocket 4 of the *DRB1* molecule ionically repulses the arginine residues in the native peptides but allows the binding of the neutral citrulline. However, a basic amino acid in position 71 alone does not dictate binding, because *DRB1*03:01* (SKR), *DRB1*07:01* (GRQ) and *DRB1*14:01* (SRE) did not show similar preferences for citrullinated peptides (Figure 2A). In contrast, the *DRB1*04:01* (VKA) allele exhibited the strongest binding of collagen²⁵⁸⁻²⁷², and this phenomenon could be completely blocked by the K71E substitution. The effect of the K71E substitution was equally dramatic in vivo, as

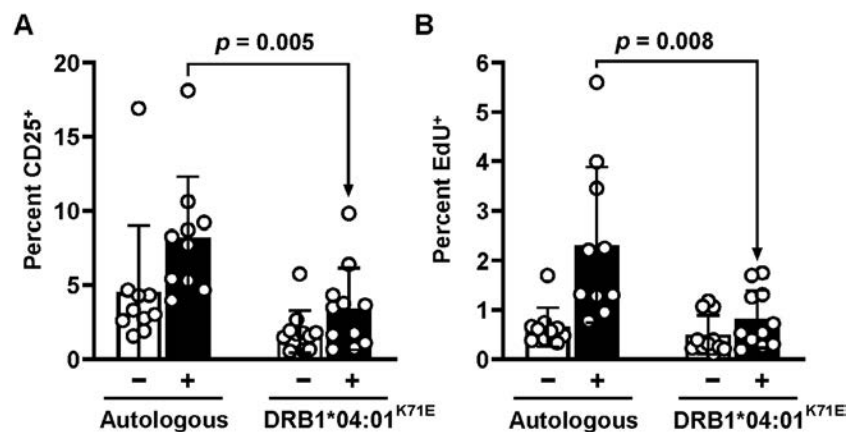


Figure 5. *DRB1*04:01^{K71E}* bone marrow transplantation renders *DRB1*04:01*-recipient mice resistant to collagen sensitization. Graphs show data from collagen injected-*DRB1*04:01* recipients of autologous ($n = 10$) or *DRB1*04:01^{K71E}* ($n = 11$) bone marrow. The percentage of lymph node CD4⁺ T cells that expressed the T cell activation marker, (A) CD25 or (B) proliferated (EdU⁺) after in vitro stimulation with (+) or without (-) the collagen²⁵⁸⁻²⁷² peptide is shown. Dots on graphs are values from individual mice, bars indicate mean values and error bars indicate SD. Data are combined from 3 independent experiments. An unpaired, two-tailed *t*-test was performed between the indicated groups in A ($t = 3.171$, $df = 19$) and in B ($t = 2.954$, $df = 19$). EdU, 5'-ethynyl-2'-deoxyuridine.

*DRB1*04:01*^{K71E} (VEA) mice were completely resistant to collagen sensitization while retaining their ability to respond to influenza HA. The HA³⁰⁶⁻³¹⁸ control peptide used throughout these experiments contains a neutral glutamine in the pocket 4 site and is therefore unaffected by the K71E substitution.

The fact that the K71E substitution in *DRB1*04:01* blocked the binding of the immunodominant peptide of collagen, but not the binding of citrullinated vimentin or α -enolase, suggests that gene editing of the bone marrow might be used to induce antigen-specific tolerance. However, it is not known if eliminating the response to a single arthritogenic peptide would be sufficient to alter the course of RA. Immune responses to citrullinated proteins occur years before the onset of joint damage, whereas immune responses to collagen are an essential component of joint erosions that ultimately manifest the disease.³⁰ *DRB1*04:01* mice transplanted with *DRB1*04:01*^{K71E} bone marrow resulted in an 81% reduction in CD4+ T cell responses to collagen (Figure 5), commensurate with the level of K71E chimerism measured in the transplanted mice (Figure 4B).

Our demonstration that *DRB1*04:01*^{K71E} bone marrow can transfer resistance to collagen sensitization into *DRB1*04:01* mice, even without complete donor chimerism, suggests that it may be possible to control joint damage by editing of the *DRB1*04:01* gene in autologous hematopoietic stem cells. The lack of acute alloreactivity is presumably because of the fact that position 71 does not come in direct contact with the T cell receptor.³¹ Although Coppin et al reported that substitution of acidic and basic amino acids in position 71 of *DRB1* resulted in a loss of responsiveness in alloreactive T cell clones, the authors conclude that the phenomenon was likely mediated by altered peptide binding.²³ Similarly, we have shown that T cell clones with specificity for *DRB1*04:01* plus collagen²⁵⁸⁻²⁷² are completely unresponsive to the same peptide presented in the context of *DRB1*04:01*^{K71E}, and that this phenomenon correlates with the loss of collagen binding.¹² Although it remains possible that the K71E substitution could introduce de novo binding of an unrelated peptide (such as the native vimentin peptide in Figure 2A) leading to allorecognition, we did not see evidence of this in the skin and bone marrow transplants (Figure 4). Taken together, these findings suggest that introduction of the K71E change into the bone marrow of *DRB1*04:01*-positive patients with RA could induce collagen-specific passive tolerance.

Although tolerance is generally thought to occur either in the thymus (central tolerance) or as a result of incomplete activation in the periphery (peripheral tolerance), it is clear from these studies that a passive form of tolerance exists at the genetic level. Though citrullinated vimentin, citrullinated α -enolase, and collagen all bound to HLA alleles associated with susceptibility to RA, they did not bind to alleles that are associated with resistance. Furthermore, editing the *DRB1*04:01* allele at a key epitope (VKA) associated with disease susceptibility blocked collagen binding and collagen sensitization by

introducing a negative charge found in resistant alleles, resulting in repulsion of the glutamic acid in the P4 position of collagen. Reversal of this phenomenon by introduction of a basic amino acid in the P4 position of collagen demonstrates the exquisite level of specificity that exists within the peptide-binding groove. In vitro collagen peptide restimulation of lymphocytes harvested from collagen immunized *DRB1*04:01* and *DRB1*04:01*^{K71E} mice revealed similar percentages of CD25⁺Foxp3⁺ regulatory T cells. This observation suggests that the tolerance induced to collagen in *DRB1*04:01*^{K71E} mice was not due to a change in the percentages of collagen-specific regulatory T cells. (Supplemental Figure 3).

The ability to edit the HLA molecule without introducing alloreactivity opens up a host of therapeutic possibilities. Several autoimmune diseases are characterized by a strong association with a single amino acid, including type 1 diabetes, celiac disease, and ankylosing spondylitis. Autologous bone marrow transplants have already been performed safely in patients with autoimmune diseases with limited long-term efficacy in RA,³² and introducing a single resistant amino acid into the bone marrow stem cells could greatly improve their efficacy.

The experiments performed in this study involved peptides that are thought to be involved in the etiology of RA but represent only a limited set of native and citrullinated peptides. In addition, the animal model employed herein allows for assessment of de novo collagen sensitization but does not exhibit autoimmune arthritis with high penetrance or recapitulate RA. It is not known if eliminating the response to a single arthritogenic peptide would be sufficient to alter the course of RA.

ACKNOWLEDGMENTS

The authors would like to acknowledge the staff in the Mouse Genetics Core Facility at National Jewish Health for generation and characterization of the transgenic mice, and the Office of Laboratory Animal Resources Mouse Breeding Core at CU Anschutz and Qiagen Genomic Services for optimizing and performing the Digital Partition PCR assay.

AUTHOR CONTRIBUTIONS





All authors contributed to at least one of the following manuscript preparation roles: conceptualization AND/OR methodology, software, investigation, formal analysis, data curation, visualization, and validation AND drafting or reviewing/editing the final draft. As corresponding author, Dr Roark confirms that all authors have provided the final approval of the version to be published, and takes responsibility for the affirmations regarding article submission (eg, not under consideration by another journal), the integrity of the data presented, and the statements regarding compliance with institutional review board/Declaration of Helsinki requirements.

REFERENCES

1. Deane KD, Demoruelle MK, Kelmenson LB, et al. Genetic and environmental risk factors for rheumatoid arthritis. *Best Pract Res Clin Rheumatol* 2017;31:3–18.

2. Gregersen PK, Silver J, Winchester RJ. The shared epitope hypothesis. An approach to understanding the molecular genetics of susceptibility to rheumatoid arthritis. *Arthritis Rheum* 1987;30(11):1205–1213.
3. Raychaudhuri S, Sandor C, Stahl EA, et al. Five amino acids in three HLA proteins explain most of the association between MHC and seropositive rheumatoid arthritis. *Nat Genet* 2012;44:291–296.
4. Viatte S, Plant D, Han B, et al. Association of HLA-DRB1 haplotypes with rheumatoid arthritis severity, mortality, and treatment response. *JAMA* 2015;313(16):1645–1656.
5. Sharma S, Plant D, Bowes J, et al. HLA-DRB1 haplotypes predict cardiovascular mortality in inflammatory polyarthritis independent of CRP and anti-CCP status. *Arthritis Res Ther* 2022;24:90.
6. MacGregor A, Ollier W, Thomson W, et al. HLA-DRB1*0401/0404 genotype and rheumatoid arthritis: increased association in men, young age at onset, and disease severity. *J Rheumatol* 1995;22:1032–1036.
7. Madsen L, Labrecque N, Engberg J, et al. Mice lacking all conventional HLA class II genes. *Proc Natl Acad Sci USA* 1999;96:10338–10343.
8. Rosloniec EF, Brand DD, Myers LK, et al. Induction of autoimmune arthritis in HLA-DR4 (DRB1*0401) transgenic mice by immunization with human and bovine type II collagen. *J Immunol* 1998;160:2573–2578.
9. Rosloniec EF, Brand DD, Myers LK, et al. An HLA-DR1 transgene confers susceptibility to collagen-induced arthritis elicited with human type II collagen. *J Exp Med* 1997;185:1113–1122.
10. Yatsuda J, Irie A, Harada K, et al. Establishment of HLA-DR4 transgenic mice for the identification of CD4+ T cell epitopes of tumor-associated antigens. *PLoS One* 2013;8:e84908.
11. Pakyari M, Farokhi A, Khosravi-Maharlooei M, et al. A new method for skin grafting in murine model. *Wound Repair Regen* 2016;24:695–704.
12. Anderson KM, Roark CL, Portas M, et al. A Molecular analysis of the shared epitope hypothesis: binding of arthritogenic peptides to DRB1*04 alleles. *Arthritis Rheumatol* 2016;68:1627–1636.
13. Scott-Browne JP, Matsuda JL, Mallevaey T, et al. Germline-encoded recognition of diverse glycolipids by natural killer T cells. *Nat Immunol* 2007;8:1105–1113.
14. Bowerman NA, Falta MT, Mack DG, et al. Mutagenesis of beryllium-specific TCRs suggests an unusual binding topology for antigen recognition. *J Immunol* 2011;187:3694–3703.
15. Roark CL, Anderson KM, Aubrey MT, et al. Arthritogenic peptide binding to DRB1*01 alleles correlates with susceptibility to rheumatoid arthritis. *J Autoimmun* 2016;72:25–32.
16. Deane KD, Norris JM, Holers VM. Preclinical rheumatoid arthritis: identification, evaluation, and future directions for investigation. *Rheum Dis Clin North Am* 2010;36:213–241.
17. Londei M, Savill CM, Verhoef A, et al. Persistence of collagen type II-specific T-cell clones in the synovial membrane of a patient with rheumatoid arthritis. *Proc Natl Acad Sci USA* 1989;86:636–640.
18. Kim HY, Kim WU, Cho ML, et al. Enhanced T cell proliferative response to type II collagen and synthetic peptide CII (255–274) in patients with rheumatoid arthritis. *Arthritis Rheum* 1999;42:2085–2093.
19. Ria F, Penitente R, De Santis M, et al. Collagen-specific T-cell repertoire in blood and synovial fluid varies with disease activity in early rheumatoid arthritis. *Arthritis Res Ther* 2008;10:R135.
20. Brand DD, Latham KA, Rosloniec EF. Collagen-induced arthritis. *Nat Protoc* 2007;2:1269–1275.
21. Malmström V, Kjellén P, Holmdahl R. Type II collagen in cartilage evokes peptide-specific tolerance and skews the immune response. *J Autoimmun* 1998;11:213–221.
22. Dessen A, Lawrence CM, Cupo S, et al. X-ray crystal structure of HLA-DR4 (DRA*0101, DRB1*0401) complexed with a peptide from human collagen II. *Immunity* 1997;7:473–481.
23. Coppin HL, Carmichael P, Lombardi G, et al. Position 71 in the alpha helix of the DR beta domain is predicted to influence peptide binding and plays a central role in allorecognition. *Eur J Immunol* 1993;23:343–349.
24. Benichou G, Yamada Y, Yun SH, et al. Immune recognition and rejection of allogeneic skin grafts. *Immunotherapy* 2011;3:757–770.
25. Yarwood A, Huizinga TW, Worthington J. The genetics of rheumatoid arthritis: risk and protection in different stages of the evolution of RA. *Rheumatology (Oxford)* 2016;55:199–209.
26. Todd JA, Wicker LS. Genetic protection from the inflammatory disease type 1 diabetes in humans and animal models. *Immunity* 2001;15:387–395.
27. Wicker LS. Major histocompatibility complex-linked control of autoimmunity. *J Exp Med* 1997;186:973–975.
28. Wicker LS, Todd JA, Peterson LB. Genetic control of autoimmune diabetes in the NOD mouse. *Annu Rev Immunol* 1995;13:179–200.
29. Ting YT, Petersen J, Ramarathnam SH, et al. The interplay between citrullination and HLA-DRB1 polymorphism in shaping peptide binding hierarchies in rheumatoid arthritis. *J Biol Chem* 2018;293:3236–3251.
30. McInnes IB, Schett G. The pathogenesis of rheumatoid arthritis. *N Engl J Med* 2011;365:2205–2219.
31. Hennecke J, Wiley DC. Structure of a complex of the human alpha/beta T cell receptor (TCR) HA1.7, influenza hemagglutinin peptide, and major histocompatibility complex class II molecule, HLA-DR4 (DRA*0101 and DRB1*0401): insight into TCR cross-restriction and alloreactivity. *J Exp Med* 2002;195:571–581.
32. Muthu S, Jeyaraman M, Ranjan R, et al. Remission is not maintained over 2 years with hematopoietic stem cell transplantation for rheumatoid arthritis: a systematic review with meta-analysis. *World J Biol Chem* 2021;12:114–130.

Development of Extramusculoskeletal Manifestations in Upadacitinib-Treated Patients With Psoriatic Arthritis or Axial Spondyloarthritis

Denis Poddubnyy,¹  Bhumik Parikh,² Dirk Elewaut,³  Victoria Navarro-Compán,⁴ Stefan Siebert,⁵ 
Michael Paley,⁶  Derek Coombs,² Ivan Lagunes,² Ana Biljan,² Priscila Nakasato,² Peter Wung,²
and Ennio Lubrano⁷

Objective. To assess the development of extramusculoskeletal manifestations (EMMs) among patients with psoriatic arthritis (PsA) or axial spondyloarthritis (axSpA) treated with upadacitinib 15 mg.

Methods. Data (cutoff: August 15, 2022) from five clinical trials in PsA (2), radiographic axSpA (r-axSpA; previously ankylosing spondylitis) (2), and nonradiographic axSpA (nr-axSpA) (1) were analyzed. Treatment-emergent adverse events of EMMs including uveitis, inflammatory bowel disease (IBD), and psoriasis were assessed in patients treated with placebo, upadacitinib 15 mg, or adalimumab (PsA only) and are reported as exposure-adjusted event rates (events per 100 patient-years [E/100 PY]).

Results. Most patients (87.1%–99.3%) did not have a history of EMMs at baseline. In PsA, development of uveitis and IBD were low regardless of treatment or prior EMM history; rates were similar with upadacitinib 15 mg and adalimumab. In r-axSpA, development of uveitis was numerically lower (E/100 PY) in patients treated with upadacitinib 15 mg (2.8) versus placebo (7.5) and in patients with no history of uveitis (upadacitinib 15 mg 0.6; placebo 1.2) versus a history of uveitis (upadacitinib 15 mg 2.1; placebo 6.2); occurrence of IBD and psoriasis were low regardless of treatment or history. In nr-axSpA, development of uveitis was low regardless of history but was numerically lower in patients treated with upadacitinib 15 mg (0.9) versus placebo (2.1); occurrence of IBD and psoriasis were low or absent.

Conclusion. In patients with spondyloarthritis, development of EMMs was generally low with upadacitinib 15 mg. Uveitis was numerically lower in patients treated with upadacitinib 15 mg versus placebo, and particularly in r-axSpA. Regardless of treatment in r-axSpA, having a history of uveitis appeared to predispose patients for future uveitis events.

INTRODUCTION

Spondyloarthritis (SpA), which includes psoriatic arthritis (PsA) and axial SpA (axSpA), encompassing both radiographic axSpA (r-axSpA; previously referred to as ankylosing spondylitis

[AS])¹ and nonradiographic axSpA (nr-axSpA), is a group of inflammatory, immune-mediated diseases characterized by peripheral arthritis and/or axial disease, enthesitis, and dactylitis.^{2–4} Extramusculoskeletal manifestations (EMMs), including uveitis, inflammatory bowel disease (IBD), and psoriasis, are

ClinicalTrials.gov identifiers: NCT03104400, NCT03104374, NCT03178487, and NCT04169373.

A portion of these data were originally presented at the Annual European Congress of Rheumatology of EULAR 2023, Milan, Italy. Poddubnyy D, Parikh B, Elewaut D, et al. Development of extra-musculoskeletal manifestations in upadacitinib-treated patients with psoriatic arthritis, ankylosing spondylitis, or non-radiographic axial spondyloarthritis. *Ann Rheum Dis* 2023;82:40–41.

Supported by AbbVie.

¹Denis Poddubnyy, MD, PhD, MSc: University of Toronto, Toronto, Ontario, Canada, and Charité-Universitätsmedizin Berlin, Germany; ²Bhumik Parikh, PharmD, MBA, Derek Coombs, BA, MPH, Ivan Lagunes, MD, Ana Biljan, BSN, RN, MBA, Priscila Nakasato, MD, Peter Wung, MD, MHS: AbbVie, Inc, North Chicago, Illinois; ³Dirk Elewaut, MD, PhD: Ghent University Hospital and Ghent University, Ghent, Belgium; ⁴Victoria Navarro-Compán, MD, PhD: Hospital Universitario La Paz, IdiPAZ, Madrid, Spain; ⁵Stefan Siebert, MBBCh, FRCP, PhD: University of Glasgow, Glasgow, United Kingdom; ⁶Michael Paley,

MD, PhD: Washington University School of Medicine, St. Louis, Missouri; ⁷Ennio Lubrano, MD, PhD, MSc: University of Molise, Campobasso, Italy.

AbbVie is committed to responsible data sharing regarding the clinical trials we sponsor. This includes access to anonymized, individual, and trial-level data (analysis data sets), as well as other information (eg, protocols, clinical study reports, or analysis plans), as long as the trials are not part of an ongoing or planned regulatory submission. This includes requests for clinical trial data for unlicensed products and indications. These clinical trial data can be requested by any qualified researchers who engage in rigorous, independent, scientific research and will be provided following review and approval of a research proposal, Statistical Analysis Plan (SAP), and execution of a Data Sharing Agreement (DSA). Data requests can be submitted at any time after approval in the United States and Europe and after acceptance of this manuscript for publication. The data will be accessible for 12 months, with possible extensions considered. For more information on the process or to submit a request, visit the following link: <https://vivli.org/ourmember/abbvie/> then select “Home.”

also commonly observed in patients with SpA.^{5,6} Uveitis (often specifically anterior uveitis) is reported in the literature to be the most common EMM in patients with SpA,⁷ with reported rates from 2.0% to 25.1% in PsA,^{7,8} 33.2% to more than 50% in r-axSpA,^{7,9,10} and 2.2% to 15.9% in nr-axSpA.^{5,11} Furthermore, patients with SpA and a history of uveitis appear to be at an increased risk of recurrence/flare compared with patients with no history, with several studies showing that most (or sometimes even all) cases of uveitis occurred in patients with a history versus new onset events.^{12–14}

EMMs are an important consideration for patients with SpA and treating clinicians, as they are often associated with higher disease activity and greater functional impairment, as well as substantial economic burden, including increased health care resource utilization and costs.¹⁵ In the latest Group for Research and Assessment of Psoriasis and Psoriatic Arthritis (GRAPPA) treatment recommendations presented in 2021,⁴ uveitis and IBD were elevated to PsA-related conditions and assessed at the same level as other PsA domains, which is a change from the previous guidance in 2015.¹⁶ Similarly, EMMs are now included as part of the mandatory Assessment of Spondyloarthritis International Society (ASAS)-Outcome Measures in Rheumatology (OMERACT) core domain set in trials assessing disease-modifying antirheumatic drug therapies.¹⁷ Combined, these guidance from clinical experts demonstrate the importance of EMMs when evaluating treatment options for patients with PsA or axSpA.

Upadacitinib is an oral JAK inhibitor with demonstrated efficacy for the treatment of PsA,^{18,19} r-axSpA,^{20,21} and nr-axSpA,²² as well as an established safety profile consistent with the observed long-term data in rheumatoid arthritis.^{23,24} However, there are limited data on the impact of JAK inhibitors, including upadacitinib, on the development of EMMs in patients with SpA. There is strong support for the use of JAK inhibitors to treat IBD²⁵ and psoriatic disease,²⁶ but more studies are needed to assess the impact of JAK inhibition on uveitis. In contrast, other advanced therapies, such as the interleukin (IL)-17 inhibitors ixekizumab, secukinumab, and bimekizumab, include mention of EMMs (ie, IBD) in the warnings and precautions section of their prescribing information, further demonstrating the importance of considering EMMs when making treatment decisions. A better understanding of the impact of upadacitinib on the occurrence of EMMs may help clinicians make informed treatment decisions and guide future treatment recommendations for patients with SpA. The objective of this post hoc analysis is to assess the development (new onset or flares) of EMMs among patients with PsA or axSpA treated with upadacitinib 15 mg, placebo, or the active

comparator adalimumab (tumor necrosis factor [TNF] inhibitor; evaluated in one PsA trial only) in the SELECT clinical trials.

MATERIALS AND METHODS

Patients and study design. This post hoc analysis describes data (cutoff August 15, 2022) from five phase 3 upadacitinib trials from the SELECT clinical program, including PsA (2 trials), r-axSpA (2 trials, 1 phase 2/3), and nr-axSpA (1 trial). In the SELECT-AXIS 1 and SELECT-AXIS 2 trials, patients were required to meet the modified New York criteria for AS based on central reading of radiographs of the sacroiliac joints to be included in the studies. For this post hoc analysis, the term r-axSpA, instead of AS, has been used throughout the manuscript to align with recent recommendations.¹

In the SELECT trials for PsA, r-axSpA, and nr-axSpA, adults (≥ 18 years of age) were randomized to receive placebo or once daily oral upadacitinib 15 mg (approved dose). Additionally, in one of the PsA studies, patients also had the opportunity to be randomized to receive the active comparator adalimumab 40 mg delivered subcutaneously every other week. An overview of the SELECT trials for PsA,^{18,19} r-axSpA,^{20,21} and nr-axSpA,²² including details about the patient populations assessed, sample size per treatment arm, and study duration, is provided in the Supplemental Materials (Supplemental Table 1).

All studies were conducted in accordance with the International Council for Harmonisation of Technical Requirements for Pharmaceuticals for Human Use (ICH) guidelines, applicable regulations governing clinical trial conduct, and the Declaration of Helsinki 1964 and its later amendments. The trial protocols were approved by an independent ethics committee/institutional review board at each study site per Good Clinical Practice. All patients provided written informed consent prior to screening.

Outcomes. EMMs, including uveitis, IBD, and psoriasis, were captured as part of the patient's general medical history at baseline and were reported as treatment-emergent adverse events (TEAEs) during the studies by the investigators. The generation of efficacy data can be challenging given the relapsing-remitting course of uveitis in SpA,^{27,28} lending support to the approach used in this analysis. As psoriasis is considered a core domain of PsA,⁴ it was only evaluated as an EMM in r-axSpA and nr-axSpA for this analysis. In one of the trials for r-axSpA (SELECT-AXIS 1), patient history of uveitis at baseline was captured using an additional form, which was not used in the other SELECT studies, which instead employed a general medical history form to capture such information. TEAEs were defined as an

Additional supplementary information cited in this article can be found online in the Supporting Information section (<http://onlinelibrary.wiley.com/doi/10.1002/art.43069>).

Author disclosures and graphical abstract are available at <https://onlinelibrary.wiley.com/doi/10.1002/art.43069>.

Address correspondence via email to Denis Poddubnyy, MD, at denis.poddubnyy@uhn.ca.

Submitted for publication April 16, 2024; accepted in revised form November 8, 2024.

adverse event (AE) with onset on or after the first dose of study drug and less than or equal to 30 days after the last dose of study drug for placebo or upadacitinib 15 mg, or less than or equal to 70 days after the last dose of study drug for adalimumab. AEs were coded according to the Medical Dictionary for Regulatory Activities version 25.0 and associated preferred terms. For this analysis, these preferred terms were manually grouped into categories representing each EMM (ie, uveitis, IBD, and psoriasis) as shown in Supplemental Table 2. For the results, events of uveitis were further categorized as anterior uveitis (including iritis and iridocyclitis) or uveitis, not otherwise specified. For IBD, events were further categorized as Crohn's disease, ulcerative colitis, and colitis, not otherwise specified. EMMs are summarized for PsA (pooled placebo, pooled upadacitinib 15 mg, and adalimumab 40 mg), r-axSpA (pooled placebo and pooled upadacitinib 15 mg), and nr-axSpA (placebo and upadacitinib 15 mg), as well as for each individual SELECT trial for PsA, r-axSpA, and nr-axSpA without being pooled across treatment groups.

Statistical analysis. For this post hoc analysis, safety data are summarized for patients treated with placebo in accordance with the study design (ie, length of double-blind placebo-controlled period), whereas upadacitinib 15 mg and adalimumab are summarized up until data cutoff. For PsA, pooled placebo was assessed up to week 24; pooled upadacitinib 15 mg and adalimumab were assessed up to the data cutoff date. For r-axSpA, pooled placebo was assessed up to week 14 and pooled upadacitinib 15 mg up to the data cutoff date. For nr-axSpA, placebo was assessed up to week 52 and upadacitinib 15 mg up to the data cutoff date. Data shown for upadacitinib 15 mg comprises patients who were originally randomized to upadacitinib 15 mg, as well as patients randomized to placebo who were later switched to upadacitinib 15 mg. In addition, EMM data that have not been pooled across treatment groups were assessed according to the timing described above and are presented separately for each SELECT trial.

EMMs are reported as exposure-adjusted event rates, defined as events per 100 patient-years (E/100 PY), with 95% confidence intervals (CIs) calculated using the exact method for the Poisson mean. Each EMM event was counted in the numerator, which may include multiple events in a single patient. Data are stratified by patients with a reported history (flare) of the respective EMM versus patients without a reported history (new onset).

To further characterize patients with a uveitis event, human leukocyte antigen B27 (HLA-B27) status in patients with r-axSpA or nr-axSpA with and without a history of uveitis was assessed. In addition, disease activity status, as determined by Axial Spondyloarthritis Disease Activity Score (ASDAS; < 2.1 vs ≥ 2.1), Bath Ankylosing Spondylitis Disease Activity Index (BASDAI; < 4.0 vs ≥ 4.0), and high-sensitivity C-reactive protein (hsCRP; ≤ 2.87 mg/L vs > 2.87 mg/L) cutoffs, in patients with axSpA (r-axSpA and nr-axSpA combined) who received upadacitinib 15 mg with

and without a uveitis event are described. Patients with axSpA who received placebo were not included in the disease activity status analysis because of the low number of events. For patients with a uveitis event, the latest available ASDAS, BASDAI, and hsCRP data prior to event onset were used. For patients without a uveitis event, disease activity was assessed at approximately 52 weeks of upadacitinib 15 mg exposure to most closely align with the median time to event in patients who experienced uveitis. Because of the low number of uveitis events in PsA, as well as the low number of IBD and psoriasis events across PsA, r-axSpA, and nr-axSpA, disease activity status was not assessed for these EMMs.

RESULTS

Analysis population. In total, data from 1,095 placebo-treated (PY = 489.1), 1,789 upadacitinib 15 mg-treated (PY = 3,689.4), and 429 adalimumab-treated (PY = 1,146.4) patients are included in this analysis. Patient baseline characteristics stratified by history of each respective EMM (ie, uveitis, IBD, and psoriasis) in PsA, r-axSpA, and nr-axSpA are shown in Supplemental Tables 3–5. Across PsA, r-axSpA, and nr-axSpA, patients with a history of uveitis or IBD at baseline tended to have longer disease durations, and a higher proportion of patients with a history of IBD at baseline were more likely to use tobacco or nicotine, compared with those without a history. In general, patients with r-axSpA or nr-axSpA who had a history of uveitis at baseline were more likely to be HLAB27 positive (HLA-B27+), and those with a history of IBD or psoriasis at baseline tended to have higher hsCRP values than those without a history. Across PsA, r-axSpA, and nr-axSpA, and regardless of study treatment (ie, placebo, upadacitinib 15 mg, or adalimumab), the majority of patients (range 87.1%–99.3%) did not report a history of EMMs at baseline (Table 1). In PsA, IBD was more frequently reported as a baseline characteristic than uveitis, whereas uveitis was the most commonly reported EMM at baseline in r-axSpA and nr-axSpA.

Development of EMMs. Uveitis. In PsA, development of uveitis, categorized as anterior uveitis (including iritis and iridocyclitis) or uveitis, not otherwise specified, was low regardless of treatment or history (Figure 1A). The rates of uveitis (new onset or recurrent flare) were similar in patients treated with upadacitinib 15 mg or adalimumab. In r-axSpA, development of uveitis was numerically lower (E/100 PY [95% CI]) in patients treated with upadacitinib 15 mg (total 2.8 [1.8–4.1]) versus placebo (total 7.5 [2.7–16.3]) and in patients with no history of uveitis (upadacitinib 15 mg 0.6 [0.2–1.4]; placebo 1.2 [0.0–6.9]) versus in those with a history (upadacitinib 15 mg 2.1 [1.3–3.3]; placebo 6.2 [2.0–14.5]) (Figure 1B). During the double-blind placebo-controlled period (14 weeks), uveitis was also numerically lower in patients with r-axSpA treated with upadacitinib 15 mg (total 1.2 [0.0–6.9]) versus placebo (total 7.5 [2.7–16.3]) and in patients with no

Table 1. History of EMMs at baseline across PsA, r-axSpA, and nr-axSpA*

EMM	PsA			r-axSpA		nr-axSpA	
	PBO, n = 635	UPA 15 mg QD ^a , n = 907	ADA 40 mg EOW, n = 429	PBO, n = 303	UPA 15 mg QD ^a , n = 596	PBO, n = 157	UPA 15 mg QD ^a , n = 286
Uveitis	5 (0.8)	8 (0.9)	3 (0.7)	39 (12.9)	76 (12.8)	11 (7.0)	21 (7.3)
IBD	10 (1.6)	13 (1.4)	5 (1.2)	7 (2.3)	16 (2.7)	6 (3.8)	8 (2.8)
Psoriasis	N/A ^b	N/A ^b	N/A ^b	10 (3.3)	19 (3.2)	4 (2.5)	7 (2.4)

* Values are the number (%). ADA, adalimumab; EMM, extramusculoskeletal manifestation; EOW, every other week; IBD, inflammatory bowel disease; N/A, not applicable; nr-axSpA, nonradiographic axial spondyloarthritis; PBO, placebo; PsA, psoriatic arthritis; QD, once daily; r-axSpA, radiographic axial spondyloarthritis; UPA, upadacitinib.

^a Includes any UPA exposure, including patients who switched from PBO to UPA 15 mg up to data cutoff (August 15, 2022).

^b As psoriasis is considered a core manifestation of PsA, it was only evaluated as an EMM in r-axSpA and nr-axSpA.

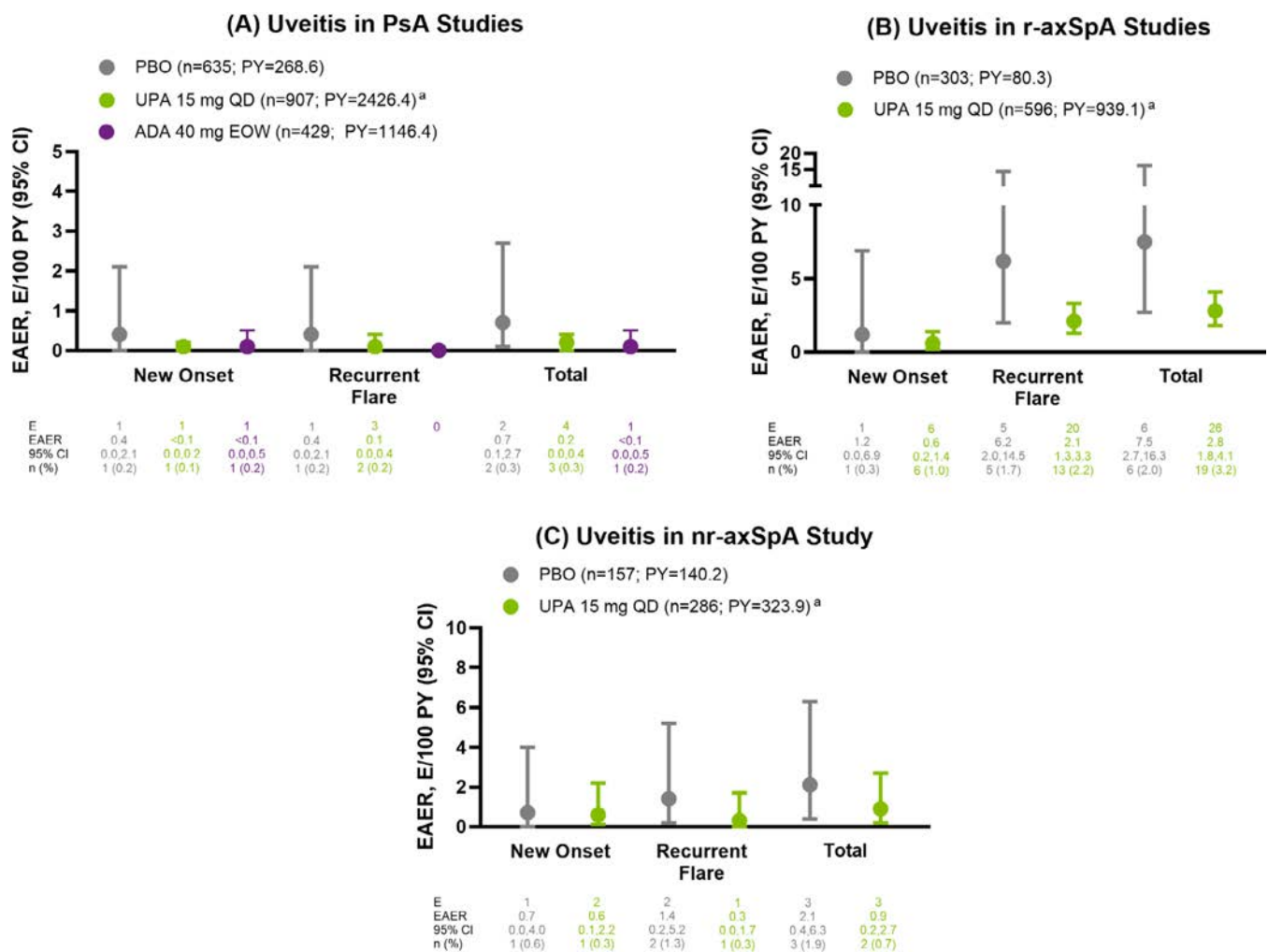


Figure 1. Development of uveitis in patients treated with upadacitinib across PsA, r-axSpA, and nr-axSpA. Development of uveitis in (A) PsA, (B) r-axSpA, and (C) nr-axSpA, stratified by history. EMM subtypes in PsA (E/100 PY [95% CI] [E]): anterior uveitis (including iritis and iridocyclitis) in PBO (0), UPA 15 mg (0.1 [0.0–0.4] [3]), and ADA (0); uveitis, not otherwise specified in PBO (0.7 [0.1–2.7] [2]), UPA 15 mg (< 0.1 [0.0–0.2] [1]), and ADA (< 0.1 [0.0–0.5] [1]). EMM subtypes in r-axSpA: anterior uveitis in PBO (5.0 [1.4–12.8] [4]) and UPA 15 mg (2.0 [1.2–3.2] [19]); uveitis, not otherwise specified in PBO (2.5 [0.3–9.0] [2]) and UPA 15 mg (0.7 [0.3–1.5] [7]). EMM subtypes in nr-axSpA: anterior uveitis in PBO (1.4 [0.2–5.2] [2]) and UPA 15 mg (0.9 [0.2–2.7] [3]); uveitis, not otherwise specified in PBO (0.7 [0.0–4.0] [1]) and UPA 15 mg (0). ^aAny exposure to UPA, including patients who switched from PBO to UPA 15 mg. ADA, adalimumab; CI, confidence interval; E/100 PY, events per 100 patient-years; E, event; EAER, exposure-adjusted event rate; EMM, extramusculoskeletal manifestation; EOW, every other week; NOS, not otherwise specified; nr-axSpA, nonradiographic axial spondyloarthritis; PBO, placebo; PsA, psoriatic arthritis; PY, patient-year; QD, once daily; r-axSpA, radiographic axial spondyloarthritis; UPA, upadacitinib.

history of uveitis (upadacitinib 15 mg 0; placebo 1.2 [0.0–6.9]) versus in those with a history (upadacitinib 15 mg 1.2 [0.0–6.9]; placebo 6.2 [2.0–14.5]) (Supplemental Table 6). In nr-axSpA, development of uveitis was low regardless of history, whereas the total rate was numerically lower in patients treated with upadacitinib 15 mg (0.9 [0.2–2.7]) versus placebo (2.1 [0.4–6.3]) (Figure 1C). During the double-blind placebo-controlled period (52 weeks), the total rate of uveitis in nr-axSpA was similar between upadacitinib 15 mg (2.2 [0.5–6.4]) and placebo (2.1 [0.4–6.3]) (Supplemental Table 6). Anterior uveitis, including iritis and iridocyclitis, was the most frequently reported subtype of uveitis in patients treated with upadacitinib 15 mg across PsA (0.1 [0.0–0.4]), r-axSpA (2.0 [1.2–3.2]), and nr-axSpA (0.9 [0.2–2.7]), with 75.8% (n = 25/33) of the total cases being identified as anterior uveitis (Table 2). Across PsA, r-axSpA, and nr-axSpA, most cases of uveitis in patients treated with upadacitinib 15 mg were mild or moderate in severity, were not identified as serious AEs, and did not lead to discontinuation of study drug (Supplemental Table 7). In r-axSpA and nr-axSpA, nearly all events of uveitis (new onset and recurrent flare) with either placebo or upadacitinib 15 mg treatment occurred in patients that were HLA-B27+ at baseline (Table 3). In axSpA (r-axSpA and nr-axSpA combined), patients treated with upadacitinib 15 mg who experienced an event of uveitis were generally in disease control, as determined by ASDAS less than 2.1, BASDAI less than 4.0, and hsCRP less than or equal to 2.87 mg/L, with no notable differences observed compared to patients without events of uveitis (Supplemental Table 8).

IBD. In PsA, development of IBD was low regardless of treatment or history (Figure 2A). Similar to uveitis, the rates of IBD (new onset or flare) were similar between upadacitinib 15 mg and adalimumab. In both r-axSpA (Figure 2B) and nr-axSpA (Figure 2C), occurrence of IBD was also low regardless of treatment or history. In PsA and r-axSpA, Crohn's disease (PsA < 0.1 [0.0–0.2]; r-axSpA 0.1 [0.0–0.6]) and colitis, not otherwise specified (PsA < 0.1 [0.0–0.3]; r-axSpA 0.1 [0.0–0.6]), were the most frequently reported subtype of IBD in patients treated with upadacitinib 15 mg, whereas ulcerative colitis (0.3 [0.0–1.7]) was most frequently reported in nr-axSpA (Table 2). Across the low number of cases of IBD in PsA, r-axSpA, and nr-axSpA in patients treated with upadacitinib 15 mg, severity varied, and no cases led to discontinuation of study drug (Supplemental Table 7).

Psoriasis. As stated previously, psoriasis was not evaluated in PsA, as it is considered a core domain of the disease. Additionally, it should be noted that the different subtypes of psoriasis being reported were not able to be differentiated by the investigators, although the majority were believed to be of the plaque subtype. In r-axSpA, development of psoriasis (new onset or flare) was infrequent in patients treated with placebo or upadacitinib 15 mg (Figure 3A), and in nr-axSpA, no events of psoriasis were reported (Figure 3B). In r-axSpA, most cases of psoriasis in patients treated with upadacitinib 15 mg were mild, no cases

Table 2. Summary of EMM subtype as event rates per 100 patient-years in patients treated with upadacitinib across PsA, r-axSpA, and nr-axSpA*

	PsA		r-axSpA		nr-axSpA	
	UPA 15 mg QD ^b , n = 907	ADA 40 mg EOW, n = 429	PBO, n = 303	UPA 15 mg QD ^b , n = 596	PBO, n = 157	UPA 15 mg QD ^b , n = 286
EMM ^a						
Total uveitis, n	2	1	6	26	3	3
Anterior uveitis (includes iritis and iridocyclitis)	0	0	5.0 (1.4–12.8) [4]	2.0 (1.2–3.2) [19]	1.4 (0.2–2.7) [2]	0.9 (0.2–2.7) [3]
Uveitis, not otherwise specified	0.7 (0.1–2.7) [2]	<0.1 (0.0–0.5) [1]	2.5 (0.3–9.0) [2]	0.7 (0.3–1.5) [7]	0.7 (0.0–4.0) [1]	0
Total IBD, n	1	0	1	2	0	1
Crohn's disease	0.4 (0.0–2.1) [1]	0	0	0.1 (0.0–0.6) [1]	0	0
Ulcerative colitis	0	0	0	0	0	0.3 (0.0–1.7) [1]
Colitis, not otherwise specified	0	0	1.2 (0.0–6.9) [1]	0.1 (0.0–0.6) [1]	0	0
Total psoriasis, n	N/A ^c	N/A ^c	1	4	0	0
Psoriasis	—	—	1.2 (0.0–6.9) [1]	0.4 (0.1–1.1) [4]	0	0

* Data are presented as EMMs, defined as E/100 PYs with (95% CI) and [number of events] shown, unless otherwise indicated. ADA, adalimumab; CI, confidence interval; E, events; EAER, exposure-adjusted event rate; EMM, extramusculoskeletal manifestation; EOW, every other week; IBD, inflammatory bowel disease; MedDRA, Medical Dictionary for Regulatory Activities; N/A, not applicable; nr-axSpA, nonradiographic axial spondyloarthritis; PBO, placebo; PsA, psoriatic arthritis; PY, patient-year; QD, once daily; r-axSpA, radiographic axial spondyloarthritis; UPA, upadacitinib.

^a MedDRA preferred terms for each EMM were defined using standardized or company MedDRA query search criteria.

^b Includes any UPA exposure, including patients who switched from PBO to UPA 15 mg up to data cutoff (August 15, 2022).

^c As psoriasis is considered a core manifestation of PsA, it was only evaluated as an EMM in r-axSpA and nr-axSpA.

Table 3. Development of uveitis by HLA-B27 status in r-axSpA and nr-axSpA*

	PBO, n = 303			UPA 15 mg QD ^a , n = 596		
	HLA-B27+, n = 241	HLA-B27–, n = 59	Missing, n = 3	HLA-B27+, n = 487	HLA-B27–, n = 107	Missing, n = 2
r-axSpA						
Patients with uveitis	6 (2.5)	0	0	18 (3.7)	1 (0.9)	0
History of uveitis	5 (2.1)	0	0	12 (2.5)	1 (0.9)	0
No history of uveitis	1 (0.4)	0	0	6 (1.2)	0	0
	PBO, n = 157			UPA 15 mg QD ^a , n = 286		
	HLA-B27+, n = 93	HLA-B27–, n = 63	Missing, n = 1	HLA-B27+, n = 167	HLA-B27–, n = 117	Missing, n = 2
nr-axSpA						
Patients with uveitis	3 (3.2)	0	0	2 (1.2)	0	0
History of uveitis	2 (2.2)	0	0	1 (0.6)	0	0
No history of uveitis	1 (1.1)	0	0	1 (0.6)	0	0

* Values are the number (%). HLA-B27 status was not determined in the PsA studies. nr-axSpA, nonradiographic axial spondyloarthritis; PBO, placebo; PsA, psoriatic arthritis; QD, once daily; r-axSpA, radiographic axial spondyloarthritis; UPA, upadacitinib.

^a Includes any UPA exposure, including patients who switched from PBO to UPA 15 mg up to data cutoff (August 15, 2022).

were identified as serious AEs, and no cases led to discontinuation of study drug (Supplemental Table 7).

EMM data for the individual SELECT trials across PsA, r-axSpA, and nr-axSpA are presented in Supplemental Table 9. In general, the findings are consistent with those observed in the aforementioned pooled analysis.

DISCUSSION

The objective of this post hoc analysis was to assess the impact of upadacitinib on the development of EMMs from the SpA SELECT clinical trials, as there are limited data on the impact of JAK inhibitors on EMMs, and in particular uveitis, in SpA. Across PsA, r-axSpA, and nr-axSpA, the development (new onset or flare) of EMMs was generally low. Of the EMMs assessed, uveitis, of which the majority of the cases were categorized as anterior uveitis (including iridocyclitis and iritis), was the most prevalent, although infrequent, with the highest rates observed in r-axSpA. Reported cases of uveitis categorized as “not otherwise specified” could not be classified more specifically because of how the verbatim term was reported by the investigator. However, based on the prevalence of anterior uveitis in the patient population with SpA,^{7,27,29} it is likely that most of these cases may have been anterior uveitis. Although the rates of EMMs in this analysis were relatively low, numerical differences were detected favoring reduced occurrence with upadacitinib 15 mg versus placebo. Additionally, we found that having a history of uveitis in r-axSpA appeared to predispose patients to recurrent flares of uveitis during the study. This finding is consistent with the literature, where it is reported that more than 50% of patients with SpA will have recurrent uveitis.⁷

Across PsA, r-axSpA, and nr-axSpA, the rate of uveitis in this analysis of the SELECT trials was numerically lower in patients treated with upadacitinib 15 mg versus placebo, which was particularly evident in patients with r-axSpA. In PsA, rates of uveitis

were similar in patients treated with upadacitinib 15 mg or adalimumab. Although an adalimumab comparator arm was not included in the axSpA SELECT studies, previously reported rates of uveitis in patients with axSpA treated with adalimumab are similar to that shown here for PsA,³⁰ with higher rates observed using registry data.^{14,31} Additionally, in the literature, a recent phase 2 study of noninfectious uveitis reported a reduced risk of flares with another JAK inhibitor (filgotinib) compared with placebo.³² Furthermore, in the current analysis, regardless of treatment, nearly all events of uveitis in r-axSpA and nr-axSpA occurred in patients that were HLA-B27+ at baseline. Of note, HLA-B27 status was not gathered in the PsA studies, and therefore could not be assessed here. Previous studies in patients with SpA have found that the development of acute anterior uveitis was greater in patients that were HLA-B27+,^{28,33} and that an HLA-B27+ status resulted in a 2.6-fold to 4.2-fold increased risk of developing uveitis.^{7,33} Finally, patients with axSpA (r-axSpA and nr-axSpA combined) treated with upadacitinib 15 mg who experienced a uveitis event had a similar disease activity state (as determined by ASDAS, BASDAI, and hsCRP cutoffs) as patients who did not have uveitis. This result is not entirely surprising, as a previous study found that patients with axSpA with current/recent anterior uveitis had lower disease activity as determined by BASDAI score than patients with no current/recent anterior uveitis.¹⁵ Overall, these data indicate that a uveitis flare may occur even in a patient with sufficient control of musculoskeletal disease activity.

Several recent reviews have summarized the impact of biologic therapies, such as TNF and IL-17 inhibitors, on the development of uveitis in patients with SpA.^{27,34,35} Adalimumab has been shown to effectively reduce the rate of anterior uveitis flares in patients with r-axSpA,¹² whereas the TNF inhibitor etanercept has been less successful in preventing uveitis flares in r-axSpA than adalimumab or infliximab,^{31,36–38} with certolizumab pegol demonstrating similar efficacy to adalimumab and infliximab.^{13,39} Evidence from several small retrospective studies suggest that

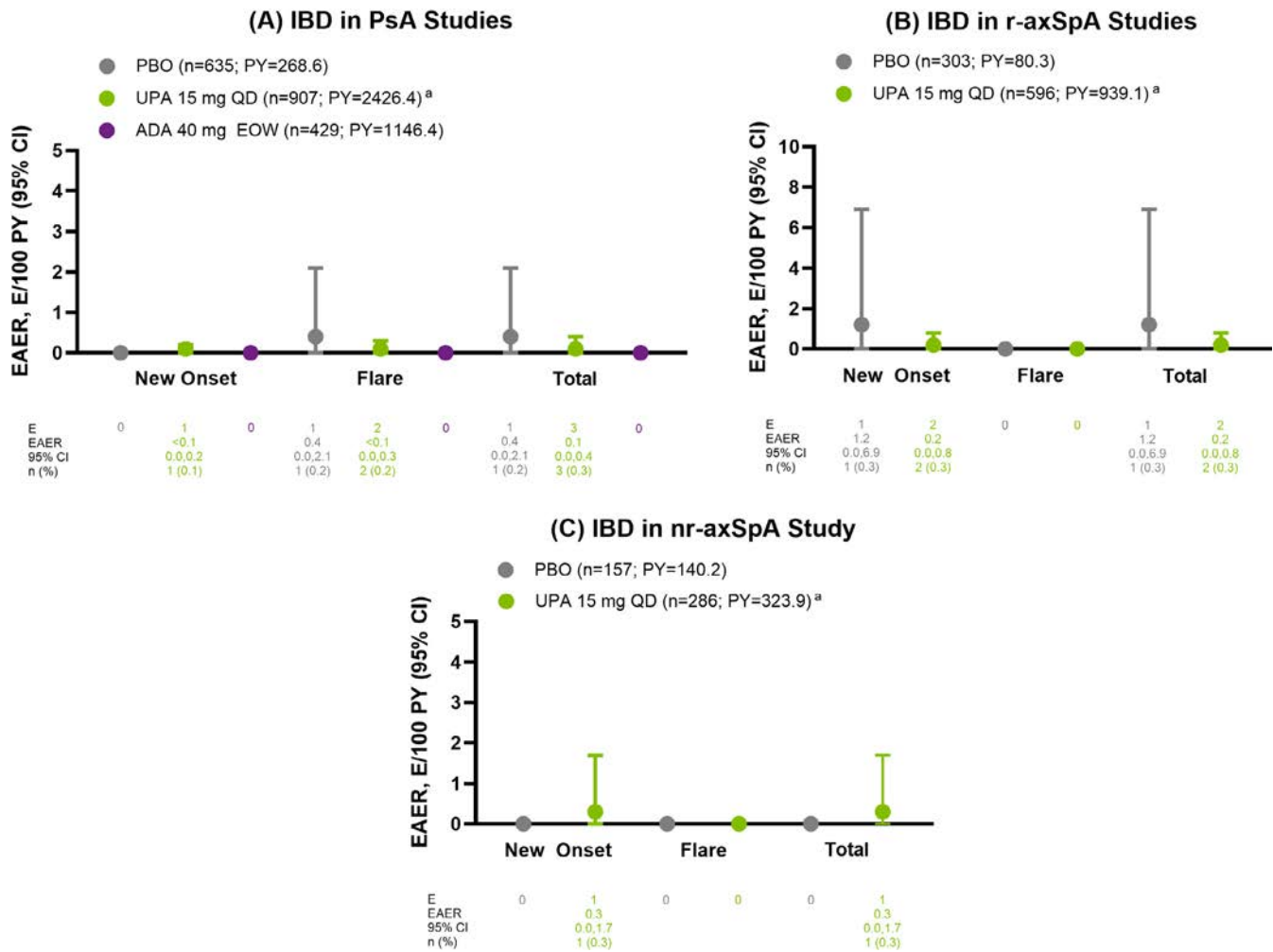


Figure 2. Development of IBD in patients treated with upadacitinib across PsA, r-axSpA, and nr-axSpA. Development of IBD in (A) PsA, (B) r-axSpA, and (C) nr-axSpA stratified by history. EMM subtypes in PsA (E/100 PY [95% CI] [E]): Crohn's disease in PBO (0.4 [0.0–2.1] [1]), UPA 15 mg (< 0.1 [0.0–0.2] [1]), and ADA (0); ulcerative colitis in PBO (0), UPA 15 mg (0), and ADA (0); colitis, not otherwise specified in PBO (0), UPA 15 mg (< 0.1 [0.0–0.3] [2]), and ADA (0). EMM subtypes in r-axSpA: Crohn's disease in PBO (0) and UPA 15 mg (0.1 [0.0–0.6] [1]); ulcerative colitis in PBO (0) and UPA 15 mg (0); colitis, not otherwise specified in PBO (1.2 [0.0–6.9] [1]) and UPA 15 mg (0.1 [0.0–0.6] [1]). EMM subtypes in nr-axSpA: Crohn's disease in PBO (0) and UPA 15 mg (0); ulcerative colitis in PBO (0) and UPA 15 mg (0.3 [0.0–1.7] [1]); colitis, not otherwise specified in PBO (0) and UPA 15 mg (0). ^aAny exposure to UPA, including patients who switched from PBO to UPA 15 mg. ADA, adalimumab; CI, confidence interval; E/100 PY, events per 100 patient-years; E, event; EAER, exposure-adjusted event rate; EMM, extramusculoskeletal manifestation; EOW, every other week; IBD, inflammatory bowel disease; NOS, not otherwise specified; nr-axSpA, nonradiographic axial spondyloarthritis; PBO, placebo; PsA, psoriatic arthritis; PY, patient-year; QD, once daily; r-axSpA, radiographic axial spondyloarthritis; UPA, upadacitinib.

golimumab may help prevent uveitis flares in patients with SpA, especially in those patients who are refractory to other TNF inhibitors^{40–42}; however, larger scale studies are needed to confirm these findings.⁴³ In contrast, secukinumab, an IL-17A inhibitor, was ineffective in treating patients with noninfectious uveitis⁴⁴ and resulted in a higher risk of anterior uveitis in patients with SpA compared with patients treated with TNF inhibitors.¹⁴ Indeed, both the GRAPPA treatment recommendations and ASAS-EULAR guidelines advise that patients with a history of recurrent uveitis be treated with a monoclonal TNF inhibitor, such as adalimumab, infliximab, certolizumab pegol, or golimumab, and do not recommend treatment with etanercept.^{3,4} However,

a recent study in patients with axSpA found a lower incidence of uveitis with bimekizumab (an IL-17A/F inhibitor) at week 16 compared with placebo, and incidence appeared to remain low with long-term treatment.⁴⁵ Altogether, results from this analysis with upadacitinib in patients with SpA showed numerically reduced rates of uveitis flare with study drug compared with placebo, contributing to our understanding of the impact of JAK inhibition on the development of uveitis in SpA.

In the SELECT trials, new onset or flares of IBD were generally low across PsA, r-axSpA, and nr-axSpA. Although total rates of IBD were numerically higher in patients treated with upadacitinib 15 mg versus placebo, these events likely occurred by chance

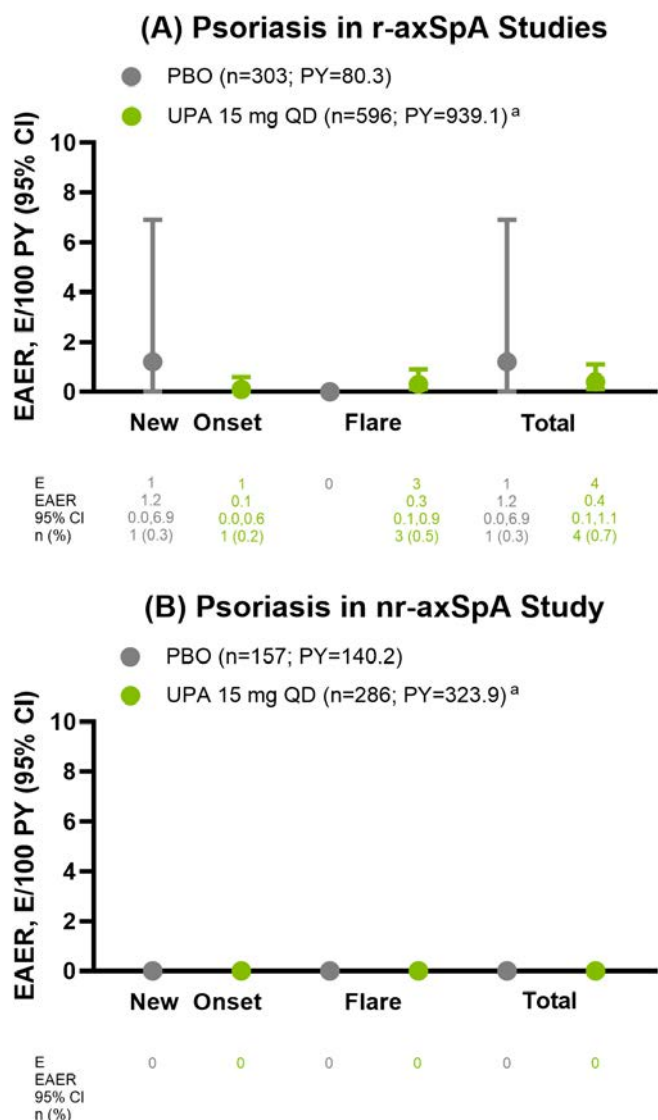


Figure 3. Development of psoriasis in patients treated with upadacitinib across r-axSpA and nr-axSpA. Development of psoriasis in (A) r-axSpA and (B) nr-axSpA stratified by history. EMM subtypes in r-axSpA (E/100 PY [95% CI] [E]): psoriasis in PBO (1.2 [0.0–6.9] [1]) and UPA 15 mg (0.4 [0.1–1.1] [4]). EMM subtypes in nr-axSpA: psoriasis in PBO (0) and UPA 15 mg (0). ^aAny exposure to UPA, including patients who switched from PBO to UPA 15 mg. CI, confidence interval; E/100 PY, events per 100 patient-years; E, event; EAER, exposure-adjusted event rate; EMM, extramusculoskeletal manifestation; nr-axSpA, nonradiographic axial spondyloarthritis; PBO, placebo; PY, patient-year; QD, once daily; r-axSpA, radiographic axial spondyloarthritis; UPA, upadacitinib.

and longer exposure to study drug may be needed to observe meaningful differences between the two treatments. Similar to the results for uveitis, rates of new onset or flares of IBD in PsA were comparable in patients treated with upadacitinib 15 mg or adalimumab. However, phase 3 studies in patients with active ulcerative colitis⁴⁶ or Crohn's disease⁴⁷ have demonstrated improved clinical and endoscopic outcomes following

upadacitinib treatment versus placebo. In the published literature, there is support for the use of TNF inhibitors, such as adalimumab and infliximab, in patients with SpA and IBD; an exception is etanercept, which does not appear to prevent flares or new onset of IBD.^{48–50} In this analysis with upadacitinib, reported rates of new onset or flares of IBD in r-axSpA and nr-axSpA were largely consistent with previously published adalimumab data.^{30,51} In contrast, IL-17 inhibitors, such as ixekizumab and secukinumab, have been associated with the occurrence of IBD in patients with SpA,⁵² resulting in inclusion of IBD in the warnings and precautions section of their prescribing information.

In this analysis, the development of psoriasis was not evaluated for PsA, as it is considered a core manifestation of the disease.⁴ Data from the phase 3 SELECT trials for PsA demonstrated the efficacy of upadacitinib for the improvement of psoriasis, including significantly better scores on the Static Investigator Global Assessment of Psoriasis and a higher percentage of patients achieving a decrease from baseline of at least 75% in the Psoriasis Area and Severity Index in both PsA trials, as well as greater change from baseline in the Self-Assessment of Psoriasis Symptoms in the SELECT-PsA 2 trial, compared with placebo.^{18,19} In patients with r-axSpA or nr-axSpA, new onset or flares of psoriasis were infrequent across the trials. Previously published rates of psoriasis in axSpA with adalimumab treatment were slightly higher than the rates observed in this analysis with upadacitinib.³⁰

In addition to the impact of study drug on the development of EMMs, it appears that having a history of an EMM may impact future events. Specifically, in this analysis, having a history of uveitis may have predisposed patients with r-axSpA for uveitis flares during the study. In an analysis of the Swedish Population Patient Register, a stronger association of uveitis flares was found in patients with r-axSpA, and the authors remarked that this likely mirrors the higher tendency for recurrence of uveitis in patients with r-axSpA compared with those with PsA or the general population.⁵³ Furthermore, an analysis of primary referral patients with acute anterior uveitis found that the number of previous relapses was significantly associated with the risk of uveitis recurrence compared with those at disease onset.⁵⁴

Several limitations of this post hoc analysis should be noted. First, this analysis describes AEs of relevant EMMs in the SpA SELECT clinical trials, as reported by the investigators. Although EMMs represent manifestations of the disease, they were collected as either previous medical history and/or TEAEs in the SELECT trials, and therefore are presented as such in this analysis. Another recent publication in patients with axSpA treated with bimekizumab used similar methods to those described here, presenting TEAE data grouped by preferred terms related to uveitis.⁴⁵ Altogether, these methods of data collection (ie, TEAEs and medical history) limited the information that could be captured, including details about the EMM subtype and specific confirmation of diagnosis by a specialist, and may have led to an underestimation

of the rate of EMMs. Second, all EMM events were reviewed by safety physicians employed by the study sponsor but were not formerly adjudicated by an independent committee. Third, in one of the SELECT clinical trials for r-axSpA, patient history of uveitis at baseline was captured using an additional form, which was not used in the other SELECT studies, and may have led to an increased likelihood of capturing history of uveitis in this r-axSpA study. Fourth, because patients were not routinely monitored for the development of EMMs outside of standard AE reporting, the impact of upadacitinib in patients with specific EMMs could not be systematically evaluated. Fifth, because of the overall low number of events observed across the SpA SELECT trials, the EMM event data should be interpreted with caution. Additional longer-term exposure data to upadacitinib are needed to confirm the results described here. An ongoing prospective, cohort study in r-axSpA (UPSTAND; NCT04846244), which aims to assess early and sustained pain control in patients treated with upadacitinib, includes the assessment of new onset or flares of uveitis and IBD and can provide real-world data on the occurrence of EMMs with upadacitinib treatment.

In summary, the development of EMMs in patients treated with upadacitinib 15 mg was generally low across PsA, r-axSpA, and nr-axSpA. Uveitis was numerically lower in patients treated with upadacitinib 15 mg versus placebo, which was particularly evident in patients with r-axSpA. Also, in r-axSpA, regardless of treatment group, having a history of uveitis appeared to predispose patients for uveitis flares. The development of uveitis and IBD were generally similar following treatment with upadacitinib 15 mg or adalimumab in patients with PsA. Altogether, findings from this post hoc analysis in patients with SpA suggest no apparent increased risk of developing EMMs with upadacitinib therapy. A better understanding of the impact of upadacitinib across EMMs in SpA, and subsequent longer-term follow-up analyses, may help clinicians make informed treatment decisions and guide future treatment recommendations to improve patient care.

ACKNOWLEDGMENTS

Medical writing support was provided by Monica R.P. Elmore, PhD, of AbbVie. Editorial support provided by Angela T. Hadsell of AbbVie.

AUTHOR CONTRIBUTIONS

All authors contributed to at least one of the following manuscript preparation roles: conceptualization AND/OR methodology, software, investigation, formal analysis, data curation, visualization, and validation AND drafting or reviewing/editing the final draft. As corresponding author, Dr Poddubnyy confirms that all authors have provided the final approval of the version to be published, and takes responsibility for the affirmations regarding article submission (eg, not under consideration by another journal), the integrity of the data presented, and the statements regarding compliance with institutional review board/Declaration of Helsinki requirements.

ROLE OF THE STUDY SPONSOR

AbbVie funded these trials and participated in the study design, research, analysis, data collection, interpretation of data, reviewing, and approval of the publication. All authors had access to relevant data and participated in the drafting, review, and approval of this publication. No honoraria or payments were made for authorship. Medical writing and editorial support were provided by employees of AbbVie.



REFERENCES

- van der Heijde D, Molto A, Ramiro S, et al. Goodbye to the term 'ankylosing spondylitis', hello 'axial spondyloarthritis': time to embrace the ASAS-defined nomenclature. *Ann Rheum Dis* 2024;83:547–549.
- Ehrenfeld M. Spondyloarthropathies. *Best Pr Res Clin Rheumatol* 2012;26:135–145.
- Ramiro S, Nikiphorou E, Sepiano A, et al. ASAS-EULAR recommendations for the management of axial spondyloarthritis: 2022 update. *Ann Rheum Dis* 2023;82:19–34.
- Coates LC, Soriano ER, Corp N, et al; GRAPPA Treatment Recommendations domain subcommittees. Group for Research and Assessment of Psoriasis and Psoriatic Arthritis (GRAPPA): updated treatment recommendations for psoriatic arthritis 2021. *Nat Rev Rheumatol* 2022;18:465–479.
- de Winter JJ, van Mens LJ, van der Heijde D, et al. Prevalence of peripheral and extra-articular disease in ankylosing spondylitis versus non-radiographic axial spondyloarthritis: a meta-analysis. *Arthritis Res Ther* 2016;18:196.
- Pittam B, Gupta S, Harrison NL, et al. Prevalence of extra-articular manifestations in psoriatic arthritis: a systematic review and meta-analysis. *Rheumatology (Oxford)* 2020;59:2199–2206.
- Zeboulon N, Dougados M, Gossec L. Prevalence and characteristics of uveitis in the spondyloarthropathies: a systematic literature review. *Ann Rheum Dis* 2008;67:955–959.
- Cantini F, Nannini C, Cassarà E, et al. Uveitis in spondyloarthritis: an overview. *J Rheumatol Suppl* 2015;93:27–29.
- van der Horst-Bruinsma IE, van Bentum RE, Verbraak FD, et al. Reduction of anterior uveitis flares in patients with axial spondyloarthritis on certolizumab pegol treatment: final 2-year results from the multicenter phase IV C-VIEW study. *Ther Adv Musculoskelet Dis* 2021; 13:1759720X211003803.
- Robinson PC, Claushuis TAM, Cortes A, et al; Spondyloarthritis Research Consortium of Canada, Australia-Anglo-American Spondylitis Consortium, International Genetics of Ankylosing Spondylitis Consortium, Wellcome Trust Case Control Study 2, Mariapia Degli-Esposti. Genetic dissection of acute anterior uveitis reveals similarities and differences in associations observed with ankylosing spondylitis. *Arthritis Rheumatol* 2015;67:140–151.
- Rudwaleit M, Haibel H, Baraliakos X, et al. The early disease stage in axial spondylarthritis: results from the German Spondyloarthritis Inception Cohort. *Arthritis Rheum* 2009;60:717–727.
- Rudwaleit M, Rødevand E, Holck P, et al. Adalimumab effectively reduces the rate of anterior uveitis flares in patients with active ankylosing spondylitis: results of a prospective open-label study. *Ann Rheum Dis* 2009;68:696–701.
- Rudwaleit M, Rosenbaum JT, Landewé R, et al. Observed incidence of uveitis following certolizumab pegol treatment in patients with axial spondyloarthritis. *Arthritis Care Res (Hoboken)* 2016;68:838–844.
- Lindström U, Bengtsson K, Olofsson T, et al. Anterior uveitis in patients with spondyloarthritis treated with secukinumab or tumour necrosis factor inhibitors in routine care: does the choice of biological therapy matter? *Ann Rheum Dis* 2021;80:1445–1452.
- Redeker I, Siegmund B, Ghoreschi K, et al. The impact of extra-musculoskeletal manifestations on disease activity, functional status,

- and treatment patterns in patients with axial spondyloarthritis: results from a nationwide population-based study. *Ther Adv Musculoskelet Dis* 2020;12:1759720X20972610.
16. Coates LC, Kavanaugh A, Mease PJ, et al. Group for Research and Assessment of Psoriasis and Psoriatic Arthritis 2015 Treatment Recommendations for Psoriatic Arthritis. *Arthritis Rheumatol* 2016; 68:1060–1071.
 17. Navarro-Compán V, Boel A, Boonen A, et al. The ASAS-OMERACT core domain set for axial spondyloarthritis. *Semin Arthritis Rheum* 2021;51:1342–1349.
 18. McInnes IB, Anderson JK, Magrey M, et al. Trial of Upadacitinib and Adalimumab for Psoriatic Arthritis. *N Engl J Med* 2021;384: 1227–1239.
 19. Mease PJ, Lertratanakul A, Anderson JK, et al. Upadacitinib for psoriatic arthritis refractory to biologics: SELECT-PsA 2. *Ann Rheum Dis* 2021;80:312–320.
 20. van der Heijde D, Song IH, Pangan AL, et al. Efficacy and safety of upadacitinib in patients with active ankylosing spondylitis (SELECT-AXIS 1): a multicentre, randomised, double-blind, placebo-controlled, phase 2/3 trial. *Lancet* 2019;394(10214):2108–2117.
 21. van der Heijde D, Baraliakos X, Sieper J, et al. Efficacy and safety of upadacitinib for active ankylosing spondylitis refractory to biological therapy: a double-blind, randomised, placebo-controlled phase 3 trial. *Ann Rheum Dis* 2022;81:1515–1523.
 22. Deodhar A, Van Den Bosch F, Poddubny D, et al. Upadacitinib for the treatment of active non-radiographic axial spondyloarthritis (SELECT-AXIS 2): a randomised, double-blind, placebo-controlled, phase 3 trial. *Lancet* 2022;400(10349):369–379.
 23. Cohen SB, van Vollenhoven RF, Winthrop KL, et al. Safety profile of upadacitinib in rheumatoid arthritis: integrated analysis from the SELECT phase III clinical programme. *Ann Rheum Dis* 2021;3: 304–311.
 24. Burmester GR, Cohen SB, Winthrop KL, et al. Safety profile of upadacitinib over 15 000 patient-years across rheumatoid arthritis, psoriatic arthritis, ankylosing spondylitis and atopic dermatitis. *RMD Open* 2023;9:e002735.
 25. Herrera-deGuise C, Serra-Ruiz X, Lastiri E, et al. JAK inhibitors: a new dawn for oral therapies in inflammatory bowel diseases. *Front Med (Lausanne)* 2023;10:1089099.
 26. Megna M, Potestio L, Ruggiero A, et al. JAK inhibitors in psoriatic disease. *Clin Cosmet Investig Dermatol* 2023;16:3129–3145.
 27. Sharma SM, Jackson D. Uveitis in the spondyloarthropathies. *Best Pract Res Clin Rheumatol* 2017;31:846–862.
 28. Biggioggero M, Crotti C, Becciolini A, et al. The management of acute anterior uveitis complicating spondyloarthritis: present and future. *BioMed Res Int* 2018;2018:9460187.
 29. Martin TM, Smith JR, Rosenbaum JT. Anterior uveitis: current concepts of pathogenesis and interactions with the spondyloarthropathies. *Curr Opin Rheumatol* 2002;14:337–341.
 30. Sieper J, van der Heijde D, Varothai NA, et al. Comparison of baseline extra-articular manifestations, comorbidities, and long-term safety in patients treated with adalimumab for ankylosing spondylitis and non-radiographic axial spondyloarthritis. Abstract presented at: American College of Rheumatology (ACR)/Association of Rheumatology Health Professionals (ARHP) Annual Meeting; November 14–19, 2014; Boston, MA.
 31. Lie E, Lindström U, Zverkova-Sandström T, et al. Tumour necrosis factor inhibitor treatment and occurrence of anterior uveitis in ankylosing spondylitis: results from the Swedish biologics register. *Ann Rheum Dis* 2017;76:1515–1521.
 32. Srivastava SK, Watkins TR, Nguyen QD, et al. A phase 2 randomized controlled trial of the Janus kinase (JAK) inhibitor filgotinib in patients with noninfectious uveitis. Abstract presented at: ARVO Annual Meeting; May 1–4, 2022; Denver, CO, and virtual.
 33. Lim CSE, Sengupta R, Gaffney K. The clinical utility of human leucocyte antigen B27 in axial spondyloarthritis. *Rheumatology (Oxford)* 2018;57:959–968.
 34. Mitulescu T-C, Trandafir M, Dimănescu M-G, et al. Advances in the treatment of uveitis in patients with spondyloarthritis - is it the time for biologic therapy? *Rom J Ophthalmol* 2018;62:114–122.
 35. Arepalli S, Rosenbaum JT. The use of biologics for uveitis associated with spondyloarthritis. *Curr Opin Rheumatol* 2019;31:349–354.
 36. Wendling D, Joshi A, Reilly P, et al. Comparing the risk of developing uveitis in patients initiating anti-tumor necrosis factor therapy for ankylosing spondylitis: an analysis of a large US claims database. *Curr Med Res Opin* 2014;30:2515–2521.
 37. Guignard S, Gossec L, Salliot C, et al. Efficacy of tumour necrosis factor blockers in reducing uveitis flares in patients with spondylarthropathy: a retrospective study. *Ann Rheum Dis* 2006;65:1631–1634.
 38. Braun J, Baraliakos X, Listing J, et al. Decreased incidence of anterior uveitis in patients with ankylosing spondylitis treated with the anti-tumor necrosis factor agents infliximab and etanercept. *Arthritis Rheum* 2005;52:2447–2451.
 39. Van der Horst-Bruinsma IE, Robinson PC, Favalli EG, et al. Certolizumab pegol treatment in patients with axial-spondyloarthritis-associated acute anterior uveitis: a narrative review. *Rheumatol Ther* 2022;9:1481–1497.
 40. Faez S, Lobo A, Sobrin L, et al. Letter to the editor: treatment of seronegative spondyloarthropathy-associated uveitis with golimumab: retrospective case series. *Clin Exp Ophthalmol* 2014;42:392–395.
 41. Yazgan S, Celik U, Işık M, et al. Efficacy of golimumab on recurrent uveitis in HLA-B27-positive ankylosing spondylitis. *Int Ophthalmol* 2017;37:139–145.
 42. Calvo-Río V, Blanco R, Santos-Gómez M, et al. Golimumab in refractory uveitis related to spondyloarthritis. Multicenter study of 15 patients. *Semin Arthritis Rheum* 2016;46:95–101.
 43. Okada K, Zhou Y, Hashida N, et al. The efficacy of golimumab against non-infectious uveitis: a PRISMA-compliant systematic review and meta-analysis. *Ocul Immunol Inflamm* 2023;31:1013–1023.
 44. Dick AD, Tugal-Tutkun I, Foster S, et al. Secukinumab in the treatment of noninfectious uveitis: results of three randomized, controlled clinical trials. *Ophthalmology* 2013;120:777–787.
 45. Brown MA, Rudwaleit M, van Gaalen FA, et al. Low uveitis rates in patients with axial spondyloarthritis treated with bimekizumab: pooled results from phase 2b/3 trials. *Ann Rheum Dis* 2024;83:1722–1730.
 46. Danese S, Vermeire S, Zhou W, et al. Upadacitinib as induction and maintenance therapy for moderately to severely active ulcerative colitis: results from three phase 3, multicentre, double-blind, randomised trials. *Lancet* 2022;399:2113–2128.
 47. Loftus EV Jr, Panés J, Lacerda AP, et al. Upadacitinib induction and maintenance therapy for Crohn's disease. *N Engl J Med* 2023;388: 1966–1980.
 48. Braun J, Baraliakos X, Listing J, et al. Differences in the incidence of flares or new onset of inflammatory bowel diseases in patients with ankylosing spondylitis exposed to therapy with anti-tumor necrosis factor α agents. *Arthritis Rheum* 2007;57:639–647.
 49. Jadon DR, Corp N, van der Windt DA, et al. Management of concomitant inflammatory bowel disease or uveitis in patients with psoriatic arthritis: an updated review informing the 2021 GRAPPA treatment recommendations. *J Rheumatol* 2023;50:438–450.
 50. Cozzi G, Scagnellato L, Lorenzin M, et al. Spondyloarthritis with inflammatory bowel disease: the latest on biologic and targeted therapies. *Nat Rev Rheumatol* 2023;19:503–518.
 51. Elewaut D, Braun J, Anderson JK, et al. Low incidence of inflammatory bowel disease adverse events in adalimumab clinical trials across

- nine different diseases. *Arthritis Care Res (Hoboken)* 2021;73: 289–295.
52. Fauny M, Moulin D, D'Amico F, et al. Paradoxical gastrointestinal effects of interleukin-17 blockers. *Ann Rheum Dis* 2020;79:1132–1138.
53. Bengtsson K, Forsblad-d'Elia H, Deminger A, et al. Incidence of extra-articular manifestations in ankylosing spondylitis, psoriatic arthritis and undifferentiated spondyloarthritis: results from a national register-based cohort study. *Rheumatology (Oxford)* 2021;60:2725–2734.
54. Natkunarajah M, Kaptoge S, Edelsten C. Risks of relapse in patients with acute anterior uveitis. *Br J Ophthalmol* 2007;91: 330–334.

Role of STING Deficiency in Amelioration of Mouse Models of Lupus and Atherosclerosis

Yudong Liu,¹ Carmelo Carmona-Rivera,²  Nickie L. Seto,² Christopher B. Oliveira,² Eduardo Patino-Martinez,² Yvonne Baumer,³ Tiffany M. Powell-Wiley,⁴ Nehal Mehta,³ Sarfaraz Hasni,² Xuan Zhang,⁵  and Mariana J. Kaplan²

Objective. Systemic lupus erythematosus (SLE) is a systemic autoimmune syndrome characterized by autoreactive responses to nucleic acids, dysregulation of the type I interferon (IFN-I) pathway, and accelerated atherosclerosis. The stimulator of IFN genes (STING), a cytosolic DNA sensor, has pathogenic implications in various inflammatory diseases. However, its specific role in SLE pathogenesis, particularly in tissue damage, remains unclear. This study aimed to elucidate the role of STING in murine models of Toll-like receptor 7 (TLR7)–driven lupus and atherosclerosis.

Methods. A TLR7-driven lupus model was induced using imiquimod (IMQ) in wild-type (WT) and STING knockout (*Sting*^{−/−}) mice on a B6 background. Mice were assessed for organ involvement, serum autoantibodies, and innate and adaptive immune responses. Additionally, *Sting*^{−/−} mice were backcrossed to apolipoprotein E knockout (*Apoe*^{−/−}) mice, and both *Apoe*^{−/−} and *Apoe*^{−/−}*Sting*^{−/−} mice were fed a high-fat chow diet to induce atherosclerosis. Phenotypic assessments were conducted.

Results. Compared with IMQ-treated WT mice, *Sting*^{−/−} mice exhibited reduced disease severity in the lupus-like phenotype, characterized by decreased splenomegaly, lower renal immune complex deposition and renal damage, diminished expansion of myeloid cells, and reduced activation of T and B lymphocytes. IMQ-induced DNA release associated with IFN-β production and subsequent IFN-induced responses were attenuated in *Sting*^{−/−} mice. DNase I treatment mitigated IMQ-induced proinflammatory responses in WT mice but had no effect in *Sting*^{−/−} mice. Furthermore, STING deficiency conferred protection against vascular damage and reduced atherosclerosis burden, accompanied by decreased IFN-I production. Human monocyte-derived macrophages treated with IFN-I significantly internalized more acetylated low-density lipoprotein when compared with untreated cells, whereas an association between oxidized nucleic acids and disease activity and vascular damage was found in human SLE.

Conclusion. These findings highlight a pathogenic role of STING and downstream IFN responses in TLR7-driven autoimmunity, vascular damage and atherosclerosis, supporting a therapeutic potential for STING inhibition in SLE treatment. Further research is warranted to elucidate the mechanisms underlying STING's involvement in these processes and to explore the feasibility of targeting STING as a therapeutic strategy in SLE and related autoimmune disorders.

INTRODUCTION

Innate immune recognition of nucleic acids is crucial for host response against infections. Dysregulation of nucleic acid-sensing

systems has been linked to several autoimmune diseases, including systemic lupus erythematosus (SLE).¹ In SLE, accelerated cell death combined with deficient chromatin clearance leads to the accumulation of modified endogenous DNA and other

Supported by the Intramural Research Program at National Institute of Arthritis and Musculoskeletal and Skin Diseases, NIH (grant ZIA-AR-041199); National Heart, Lung, and Blood Institute, NIH (grants ZIA-HL-006168, ZIA-HL-006225, and ZIA-HL-006252); National Institute on Minority Health and Health Disparities, NIH (grant ZIJ-MD-000010); and National Natural Science Foundation of China (grant 81971521).

¹Yudong Liu, MD, PhD: National Center for Clinical Laboratories, Institute of Geriatric Medicine, Chinese Academy of Medical Sciences, Beijing Hospital/National Center of Gerontology, Beijing, China, and National Institute of Arthritis and Musculoskeletal and Skin Diseases, NIH, Bethesda, Maryland; ²Carmelo Carmona-Rivera, PhD, Nickie L. Seto, MD, Christopher B. Oliveira, BS, Eduardo Patino-Martinez, PhD, Sarfaraz Hasni, MD, Mariana J. Kaplan, MD: National Institute of Arthritis and Musculoskeletal and Skin Diseases,

NIH, Bethesda, Maryland; ³Yvonne Baumer, PhD, Nehal Mehta, MD: National Heart Lung and Blood Institute, NIH, Bethesda, Maryland; ⁴Tiffany M. Powell-Wiley, MD, MPH: National Heart Lung and Blood Institute, NIH and National Institute on Minority Health and Health Disparities, NIH, Bethesda, Maryland; ⁵Xuan Zhang, MD: Beijing Hospital, National Center of Gerontology, Institute of Geriatric Medicine, Clinical Immunology Center, Graduate School of Peking Union Medical College, Chinese Academy of Medical Sciences, Beijing, China.

Drs Liu and Carmona-Rivera contributed equally to this work.

Additional supplementary information cited in this article can be found online in the Supporting Information section (<https://acrjournals.onlinelibrary.wiley.com/doi/10.1002/art.43062>).

Author disclosures and graphical abstract are available at <https://onlinelibrary.wiley.com/doi/10.1002/art.43062>.

autoantigens. In genetically predisposed individuals, this accumulation promotes autoantibody and immune complex formation, fueling systemic inflammation through aberrant synthesis of type I interferon (IFN-I).²

Various intracellular systems, including endosomal Toll-like receptors (TLRs), sense DNA. Previous studies, including our own, have shown that deficiency in TLR9, a key intracellular DNA sensor, exacerbates lupus severity.³ Another cytosolic DNA sensing system, the cyclic-GMP-AMP (cGAMP) synthase (cGAS) stimulator of IFN genes (STING) pathway, has garnered attention for its role in SLE.⁴ Hyperactivity of STING has been reported in some patients with SLE, along with elevated levels of circulating cGAMP and increased STING expression in monocytes.⁵ SLE serum can induce IFN-I responses via STING pathway activation.⁶ SLE monocytes show higher expression of the IFN-inducible gene with tetratricopeptide repeats 3 (IFIT3), a downstream player in the cGAS-STING pathway, suggesting aberrant cGAS-STING activation in SLE pathogenesis.⁷

The cGAS-STING pathway is implicated in several lupus-like models. Our previous work demonstrated that oligomerization of the voltage-dependent anion channel protein-1 promotes the formation of pores in the outer mitochondrial membrane, allowing mitochondrial DNA (mtDNA) fragments to leak into the cytosol and activate STING signaling, which contributes to lupus-like disease.⁸ We also found that neutrophil extracellular traps (NETs) enriched in oxidized mtDNA activate STING, but not endosomal TLRs, contributing to lupus-like disease.⁹ However, the relevance of the STING pathway in lupus remains complex, as some mouse models suggest a protective effect.^{10,11}

Among various lupus models, an inducible lupus-like model using epicutaneous application of a TLR7/8 agonist (imiquimod [IMQ]) has been described. This model resembles human lupus phenotypically and functionally, including the development of anti-nuclear antibodies, renal immune complex deposition, IFN-1 responses, and immune activation, without the confounding factors of complex murine genetics.³

In addition to exploring the role of STING in endosomal TLR-induced mouse lupus, we also assessed its role in vascular damage and atherosclerosis, conditions prominently associated with lupus. To study atherosclerosis in the context of lupus, we used a mouse model with apolipoprotein E deficiency (*Apoe*^{-/-}), which is prone to developing atherosclerosis. By generating mice with both *Apoe* and STING deficiencies (*Apoe*^{-/-}*Sting*^{-/-}), we aimed to investigate the impact of STING on the development of atherosclerosis in lupus. This dual-knockout model allows us to dissect the contributions of STING to both lupus pathogenesis and atherosclerosis, providing a comprehensive understanding of the interplay between these conditions.

MATERIALS AND METHODS

Mice. STING wild-type (WT) and STING knockout (*Sting*^{-/-}) breeding pairs were kindly provided by Dr Glen N. Barber (University of Miami, FL). *Apoe*^{-/-} (B6.129P2-Apoetm1Unc/J) mice were purchased from The Jackson Laboratory. *Sting*^{-/-} mice were backcrossed to *Apoe*^{-/-} mice to generate *Apoe*^{-/-}*Sting*^{-/-} mice. All mice were bred and maintained under specific pathogen-free conditions, and experiments were performed under approved animal study protocol #A019-05-03 and under the approved animal study protocol #2022BJYEC-176-01.

Human participants. Blood samples from healthy controls were obtained at the clinical center, NIH. Patients met the American College of Rheumatology revised diagnostic criteria for SLE.¹² All individuals signed informed consent. Protocols were approved by the NIH institutional review board. Demographic and clinical characteristics of the patients are shown in Supplementary Tables 1 and 2.

IMQ-induced lupus model and atherosclerosis

model. Eight- to ten-week-old WT and *Sting*^{-/-} mice were treated epicutaneously with IMQ cream on both ears three times per week for four weeks, as previously described.¹³ For DNase I treatment, eight-week-old WT or *Sting*^{-/-} mice were epicutaneously treated with Fougera IMQ CREAM 5% on both ears three times per week for four weeks. On the first day of IMQ treatment, mice were intravenously injected with 400 U DNase I (Sigma) in 200 μ L phosphate-buffered saline (PBS) or 200 μ L PBS alone as a control three times weekly for four weeks. For H-151 treatment, eight- to ten-week-old WT mice were treated with epicutaneous IMQ on both ears three times per week for five weeks. From the first day of the third week of the IMQ treatment, mice were intravenously injected with 200 μ L of H-151 (750 nM) (InvivoGen)¹⁴ in PBS containing 10% Tween-80 or 200 μ L vehicle control three times weekly for three weeks. For the mouse model of atherosclerosis, *Apoe*^{-/-} mice and *Apoe*^{-/-}*Sting*^{-/-} mice were fed high-fat diet (HFD) (Envigo TD.88137, 42% from fat) for the indicated time points, as previously described.¹⁵

Cell isolation and flow cytometry analysis. Spleens were harvested, weighed, and processed into single-cell suspensions. Total splenocyte numbers were counted, and splenocytes were stained with the following anti-mouse antibodies: anti-B220 (RA3-6B2), anti-CD3 (17A2), anti-CD4 (GK1.5), anti-CD11b (M1/70), anti-CD11c (N418), anti-CD19 (6D5), anti-CD45 (30-F11), anti-Ly6C (HK1.4), anti-Ly6G (1A8), and anti-PDCA-1 (927). All antibodies were from Biolegend. The LIVE/DEAD Fixable Aqua Dead Cell Stain Kit (Thermo Fisher Scientific)

Address correspondence via email to Mariana J. Kaplan, MD, at mariana.kaplan@nih.gov.

Submitted for publication July 19, 2024; accepted in revised form November 13, 2024.

was used to exclude dead cells in all flow experiments. Cells were analyzed using a FACS Fortessa analyzer (BD Biosciences), and data were processed with FlowJo software (Tree Star).

Kidney harvesting, urinalysis, histology, and immunofluorescence. Kidney harvesting and urinalysis were performed as previously described.¹⁶ Urine was collected at euthanasia, and albumin/creatinine ratio was determined by the Albuwell M and Creatinine Companion kits (Exocell). Hematoxylin and eosin (H&E) staining of kidney tissue was performed as previously described.¹³ Slides were scored based on histopathological criteria by a pathologist, who was masked to the genetic background for all samples, as previously described.^{13,17,18} For the kidney immunofluorescence staining, mice were anesthetized, and kidneys were perfused with cold PBS via left-sided cardiac puncture. Kidneys were frozen in Tissue-Tek OCT Compound and stored at -80°C until sectioning for immunofluorescence staining. Immune complex deposition was assessed by immunofluorescence staining of IgG and C3 on frozen kidney sections, as previously described.¹⁶ Glomerular staining for IgG and C3 was graded in a anonymized manner by intensity on a 0 to 3+ scale for at least 10 glomeruli per mouse; an average score was calculated.

Characterization and quantification of atherosclerotic lesions. To assess atherosclerotic plaques, the vasculature was perfused with PBS. For aortic roots, the heart was removed, fixed in 4% paraformaldehyde (PFA) in 5% sucrose solution, embedded in OCT, frozen, and serial sectioned with a cryostat at $10\ \mu\text{m}/\text{section}$. Serial sections were stained with Oil Red O and counterstained with hematoxylin, as previously described.¹⁵ Necrotic lesions were assessed on the aortic root frozen sections with H&E staining. Necrotic core size, as determined by nuclei-free area, was quantified with ImageJ. The percentage of necrotic lesions was calculated as the size of the necrotic core divided by the total plaque size. The presence of cholesterol crystals (CCs) was assessed by a polarized light microscope on the aortic root frozen sections. The crystal content was calculated as the size of the crystal area, which was quantified with ImageJ, divided by the total plaque size. For en face atherosclerotic lesion quantification in the aorta, the aorta was cleaned of adventitial fat under a dissection microscope until the ileal bifurcation. The thoracic part of the aorta was subsequently opened longitudinally, transferred to a wax coated dissection tray, and pinned using micro pins. Afterwards, the aorta was fixed in 4% PFA solution for 5 minutes, washed in water, incubated with 60% isopropanol for 5 minutes, stained with Oil Red O solution for 15 minutes, washed 3 \times for 5 minutes each in 60% isopropanol, and finally washed and submerged for imaging in water. Quantification of aortic plaques was performed with ImageJ. The abdominal part of the cleaned aortae was used for gene expression analysis.

Immunofluorescence staining. Immunofluorescence staining of spleen and aortic root was performed as previous described.¹⁵ Briefly, frozen sections were fixed with 4% PFA for 10 minutes, followed by permeabilization in 0.2% Triton X-100 for 8 minutes. The sections were blocked by 1% bovine serum albumin (BSA) plus 1% donkey serum in PBS for 30 minutes. Sections were then stained with primary antibodies when application: rat anti-mouse Ly6G (BioLegend), rat anti-mouse CD68 (BioLegend), rabbit anti- α smooth muscle actin (Abcam), and rabbit anti-citrullinated histone 3 (Abcam), followed by staining with Alexa Fluor 488-conjugated goat anti-mouse IgM (Abcam), Alexa Fluor 488-conjugated donkey anti-rat IgG, Alexa Fluor 555-conjugated donkey anti-rat IgG, Alexa Fluor 555-conjugated donkey anti-rabbit IgG, and Alexa Fluor 647-conjugated donkey anti-rabbit IgG (all from Thermo Fisher Scientific). Cells and tissue sections were counterstained with DAPI (Thermo Fisher Scientific) before being mounted in ProLong Gold (Thermo Fisher Scientific) and examined by confocal microscopy. Quantification of macrophages, α smooth muscle actin, and neutrophils was performed with ImageJ. The percentage of macrophages, smooth muscle cell activation, and neutrophils was calculated as the size of CD68 $^{+}$ area, α smooth muscle actin $^{+}$ area, and Ly6G $^{+}$ area divided by the total plaque size.

Endothelium-dependent vasorelaxation assays. Aortic rings ($\sim 2\ \text{mm}$) from HFD were excised and mounted in a myograph system (Danish Myo Technology A/S) containing physiologic salt solution (PSS) with aeration (95% $\text{O}_2/5\% \text{CO}_2$). Aortic rings were equilibrated at 700 mg passive tension for 1 hour with buffer changes every 30 minutes. Contraction was achieved with PSS containing 100 mM potassium chloride before collecting contraction/relaxation measurements. Phenylephrine (PE)-induced contraction was allowed to reach a stable plateau. Vasorelaxation was assessed by the addition of acetylcholine (ACh) ($1 \times 10^{-9}\ \text{M}$ to $1 \times 10^{-3}\ \text{M}$). Results were reported as the percentage of PE contraction.

Quantification of serum autoantibodies and oxidized DNA. Serum total IgM, IgG, and anti-double-stranded DNA (dsDNA) were determined by enzyme-linked immunosorbent assay (ELISA) according to manufacturer's instructions (Thermo Fisher Scientific and Alpha Diagnostics, respectively). Anti-histone autoantibodies were quantified as previously described.^{3,13} Serum oxidized DNA was determined by ELISA. Briefly, serum DNA extracted using a serum DNA isolation kit (Abcam) was precoated on Nunc MaxiSorp ELISA plates (500 $\mu\text{g}/\text{mL}$). Plates were blocked with 1% BSA for two hours at room temperature (RT), washed, and incubated with 1:1,000 dilutions of anti-DNA/RNA Damage antibody (Abcam) for 1 hour at RT. Plates were washed and incubated with a 1/10,000 dilution of horseradish peroxidase-conjugated donkey anti-mouse IgG

(Southern Biotech) for one hour at 37°C, then developed with a 3,3',5,5'-tetramethylbenzidine substrate.

Quantification of 8-oxo-2'-deoxyguanosine (8-oxo-dG). Cell-free DNA was isolated from patients with lupus serum and quantified using the Quant-iT PicoGreen dsDNA Assay Kit (Thermo Fisher Scientific) according to the manufacturer's instructions. Serum oxidized DNA from patients with lupus and isolated NETs were determined by ELISA (R&D) according to the manufacturer's recommendations.

Measurements of vascular disease in human SLE. ¹⁸F-fluorodeoxyglucose–positron emission tomography/computed tomography (FDG-PET CT) and cardio-ankle vascular index were performed as previously described.¹⁹

Quantification of gene expression in splenocytes, peripheral blood mononuclear cells, and serum. Spleens were processed into single-cell suspensions. Splenocytes were resuspended in Trizol reagent (Invitrogen) for RNA extraction using the Qiagen RNeasy kit. Peripheral blood mononuclear cells (PBMCs) were isolated from peripheral blood by density gradient centrifugation on Histopaque 1119 and 1077 (Sigma) and resuspended in Trizol reagent. Complementary DNA was synthesized using BIO-RAD iScript reverse transcription supermix according to the manufacturer's instructions. Quantitative real-time polymerase chain reaction (PCR) was performed on a BIO-RAD CFX96 Real-Time System thermocycler (BIO-RAD, Hercules, CA) using specific TaqMan primers and probes (Thermo Fisher Scientific). Gapdh was used as the housekeeping gene to normalize the expression of the target genes, and the WT IMQ-treated mice Ct was used in the delta delta cycle threshold (ct) calculations for determining fold gene expression. The primers (assay ID) were as follows: *Gapdh*, Mm99999915_g1; *Mx-1*, Mm00487796_m1; *Isg15*, Mm01705338_s1; *Irf7*, Mm00516793_g1, *Nfkb1*, Mm00476361_m1; *Il1b*, Mm00434228_m1.

Quantification of DNA in serum. Serum DNA was directly measured using specific TaqMan primers and probes (Thermo Fisher Scientific) on a BIO-RAD CFX96 Real-Time System thermocycler (BIO-RAD). Briefly, serum was diluted at a 1:5 ratio in water. MgCl₂ was added to the PCR system at a final concentration of 4 mM, and 18S ribosomal RNA was quantified as an indicator of serum DNA using quantitative real-time PCR. The assay ID for 18S ribosomal RNA was Mm03928990_g1 (Thermo Fisher Scientific).

Low-density lipoprotein internalization by macrophages. CD14⁺ monocytes were isolated from human peripheral blood according to manufacturer's recommendation (Miltenyi Biotec). Cells were polarized with macrophage colony-

stimulating factor for seven days. M2-polarized macrophages were primed with 1,000 U of IFN- γ , 100 ng/mL of IFN- β or 50 μ g of purified NETs for 24 hours in RPMI containing 0.3% BSA. Cells were incubated with 5 μ g/mL of low-density lipoprotein (LDL), oxidized LDL, or acetylated LDL Dil complex (Invitrogen) for 3 hours. Plate was read on a plate reader at ex 520/em 571.

Statistical analysis. Statistical analysis was performed using the Mann-Whitney U test in GraphPad Prism (GraphPad Software). Multiple comparisons were analyzed by one-way analysis of variance. For endothelium-dependent vasorelaxation, curves were first analyzed using an asymmetric (five-parameter) logistic equation, and the significance of each data point was determined by two-way analysis of variance. A *P*-value less than 0.05 was considered significant.

RESULTS

STING pathway regulation of systemic inflammation triggered by IMQ. To test the role of STING in lupus, WT and *Sting1*^{-/-} mice were treated with the TLR7/8 agonist IMQ for 5 weeks. WT animals treated with IMQ exhibited marked alterations in spleen size and splenocyte phenotype compared with untreated controls. Specifically, IMQ treatment led to significant splenomegaly, characterized by a substantial increase in spleen size relative to untreated animals (Figure 1A). Quantitative analysis revealed a robust elevation in the number of splenocytes in IMQ-treated WT mice compared with controls (Figure 1B). Further characterization of the splenocyte populations demonstrated significant increases in neutrophils (CD11b⁺, Ly6G⁺) (Figure 1C), inflammatory monocytes (CD11b⁺, CD11c⁺) (Figure 1D), plasmacytoid dendritic cells (pDCs; CD138⁺, CD317⁺) (Figure 1E), and CD19⁺ B cells (Figure 1F) after IMQ treatment. *Sting1*^{-/-} mice treated with IMQ displayed strikingly different responses compared with their WT counterparts. Notably, IMQ-treated *Sting1*^{-/-} mice exhibited significant reduction in splenomegaly (Figure 1A). Analysis of splenocyte numbers in *Sting1*^{-/-} mice revealed a marked attenuation in the IMQ-induced increases observed in WT mice (Figure 1B). Specifically, the populations of neutrophils (CD11b⁺, Ly6G⁺) (Figure 1C), inflammatory monocytes (CD11b⁺, CD11c⁺) (Figure 1D), and pDCs (CD138⁺, CD317⁺) (Figure 1E) were significantly lower in IMQ-treated *Sting1*^{-/-} mice compared with IMQ-treated WT mice. No significant differences were observed between IMQ-treated WT and *Sting1*^{-/-} mice in CD19⁺ B cells (Figure 1F), CD4⁺ T cells (Figure 1G), and CD3⁺ T cells (Figure 1H) within the spleen. In addition, no significant differences in levels of total IgM, total IgG, anti-dsDNA, and anti-histone autoantibodies were observed between IMQ-treated WT and *Sting1*^{-/-} mice (Supplementary Figure 1). These results highlight the involvement of the STING pathway in regulating systemic inflammatory responses triggered by IMQ.

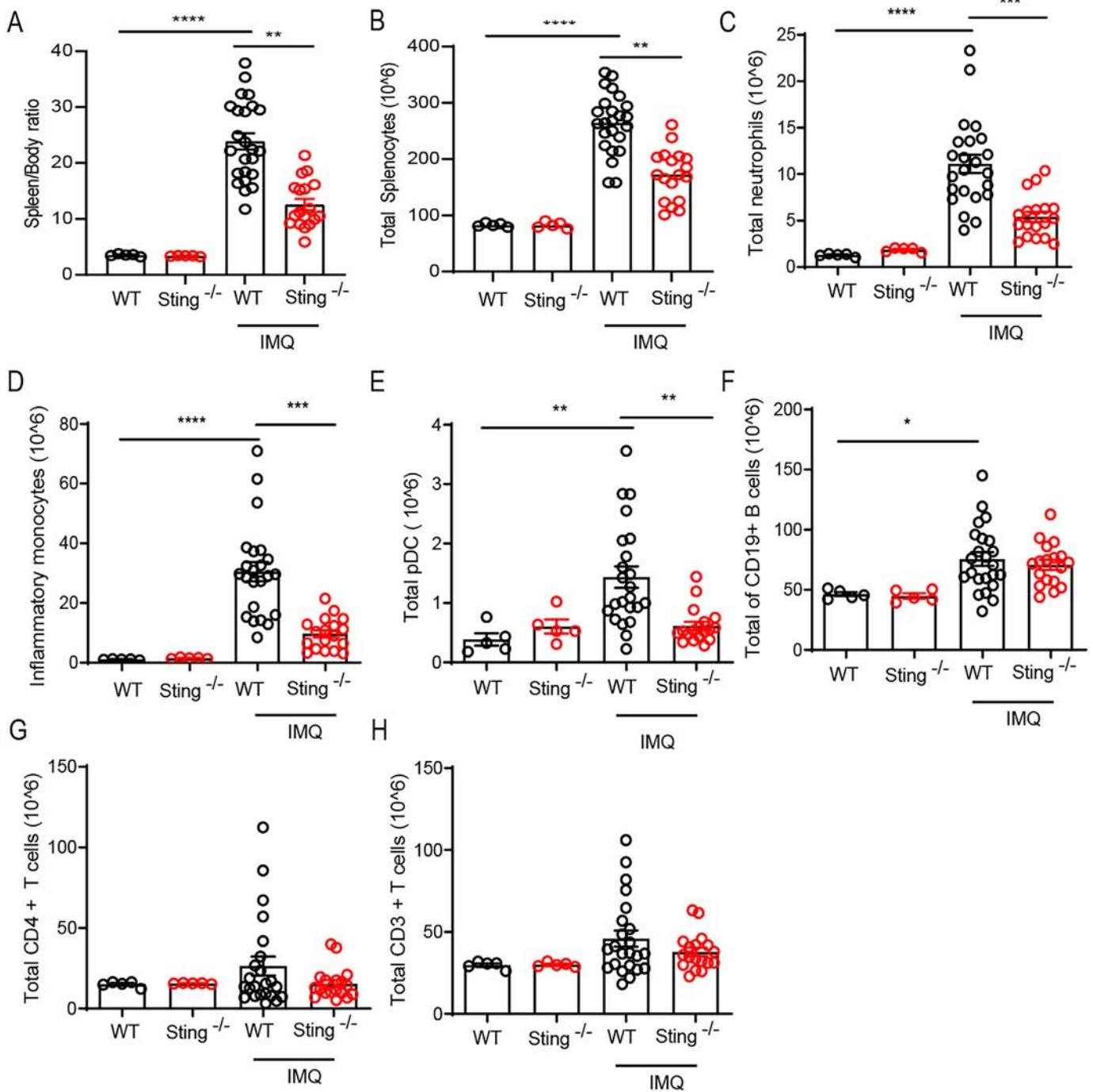


Figure 1. IMQ-induced splenomegaly and myeloid expansion are decreased in the absence of STING. (A and B) Spleen/body weight ratios and total numbers of splenocytes of untreated and IMQ-treated WT and *Sting*^{-/-} mice are shown (WT-untreated, n = 5; *Sting*^{-/-}-untreated, n = 5; WT-IMQ, n = 24; *Sting*^{-/-}-IMQ, n = 18). (C–E) Splenocytes from untreated and IMQ-treated WT and *Sting*^{-/-} mice were analyzed by flow cytometry to quantify neutrophils (CD11b⁺, Ly6G⁺), inflammatory monocytes (CD11b⁺, CD11c⁺), and pDCs (CD138⁺, CD317⁺), respectively. (F–H) Splenocytes from untreated and IMQ-treated WT and *Sting*^{-/-} mice were analyzed by flow cytometry to quantify (F) CD19⁺ B cells, (G) CD4⁺ T cells, and (H) CD3⁺ T cells, respectively (WT-untreated, n = 5; *Sting*^{-/-}-untreated, n = 5; WT-IMQ, n = 23; *Sting*^{-/-}-IMQ, n = 18). **P* < 0.05, ***P* < 0.01, ****P* < 0.001, *****P* < 0.0001. Kruskal-Wallis test was used to compare differences among groups. IMQ, imiquimod; pDC, plasmacytoid dendritic cell; STING, stimulator of interferon genes; WT, wild type.

STING pathway modulation of renal manifestations in lupus. To investigate the role of STING in renal manifestations, we assessed levels of albumin:creatinine in the urine and by

assessing complement C3 and IgG deposition in the kidneys of WT and *Sting*^{-/-} mice. A trend toward lower levels of proteinuria in the urine was observed in IMQ-treated *Sting*^{-/-} mice

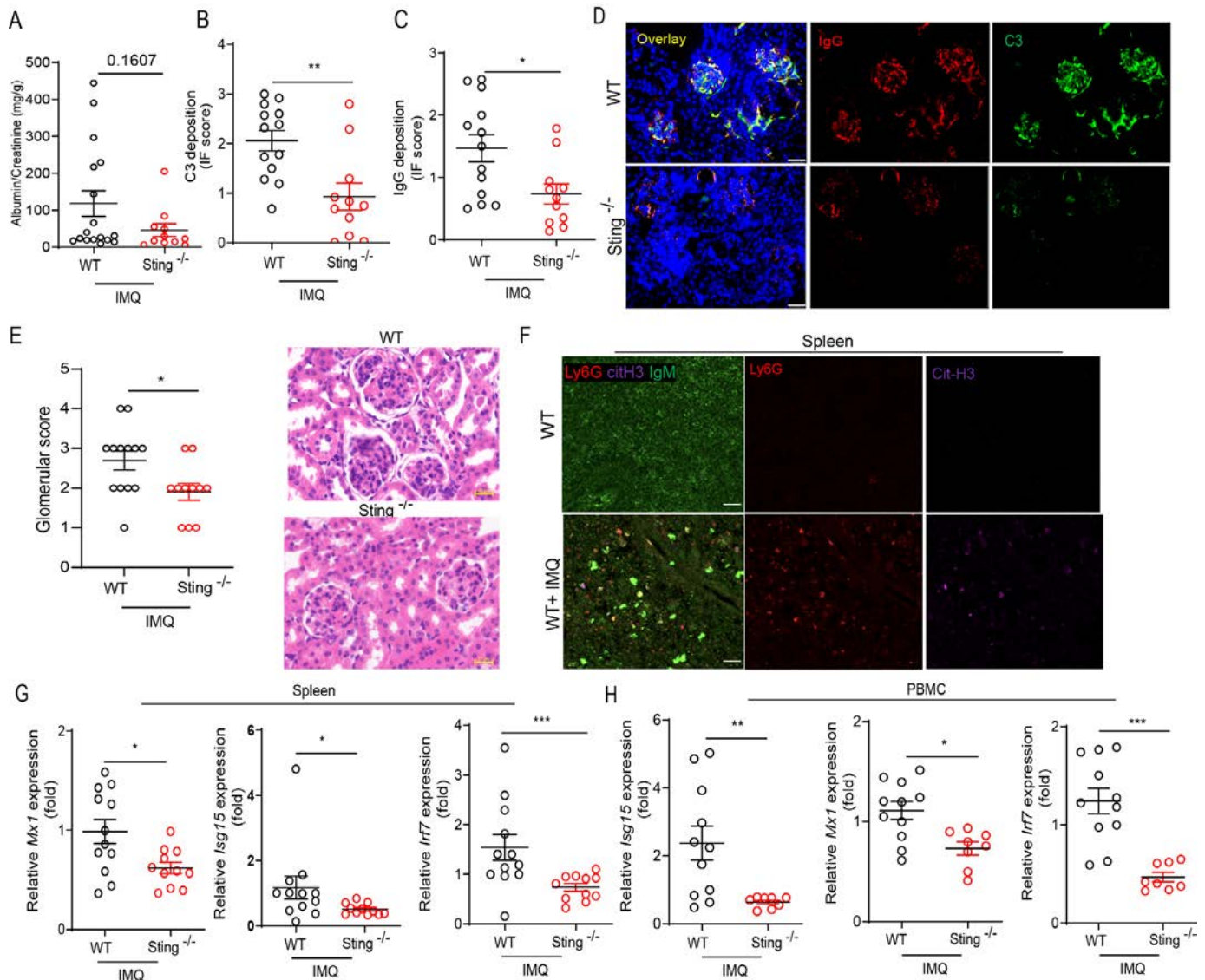


Figure 2. STING deficiency ameliorates IMQ-induced renal immune complex deposition and kidney pathology and mitigates type I interferon responses. (A) Albumin creatinine ratios measured in IMQ-treated WT and *Sting*^{-/-} mice at euthanasia (WT-IMQ, n = 18; *Sting*^{-/-}-IMQ, n = 12). (B and C) Quantitative analysis of kidney immune complex deposition is shown (WT-IMQ, n = 13; *Sting*^{-/-}-IMQ, n = 11). (D) Representative images of kidney sections stained for immune complex deposition are shown: C3, green; IgG, red; Hoechst, blue. Scale bar, 100 μm. (E) Kidney pathology score and representative kidney tissue images stained with H&E are shown. Scale bar, 1,000 μm. (F) Representative images of spleen sections from untreated and IMQ-treated WT mice stained for anti-IgM (green), Ly6G (red), and Cit-H3 (purple) and Hoechst (blue) are given. Quantitative PCR analysis of *mx-1*, *isg15*, and *irf7* genes in (G) splenocytes and (H) PBMCs from IMQ-treated WT mice (n = 11) and *Sting*^{-/-} mice (n = 8) is shown. *P < 0.05, **P < 0.01, ***P < 0.001 by Mann-Whitney test. H&E, hematoxylin and eosin; IF, Immunofluorescence; IMQ, imiquimod; PBMC, peripheral blood mononuclear cell; STING, stimulator of interferon genes; WT, wild type.

compared with IMQ-treated WT mice, although it was not significant (Figure 2A). Immunofluorescence staining revealed a significant decrease in C3 and IgG deposition in *Sting*^{-/-} mice treated with IMQ compared with IMQ-treated WT mice (Figure 2B–D). H&E staining also demonstrated lower glomerular and interstitial scores in IMQ-treated *Sting*^{-/-} mice compared with IMQ-treated WT mice (Figure 2E). Concurrently, IMQ treatment induced an increase in NETs in the spleen, as indicated by elevated levels of citrullinated histone H3 (Figure 2F).

Quantitative PCR (qPCR) analysis demonstrated a noteworthy reduction in IFN-regulated genes, including *Mx1*, *Isg15*, and *Irf7*, in both the spleen and PBMCs of *Sting*^{-/-} mice treated with IMQ relative to IMQ-treated WT mice (Figure 2G and H). To further corroborate STING involvement, we administered an inhibitor of this molecule, H-151, to IMQ-treated animals. Administration of H-151 significantly attenuated IMQ-induced splenomegaly, as assessed by lower spleen weight and lower total splenocyte numbers, in comparison with the vehicle control

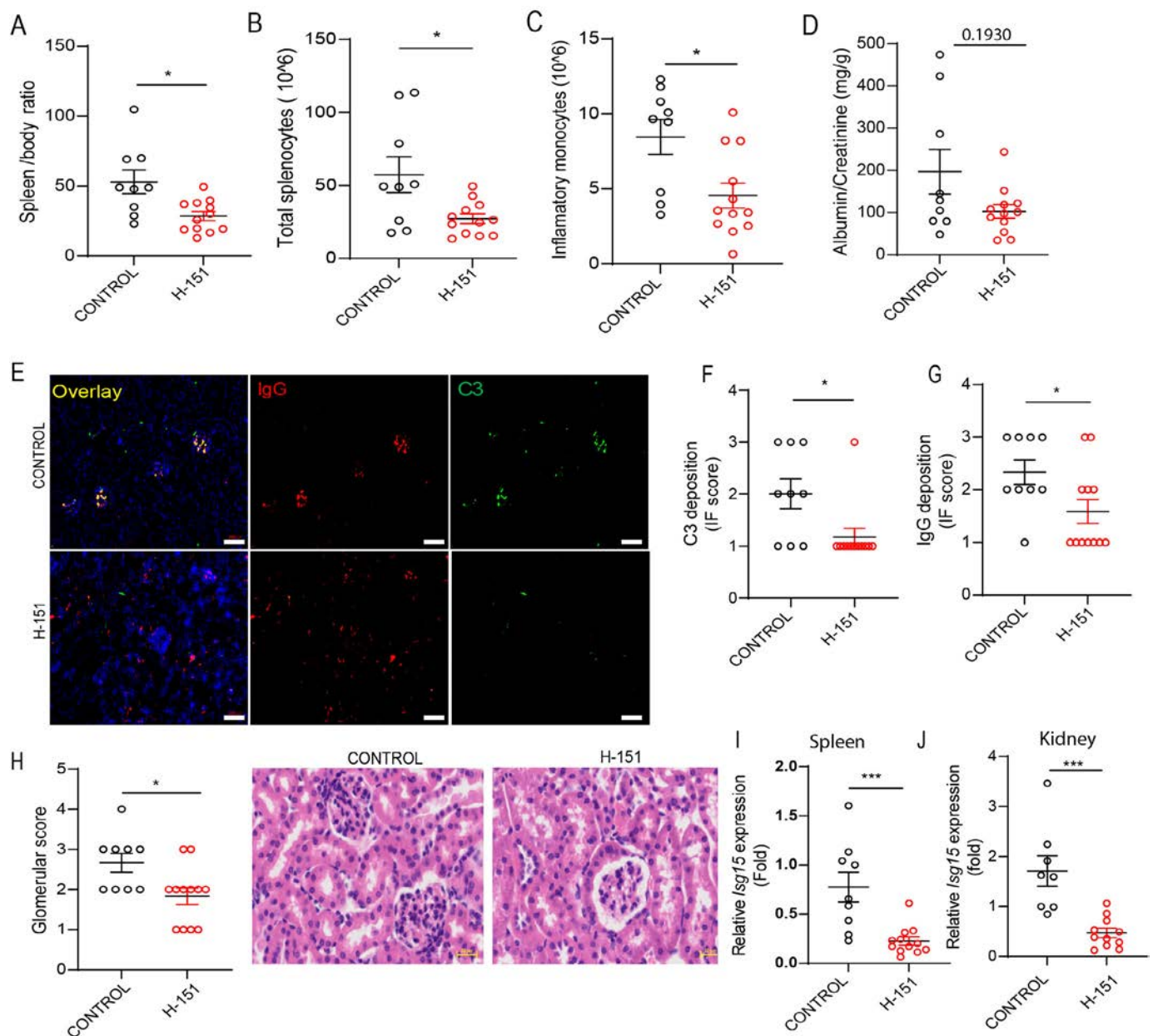


Figure 3. Pharmacological inhibition of STING with H-151 ameliorates IMQ-induced renal immune complex deposition. (A) Spleen/body weight and albumin:creatinine ratios of IMQ-treated wild-type mice (CONTROL) in the absence or presence of STING inhibitor H-151 are shown. (B and C) Splenocytes and inflammatory monocytes (CD11b⁺, CD11c⁺) of IMQ-treated wild-type mice (CONTROL) in the absence or presence of H-151 are shown. (D) Proteinuria assessment in IMQ-treated mice at death is shown (CONTROL, n = 9; H-151, n = 12). (E) Representative images of kidney sections stained for immune complex deposition are given: C3, green; IgG, red; Hoechst, blue. Scale bar, 100 μ m. (F and G) Quantitative analysis of kidney immune complex deposition of IMQ-treated wild-type mice (CONTROL) in the absence or presence of H-151 is shown. (H) Kidney pathology score and representative kidney tissue images stained with H&E are shown. Scale bar, 1,000 μ m. Quantitative PCR analysis of *Isg15* in (I) splenocytes and (J) kidney from IMQ-treated mice is given. * P < 0.05 by Mann-Whitney test. H&E, hematoxylin and eosin; IF, Immunofluorescence; IMQ, imiquimod; PCR, polymerase chain reaction; STING, stimulator of interferon genes.

group (Figure 3A and B). In addition, the expansion of proinflammatory monocytes (CD11b⁺Ly6C⁺Ly6G[−]) was substantially reduced in the H-151-treated group compared with the control group (Figure 3C). Furthermore, a trend toward lower levels of proteinuria in the urine was observed in IMQ-treated mice with STING inhibition, but it was not statistically significant

(Figure 3D). This was accompanied with significant reduction of glomerular C3 and IgG deposition (Figure 3E–G) and glomerular and interstitial scores (Figure 3H). Moreover, the gene expression levels of *Isg15* in spleen and kidney was dampened in the presence of H-151 (Figure 3I and J). These results support a role for STING in driving TLR7/8-induced autoimmunity.

Oxidized DNA elevation in mouse and human lupus in association with kidney and cardiovascular manifestations.

In patients with SLE, the presence of oxidized DNA and mtDNA has been well documented,^{9,20,21} highlighting their potential roles in disease pathogenesis. Oxidative stress contributes to cellular damage and is crucial for activating the STING pathway. Therefore, we aimed to assess the levels of DNA and their oxidation status in our IMQ-treated mice. Levels of genomic DNA, assessed by PCR targeting 18S, were significantly elevated in the serum of WT mice after IMQ treatment compared with untreated controls (Figure 4A). In contrast, there was no significant difference observed in the levels of the mtDNA marker 16S among all these groups (Figure 4B). Treatment with DNase1 reduced genomic DNA levels in the serum (Figure 4C), concomitant with a significant decrease in IFN-regulated genes in both WT and *Sting1*^{-/-} mice treated with IMQ (Figure 4D). Overall, these results indicate that IMQ treatment induced increases in genomic, but not mitochondrial, DNA release, but this was not modulated by the absence of STING.

IMQ treatment induced a marked increase in levels of oxidized circulating DNA in WT mice, as measured by ELISA (Figure 4E). Notably, NETs were significantly elevated in the serum of WT mice treated with IMQ after three to five weeks compared with untreated controls (Figure 4F). In humans, neutrophils exposed to IMQ in vitro demonstrated release of NETs with increased levels of oxidation of nucleic acids when compared with phorbol 12-myristate 13-acetate (PMA)-treated neutrophils (Figure 4G). To explore the clinical relevance of this finding, oxidized DNA levels were quantified in sera from patients with lupus, revealing a significant association with those diagnosed with lupus nephritis ($r = 0.5314$; $P = 0.0462$) (Figure 4H). Additionally, levels of DNA oxidation in serum were associated with enhanced vascular wall inflammation (reported as target:background ratio, as assessed by FDG-PET CT) in patients with lupus ($r = 0.4526$; $P = 0.0451$) (Figure 4I) and urine protein ($r = 0.4051$; $P = 0.0427$) (Figure 4J). Levels of DNA oxidation were negatively associated with serum C3 ($r = -0.5028$; $P = 0.0119$) (Figure 4K) and patients' age ($r = -0.4291$; $P = 0.0295$) (Figure 4L). We did not find associations between oxidized nucleic acids and specific lupus medications (azathioprine: $r = 0.1196$, $P = 0.3077$; methotrexate: $r = 0.1775$, $P = 0.2270$; mycophenolate mofetil: $r = 0.01435$, $P = 0.2730$; prednisone: $r = 0.3814$, $P = 0.0971$; hydroxychloroquine: $r = 0.3546$, $P = 0.0625$). There was a significant association between use of statins and levels of oxidized nucleic acids ($r = 0.4500$; $P = 0.0232$). The demographics of the patients are listed in Supplementary Tables 1 and 2. Overall, these results indicate that enhanced DNA oxidation in SLE is associated with clinical markers of disease activity, renal dysfunction, and vascular inflammation.

Critical role of STING in exacerbating vascular inflammation and promoting atherogenesis. To further elucidate the role of STING in vascular inflammation which can

contribute to an increased risk of atherosclerosis, a feature of SLE and other autoimmune diseases, we investigated the impact of this pathway in *Apoe*^{-/-} mice, a model of accelerated atherosclerosis, reminiscent of what is observed in SLE. Given the observation that increased levels of DNA oxidation are associated with vascular inflammation, we generated *Apoe*^{-/-}*Sting1*^{-/-} mice. The qPCR analysis confirmed a significant reduction in STING messenger RNA levels in the aortas of *Apoe*^{-/-}*Sting1*^{-/-} mice compared with *Apoe*^{-/-} mice (Figure 5A). This reduction was accompanied by a significant decrease in serum levels of IFN-1 (IFN- α and β), whereas type II IFN levels remained unchanged (Figure 5B–D). Functional assessments of vascular health revealed improved endothelium-dependent vasorelaxation in *Apoe*^{-/-}*Sting1*^{-/-} precontracted thoracic aortas after Ach administration when compared with *Apoe*^{-/-} mice (Figure 5E). Morphometric analysis of atherosclerotic lesions showed a notable reduction in plaque burden in both the thoracic aorta (Figure 5F) and aortic root (Figure 6A) of HFD *Apoe*^{-/-}*Sting1*^{-/-} mice compared with *Apoe*^{-/-} mice. Furthermore, quantification of necrotic lesions and Crystal content demonstrated a significant decrease in *Apoe*^{-/-}*Sting1*^{-/-} mice, indicating reduced disease severity (Figure 6B and C).

Immunofluorescence analysis of aortic sections revealed significant reduction of macrophages and alpha smooth muscle actin in *Apoe*^{-/-}*Sting1*^{-/-} mice, indicative of attenuated inflammation and smooth muscle cell activation (Figure 6D). Additionally, reduced numbers of neutrophils and NETs were observed in the absence of STING (Figure 6E and Supplementary Figure 2). Further molecular analysis via qPCR demonstrated decreased expression levels of adhesion molecules (intercellular adhesion molecule, vascular cell adhesion molecule, E-selectin) (Figure 6F–H) and inflammatory mediators (interleukin-1 β , NF- κ B) in the aortas of HFD *Apoe*^{-/-}*Sting1*^{-/-} mice compared with *Apoe*^{-/-} mice (Figure 6I and J). To further elucidate the role of IFN- β in plaque formation, human M2 macrophages were primed with IFN- β , IFN- $\alpha\beta$ (IFN-1), or purified NETs for 24 hours, and internalization of native LDL, oxidized LDL, or acetylated LDL was quantified (6K–N). No significant differences were seen in the internalization of LDL or oxidized LDL after priming with IFN- β , IFN- $\alpha\beta$, or NETs (Figure 6K and L). In contrast, IFN- β and IFN- $\alpha\beta$ -primed macrophages displayed enhanced internalization of acetylated oxidized LDL when compared with untreated cells (Figure 6M and N). These findings collectively underscore the critical role of STING in exacerbating vascular inflammation and promoting atherogenesis in the context of APOE deficiency, resembling features observed in patients with lupus.

DISCUSSION

The role of the STING pathway in SLE has garnered increasing interest, yet significant discrepancies in findings across different experimental models highlight the complexity of its

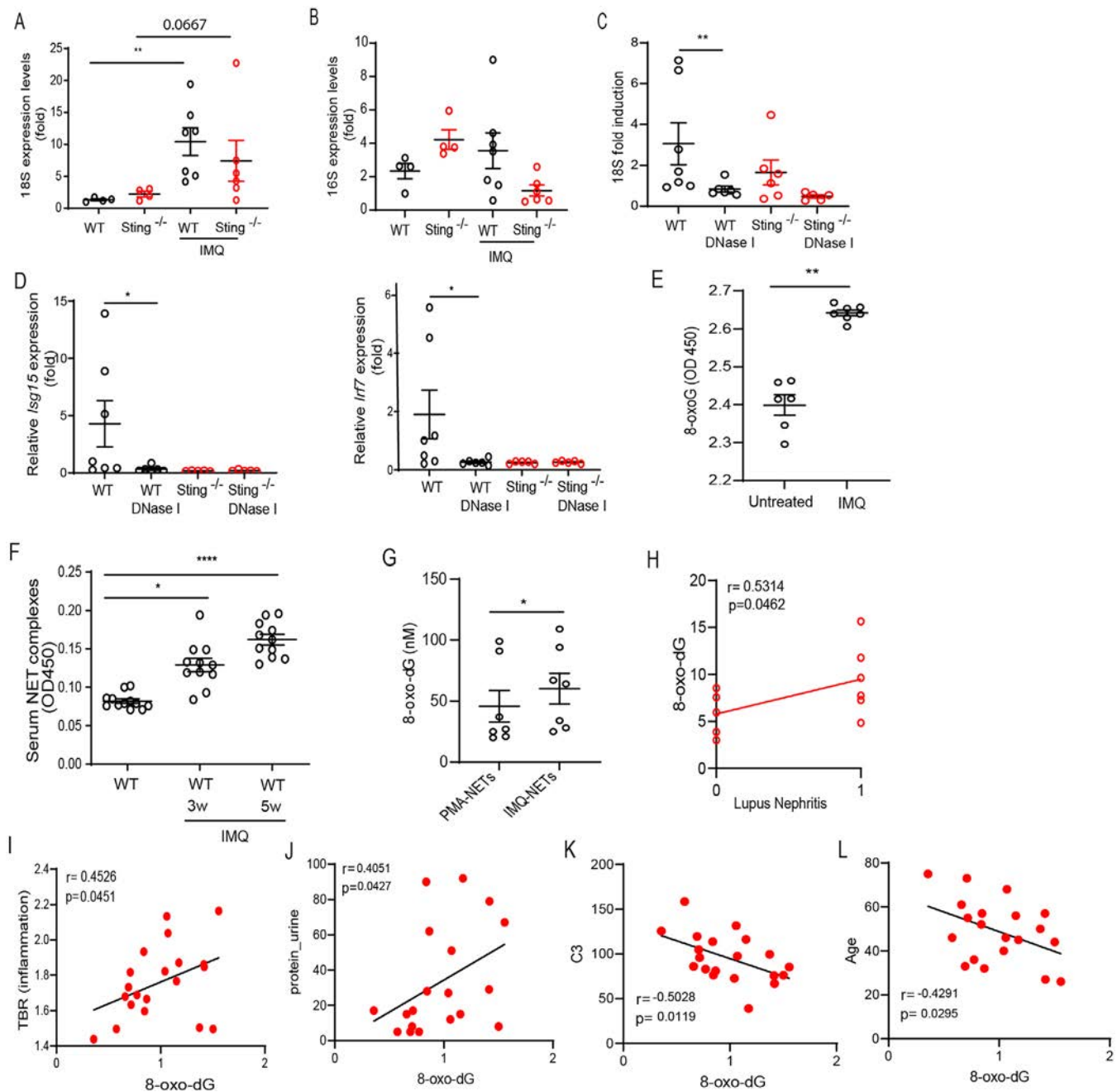


Figure 4. Levels of oxidized DNA are elevated in IMQ-treated animals and in patients with lupus in association with parameters of kidney injury and cardiovascular inflammation. (A–C) Quantitative PCR analysis of genomic, 18S, and mitochondrial 16S genes in the serum from untreated or IMQ-treated or DNase I-treated mice is shown; $n = 4$ –7 mice per group. (D) Quantitative PCR analysis of *Isg15* and *Irf7* in splenocytes from IMQ-treated WT mice and *Sting*^{-/-} mice in the presence or absence of DNase I treatment is shown (WT-Control, $n = 7$; WT-DNase I, $n = 6$; *Sting*^{-/-}-Control, $n = 6$; *Sting*^{-/-}-DNase I, $n = 5$). (E) ELISA analysis of oxidized DNA in the serum from untreated and IMQ-treated WT is shown; $n = 6$ –7 mice per group. (F) ELISA analysis of MPO-DNA complexes in the serum from untreated and IMQ-treated WT mice at indicated time points is shown. (G) Levels of 8-oxo-dG measured in purified NETs isolated from human control neutrophils after four hours of treatment with PMA or IMQ are shown. Mann-Whitney was used. (H) Analysis of serum samples from patients with SLE with ($n = 6$) and without lupus nephritis ($n = 5$) for the presence of 8-oxo-dG is given. Correlation between lupus nephritis and 8-oxo-dG levels was assessed using the Spearman correlation test. (I) Levels of 8-oxo-dG were measured in serum from patients with lupus. Correlation between levels of 8-oxo-dG and (I) vascular inflammation, expressed as TBR quantified by FDG-PET CT; (J) urine protein, (K) serum C3, and (L) age, was analyzed by Spearman. * $P < 0.05$, ** $P < 0.01$, *** $P < 0.001$, **** $P < 0.0001$. ELISA, enzyme-linked immunosorbent assay; FDG-PET CT, ¹⁸F-fluorodeoxyglucose-positron emission tomography/computed tomography; IMQ, imiquimod; MPO, myeloperoxidase; NET, neutrophil extracellular trap; OD, optical density; PCR, polymerase chain reaction; PMA, phorbol 12-myristate 13-acetate; SLE, systemic lupus erythematosus; STING, stimulator of interferon genes; TBR, target:background ratio; WT, wild type; 8-oxo-dG, 8-hydroxy 2-deoxyguanosine

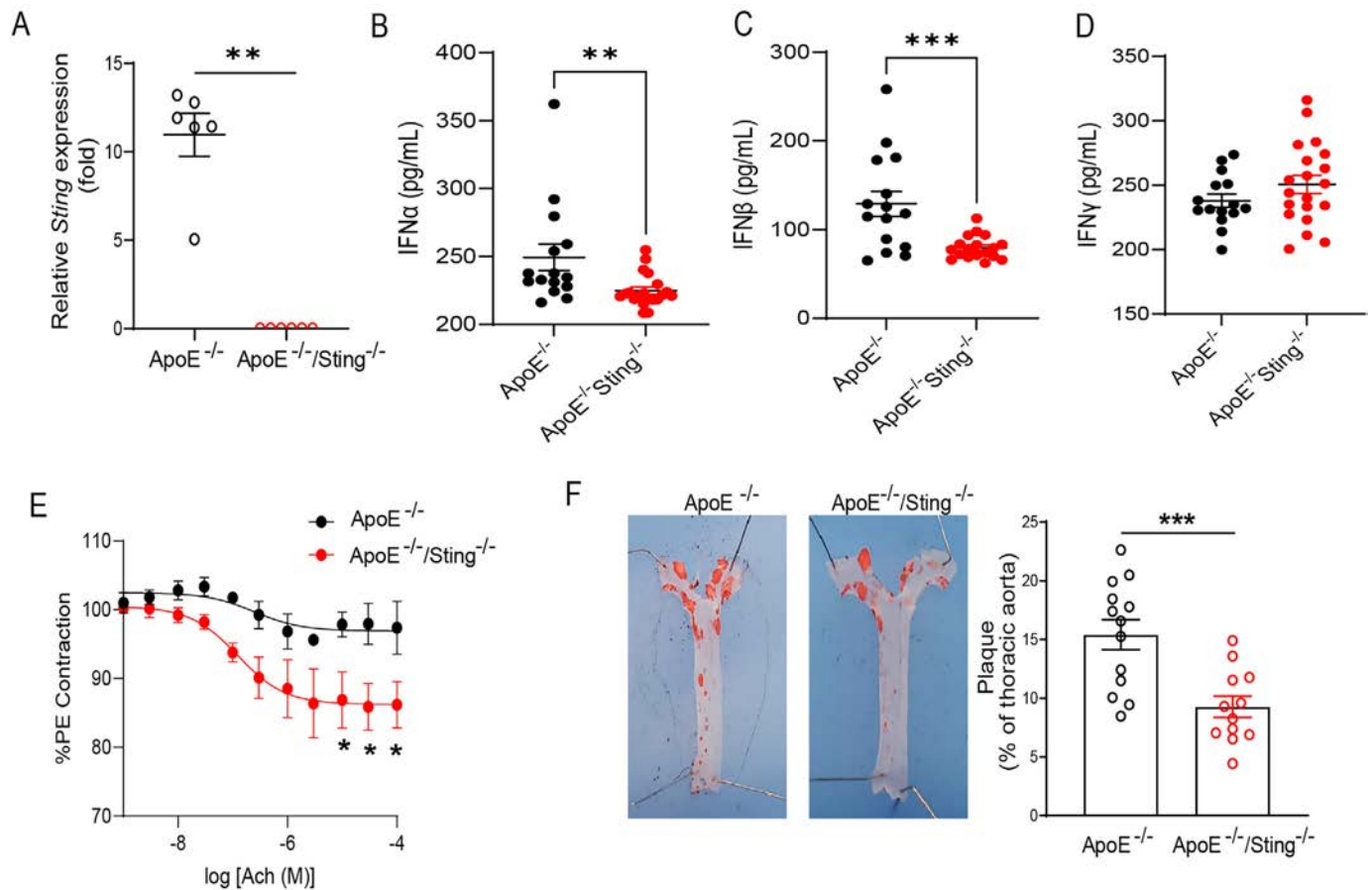


Figure 5. STING deficiency mitigates vascular damage and reduces atherosclerosis burden in association with diminished type I IFN production in animals fed with HFD. (A) mRNA levels of STING in aorta of ApoE^{-/-} (n = 6) and ApoE^{-/-}Sting^{-/-} mice (n = 6) are shown. Serum levels of (B) IFNα, (C) IFNβ, and (D) IFNγ measured in ApoE^{-/-} (n = 15) and ApoE^{-/-}Sting^{-/-} (n = 20) in mice are shown. **P < 0.01, ***P < 0.001 by Mann-Whitney test. (E) Ach-dependent vasoelaxation after PE precontraction was determined in thoracic aortas of ApoE^{-/-} and ApoE^{-/-}Sting^{-/-} (n = 4 mice/group). Results represent mean ± SEM % vasorelaxation; *P < 0.05. A two-way ANOVA with post hoc Tukey's test was used to compare differences among the groups. (F) Representative images and quantification of plaque area of en face preparations of intact aortas from ApoE^{-/-} and ApoE^{-/-}Sting^{-/-} mice placed on HFC for 10 weeks and stained with Sudan IV (red) are shown. Results are mean ± SEM, and Mann-Whitney analysis was used. Ach, acetylcholine; ANOVA, analysis of variance; ApoE, apolipoprotein E; HFC, high-fat chow; HFD, XXXX; IFN, interferon; mRNA, messenger RNA; PE, phenylephrine; STING, stimulator of interferon genes.

involvement in the disease. This is likely a reflection of the heterogeneous nature of human SLE, where multiple genetic and environmental factors converge to drive disease pathogenesis. Research has demonstrated that the involvement of STING in lupus pathogenesis can vary significantly across different mouse models.^{10,11,22,23} Furthermore, oxidative stress generates oxidized DNA and RNA, which can activate STING more robustly than unmodified nucleic acids.^{5-7,10,11,22,23}

The IMQ-induced lupus model exhibits pronounced activation of the STING pathway, which has been linked to elevated levels of nucleic acid oxidation and was the model we tested in this study, and it demonstrated that STING signaling plays a critical role in promoting proinflammatory responses that drive lupus-associated pathology. STING deficiency attenuated systemic inflammation and renal immune complex deposition induced by IMQ, emphasizing its pathogenic role in TLR7/8-driven

autoimmunity. Mechanistically, we observed that STING activation, likely driven by aberrant accumulation of oxidized genomic DNA and excessive NET formation, promoted IFN-I responses, which are considered to play important roles in SLE pathogenesis.

Conflicting results in various lupus-prone mouse models underscore the complexity of STING's involvement in SLE. STING deficiency exacerbated lupus-like symptoms in MRL/Fas/pr mice and accelerated lupus development in the pristane-induced lupus model,^{10,11} whereas it ameliorated disease phenotypes in DNase II-deficient mice²⁴ and Fcgr2b-deficient mice.²² The loss of STING function in Goldenticket mutant mice rescued the autoimmune symptoms in a pristane-induced lupus model.²³ Besides genetic background differences, it is also possible that variation in levels of oxidized nucleic acids and the role of IFN-1 and NETs in specific models may determine the role of STING in

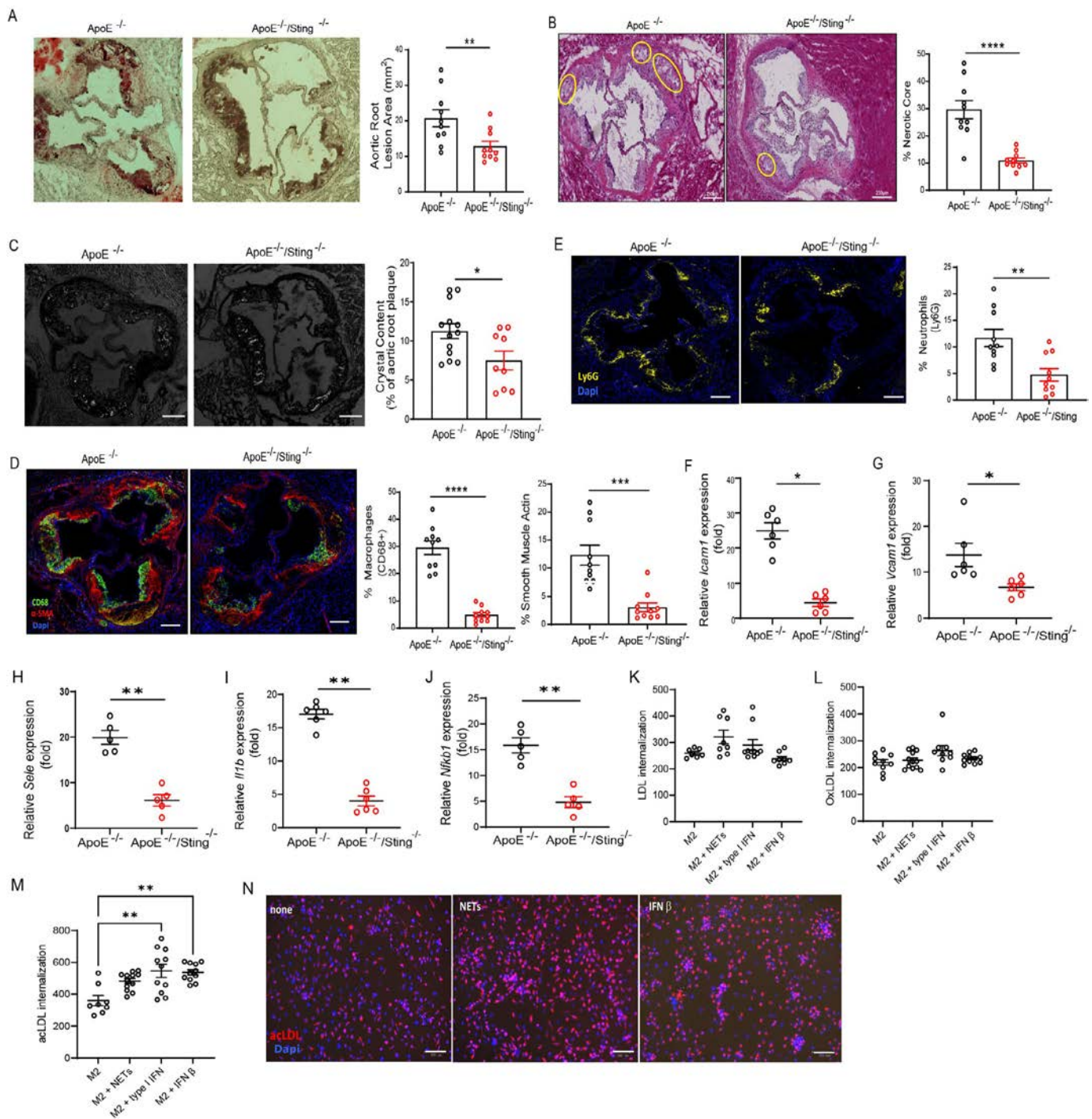


Figure 6. STING deficiency reduces atherosclerosis burden in animals fed with HFD, whereas type I IFNs enhance acLDL internalization in M2 macrophages. Representative images and quantitation of (A) plaque area relative to the aortic lumen area of aortic root sections and (B) necrotic core area of aortic root sections are shown. (C) Crystal content area of aortic root sections of *ApoE*^{-/-} and *ApoE*^{-/-}*Sting*^{-/-} mice are shown; n = 10/group in 2 independent experiments. Results are mean ± SEM, and Mann-Whitney analysis was used. (D and E) Representative immunofluorescence images and quantitation of CD68⁺ macrophages (green), alpha smooth muscle actin, and Ly6G⁺ neutrophils (yellow) in the plaque area are shown. Results are mean ± SEM. Quantitative PCR analysis of (F) *Icam1*, (G) *Vcam1*, (H) *Sele* (E-selectin), (I) *Il1b*, and (J) *Nfkb1* in aorta of *ApoE*^{-/-} (n = 6) and *ApoE*^{-/-}*Sting*^{-/-} mice (n = 6) is shown. **P* < 0.05, ***P* < 0.01, ****P* < 0.001, *****P* < 0.0001 by Mann-Whitney test. Human monocyte-derived M2 macrophages were preincubated with NETs, IFNα/β, or just IFNβ for 24 hours. Cells were then incubated with different forms of LDL. (K–N) Quantification and representative images of macrophages incubated with LDL (K), oxLDL (L), or acLDL (M and N) for three hours are shown. Results are mean ± SEM, and Kruskal-Wallis analysis was used. ***P* < 0.01. ac, acetylated; ApoE, apolipoprotein E; HFD, High-fat diet; ICAM, intercellular adhesion molecule; IFN, interferon; Il, interleukin; LDL, low-density lipoprotein; NET, neutrophil extracellular trap; ox, oxidized; PCR, polymerase chain reaction; STING, stimulator of interferon genes; VCAM, vascular cell adhesion molecule.

pathogenesis. This discrepancy highlights the influence of genetic predispositions on STING-mediated responses and the importance of choosing appropriate models for studying specific aspects of lupus. The prominent nucleic acid oxidation observed in the IMQ-induced lupus model may serve as a critical driver of STING activation, distinguishing it from other models.

Future studies should further evaluate other potential reasons for these discrepancies, quite reminiscent of human SLE. The genetic landscape of SLE is complex, involving multiple susceptibility loci. Variations in genes that regulate the immune response, including those involved in nucleic acid sensing and clearance, can influence the extent to which STING contributes to lupus pathogenesis. Polymorphisms in the *IRF5* and *TYK2* genes, which play roles in the IFN-1 pathway, can modulate the severity of disease manifestations in patients with SLE.²⁵ The interplay between these genetic factors and environmental triggers further complicates our understanding of STING's role in SLE.

Our study also linked STING activation to endothelial dysfunction and accelerated atherosclerosis, common comorbidities in SLE. STING deficiency protected against endothelial dysfunction and reduced atherosclerotic lesion development in ApoE^{-/-} mice, implicating STING-mediated IFN-I responses in vascular injury and inflammation. These findings are consistent with previous reports linking STING activation to vascular inflammation and atherogenesis in other disease contexts.²⁶

Therapeutically, our study supports the potential of STING inhibition as an approach to mitigate endosomal TLR-driven autoimmunity and its complications. These results underscore the promise of STING pathway inhibition in clinical settings, suggesting that it may benefit subsets of patients with SLE characterized by TLR7/8-driven immune dysregulation.

In conclusion, our findings contribute to a deeper understanding of the putative diverse roles of STING in lupus pathogenesis, highlighting its contributions to systemic immune dysregulation, vascular injury, and potential therapeutic avenues. Future studies should further explore the molecular mechanisms underlying STING activation in lupus and evaluate the efficacy of STING-targeted therapies across different lupus models and patient subsets. This approach is crucial for identifying optimal conditions and patient populations that may benefit most from STING modulation in the treatment of SLE and related autoimmune diseases.

ACKNOWLEDGMENTS

We acknowledge Randall Kennedy for technical assistance and the Office of Science and technology at NIAMS, NIH for technical support.

AUTHOR CONTRIBUTIONS

All authors contributed to at least one of the following manuscript preparation roles: conceptualization AND/OR methodology, software,



investigation, formal analysis, data curation, visualization, and validation AND drafting or reviewing/editing the final draft. As corresponding author, Dr Kaplan confirms that all authors have provided the final approval of the version to be published, and takes responsibility for the affirmations regarding article submission (eg, not under consideration by another journal), the integrity of the data presented, and the statements regarding compliance with institutional review board/Declaration of Helsinki requirements.

REFERENCES

1. Crowl JT, Gray EE, Pestal K, et al. Intracellular nucleic acid detection in autoimmunity. *Annu Rev Immunol* 2017;35:313–336.
2. Crow MK. Pathogenesis of systemic lupus erythematosus: risks, mechanisms and therapeutic targets. *Ann Rheum Dis* 2023;82:999–1014.
3. Liu Y, Seto NL, Carmona-Rivera C, et al. Accelerated model of lupus autoimmunity and vasculopathy driven by toll-like receptor 7/9 imbalance. *Lupus Sci Med* 2018;5:e000259.
4. Liu Y, Jesus AA, Marrero B, et al. Activated STING in a vascular and pulmonary syndrome. *N Engl J Med* 2014;371:507–518.
5. Murayama G, Chiba A, Kuga T, et al. Inhibition of mTOR suppresses IFN α production and the STING pathway in monocytes from systemic lupus erythematosus patients. *Rheumatology (Oxford)* 2020;59:2992–3002.
6. Kato Y, Park J, Takamatsu H, et al. Apoptosis-derived membrane vesicles drive the cGAS-STING pathway and enhance type I IFN production in systemic lupus erythematosus. *Ann Rheum Dis* 2018;77:1507–1515.
7. Wang J, Dai M, Cui Y, et al. Association of abnormal elevations in IFIT3 with overactive cyclic GMP-AMP synthase/stimulator of interferon genes signaling in human systemic lupus erythematosus monocytes. *Arthritis Rheumatol* 2018;70:2036–2045.
8. Kim J, Gupta R, Blanco LP, et al. VDAC oligomers form mitochondrial pores to release mtDNA fragments and promote lupus-like disease. *Science* 2019;366:1531–1536.
9. Lood C, Blanco LP, Purmalek MM, et al. Neutrophil extracellular traps enriched in oxidized mitochondrial DNA are interferogenic and contribute to lupus-like disease. *Nat Med* 2016;22:146–153.
10. Motwani M, McGowan J, Antonovitch J, et al. cGAS-STING pathway does not promote autoimmunity in murine models of SLE. *Front Immunol* 2021;12:605930.
11. Sharma S, Campbell AM, Chan J, et al. Suppression of systemic autoimmunity by the innate immune adaptor STING. *Proc Natl Acad Sci U S A* 2015;112:E710–E717.
12. Hochberg MC. Updating the American College of Rheumatology revised criteria for the classification of systemic lupus erythematosus. *Arthritis Rheum* 1997;40:1725.
13. Goel RR, Wang X, O'Neil LJ, et al. Interferon lambda promotes immune dysregulation and tissue inflammation in TLR7-induced lupus. *Proc Natl Acad Sci U S A* 2020;117:5409–5419.
14. Haag SM, Gulen MF, Reymond L, et al. Targeting STING with covalent small-molecule inhibitors. *Nature* 2018;559:269–273.
15. Liu Y, Carmona-Rivera C, Moore E, et al. Myeloid-specific deletion of peptidylarginine deiminase 4 mitigates atherosclerosis. *Front Immunol* 2018;9:1680.
16. Liu Y, Lightfoot YL, Seto N, et al. Peptidylarginine deiminases 2 and 4 modulate innate and adaptive immune responses in TLR-7-dependent lupus. *JCI Insight* 2018;3:e124729.
17. Kuriakose J, Redecke V, Guy C, et al. Patrolling monocytes promote the pathogenesis of early lupus-like glomerulonephritis. *J Clin Invest* 2019;129:2251–2265.

18. Weening JJ, D'Agati VD, Schwartz MM, et al. The classification of glomerulonephritis in systemic lupus erythematosus revisited. *Kidney Int* 2004;65:521–530.
19. Carlucci PM, Purmalek MM, Dey AK, et al. Neutrophil subsets and their gene signature associate with vascular inflammation and coronary atherosclerosis in lupus. *JCI Insight* 2018;3:e99276.
20. Tumurkhuu G, Chen S, Montano EN, et al. Oxidative DNA damage accelerates skin inflammation in pristane-induced lupus model. *Front Immunol* 2020;11:554725.
21. Caielli S, Athale S, Domic B, et al. Oxidized mitochondrial nucleoids released by neutrophils drive type I interferon production in human lupus. *J Exp Med* 2016;213:697–713.
22. Thim-Uam A, Prabakaran T, Tansakul M, et al. STING mediates lupus via the activation of conventional dendritic cell maturation and plasmacytoid dendritic cell differentiation. *iScience* 2020;23:101530.
23. Vejvisithsakul PP, Thumarat C, Leelahavanichkul A, et al. Elucidating the function of STING in systemic lupus erythematosus through the STING Goldenticket mouse mutant. *Sci Rep* 2024;14:13968.
24. Gao D, Li T, Li XD, et al. Activation of cyclic GMP-AMP synthase by self-DNA causes autoimmune diseases. *Proc Natl Acad Sci U S A* 2015;112:E5699–E5705.
25. Hellquist A, Järvinen TM, Koskenmies S, et al. Evidence for genetic association and interaction between the TYK2 and IRF5 genes in systemic lupus erythematosus. *J Rheumatol* 2009;36:1631–1638.
26. Pham PT, Fukuda D, Nishimoto S, et al. STING, a cytosolic DNA sensor, plays a critical role in atherogenesis: a link between innate immunity and chronic inflammation caused by lifestyle-related diseases. *Eur Heart J* 2021;42:4336–4348.

Safety and Efficacy of Ianalumab in Patients With Sjögren's Disease: 52-Week Results From a Randomized, Placebo-Controlled, Phase 2b Dose-Ranging Study

Thomas Dörner,¹  Simon J. Bowman,² Robert Fox,³ Xavier Mariette,⁴ Athena Papas,⁵ Thomas Grader-Beck,⁶ Benjamin A. Fisher,⁷ Filipe Barcelos,⁸ Salvatore De Vita,⁹ Hendrik Schulze-Koops,¹⁰  Robert J. Moots,¹¹ Guido Junge,¹² Janice Woznicki,¹³ Monika Sopala,¹² Alexandre Avrameas,¹² Wen-Lin Luo,¹³ and Wolfgang Hueber¹²

Objective. The objective of this study was to report 52-week safety and efficacy of ianalumab from phase 2b dose-finding study in patients with Sjögren's disease (SjD).

Methods. Patients randomly received (1:1:1:1) ianalumab (5, 50, or 300 mg) or placebo subcutaneously every 4 weeks until week 24 (treatment period [TP]1). At week 24, patients on 300 mg were rerandomized to continue 300 mg or receive placebo until week 52 (TP2), patients on placebo were switched to ianalumab 150 mg, and patients on 5 and 50 mg directly entered posttreatment safety follow-up. Patients who discontinued treatment early or completed treatment entered safety follow-up (≥ 20 weeks).

Results. During TP1, 190 patients were randomized (placebo = 49, 5 mg = 47, 50 mg = 47, 300 mg = 47). Of these 190 patients, 90 (47.4 %; 43 continued 300 mg and 47 received placebo) entered TP2, and 81 of 90 (90.0%) completed the study treatment. By week 52, efficacy was sustained in patients who continued 300 mg in TP2 (EULAR Sjögren's Syndrome Disease Activity Index, EULAR Sjögren's Syndrome Patient Reported Index, patient global assessment, and physician global assessment change from week 24: -1.45 , -0.46 , -4.69 , and -6.86 , respectively). Stimulated salivary flow rates and autoantibody levels numerically improved in the 300 mg group. Treatment-emergent adverse events were not dose-dependent, except for injection-site reactions. Cases of decreased neutrophil counts (Common Terminology Criteria for Adverse Events v4.03 grade 3 according to laboratory listings) were observed in three patients during the posttreatment follow-up, occurring at 3.5, 5.5, and 3 months, after the last ianalumab administration. None were associated with infection except one incidental finding of asymptomatic cytomegalovirus infection (IgM-positive).

Conclusion. In patients with SjD, ianalumab 300 mg demonstrated sustained efficacy through week 52 and a favorable safety profile up to two years of follow-up.

INTRODUCTION

Sjögren's disease (SjD) is an autoimmune disease characterized by lymphocytic infiltration, malfunction, and progressive

destruction of exocrine glands. The clinical features range from mucosal dryness, fatigue, and pain, affecting nearly all patients, to severe extraglandular disease manifestations with an increased risk for lymphoma development in a subset of patients.¹ The

ClinicalTrials.gov identifier: NCT02962895.

Supported by Novartis Pharma AG.

¹Thomas Dörner, MD: Charité Universitätsmedizin, Berlin, Germany; ²Simon J. Bowman, PhD, FRCP: University Hospitals Birmingham NHS Foundation Trust, Birmingham, United Kingdom; ³Robert Fox, MD, PhD: Scripps Memorial Hospital and Research Institute, La Jolla, California; ⁴Xavier Mariette, MD: Université Paris-Saclay, Paris, France, and Hôpital Bicêtre, AP-HP, Le Kremlin Bicêtre, France; ⁵Athena Papas, MD, PhD: Tufts School of Dental Medicine, Boston, Massachusetts; ⁶Thomas Grader-Beck, MD: Johns Hopkins School of Medicine, Baltimore, Maryland; ⁷Benjamin A. Fisher, MD: University Hospitals Birmingham NHS Foundation Trust, University of Birmingham, and NIHR Birmingham Biomedical Research Centre, Birmingham, United Kingdom; ⁸Filipe Barcelos, MD: Instituto Português de Reumatologia, Lisbon, Portugal; ⁹Salvatore De Vita, MD: University Hospital of Udine, Udine, Italy; ¹⁰Hendrik Schulze-Koops, MD, PhD: Ludwig Maximilians University of

Munich, Munich, Germany; ¹¹Robert J. Moots, MD, PhD: Aintree University Hospital, Liverpool, United Kingdom, and Edge Hill University, Ormskirk, United Kingdom; ¹²Guido Junge, PhD, Monika Sopala, PhD, Alexandre Avrameas, PhD, Wolfgang Hueber, MD: Novartis Pharma AG, Basel, Switzerland; ¹³Janice Woznicki, BSc, Wen-Lin Luo, PhD: Novartis Pharmaceuticals Corporation, East Hanover, New Jersey.

Additional supplementary information cited in this article can be found online in the Supporting Information section (<https://acrjournals.onlinelibrary.wiley.com/doi/10.1002/art.43059>).

Author disclosures are available at <https://onlinelibrary.wiley.com/doi/10.1002/art.43059>.

Address correspondence via email to Thomas Dörner, MD, at thomas.doerner@charite.de.

Submitted for publication February 7, 2024; accepted in revised form November 6, 2024.

treatment goals in patients with SjD are alleviation of symptoms of dry eye and mouth, control of systemic manifestations, and improvement in quality of life.² Currently available treatments for SjD are limited to symptomatic care for mucosal signs and symptoms.^{3,4} Although conventional disease-modifying antirheumatic drugs and glucocorticoids have been shown to reduce severe inflammation and delay the progression of systemic disease, they are often prescribed for off-label use and reported to be ineffective in improving the symptoms of dryness and fatigue.⁵ Over the past two decades, a number of disease-modifying treatments targeting specific elements of the immune system have been evaluated in SjD.²

Recent advances in the understanding of the pathogenesis of SjD have shown that B cells play a key role in the disease development and progression.^{6,7} Biologic therapies directed against cellular B cell targets, including rituximab and epratuzumab, or against the soluble cytokine B cell activating factor (BAFF) (belimumab) have not shown potential benefits in treating patients with SjD.^{8–13} A meta-analysis of rituximab trials showed weak effects on salivary and tear flow but no improvement in fatigue or other global measures of well-being.^{8–10} Treatment with epratuzumab improved symptoms only in some patients in an open-label phase 1/2 study¹¹ and in a subgroup of patients with systemic lupus erythematosus (SLE) with associated SjD.¹⁴ Belimumab improved fatigue in open-label phase 2 studies but was not effective in improving symptoms of dryness.^{12,13} The combination of rituximab and belimumab has been shown to enhance the depletion of salivary gland B cells and improve clinical outcomes.¹⁵ However, available data are limited to a single randomized controlled SjD trial, and further studies are needed to delineate the benefit and risk of this approach.

Ianalumab (VAY736) is a novel B cell–targeting human monoclonal antibody that combines profound B cell depletion via antibody-dependent cellular cytotoxicity with blockade of the BAFF receptor (BAFF-R), interrupting BAFF-mediated signaling for B cell maturation, proliferation, and survival, and is hypothesized to prevent reactivation of residual pathogenic B cell clones in the target tissue. In this paradigm, suppression of these B cell clones despite continued BAFF upregulation may play a role in the long-term maintenance of the treatment response to ianalumab after initial cell depletion.

A phase 2b dose-finding study evaluated three dose levels of ianalumab versus placebo in patients with moderate to severe SjD.¹⁶ The study met its primary end point at week 24; ianalumab treatment resulted in improvements in the EULAR Sjögren's Syndrome Disease Activity Index (ESSDAI), demonstrating a statistically significant dose-response relationship. Ianalumab was well tolerated with no dose-dependent increase in infections until week 24. Trends in other outcome measures and significant improvements in stimulated salivary flow further support the findings of a positive risk-benefit of ianalumab in this trial.¹⁶ Herein, we report the 52-week safety and additional exploratory efficacy results of this study.

PATIENTS AND METHODS

Study design and patients. This study was a randomized, parallel, double-blind, placebo-controlled, phase 2b multicenter (65 sites in 19 countries) dose-finding trial of ianalumab in patients with SjD. The detailed study design and patient inclusion and exclusion criteria have been previously reported.¹⁶ Briefly, patients aged 18 to 75 years who fulfilled the American European Consensus Group classification criteria¹⁷ were included. In addition, eligible patients were positive for anti-Ro/SSA antibody, had an ESSDAI score of 6 or more at screening (eligibility score based on weighted scores of the biologic, hematologic, articular, cutaneous, glandular, lymphadenopathy, and constitutional domains), and had a EULAR Sjögren's Syndrome Patient Reported Index (ESSPRI) score of 5 or more at baseline and stimulated whole salivary flow rate of more than 0.1 mL/min (minimal level of saliva production) at screening.

Key exclusion criteria were evidence of SjD associated with other autoimmune diseases, serious diseases or uncontrolled conditions, active infection, malignancy within the past five years (other than localized basal cell carcinoma of the skin, in situ cervical cancer or SjD-related lymphoma), pregnancy, recent change in allowed background therapy, and prior exposure to biologics within 180 days before randomization. After a screening period of four weeks, eligible patients were randomized equally to receive subcutaneous (SC) doses of ianalumab (5, 50, or 300 mg) or placebo every four weeks up to week 24. Per the study design, at week 24, after completion of the first blinded treatment period (TP)1, patients on ianalumab 300 mg were rerandomized (1:1) to continue 300 mg or receive placebo every 4 weeks up to week 52 in TP2, and patients on placebo were switched to ianalumab 150 mg every 4 weeks up to week 52. Patients in the ianalumab 5 and 50 mg groups directly entered safety follow-up. Patients who prematurely discontinued the study treatment at any time point or completed the treatment as planned entered the safety follow-up period for ≥ 20 weeks posttreatment (Supplementary Figure 1). The duration of safety follow-up was up to two years from the last dose of the study treatment, and it was defined for each patient based on the level of recovery of CD19–positive (CD19+) B cells.

All patients provided written informed consent before inclusion in the study. The trial was conducted according to Good Clinical Practice and the Declaration of Helsinki. The review board at each site approved the protocol. Data obtained at each site were monitored and analyzed by Novartis personnel.

Outcomes and assessments. As previously reported,¹⁶ the primary outcome was the change in the ESSDAI score from baseline at week 24. The exploratory outcomes up to week 52 included changes from baseline in ESSDAI, ESSPRI, physician global assessment (PhGA), patient global assessment (PaGA), Functional Assessment of Chronic Illness Therapy Fatigue

(FACIT-F), 36-Item Short Form Health Survey (SF-36) scores, and change from baseline in the levels of soluble BAFF, IgG, rheumatoid factor (RF), and autoantibody (anti-SSA/Ro60 and 52, anti-SSB/La).

The secondary outcomes related to objective measures included (1) change from baseline in stimulated salivary flow at week 24 and (2) change from baseline in whole-blood CD19⁺ B cell counts and time to recovery defined as $\geq 80\%$ of baseline or ≥ 50 cells/ μL .

Regular safety monitoring was performed: patient on-site visits occurred every four weeks and included a physical examination, routine laboratory tests, and evaluation and collection of adverse event (AE) details. Serious AEs (SAEs) were reported upon occurrence. The AE severity was graded as low, moderate, or severe. Clinical efficacy measurements, including ESSDAI and PhGA, and patient-reported outcome (PRO) measures, ESSPRI, SF-36, FACIT-F, and PaGA were collected at baseline and every four weeks during TP1 and TP2. Stimulated salivary flow was assessed at baseline and at weeks 12, 24, 28, 36, and 48.

Statistical analysis. The full analysis set (FAS) comprised all randomized patients to whom the study treatment was assigned. FAS was used for all efficacy variables unless otherwise stated. The safety set included all patients who received at least one dose of the study medication. The safety set was used in the analysis of all the safety variables. Demographics and baseline characteristics were descriptively summarized for the treatment groups using frequencies, percentages, or means (SD), as appropriate. For the secondary variables, ESSPRI and FACIT-F score dose-response analysis using Multiple Comparison Procedure–Modeling was performed, and all other secondary end points were analyzed using a mixed-effect model for repeated measures. Descriptive statistics were provided for ESSDAI, ESSPRI, FACIT-F, PhGA, PaGA, and SF-36. Continuous efficacy data were analyzed as the change from baseline with a linear mixed-effect model for repeated measures. The percentage change from baseline in B cell counts before, during, and after treatment with ianalumab, as well as the time to recover to baseline-like values (defined as at least 80% of baseline counts or ≥ 50 cells/ μL), were descriptively summarized. Post hoc analysis of the relationship between baseline BAFF concentrations and ESSDAI response at week 24 was performed using the one-sided *t*-test.

RESULTS

Patient disposition and characteristics. Of the 190 patients randomized in TP1 (placebo, $n = 49$; ianalumab 5 mg, $n = 47$; ianalumab 50 mg, $n = 47$; ianalumab 300 mg, $n = 47$), 178 (93.7%) completed TP1 as planned. As per protocol, 47 patients each in the ianalumab 5 and 50 mg groups entered the safety follow-up period directly from TP1.

A total of 90 of 190 (47.4%; ianalumab 300 mg, $n = 43$; placebo, $n = 47$) patients entered TP2.¹⁶ At week 24, patients who received ianalumab 300 mg were rerandomized to the placebo ($n = 22$) or ianalumab 300 mg ($n = 21$) group, and patients in the placebo group were switched to ianalumab 150 mg ($n = 47$). A total of 81 patients (90.0%) completed the planned study treatment in TP2, and 9 (10%) discontinued prematurely. The most common reason for discontinuation was AEs ($n = 7$; 7.8%). A total of 88 patients (placebo to ianalumab 150 mg, $n = 46$; ianalumab 300 mg to placebo, $n = 22$; ianalumab 300 mg to ianalumab 300 mg, $n = 20$) from TP2 continued to the safety follow-up period.

Demographics and baseline clinical characteristics were comparable between groups in TP2 (Table 1). Overall, the mean ESSDAI score was ≥ 10 for more than 70% of patients in each treatment group, with a mean ESSDAI score of 13.5 in the ianalumab 300 mg to ianalumab 300 mg group.

Efficacy. Primary outcome. As reported previously, the primary end point was met¹⁶; statistically significant dose-related decrease in disease activity, measured by ESSDAI, was observed at week 24. Briefly, the largest ESSDAI improvement was 1.92 points more reduction with ianalumab 300 mg versus placebo at week 24.

Exploratory and secondary outcomes. For TP2, one of the main objectives was to descriptively evaluate differences within the patient group on 300 mg who either discontinued or continued ianalumab 300 mg by week 24. At week 52, efficacy was sustained for patients who continued ianalumab 300 mg ($n = 21$) in TP2 (ESSDAI, ESSPRI, PaGA, and PhGA change from week 24: -1.45 , -0.46 , -4.69 , -6.86 , respectively; Supplementary Table 1). By week 52, improvement was also noted for patients in the placebo group who switched to ianalumab 150 mg. At the same time point, some loss of week 24 improvements in PROs (FACIT-F, PaGA, and SF-36) was observed in patients who switched to placebo at week 24. The changes between weeks 24 and 52 were numerically smallest for ESSPRI. Figure 1 shows a summary of the key exploratory efficacy parameters at week 52 compared to week 24.

Biomarker analysis. A greater maximum reduction in CD19⁺ B cells and IgG levels was observed at week 24 for the 50 mg and 300 mg groups compared to the 5 mg group (Figure 2 A–C). Across all treatment groups, BAFF sharply increased from baseline and promptly decreased after treatment discontinuation (Figure 2A). In the placebo to ianalumab 150 mg group, BAFF remained at baseline levels until week 24 and showed a respective increase upon the start of ianalumab after week 24, which was sustained until week 48 (last testing time point).

Per protocol, in TP1, the number of CD19⁺ cells was measured before the first dose of the study treatment (baseline) and at the week-24 visit. At week 24, the mean B cell counts remained at the baseline level in the placebo-treated group, whereas all

Table 1. Baseline demographic and clinical characteristics of patient subgroups treated in treatment period 2*

Variables	Placebo to ivalumab 150 mg (n = 47)	ivalumab 300 mg to placebo (n = 22)	ivalumab 300 mg to ivalumab 300 mg (n = 21)
Age, y	47.6 (12.6)	48.7 (16.8)	48.7 (14.7)
Female, n (%)	45 (95.7)	21 (95.5)	21 (100)
ESSDAI	12.9 (6.7)	13.7 (7.1)	13.5 (6.7)
ESSPRI	7.3 (1.1)	6.7 (1.9)	6.9 (1.5)
FACIT-F score	23.2 (9.1)	28.3 (11.5)	26.9 (10.5)
PhGA	51.8 (16.9)	53.6 (14.3)	51.4 (15.8)
PaGA	61.6 (17.4)	68 (24.0)	56.5 (18.8)
Stimulated salivary flow rate (mL/min), [min–max]	0.54 (0.74) [0.0–3.7]	0.92 (1.13) [0.0–5.1]	0.70 (0.58) [0.0–1.9]
Schirmer's test: left eye, mm	7.3 (8.8)	10.4 (11.7)	7.6 (8.1)
Schirmer's test: right eye, mm	6.6 (6.8)	8.6 (9.9)	5.7 (7.6)
Positive anti-Ro/SSA status, n (%)	47 (100)	22 (100)	21 (100)
IgG, g/L	17.4 (7.1)	18.0 (6.7)	17.7 (8.6)
IgM, g/L	1.7 (1.5)	1.3 (0.8)	1.3 (1.2)
B cell count, cells/ μ L	199.6 (146.8)	265.2 (267.1)	278.5 (156.2)
Use of DMARDs, n (%)	27 (57.4)	12 (54.5)	10 (47.6)
Hydroxychloroquine, n (%)	25 (53.2)	11 (50.0)	8 (38.1)
Methotrexate, n (%)	4 (8.5)	5 (22.7)	2 (9.5)
Steroid therapy, n (%)	14 (29.8)	5 (22.7)	7 (33.3)

* Values are in mean (SD), unless specified otherwise. Baseline medications were taken before the first dose and continued through the treatment period with a missing stop date or with a stop date on or after the first dose. DMARD, disease-modifying antirheumatic drug; ESSDAI, EULAR Sjögren's Syndrome Disease Activity Index; ESSPRI, EULAR Sjögren's Syndrome Patient Reported Index; FACIT-F, Functional Assessment of Chronic Illness Therapy Fatigue; PaGA, patient global assessment; PhGA, physician global assessment.

ivalumab-treated patients showed a sharp decline. However, there was a greater maximum reduction in mean CD19 B cell counts observed for 50 and 300 mg than for 5 mg. Following a treatment switch from placebo to ivalumab 150 mg, a sharp drop in B cell counts was observed at week 28. The B cell counts remained suppressed in all treatment groups up to week 48; depletion was maintained in patients who continued to receive ivalumab 300 mg up to week 48, and a marked return of B cell counts was observed after week 36 in patients who switched from ivalumab 300 mg to placebo at week 24. The time to CD19⁺ B cell recovery after stopping the study treatment was dose-proportional; the median time to B cell recovery was 3.8 months for ivalumab 5 mg, 4.8 months for ivalumab 50 mg, 8.4 months for ivalumab 300 mg (24 weeks), 6.8 months for placebo to ivalumab 150 mg (28 weeks), and 6.5 months for ivalumab 300 mg (52 weeks) groups (Supplementary Figure 2).

A reduction in IgM RF and serum IgG levels was observed across all treatment groups. The anti-Ro60/52 and anti-La autoantibody levels demonstrated a reduction of 15% to 20% from baseline at week 24 in the 50 and 300 mg groups. Notably, the decrease in anti-Ro60/52 levels was less prominent in the 5 mg group. Anti-Ro60/52 and anti-La autoantibody levels returned to baseline 6 months after discontinuation of ivalumab 300 mg. In contrast, continued treatment with ivalumab 300 mg showed stable or further decline in autoantibody levels (Figure 2D–G).

Other secondary outcomes. The stimulated whole salivary flow rate improved from baseline over time. The highest increase

was observed with ivalumab 300 mg at week 24,¹⁶ rising by 0.20 mL/min above placebo (95% confidence interval [CI]: 0.01–0.38; $P = 0.037$). At the last available assessment time point of flow rates (week 48), further improvement was observed in the ivalumab 300 mg group; stimulated salivary flow rate improvements remained numerically higher in the ivalumab 300 mg continued treatment group compared to the group that switched to placebo at week 24 (least squares mean change from baseline: 0.45 mL/min versus 0.22 mL/min; Figure 3). Supplementary Table 2 shows the proportion of patients with stimulated salivary flow response rate of at least 0.25 mL/min, and 0.50 mL/min over baseline. Figure 4 shows the potential associations between baseline BAFF levels with week 24 ESSDAI response in patients receiving an efficacious dose (50 and 300 mg pooled; analysis done for TP1 only). In this post hoc analysis, no statistical difference was observed between ESSDAI responders and nonresponders at the group level.

Safety. Safety data are presented for TP1, TP2, and post-treatment follow-ups. The 150 mg group includes TP1 placebo-treated patients who switched to ivalumab 150 mg at week 24 and “any 300 mg” group includes patients treated with ivalumab 300 mg up to week 24 plus those who continued 300 mg to week 52. The “any ivalumab”-treated group includes patients who received ivalumab treatment in TP1 or TP2.

Overall, a total of 176 of 188 patients (93.6%) who received ivalumab had at least one AE. The most frequent treatment-emergent AE (TEAE) per system organ class was “infections and infestations” (73.4%) followed by “general disorders and

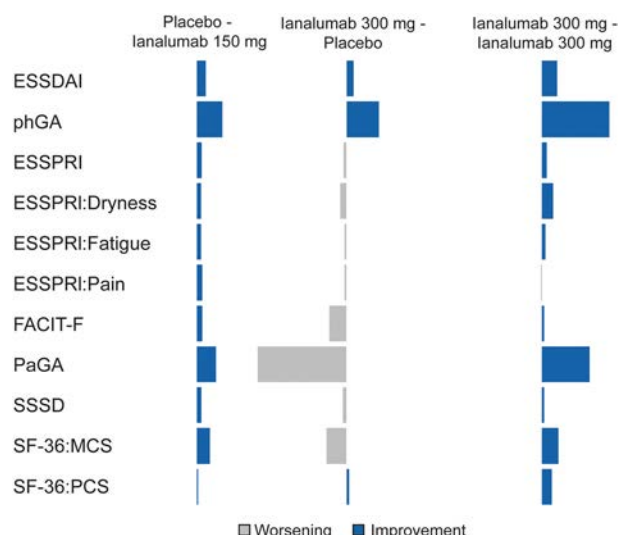


Figure 1. Summary of efficacy data at week 52 compared to week 24. Only patients with week 24 measurements and at least one measurement after week 24 were included. Least square means were derived from a mixed model for repeated measures that included treatment, visit, treatment by visit interaction, stratification factor, baseline ESSDAI score, and region as factors, and week 24 measurement as a continuous covariate. ESSDAI, EULAR Sjögren's Syndrome Disease Activity Index; ESSPRI, EULAR Sjögren's Syndrome Patient Reported Index; FACIT-F, Functional Assessment of Chronic Illness Therapy Fatigue; MCS, mental component summary; PCS, physical component summary; PaGA, patient global assessment; PhGA, physician global assessment; SSSD, Sjögren's syndrome symptom diary; SF-36, 36-Item Short Form Health Survey.

administration site conditions" (43.1%). Overall, a higher proportion of TEAEs was observed in the groups treated with ianalumab 300 mg, and these results were driven by mild to moderate injection-site reactions. One patient in the ianalumab 150 mg group reported a severe injection-site reaction and discontinued the study treatment. Overall, infections were mostly mild or moderate. The most commonly reported infections were nasopharyngitis (16.5%), upper respiratory tract infections (17.6%), urinary tract infections (13.8%), sinusitis (9.6%), bronchitis (8.0%), oral herpes (6.4%), and conjunctivitis (6.4%). A summary of AEs by treatment groups is provided in Table 2.

Serious infections were reported in eight patients treated with any ianalumab dose. The five SAEs of infections (Supplementary Table 3) were considered by the investigators to be treatment-related: candida infection ($n = 1$ in 5 mg group), tubo-ovarian abscess plus appendicitis ($n = 1$ in 50 mg group), and bronchitis and respiratory syncytial virus bronchiolitis ($n = 1$ in 150 mg group, in a patient with interstitial lung disease). The other three SAEs were not considered to be treatment-related: pneumonia (1 community-acquired, associated with chronic obstructive pulmonary disease in 150 mg group and 1 associated with newly diagnosed sarcoidosis in 300 mg group), wound infection ($n = 1$ in 50 mg group), sinusitis ($n = 1$ in 150 mg group), and COVID-19 and COVID-19 pneumonia

($n = 1$ in 300 mg group; both occurred 740 days after the last dose of ianalumab).

Malignancies were reported in two patients. A patient with previously treated human epidermal growth factor receptor-positive breast cancer was considered cured approximately 10 years previously and was randomized to ianalumab 5 mg. Nine months later, the patient had chest pain, and recurrence of breast cancer was suspected (treatment-emergent SAE). Positron emission tomography scan showed a rib fracture that was considered traumatic in nature. A course of trastuzumab treatment was initiated. No biopsy was performed; therefore, no tissue confirmation of the suspicion of recurrence of metastatic breast cancer was available. Based on the information obtained in April 2021, no further details related to the treatment and outcome of this case was available. The second malignancy case was deterioration of the concurrent extranodal marginal zone B cell lymphoma (mucosa-associated lymphoid tissue [MALT] type, SjD associated). One month before the start of study treatment with placebo, the patient experienced recurrence of the MALT lymphoma. Although further deterioration of lymphadenopathy was reported in TP2 (after the patient was rerandomized to ianalumab 150 mg), it was deemed unrelated to the study treatment by the investigator, and the treatment was continued. Some improvement of the lymphoma condition was noted three months later.

A total of 11 of 188 patients (5.9%) discontinued the study treatment due to AEs: 2 of 47 patients in the 5 mg group for bronchitis and decreased lymphocyte count; 2 of 47 patients in the 50 mg group for wound infection and injection-site reaction; 5 of 47 patients in the 150 mg group for herpes zoster, esophagitis, rash and vasculitis (occurred in the same patient), injection-site reaction, and systemic injection-related reaction; 2 of 21 patients in the 300-mg group for (1) pulmonary sarcoidosis and (2) arthralgia and dermatosis.

Lymphopenia and neutropenia were mostly grade 1 and grade 2. Cases of decreased neutrophil counts (Common Terminology Criteria for Adverse events [CTCAE] v4.03 grade 3 according to laboratory listings) were observed in three patients during the posttreatment follow-up, occurring at 3.5 months, 5.5 months, and 3 months after the last administration of ianalumab. All three patients had ongoing history of neutropenia CTCAE grade 1 (2 patients) or CTCAE grade 2 (1 patient) documented at screening or baseline visit. None were associated with infection except for a single incidental finding of an asymptomatic viral infection (cytomegalovirus [CMV] IgM-positive). Two patients had pre-existing grade 1 neutropenia, whereas one patient had pre-existing grade 2 neutropenia. No grade 4 neutropenia was reported. Two patients ($n = 1$ each in the 5 mg and 50 mg groups) entered the study (screening/baseline) with IgG levels below lower limit of normal (LLN), and their IgG levels remained below LLN until end of the study.

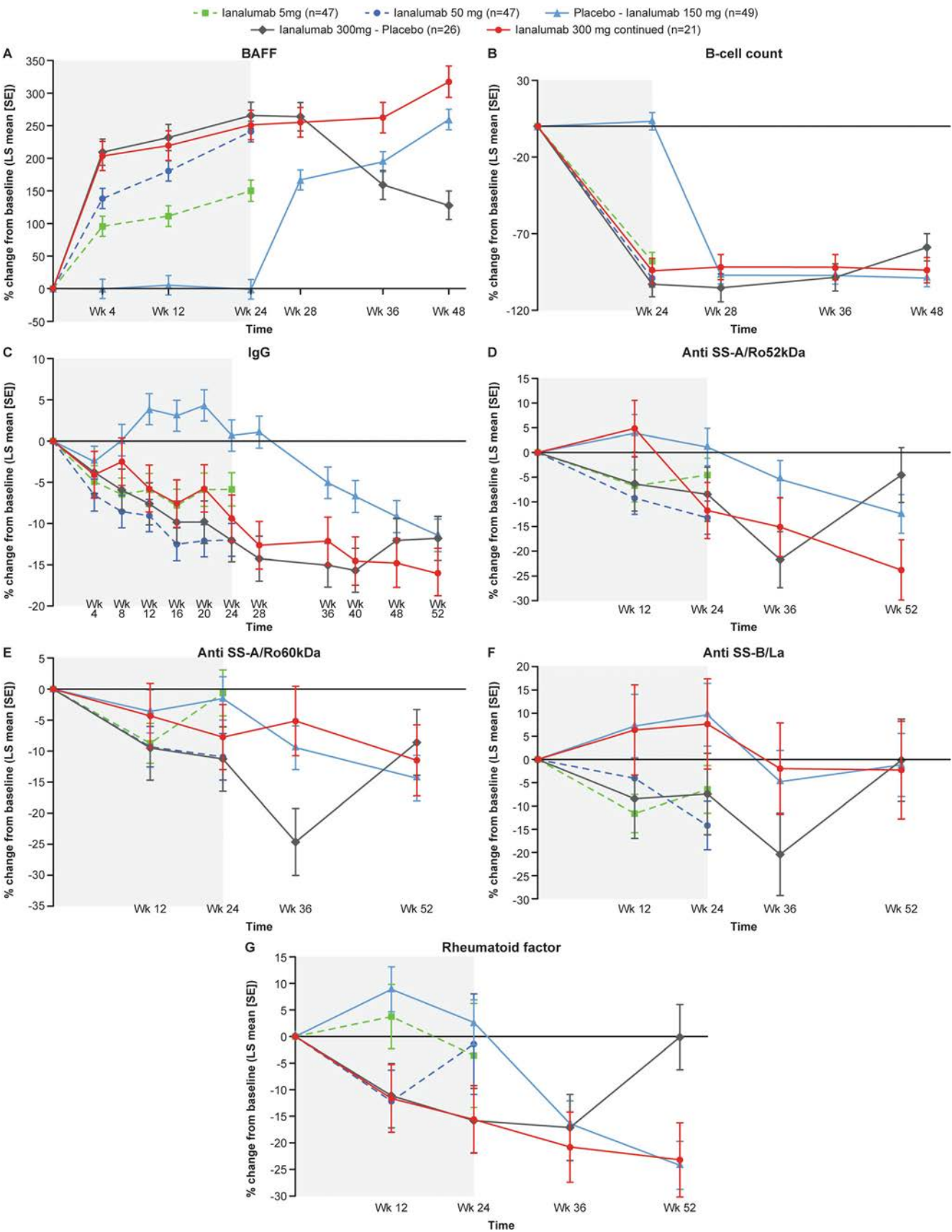


(Figure legend continues on next page.)

(Figure legend continued from previous page.)

Figure 2. Serum BAFF, B cells, IgG, and autoantibody concentrations by treatment group. The gray shaded area shows the placebo-controlled period. Patients who received 5 and 50 mg of ionalumab proceeded directly to the follow-up period. Therefore, no measurements were available for these cohorts after week 24. For (D)–(G), $n = 47$ for the placebo to ionalumab 150 mg and $n = 22$ for the ionalumab 300 mg to placebo groups. (A) LS mean change in BAFF concentration from baseline (pg/mL); (B) LS mean change in B cell count from baseline (cells/ μ L); (C) LS mean change in IgG concentration from baseline (g/L); (D–G) LS mean \pm SE of change from baseline of biomarkers presented up to week 52. BAFF, B cell activating factor; LS, least squares.

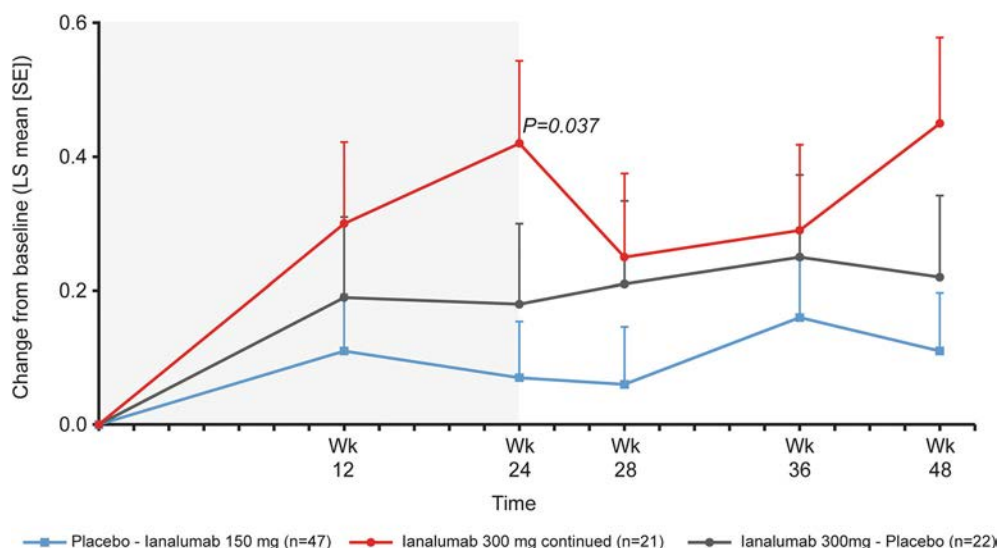


Figure 3. Stimulated salivary flow rate over time up to week 48, the last testing time point (primary end point at week 24). The gray shaded area shows the placebo-controlled period. Stimulated whole salivary flow significantly increased with 300 mg at week 24, rising by 0.20 mL/min above placebo (95% CI: 0.01–0.38; $P = 0.037$). Per protocol, no formal significance testing was performed for the exploratory time points after week 24. The figure presents data as the change from baseline for dose arms studied in TP2 following the new treatment assignment at week 24. Baseline is defined as the last assessment performed on or before the date of administration of the first dose of the study treatment. Only patients with baseline measurements and at least one measurement postbaseline were included. LS means were derived from a mixed model for repeated measures that included treatment, visit, treatment by visit interaction, stratification factor, baseline ESSDAI score, and region as factors and baseline value as a continuous covariate. CI, confidence interval; ESSDAI, EULAR Sjögren's Syndrome Disease Activity Index; LS, least squares; TP, treatment period.

DISCUSSION

As previously reported,¹⁶ the phase 2b study of ionalumab in moderate to severe active SjD achieved its primary objective, showing a dose-dependent reduction in disease activity at week 24. A dose of 300 mg administered once a month showed the greatest improvement in several outcome measures.¹⁶ The strength of the study design was the blinded prospective evaluation of efficacy with or without continuation of the investigational drug after the first blinded treatment period, between weeks 24 and 52. These exploratory efficacy results are the focus of the present paper, complemented by a detailed report of the final safety profile of ionalumab in SjD, including up to two years of drug-free follow-up.

After six months of treatment with the highest dose of ionalumab 300 mg every four weeks, patients were rerandomized to either discontinue or continue treatment with the same dose up to the end of TP2 at week 52. Although the results from

physician-reported outcome instruments mostly remained stable, results from PRO instruments suggested an increase of disease activity approximately six months after discontinuation of ionalumab 300 mg. At the molecular level, IgM RFs, anti-SSA/Ro52 and 60, and anti-SSB/La autoantibody levels returned to baseline concentrations in patients who discontinued ionalumab, whereas continued ionalumab treatment showed sustained autoantibody responses or further declines. The differences in anti-La reductions between the two patient groups, both receiving 300 mg, from week 24 to 52 was unexpected and could be due to random variation and the small sample size. In summary, these insights support the notion that molecular changes related to B cell depletion or the BAFF/BAFF-R axis and reductions in autoantibody concentrations are related to the clinical benefit experienced by patients with SjD.

In line with the cellular and molecular mechanisms of action of ionalumab, a dose-response relationship for the pharmacodynamic markers serum BAFF and CD19⁺ B cell count was

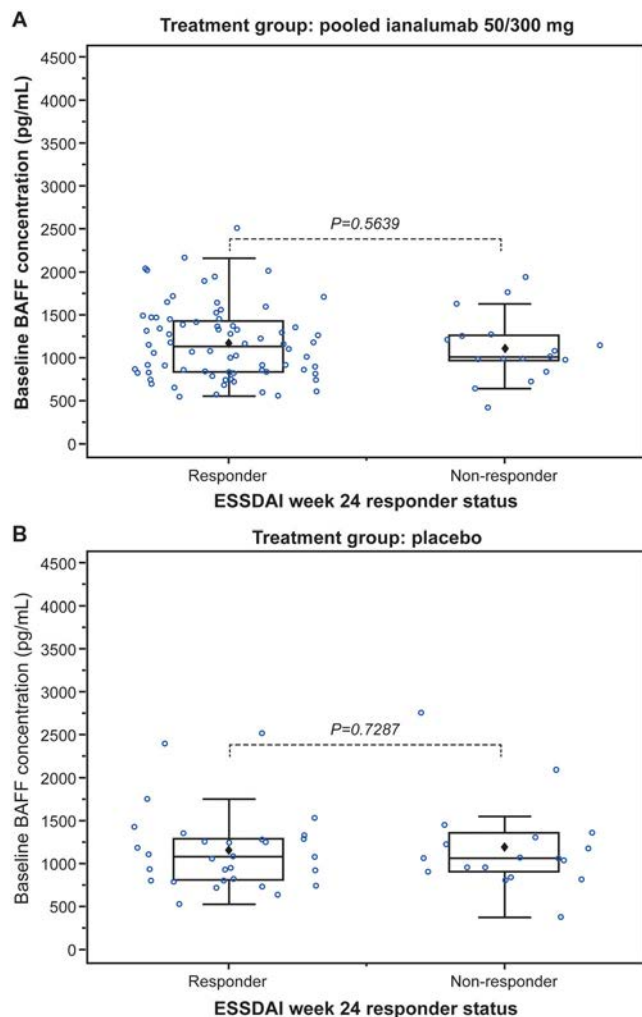


Figure 4. BAFF levels at baseline and by ESSDAI response at week 24. (A) Treatment group: pooled ianalumab 50/300 mg; (B) Treatment group: placebo. The plot shows boxes (25th–75th percentiles) with median as horizontal line. The whiskers indicate the minimum and maximum values. Each dot represents an observation. BAFF, B cell activating factor; ESSDAI, EULAR Sjögren’s Syndrome Disease Activity Index.

observed up to weeks 24 and 52. As expected, B cell depletion was accompanied by a rapid increase in BAFF in a dose-dependent manner. Conversely, repopulation of B cells was paralleled by a decline in BAFF.

Assessment of the time to recovery of CD19⁺ B cells in peripheral blood is generally used to monitor the B cell compartment after B cell depletion therapy (BCDT), whereby time to recovery can vary between different autoimmune diseases.¹⁸ In our study, the median time to recovery was dose-dependent but not dependent on pretreatment B cell counts and was comparable to experience with B cell depletion in lupus or rheumatoid arthritis.^{19,20} However, our phase 2b study provided limited exposure to ianalumab for 6 to 12 months (only 300 mg dose), and no enumeration of B cell subsets was performed.

Therefore, it is currently unknown whether treatment with ianalumab (or extended treatment with ianalumab at a steady state of BAFF-R engagement) might change the kinetics of B cell repopulation, the composition of the repopulated B cell compartment, or ianalumab’s impact on autoantibody-producing plasma cells, memory B cells, and other cell types remains of interest.

Important factors associated with incomplete or no response to BCDT include excess BAFF^{21,22} and persistence of certain B cell receptor clones.²³ It was hypothesized that serum BAFF levels reduce the threshold for autoreactive B cell survival and expansion, thereby stimulating autoantibody production. The activated BAFF/BAFF-R axis may therefore play a role in the recurrence of symptoms in rituximab-treated patients.^{22,24} In a post hoc analysis, we found that high pretreatment BAFF levels were not associated with lesser responses (ESSDAI response) to ianalumab. In contrast, increased resistance to BCDT was reported in high-BAFF patients with lupus who were treated with rituximab.^{19,24} These findings are consistent with the first results of trials combining treatment with BCDT and soluble BAFF blockade in SLE²⁵ and SjD.¹⁵

Significant stimulated whole salivary flow improvements were seen at week 24 for the ianalumab 300 mg group and were maintained up to the last measurement at week 48; further improvement was observed in the ianalumab 300 mg group that continued treatment versus placebo. The observed effect size of 0.45 mL/min flow improvement is clinically important as it might translate into fewer complications related to dryness, including problems in speaking and eating, emergence of oral candidiasis, and accelerated tooth decay.²⁶

Exploratory efficacy results suggest that continuous dosing of 300 mg SC every 4 weeks is required for continued clinical benefit, supported by further numerical improvements in outcome measures, compared to patients who discontinued after six months of dosing and experienced worsening. Clinical improvements achieved with ianalumab 300 mg at week 24 were maintained across several end points. Due to study design limitations, no efficacy comparisons between ianalumab- and placebo-treated patients were possible after week 24. However, patients who switched from placebo to ianalumab 150 mg experienced improvements between weeks 24 and 52. Although certain PRO instruments, including PaGA, FACIT-F, and SF-36 mental component, showed consistent signals of improvement after week 24, changes in ESSPRI were small. A small further improvement (–0.95 ESSPRI points from weeks 24 to 52) was observed in patients switching from placebo to ianalumab 150 mg. A reduction of 3 points in ESSDAI and a reduction of 1 point or 15% in ESSPRI indicate clinically relevant improvement, reflecting meaningful reduction in global disease activity and symptom burden, respectively.²⁷ As elaborated previously,¹⁶ the design features of this phase 2b trial may have caused a larger than expected ESSPRI placebo response, impeding the ability to

Table 2. Summary of adverse events*

Treatment group, treatment period (duration, wk)	lanalumab 5 mg, TP1 (24 wk), n = 47	lanalumab 50 mg, TP1 (24 wk), n = 47	Placebo to lanalumab 150 mg, ^a TP2 (28 wk), n = 47	lanalumab 300 mg, ^b TP1 (24 wk), n = 26	lanalumab 300 mg to lanalumab 300 mg, TP1, TP2 (52 wk), n = 21
Median duration of follow-up, mo	3.8	4.8	6.8	8.4	6.5
Any TEAE	43 (91.5)	43 (91.5)	45 (95.7)	25 (96.2)	20 (95.2)
Serious TEAEs	3 (6.4)	7 (14.9)	9 (19.1)	5 (19.2)	5 (23.8)
TEAEs leading to study treatment discontinuation	2 (4.3)	2 (4.3)	5 (10.6)	0 (0.0)	2 (9.5)
Deaths	0 (0.0)	0 (0.0)	0 (0.0)	0 (0.0)	0 (0.0)
Safety topics of interest					
Local injection reaction	4 (8.5)	9 (19.1)	17 (36.2)	13 (50.0)	14 (66.7)
Systemic injection reaction	6 (12.8)	5 (10.6)	8 (17.0)	2 (7.7)	2 (9.5)
Any infections	33 (70.2)	30 (63.8)	38 (80.9)	21 (80.8)	18 (85.7)
Nasopharyngitis	7 (14.9)	4 (8.5)	11 (23.4)	5 (19.2)	4 (19.0)
Upper respiratory tract infection	7 (14.9)	9 (19.1)	7 (14.9)	8 (30.8)	2 (9.5)
Acute sinusitis	3 (6.4)	0 (0.0)	2 (4.3)	0 (0.0)	1 (4.8)
Urinary tract infection	9 (19.1)	5 (10.6)	7 (14.9)	2 (7.7)	3 (14.3)
Conjunctivitis	3 (6.4)	5 (10.6)	2 (4.3)	2 (7.7)	0 (0.0)
Gastroenteritis	1 (2.1)	2 (4.3)	1 (2.1)	2 (7.7)	1 (4.8)
Cystitis	0 (0.0)	1 (2.1)	2 (4.3)	2 (7.7)	1 (4.8)
Parotitis	2 (4.3)	0 (0.0)	3 (6.4)	1 (3.8)	0 (0.0)
Influenza	0 (0.0)	1 (2.1)	0 (0.0)	1 (3.8)	3 (14.3)
Rhinitis	1 (2.1)	0 (0.0)	1 (2.1)	1 (3.8)	1 (4.8)
Pneumonia	1 (2.1)	0 (0.0)	1 (2.1)	1 (3.8)	1 (4.8)
Tracheobronchitis	1 (2.1)	0 (0.0)	0 (0.0)	1 (3.8)	2 (9.5)
Viral upper respiratory tract infection	1 (2.1)	1 (2.1)	0 (0.0)	2 (7.7)	0 (0.0)
Blood and lymphatic disorders	8 (17.0)	10 (21.3)	6 (12.8)	4 (15.4)	5 (23.8)
Leukopenia	3 (6.4)	3 (6.4)	4 (8.5)	2 (7.7)	4 (19.0)
Lymphopenia	4 (8.5)	4 (8.5)	3 (6.4)	1 (3.8)	1 (4.8)
Neutropenia ^c , n/m (%)					
<LLN– 1.5×10^9 /L (grade 1)	12/38 (31.6)	4/40 (10.0)	7/43 (16.3)	2/24 (8.3)	3/19 (15.8)
< 1.5 – 1.0×10^9 /L (grade 2)	9/45 (20.0)	5/45 (11.1)	6/45 (13.3)	5/25 (20.0)	2/21 (9.5)
< 1.0 – 0.5×10^9 /L (grade 3)	2/47 (4.3)	1/45 (2.2)	0/46 (0)	0/26 (0)	2/21 (9.5)
< 0.5×10^9 /L (grade 4)	0/47 (0)	0/45 (0)	0/46 (0)	0/26 (0)	0/21 (0)
Malignancies	1 (2.1)	0	1 (2.1)	0 (0.0)	0 (0.0)
Other common TEAEs ($\geq 5\%$ in any treatment group) by preferred term					
Abdominal pain	0 (0.0)	3 (6.4)	1 (2.1)	0 (0.0)	0 (0.0)
Arthralgia	3 (6.4)	1 (2.1)	7 (14.9)	2 (7.7)	3 (14.3)
Back pain	3 (6.4)	4 (8.5)	6 (12.8)	4 (15.4)	2 (9.5)
Blood creatinine	3 (6.4)	1 (2.1)	1 (2.1)	1 (3.8)	0 (0.0)
Increased					
Bronchitis	3 (6.4)	3 (6.4)	5 (10.6)	2 (7.7)	2 (9.5)
Cough	3 (6.4)	0 (0.0)	2 (4.3)	2 (7.7)	0 (0.0)
Diarrhea	3 (6.4)	3 (6.4)	2 (4.3)	3 (11.5)	4 (19.0)
Dizziness	2 (4.3)	1 (2.1)	0 (0.0)	2 (7.7)	2 (9.5)
Fall	0 (0.0)	0 (0.0)	2 (4.3)	1 (3.8)	2 (9.5)
Gastro-esophageal reflux disease	1 (2.1)	4 (8.5)	0 (0.0)	0 (0.0)	1 (4.8)
Headache	5 (10.6)	5 (10.6)	4 (8.5)	4 (15.4)	2 (9.5)
Hypertension	4 (8.5)	2 (4.3)	2 (4.3)	0 (0.0)	0 (0.0)
Influenza like illness	0 (0.0)	4 (8.5)	1 (2.1)	2 (7.7)	2 (9.5)
Injection-related reaction	6 (12.8)	5 (10.6)	8 (17.0)	2 (7.7)	2 (9.5)
Injection-site reaction	4 (8.5)	9 (19.1)	17 (36.2)	13 (50.0)	14 (66.7)
Insomnia	0 (0.0)	0 (0.0)	3 (6.4)	0 (0.0)	3 (14.3)
Iron deficiency anemia	1 (2.1)	3 (6.4)	0 (0.0)	0 (0.0)	0 (0.0)
Joint swelling	2 (4.3)	0 (0.0)	0 (0.0)	2 (7.7)	1 (4.8)
Lymphocyte count decreased	4 (8.5)	0 (0.0)	1 (2.1)	0 (0.0)	2 (9.5)
Myalgia	2 (4.3)	0 (0.0)	4 (8.5)	1 (3.8)	2 (9.5)
Neutrophil count decreased	3 (6.4)	0 (0.0)	1 (2.1)	1 (3.8)	1 (4.8)
Edema peripheral	0 (0.0)	2 (4.3)	0 (0.0)	2 (7.7)	1 (4.8)
Oral candidiasis	0 (0.0)	0 (0.0)	1 (2.1)	2 (7.7)	1 (4.8)
Oral herpes	4 (8.5)	2 (4.3)	2 (4.3)	1 (3.8)	3 (14.3)
Pain in extremity	3 (6.4)	4 (8.5)	2 (4.3)	2 (7.7)	0 (0.0)

(Continued)

Table 2. (Cont'd)

Treatment group, treatment period (duration, wk)	Ianalumab 5 mg, TP1 (24 wk), n = 47	Ianalumab 50 mg, TP1 (24 wk), n = 47	Placebo to Ianalumab 150 mg, ^a TP2 (28 wk), n = 47	Ianalumab 300 mg, ^b TP1 (24 wk), n = 26	Ianalumab 300 mg to Ianalumab 300 mg, TP1, TP2 (52 wk), n = 21
Pruritus	2 (4.3)	1 (2.1)	2 (4.3)	3 (11.5)	1 (4.8)
Pyrexia	0 (0.0)	1 (2.1)	3 (6.4)	3 (11.5)	0 (0.0)
Rash	6 (12.8)	3 (6.4)	3 (6.4)	2 (7.7)	2 (9.5)
Sinusitis	5 (10.6)	3 (6.4)	7 (14.9)	2 (7.7)	1 (4.8)
Sjögren's syndrome	0 (0.0)	4 (8.5)	1 (2.1)	0 (0.0)	2 (9.5)
White blood cell count decreased	3 (6.4)	1 (2.1)	0 (0.0)	1 (3.8)	1 (4.8)

* Includes all safety data from TP1, TP2, and posttreatment follow-up. Data are n (%) unless otherwise specified. A patient with multiple occurrences of an AE under one treatment is counted only once in the AE category for that treatment at the maximum severity grade; preferred terms are sorted by alphabetical order. AE, adverse event; CTCAE, Common Terminology Criteria for Adverse Events; LLN, lower limit of normal; m, number of patients with evaluable criterion who were better than the criterion at baseline; SAE, serious adverse event; TEAE, treatment-emergent adverse event; TP, treatment period.

^a 150 mg also includes placebo-treated patients who were switched to Ianalumab 150 mg at week 24.

^b 300 mg 24 weeks group includes patients treated with 300 mg up to week 24 and switched to placebo every 4 weeks up to week 52 in TP2.

^c Neutrophil count based on CTCAE grades.

detect patient benefit with Ianalumab compared to placebo. Early and large reductions in ESSPRI scores across all arms, specifically 300 mg, may explain why only marginal further ESSPRI improvements were seen between weeks 24 and 52.

The safety events of interest include neutropenia, infections, malignancies, and injection-related systemic reactions. Hypogammaglobulinemia is known to occur because of long-term B cell depletion and may be associated with infections; hence, IgG monitoring is recommended.²⁸ In the current phase 2b study, safety follow-up was up to two years, and only two patients showed reductions below LLN in IgG without reports of contemporaneous infection. Likewise, a very low rate of decreased neutrophil counts was reported, and none were associated with infections except for a single incidental finding of an asymptomatic viral infection (CMV, IgM-positive). As BAFF may play a role in the development of late-onset neutropenia in patients with SLE²⁹ and BAFF downstream cellular effects are inhibited by the BAFF-R blocker Ianalumab, it is reasonable to speculate that the combination of BCDT with BAFF-R blockade may be advantageous compared to BCDT alone. Ongoing larger trials will shed further light on these relationships.

Infections were seen more frequently with Ianalumab compared to placebo, and events included bacterial and viral infections. No severe or systemic opportunistic infections were observed in this phase 2 trial. Patients with SjD generally have fewer background immunosuppressive treatments compared to patients with SLE. Ongoing phase 3 trials will provide additional insights into potential events that occur rarely under BCDT.

The limitations of this study include the small sample size after week 24 for the 300 mg subgroup comparisons, which were descriptive only and not powered for statistical significance, and no collection of efficacy data for the lower doses of 5 and 50 mg after the primary endpoint at week 24. The placebo group in

TP2 was not designed to control for efficacy; therefore formal statistical comparisons between treatment groups during TP2 was not feasible.

In conclusion, week 52 results of Ianalumab in SjD, including up to two years of safety follow-up, yielded a positive risk-benefit profile and provided additional insights into the kinetics of biomarkers during treatment and after treatment discontinuation. The findings suggest that Ianalumab treatment should be administered for longer than six months because continued treatment resulted in additional benefit and no new safety concerns, whereas discontinuation after six months (ie, shortly after steady state is achieved) resulted in rebound of disease activity in some patients.

AUTHOR CONTRIBUTIONS

All authors contributed to at least one of the following manuscript preparation roles: conceptualization AND/OR methodology, software, investigation, formal analysis, data curation, visualization, and validation AND drafting or reviewing/editing the final draft. As corresponding author, Dr Dörner confirms that all authors have provided the final approval of the version to be published and takes responsibility for the affirmations regarding article submission (eg, not under consideration by another journal), the integrity of the data presented, and the statements regarding compliance with institutional review board/Declaration of Helsinki requirements.

ROLE OF THE STUDY SPONSOR

The study was designed by the authors including Novartis personnel. All authors had access to the data, contributed to the interpretation, and collaborated in the development of the manuscript. Statistical analyses were performed by statisticians employed by the study sponsor (Novartis Pharma AG, Basel, Switzerland). Publication of this article was not contingent upon approval by Novartis. Medical writing and editorial assistance were provided by Divya Chandrasekhar, PhD (Novartis Healthcare Pvt. Ltd., India), and Ramji Narayanan, M Pharm (Novartis Ireland Limited), which was funded by Novartis Pharma AG.







DATA AVAILABILITY STATEMENT

All data relevant to the study are included in the article or uploaded as supplementary information. Novartis is committed to sharing, with qualified external researchers, access to patient-level data and supporting clinical documents from eligible trials. These requests are reviewed and approved by an independent review panel on the basis of scientific merit. All data provided are anonymised to respect the privacy of patients who have participated in the trials in line with applicable laws and regulations.

REFERENCES

- Nocturne G, Pontarini E, Bombardieri M, et al. Lymphomas complicating primary Sjögren's syndrome: from autoimmunity to lymphoma. *Rheumatology (Oxford)* 2021;60(8):3513–3521.
- Seror R, Nocturne G, Mariette X. Current and future therapies for primary Sjögren syndrome. *Nat Rev Rheumatol* 2021;17(8):475–486.
- Ramos-Casals M, Tzioufas AG, Stone JH, et al. Treatment of primary Sjögren syndrome: a systematic review. *JAMA* 2010;304(4):452–460.
- Ramos-Casals M, Brito-Zerón P, Sisó-Almirall A, et al. Topical and systemic medications for the treatment of primary Sjögren's syndrome. *Nat Rev Rheumatol* 2012;8(7):399–411.
- Brito-Zerón P, Retamozo S, Kostov B, et al. Efficacy and safety of topical and systemic medications: a systematic literature review informing the EULAR recommendations for the management of Sjögren's syndrome. *RMD Open* 2019;5(2):e001064.
- Ambrus JL, Suresh L, Peck A. Multiple roles for B-lymphocytes in Sjögren's syndrome. *J Clin Med* 2016;5(10):87.
- Nocturne G, Mariette X. B cells in the pathogenesis of primary Sjögren syndrome. *Nat Rev Rheumatol* 2018;14(3):133–145.
- Devauchelle-Pensec V, Mariette X, Jousse-Joulin S, et al. Treatment of primary Sjögren syndrome with rituximab: a randomized trial. *Ann Intern Med* 2014;160(4):233–242.
- Souza FB, Porfirio GJ, Andriolo BN, et al. Rituximab effectiveness and safety for treating primary Sjögren's syndrome (pSS): systematic review and meta-analysis. *PLoS One* 2016;11(3):e0150749.
- Bowman SJ, Everett CC, O'Dwyer JL, et al. Randomized controlled trial of rituximab and cost-effectiveness analysis in treating fatigue and oral dryness in primary Sjögren's syndrome. *Arthritis Rheumatol* 2017;69(7):1440–1450.
- Steinfeld SD, Tant L, Burmester GR, et al. Epratuzumab (humanised anti-CD22 antibody) in primary Sjögren's syndrome: an open-label phase I/II study. *Arthritis Res Ther* 2006;8(4):R129.
- De Vita S, Quartuccio L, Seror R, et al. Efficacy and safety of belimumab given for 12 months in primary Sjögren's syndrome: the BELISS open-label phase II study. *Rheumatology (Oxford)* 2015;54(12):2249–2256.
- Mariette X, Seror R, Quartuccio L, et al. Efficacy and safety of belimumab in primary Sjögren's syndrome: results of the BELISS open-label phase II study. *Ann Rheum Dis* 2015;74(3):526–531.
- Gottenberg JE, Dörner T, Bootsma H, et al. Efficacy of epratuzumab, an anti-CD22 monoclonal IgG antibody, in systemic lupus erythematosus patients with associated Sjögren's syndrome: post hoc analyses from the EMBODY trials. *Arthritis Rheumatol* 2018;70(5):763–773.
- Mariette X, Barone F, Baldini C, et al. A randomized, phase II study of sequential belimumab and rituximab in primary Sjögren's syndrome. *JCI Insight* 2022;7(23):e163030.
- Bowman SJ, Fox R, Dörner T, et al. Safety and efficacy of subcutaneous ianalumab (VAY736) in patients with primary Sjögren's syndrome: a randomised, double-blind, placebo-controlled, phase 2b dose-finding trial. *Lancet* 2022;399(10320):161–171.
- Vitali C, Bombardieri S, Jonsson R, et al; European Study Group on Classification Criteria for Sjögren's Syndrome. Classification criteria for Sjögren's syndrome: a revised version of the European criteria proposed by the American-European Consensus Group. *Ann Rheum Dis* 2002;61(6):554–558.
- Thiel J, Rizzi M, Engesser M, et al. B cell repopulation kinetics after rituximab treatment in ANCA-associated vasculitides compared to rheumatoid arthritis, and connective tissue diseases: a longitudinal observational study on 120 patients. *Arthritis Res Ther* 2017;19(1):101.
- Levesque MC, St Clair EW. B cell-directed therapies for autoimmune disease and correlates of disease response and relapse. *J Allergy Clin Immunol* 2008;121(1):13–21.
- Dörner T. Crossroads of B cell activation in autoimmunity: rationale of targeting B cells. *J Rheumatol Suppl* 2006;77:3–11.
- Thien M, Phan TG, Gardam S, et al. Excess BAFF rescues self-reactive B cells from peripheral deletion and allows them to enter forbidden follicular and marginal zone niches. *Immunity* 2004;20(6):785–798.
- Becerra E, De La Torre I, Leandro MJ, et al. B cell phenotypes in patients with rheumatoid arthritis relapsing after rituximab: expression of B cell-activating factor-binding receptors on B cell subsets. *Clin Exp Immunol* 2017;190(3):372–383.
- Pollastro S, Klarenbeek PL, Doorenspleet ME, et al. Non-response to rituximab therapy in rheumatoid arthritis is associated with incomplete disruption of the B cell receptor repertoire. *Ann Rheum Dis* 2019;78(10):1339–1345.
- Carter LM, Isenberg DA, Ehrenstein MR. Elevated serum BAFF levels are associated with rising anti-double-stranded DNA antibody levels and disease flare following B cell depletion therapy in systemic lupus erythematosus. *Arthritis Rheum* 2013;65(10):2672–2679.
- Shipa M, Embleton-Thirsk A, Parvaz M, et al; BEAT-LUPUS Investigators. Effectiveness of belimumab after rituximab in systemic lupus erythematosus: a randomized controlled trial. *Ann Intern Med* 2021;174(12):1647–1657.
- Bookman AA, Shen H, Cook RJ, et al. Whole stimulated salivary flow: correlation with the pathology of inflammation and damage in minor salivary gland biopsy specimens from patients with primary Sjögren's syndrome but not patients with sicca. *Arthritis Rheum* 2011;63(7):2014–2020.
- Seror R, Bootsma H, Saraux A, et al; EULAR Sjögren's Task Force. Defining disease activity states and clinically meaningful improvement in primary Sjögren's syndrome with EULAR primary Sjögren's syndrome disease activity (ESSDAI) and patient-reported indexes (ESSPRI). *Ann Rheum Dis* 2016;75(2):382–389.
- Roberts DM, Jones RB, Smith RM, et al. Rituximab-associated hypogammaglobulinemia: incidence, predictors and outcomes in patients with multi-system autoimmune disease. *J Autoimmun* 2015;57:60–65.
- Parodis I, Söder F, Faustini F, et al. Rituximab-mediated late-onset neutropenia in systemic lupus erythematosus - distinct roles of BAFF and APRIL. *Lupus* 2018;27(9):1470–1478.

Autologous Nonmyeloablative Hematopoietic Stem Cell Transplantation for Diffuse Cutaneous Systemic Sclerosis: Identifying Disease Risk Factors for Toxicity and Long-Term Outcomes in a Prospective, Single-Arm Trial

George E. Georges,¹  Dinesh Khanna,²  Mark H. Wener,³ Matthew G. Mei,⁴ Maureen D. Mayes,⁵ 
Robert W. Simms,⁶ Vaishali Sanchowala,⁶ Chitra Hosing,⁷ Suzanne Kafaja,⁸ Attaphol Pawarode,²
Leona A. Holmberg,⁹ Jason Kolfenbach,¹⁰  Daniel E. Furst,⁸  Keith M. Sullivan,¹¹  Suiyuan Huang,²
Ted Gooley,¹² and Richard A. Nash¹³

Objective. Two randomized trials for patients with diffuse systemic sclerosis (SSc) demonstrated an overall survival (OS) and event-free survival (EFS) advantage of autologous hematopoietic stem cell transplantation (AHSCT) using CD34+ selected peripheral blood stem cells (PBSCs) compared with monthly cyclophosphamide (CY). We asked if an unmodified PBSC graft followed by maintenance mycophenolate mofetil (MMF) after AHSCT, instead of a CD34+ selected graft, could provide comparable AHSCT outcomes.

Methods. Twenty patients with high-risk SSc were enrolled in a prospective, single-arm trial with CY 200 mg/kg and horse antithymocyte globulin (ATG; CY200/ATG), followed by unmanipulated autologous PBSC, and then MMF maintenance starting at 2 months after AHSCT.

Results. Point estimates of OS and EFS at 5 years after AHSCT were 85% (95% confidence interval [CI] 60.4%–94.9%) and 75% (95% CI 50%–88.7%), respectively. Median follow-up was 7.5 years (range 5.6–11.6) after transplant for living patients. Eight patients (40%) required intensive care unit treatment early after transplant. Early transplant-related mortality occurred in two patients (10%). Five patients developed relapse/progression of SSc after AHSCT. Four of nine patients with anti-RNA polymerase III antibodies had prior scleroderma renal crisis and the lowest quartile of estimated glomerular filtration rate (eGFR) on study entry; all four patients developed prolonged organ failure/death early after transplant.

Conclusion. We observed favorable OS and EFS after AHSCT for patients with SSc, using CY200/ATG, unmanipulated PBSCs, and MMF posttransplant maintenance, which was comparable to trials with CD34+ graft selection. We identified a possible risk factor, pretransplant low eGFR, for adverse outcomes after AHSCT.

INTRODUCTION

Diffuse cutaneous systemic sclerosis (dcSSc) is a devastating autoimmune disorder that is often fatal owing to progressive internal organ involvement.^{1–3} Although disease-modifying anti-rheumatic drugs (DMARDs) and biologics have been studied,

none have shown sustained survival benefit.^{4–6} Two large randomized clinical trials demonstrated an overall survival (OS) and event-free survival (EFS) advantage of autologous hematopoietic stem cell transplantation (AHSCT) compared with an effective DMARD, consisting of monthly cyclophosphamide (CY; 750 mg/m² for 12 months).^{7,8} The nonmyeloablative conditioning

[ClinicalTrials.gov](https://clinicaltrials.gov/ct2/show/study/NCT01413100) identifier: NCT01413100.

¹George E. Georges, MD, Northwestern University Feinberg School of Medicine, Chicago; Fred Hutchinson Cancer Center and University of Washington, Seattle; ²Dinesh Khanna, MD, MSc, Attaphol Pawarode, MD, Suiyuan Huang, MPH: University of Michigan, Ann Arbor; ³Mark H. Wener, MD: University of Washington, Seattle; ⁴Matthew G. Mei, MD: City of Hope National Medical Center, Duarte, California; ⁵Maureen D. Mayes, MD, MPH: University of Texas Houston, Houston; ⁶Robert W. Simms, MD (current address: Dartmouth Geisel School of Medicine, Hannover, New Hampshire), Vaishali Sanchowala, MD: Boston Medical Center and Boston University, Boston, Massachusetts; ⁷Chitra Hosing, MD: M. D. Anderson Cancer Center, Houston, Texas; ⁸Suzanne Kafaja, MD, Daniel E. Furst, MD: University of

California Los Angeles, Los Angeles; ⁹Leona A. Holmberg, MD, PhD: Fred Hutchinson Cancer Center and University of Washington, Seattle; ¹⁰Jason Kolfenbach, MD: University of Colorado Anschutz, Aurora; ¹¹Keith M. Sullivan, MD: Duke University, Durham, North Carolina; ¹²Ted Gooley, PhD: Fred Hutchinson Cancer Center, Seattle, Washington; ¹³Richard A. Nash, MD: Colorado Blood Cancer Institute, Denver, Colorado.

Author disclosures are available at <https://onlinelibrary.wiley.com/doi/10.1002/art.43072>.

Address correspondence via email to George E. Georges, MD, at georges@northwestern.edu.

Submitted for publication August 5, 2024; accepted in revised form November 13, 2024.

regimen for the first trial (Autologous Stem Cell Transplantation International Scleroderma [ASTIS]) consisted of CY 200 mg/kg plus rabbit antithymocyte globulin (ATG) 7.5 mg/kg followed by CD34+ immunomagnetically selected autologous peripheral blood stem cells (PBSCs).⁷ In the AHSCT arm, the transplant-related mortality (TRM) was 10.1%, and the 5-year OS and EFS were 81% and 78%, respectively.⁷ The second trial (Scleroderma Cyclophosphamide or Transplant [SCOT]) consisted of myeloablative fractionated total body irradiation (TBI) 8 Gray (with lung and kidney shielding limiting the radiation dose to 2 Gray), CY 120 mg/kg, and horse ATG 90 mg/kg (TBI/CY/ATG), followed by infusion of CD34+ selected autologous PBSCs.⁸ In the per protocol AHSCT arm, the TRM was 6% at 72 months (because of myelodysplastic syndrome [MDS]), and the 72-month OS and EFS were 86% and 74%, respectively.⁸

Between the publication of the ASTIS and SCOT trials, we conducted a multicenter, single-arm trial evaluating the efficacy of irradiation-free, nonmyeloablative CY 200 mg/kg plus horse ATG conditioning (CY200/ATG) followed by unselected autologous PBSC infusion and maintenance mycophenolate mofetil (MMF) for patients with high-risk dcSSc, using the eligibility criteria of the SCOT trial. CD34+ selection was not used primarily because of limited availability, regulatory burden, added cost, and potential increased risk of opportunistic infections. MMF was given after AHSCT to prevent disease relapse. The primary outcome measure was EFS, defined as survival without prolonged organ damage. Secondary objectives included safety and time to disease relapse requiring treatment with additional DMARDs. We sought to evaluate the overall safety and potential efficacy of the conditioning regimen with posttransplant MMF maintenance therapy given in place of CD34+ selection of the autologous graft.

PATIENTS AND METHODS

Trial design, interventions, and oversight. This investigator-initiated phase 2 trial was conducted at six paired US rheumatology and transplant centers. The trial ended when the last participant completed 5 years of follow-up, with a maximum follow-up of 11.6 years. Participants were observed annually for 5 years after AHSCT and at study completion. The trial was registered with [ClinicalTrials.gov](https://clinicaltrials.gov/ct2/show/study/NCT01413100) (NCT01413100). An independent data safety monitoring board consisting of two rheumatologists, one transplant physician, and one biostatistician met every 6 to 12 months to review data. All participants provided informed written consent before trial participation. The trial was conducted in accordance with Declaration of Helsinki and Good Clinical Practice guidelines. The protocol was approved by each site's institutional review board. Participant race and ethnicity was self-reported.

Participant inclusion and exclusion criteria were as follows: the diagnosis of SSc (American College of Rheumatology/EULAR 2013 criteria⁹) with diffuse subset and disease duration of

≤5 years from the first non-Raynaud sign or symptom, with either pulmonary/renal involvement or rapidly progressive, extensive, severe skin involvement for ≤2 years. Pulmonary involvement required active interstitial lung disease determined by chest computed tomography scan plus forced vital capacity (FVC) or lung diffusing capacity for carbon monoxide (DL_{CO}, adjusted for hemoglobin) <70% predicted value. Renal involvement required previous scleroderma-related renal disease. Patients had received either MMF, mycophenolic acid (MPA), or CY for ≥4 months with no clinical benefit. The exclusion criteria included active gastric antral vascular ectasia, DL_{CO}, and FVC <40% and <45% predicted value, respectively, left ventricular ejection fraction (LVEF) <50%, and serum creatinine level ≥2.0 mg/dL. Patients with evidence of SSc cardiac involvement or pulmonary arterial hypertension (mean pulmonary arterial pressure >40 mm Hg) were excluded.

Mobilization of autologous PBSCs used granulocyte colony-stimulating factor (filgrastim) 16 µg/kg/day subcutaneous for 5 days. Prednisone 0.5 mg/kg/day was administered during granulocyte colony-stimulating factor and for 5 days afterward to prevent flare of autoimmune disease. Apheresis and cryopreservation were completed in compliance with certified institutional practice.

All DMARDs were stopped before conditioning. Between 6 and 21 days after completion of apheresis, patients were admitted to the HSCT unit and began conditioning with intravenous CY 50 mg/kg/day (days -5 to -2, total dose 200 mg/kg), an equal Mesna dose, and horse ATG 15 mg/kg/day (days -5, -3, -1, +1, +3, and +5). Intravenous methylprednisolone 1 mg/kg was administered before each ATG dose. Autologous PBSCs (cell dose >2.5 × 10⁶ CD34/kg) were thawed and infused on day 0. Prophylactic antibiotic, antiviral, and antifungal medications were administered per standard institutional practice. Lisinopril was administered to maintain systolic blood pressure between 90 and 110 mm Hg. Maintenance MMF/MPA was started 2 to 4 months after HSCT; the dose was titrated to tolerance (target dose MMF 1 g or MPA 720 mg twice daily), with a plan to continue maintenance treatment for ≥2 years.

Kaplan-Meier estimates of OS, EFS, and additional DMARD-free EFS (DEFS) were obtained with a focus on point estimates at 5 and 10 years. EFS was defined as survival without meeting the protocol-defined endpoint of organ injury (kidney injury requiring renal replacement dialysis for >6 months, sustained LVEF <30%, or sustained decline of FVC >20%), similar to prior trials.^{7,8} DEFS was defined as survival without meeting the EFS endpoint and without additional DMARD treatment. Patients were evaluable for disease response if they survived >3 months after HSCT. TRM was defined as death before day +90 after HSCT. Data were censored at last follow-up. The analysis used Prism software (version 10.0, GraphPad Software). Changes in least squares means were based on the linear mixed effect model, where change from baseline was the outcome and baseline value and study time

were the covariates. Models were fitted with the random effect of the intercept. Local institutional funding supported the collection and reporting of the data. The data cutoff was December 1, 2023. The data will be shared in a public repository.

RESULTS

Patient characteristics. Twenty patients with dcSSc meeting the entry criteria were enrolled and completed AHSCT between January 2012 and September 2018. The baseline characteristics are shown in Table 1. The mean age of study participants was 46 years (range 13–70 years), with 15 women and 5 men. The median time from disease onset to HSCT was 18 months (range 6–59 months). The mean number of prior (failed) DMARDs for SSc was 2 (range 1–5). At pretransplant evaluation, the mean modified Rodnan skin score (mRSS) was 34 (range 8–46). Eighteen patients (90%) had interstitial lung disease, and five patients (25%) had a history of scleroderma renal crisis (SRC) before enrollment. The mean baseline adjusted DLco was 62% predicted value (range 41%–91%), and the mean FVC was 76% (range 50%–111%). Four participants (20%) had a history of tobacco smoking. The median estimated glomerular filtration rate (eGFR, mL/min/1.73m²) was 105 (range 33–150, Chronic Kidney Disease Epidemiology Collaboration 2021 equation¹⁹).

All participants had baseline antinuclear antibody (ANA) titer of $\geq 1:320$. Eight participants (40%) were antitopoisomerase 1 (scleroderma-70 [Scl-70]) positive (ATA+), nine (45%) were anti-RNA polymerase III positive (ARA+), and one patient was positive for both. No one was anticentromere positive.

Engraftment. The median CD34+ cell dose of the unmodified autologous PBSCs infused at transplant was 5.57 (range 2.8–15.56) $\times 10^6$ /kg. All patients had sustained neutrophil engraftment (range 8–13 days) after transplant followed by sustained platelet engraftment.

OS and EFS. Sixteen patients were alive at the last follow-up (Figure 1). The median follow-up of the surviving patients was 7.5 years after transplant (range 5.6–11.6 years). The 5- and 10-year OS estimates were 85% (95% confidence interval [CI] 60.4%–94.9%) and 77% (95% CI 49%–91%), respectively (Figure 2A). There were six events (four deaths and two patients who developed prolonged organ failure). The 5- and 10-year EFS estimates were 75% (95% CI 50%–88.7%) and 67% (95% CI 40.5%–84.3%), respectively (Figure 2B).

TRM and adverse events. TRM occurred in two patients (Figure 1) on days +37 and +44 after HSCT, indicating a 1-year TRM of 10% (95% CI 2.6%–34.6%). The patient (#14) who had TRM at day +37 developed fever, hypoxemia, skin rash, and pulmonary infiltrates on day +10 after transplant, consistent with

engraftment syndrome.¹¹ Despite therapy, respiratory symptoms worsened by day +13, requiring intubation and mechanical ventilation. Acute kidney injury (AKI) and anuria developed, requiring daily renal replacement therapy beginning on day +14. Echocardiogram results showed global hypokinesis with an LVEF of 25%. After transient stabilization, the patient developed recurrent fevers with hypotension. Despite maximal pressor support and anti-infective agents, the clinical status worsened with development of multiple brain infarcts, acute hepatic injury, and coagulopathy, followed by progressive multi-organ failure, leading to death on day +37. An autopsy showed diffuse pulmonary fibrosis, diffuse alveolar damage, small vessel sclerosis, patchy fibrin exudates, and airways with extensive mucous plugging. The heart showed remote inferoposterior LV myocardial infarction. Kidneys showed medullary casts, focal glomerulosclerosis, and focal neointimal formation, but no microthrombi. The brain cortex showed acute ischemic injury of the left parietal and occipital regions. The liver showed centrilobular atrophy/dropout and fibrosis.

The patient (#9) who had TRM on day +44 developed progressive pulmonary edema with mild cardiac hypokinesis starting on day +1 after HSCT with concurrent worsening renal function and was initially stabilized with diuresis. On day +13, cardiac failure worsened, with LVEF 20% to 25% combined with volume overload and anuria, and renal replacement therapy was initiated. Symptoms gradually improved, and the patient was discharged from the hospital on day +43 with planned thrice-weekly hemodialysis. Within 20 minutes of the first outpatient hemodialysis, the patient developed fever and hypotension, then acute respiratory failure and cardiac arrest. Despite a prolonged resuscitation effort, the patient died. Death was due to sepsis in the setting of AKI with SRC.

Both patients with early TRM developed evidence of SRC with AKI progressively developing between 7 and 14 days after HSCT with concurrent engraftment syndrome and evidence of CY-induced cardiomyopathy. Terminal events included acute respiratory failure, sepsis physiology, and multi-organ injury.

Thirteen patients (65%) developed at least one grade ≥ 3 adverse event, which were outside of the expected, time-limited hematologic/gastrointestinal toxicity of HSCT. In addition to the two patients with early TRM, three patients (#7, #12, and #15) developed at least two grade 4 adverse events after HSCT requiring intensive care unit (ICU) stay for the treatment of combined AKI requiring renal replacement therapy and limited-duration intubation with mechanical ventilation for alveolar hemorrhage ($n = 1$) or respiratory distress owing to volume overload ($n = 2$) during the first month after transplant. The patient (#12) with alveolar hemorrhage recovered lung and renal function by 3 and 4 months after HSCT, respectively. The remaining two patients promptly recovered lung function but required ongoing hemodialysis for >6 months because of prolonged renal injury. One patient (#7) with prolonged renal injury also developed ruptured a left renal

Table 1. Baseline characteristics of enrolled patients and select final outcomes*

Pt no.	Age at HSCT, y	Sex	Dx to HSCT, mo	Prior failed DMARDs, x duration in months	SRC pre-HSCT?	S creat	eGFR	ILD?	FVC, %	DLco corr %	mRSS	Scl-70	RNA pol III	Final outcomes after HSCT			
														Organ fail sust?	Relapse SSC?	Alive? U, y	Other F/ U, y
1	64	M	11	MMFx7, pred	N	1.1	75	N	95	83	31	Neg	Neg	N	N	Y	9.2
2	53	F	59	MTXx15, Cyx6, MMFx30, Cyx6	N	0.6	107	Y	64	63	8	>8.0	46	N	N	Y	11.6
3	55	F	18	MTXx7, Cyx6, pred	N	0.7	101	Y	75	56	33	3.4	Neg	N	N	N	8.0 2nd AML
4	55	M	10	MMFx9, pred	N	0.65	111	Y	67	46	31	Neg	Neg	N	N	Y	10.5
5	19	F	6	MMFx1, MPax4	N	0.73	121	Y	63	77	41	Neg	Neg	N	N	Y	8.8
6	13	F	43	MTXx37, MMFx34, Cyx4, RTX2, pred	N	0.43	150	Y	66	47	46	>8.0	Neg	N	Y	Y	8.5
7	53	F	18	Cyx5	Y	1.8	33	Y	69	70	32	Neg	>150	Y	N	Y	8.4 Ren Tx
8	38	F	15	MTXx6, MMFx7, RTX2, pred	N	0.52	121	Y	70	64	39	>8.0	Neg	N	N	Y	8.3
9	60	F	22	MMFx4.5	Y	1.1	57	N	91	91	41	Neg	182	Y	n/a	N	0.1
10	50	M	11	MTXx2, MMFx6, Cyx4	N	0.72	111	Y	68	70	46	Neg	149	N	Y	Y	8.2
11	34	F	18	PIRFx9, TOCIX2, MMFx5,	N	0.56	123	Y	50	61	26	165	Neg	N	N	Y	8.3
12	70	F	22	MTXx1, Cyx6, MMFx6, RTX2	N	0.53	99	Y	86	51	33	52	Neg	N	N	Y	8.1
13	35	F	36	Cyx12, RILOx3	Y	0.62	119	Y	61	43	26	Neg	Neg	N	N	Y	7.4
14	52	M	14	MMFx0.5, Cyx6	Y	1.84	43	Y	61	41	39	Neg	87	Y	n/a	N	0.1
15	48	M	11	MMFx4, Cyx6	Y	1.4	62	Y	111	62	41	Neg	>80	Y	N	Y	7.0
16	49	F	16	MTXx4, MMFx10	N	0.71	104	Y	106	58	44	Neg	127	N	Y	Y	6.8
17	25	F	30	MTXx6, MMFx18	N	0.84	99	Y	81	65	26	>8.0	Neg	N	N	Y	6.5
18	41	F	15	MTXx2, MMFx11, pred	N	0.45	123	Y	97	67	32	Neg	56	N	Y	Y	5.6
19	43	F	36	ETANx3, RILOx3, MMFx12	N	0.71	108	Y	72	68	29	Neg	123	N	N	Y	5.8
20	52	F	30	MTXx6, MMFx1, MPax10	N	0.73	99	Y	75	60	46	>8.0	Neg	N	Y	N	3.3

* Eighteen patients had ILD progression (in addition to increasing mRSS) as the primary indication for autologous HSCT. Two patients (#1 and #9) had rapidly increasing mRSS (one patient [#9] also had a history of SRC) as the primary indication for HSCT. Thirteen participants identified as non-Hispanic White, five as non-Hispanic Black, and one as Hispanic. 2nd AML, secondary acute myeloid leukemia; Cy, cyclophosphamide; DLco corr%, diffusion lung capacity carbon monoxide corrected for hemoglobin percent predicted value; DMARD, disease-modifying antirheumatic drug (shown in the sequence administered); Dx, diagnosis (interval time from scleroderma diagnosis); eGFR, estimated glomerular filtration rate based on the Chronic Kidney Disease Epidemiology Collaboration 2021 equation (formula including sex and age; patient #6 used Schwartz pediatric bedside eGFR equation); ETAN, etanercept; F, female; fail sust, sustained organ failure >6 months (if alive); F/U, follow-up after hematopoietic stem cell transplantation at last contact; FVC, forced vital capacity percent predicted value; HSCT, hematopoietic stem cell transplantation; ILD, interstitial lung disease; M, male; MMF, mycophenolate mofetil; MPA, mycophenolic acid; mRSS, modified Rodnan skin score (maximum score 51); MTX, methotrexate; N, no; n/a, not applicable; neg, negative clinical test range autoantibody value; PIRF, pirfenadone; pred, prednisone (at various doses >20 milligram per day for varying duration); Pt, patient; Ren Tx, renal transplant; RILO, rilonacept; RTX, rituximab; RNA pol III, RNA polymerase-3 (values in positive range are shown in units per milliliter); Scl-70, scleroderma-70 autoantibody measured in arbitrary units per milliliter (values in positive range are shown and are dependent on laboratory-specific clinical tests); S creat, serum creatinine before hematopoietic stem cell transplantation; SRC, scleroderma renal crisis; SSC, systemic sclerosis; TOC1, tocilizumab; Y, yes.

artery aneurysm day +77 after transplant and was treated with embolization. This patient proceeded to a successful living donor kidney transplant 2 years after HSCT. The second patient (#15) recovered renal function by 18 months and discontinued hemodialysis; however, they had persistent cardiomyopathy after transplant with LVEF of 25% to 30%. The two patients with renal failure >6 months after HSCT met the protocol endpoint of organ failure.

One patient (#8) with rSr' right ventricular conduction delay on electrocardiogram before HSCT developed persistent, refractory ventricular tachycardia at day +10 after transplant, requiring ICU and intravenous anti-arrhythmia drug treatment. This patient underwent successful right cardiac ablation 1 month after transplant, followed with oral diltiazem, with no recurrence of significant arrhythmia beyond 2 months after HSCT. In total, eight patients (40%, #7, #8, #9, #10, #11, #12, #14, and #15) received ICU treatment early after transplant for a median of 27 (range 4–50) days.

Three patients (15%) had a transient, low-level reactivation of Epstein-Barr virus during the first 100 days after transplant, but none required treatment. The two patients with early TRM had cytomegalovirus reactivation after HSCT that responded to ganciclovir treatment.

In addition to the two patients with early TRM, one patient (#20) died at 40 months after transplant because of sepsis/infection unrelated to HSCT. This patient did not take MMF maintenance therapy and initially had an excellent response in skin tightness symptoms. However, beginning at 34 months after transplant, the patient reported increasing diffuse skin tightness but was not started on DMARDs because of patient preference. They had a non-ST elevation myocardial infarct with concurrent pericardial effusion at month 39. The pericardial effusion cytology was hypocellular, containing histiocytes, mesothelial cells, and few lymphocytes. At month 40 after transplant, the patient was found unresponsive and died shortly after arrival to hospital because of overwhelming sepsis. Recurrence of SSc disease activity likely contributed to this patient's death; no autopsy was obtained.

There was one late death at 8 years after transplant. This patient (#3) developed low-grade MDS with complex cytogenetics at 6.2 years after HSCT attributable to late effects of the conditioning regimen or prior CY. The malignancy progressed to high-grade MDS by 7 years after HSCT and did not respond to three cycles of decitabine/venetoclax. The MDS progressed to secondary acute myelogenous leukemia (AML), and the patient died of AML complications without recurrence of SSc disease.

SSc response to treatment. Eighteen of 20 patients were evaluable for disease response to HSCT. Thirteen (72%) of 18 patients initiated and were compliant with MMF/MPA maintenance therapy with treatment duration ranging from 9 months to ≥5 years after HSCT (Figure 1). Reasons for not starting

after transplant MMF/MPA included patient/physician preference (n = 3) or AKI (n = 2). There were no significant adverse events reported among the patients treated with MMF/MPA maintenance other than mild upper respiratory infection ([URI], n = 2). Reasons for discontinuation of MMF/MPA <2 years after transplant included SSc progression/relapse (n = 1) and URI (n = 2). Seven patients (39%) continued MMF/MPA for ≥5 years after HSCT.

Excluding the four patients who met an early posttransplant EFS endpoint, renal function was stable or improved compared with baseline among all surviving patients at time points >3 months after transplant. In addition, available follow-up echocardiogram and electrocardiogram results for the 14 patients with long-term EFS were stable/unchanged.

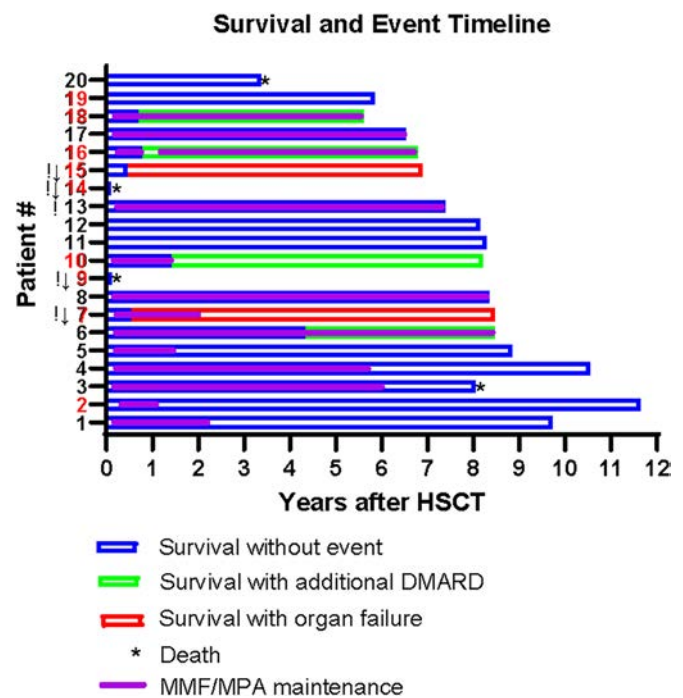


Figure 1. Swimmer plot of survival and events for 20 patients with diffuse cutaneous systemic sclerosis enrolled in this autologous HSCT trial. The patient number is shown as identified in Table 1 in ascending sequence of trial enrollment. A red font patient number indicates anti-RNA-polymerase III seropositive before HSCT. The exclamation mark indicates a history of scleroderma renal crisis, “↓” indicates baseline pre-HSCT decreased renal function (estimated glomerular filtration rate <65 mL/min/1.73m²), and the asterisk indicates death. The blue bar border indicates survival without event. The red bar border indicates survival after meeting the protocol-defined organ failure event endpoint. The green bar border indicates survival after the addition of a DMARD for the treatment of clinical systemic sclerosis progression or disease activity. The purple fill indicates treatment duration with protocol-prescribed maintenance MMF or MPA. All patients received an unmodified (not CD34+ selected) autologous peripheral blood stem cell graft at time point 0, and the follow-up is shown in years. DMARD, disease-modifying antirheumatic drug; HSCT, hematopoietic stem cell transplantation; MMF, mycophenolate mofetil; MPA, mycophenolic acid.

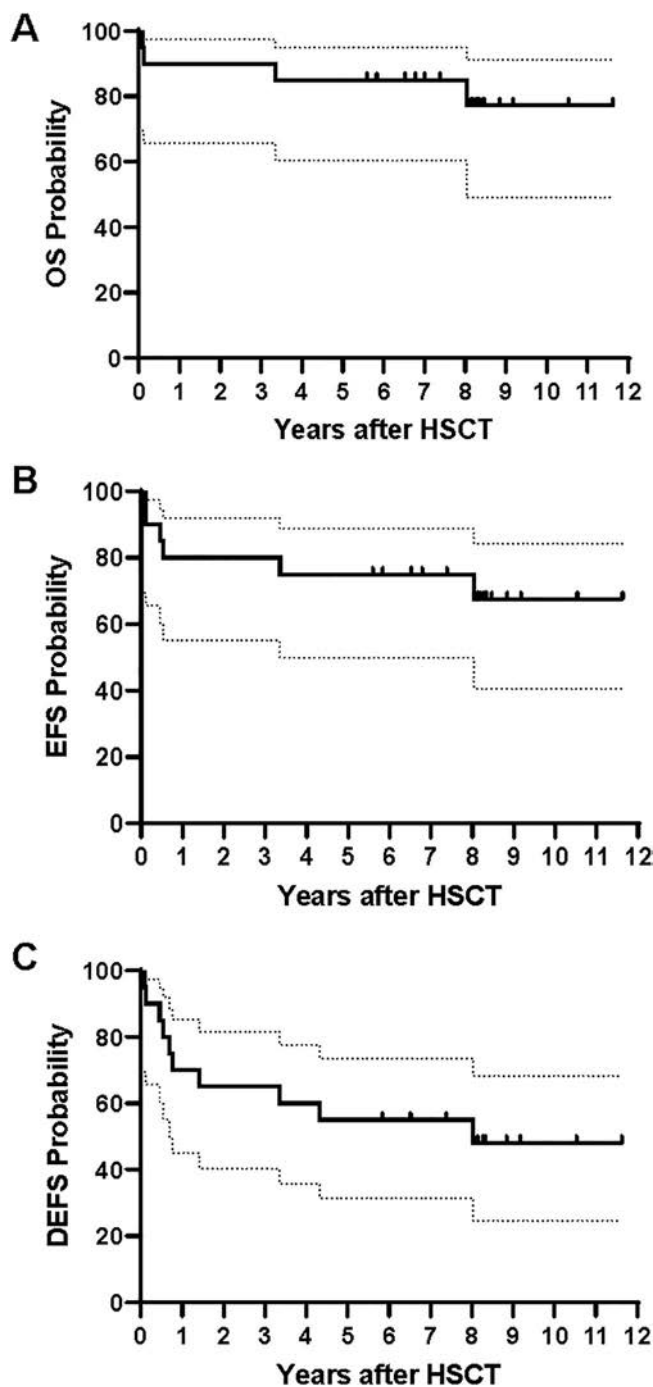


Figure 2. Kaplan-Meier survival curves of (A) OS, (B) EFS, and (C) DEFS for the entire cohort of 20 systemic sclerosis patients after HSCT. The EFS endpoint included death or meeting the defined organ failure criteria for longer than 6 months. The DEFS endpoint included death, organ failure, or initiation of additional disease-modifying antirheumatic drugs (indicator of disease relapse/recurrence after transplant). Tick marks show the time of censorship and status at time of last contact. The dotted lines indicate the 95% confidence interval. DEFS, composite of additional disease-modifying antirheumatic drug and event-free survival; EFS, event-free survival; HSCT, hematopoietic stem cell transplantation; OS, overall survival.

Table 2. LS mean changes in skin score, pulmonary function, and disability index*

Variable	Value
Baseline mRSS score, n	20
Mean (SD)	34.5 (9.3)
Median (Q1–Q3)	33.0 (30.0–41.0)
Change in mRSS at last assessment, n	18
Mean (SD)	–20.3 (11.3)
Median (Q1–Q3)	–22.5 (–29.0 to –14.0)
P value	<0.0001
LS mean change in mRSS at year 5, n	18
LS mean	–25.1
95% CI	–29.8 to –20.4
P value	<0.0001
Baseline FVC% predicted, n	20
Mean (SD)	76.4 (16.3)
Median (Q1–Q3)	71.0 (65.0–88.5)
Change in FVC% at last assessment, n	17
Mean (SD)	8.7 (11.9)
Median (Q1–Q3)	9.0 (0.0–19.0)
P value	0.0127
LS mean change in FVC% at year 5, n	17
LS mean	10.5
95% CI	5.4–15.6
P value	0.0001
Baseline DLco% predicted, n	20
Mean (SD)	61.7 (13.2)
Median (Q1–Q3)	62.5 (50.5–69.0)
Change in DLco% at last assessment, n	17
Mean (SD)	11.2 (14.4)
Median (Q1–Q3)	8.0 (2.0–17.0)
P value	0.0020
LS mean change in DLco% at year 5, n	17
LS mean	12.4
95% CI	5.5–19.3
P value	0.0006
Baseline HAQ-DI, n	19
Mean (SD)	2.1 (0.9)
Median (Q1–Q3)	2.4 (1.8–2.8)
Change in HAQ-DI at last measure, n	15
Mean (SD)	–0.8 (1.0)
Median (Q1–Q3)	–0.5 (–1.9 to –0.1)
P value	0.0079
LS mean change in HAQ-DI at year 4, n	15
LS mean	–1.1
95% CI	–1.6 to –0.6
P value	0.0004

* We assessed the change from baseline in four outcome measures: mRSS, FVC%, DLco%, and HAQ-DI. LS mean change at year 5 was reported for mRSS, FVC%, and DLco%. LS mean change at year 4 was reported for HAQ-DI (because there was incomplete year 5 HAQ-DI data). There was no significant difference in the change in mRSS at last assessment between patients in the two autoantibody subgroups (scleroderma-70+ and RNA polymerase III+). CI, confidence interval; DLco%, diffusion lung capacity carbon monoxide corrected for hemoglobin percent predicted value; FVC%, forced vital capacity percent predicted value; HAQ-DI, Health Assessment Questionnaire Disability Index, (score range 0–3.0); LS, least square; mRSS, modified Rodnan skin score; Q, quartile.

Among the 18 evaluable patients, 12 (67%) achieved a sustained $\geq 50\%$ reduction in skin scores at a median of 12 (range 2–60) months after HSCT without additional DMARD treatment. Eight (44%) of 18 patients achieved a sustained

$\geq 10\%$ improvement in predicted FVC at a median of 18 (range 12–60) months after transplant. Seven (39%) of 18 patients achieved a sustained $\geq 15\%$ improvement in predicted DLco at a median of 4 (range 2–5) years after transplant. No patient met the lung function failure endpoint. Table 2 and Figure 3 show the least squares mean change in four outcome measures: mRSS, FVC, DLco, and Health Assessment Questionnaire Disability Index. There were significant improvements in all four outcome measures over the course of the trial with improvements seen at ≤ 1 year after AHSCT with continuing improvement/stabilization.

A minority of patients who were positive for SSc autoantibodies at pretransplant evaluation became negative (below the clinically positive range) after transplant. Of the eight patients who were ATA+, three (38%) became autoantibody negative by 1 to 4 years after transplant. Of the nine patients who were ARA+, four (44%) had decreased levels to the negative range by 2 years after transplant (using the same assay platform). Of the 20 patients who were ANA+ before transplant, 7 (35%) became ANA negative, 7 patients had decreased or unchanged ANA titer, and 6 (30%) had no follow-up testing.

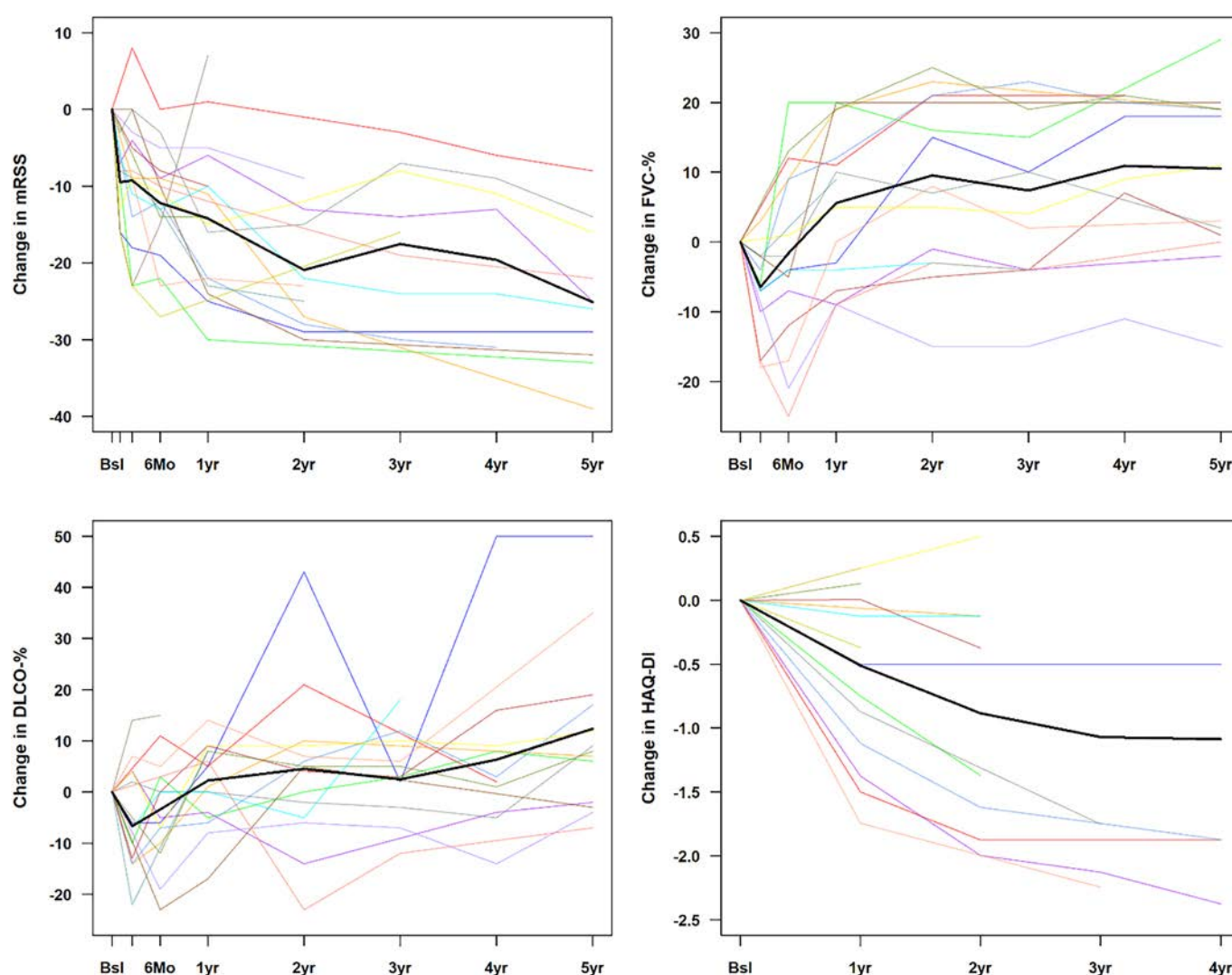


Figure 3. Rate of change in skin score, lung function, and HAQ-DI score after nonmyeloablative autologous hematopoietic stem cell transplantation. The Bsl values and statistical analysis of change over time is shown in Table 2. The colored lines are spaghetti plots of change from the pretransplant Bsl for each patient, and the bold black lines are the overall change trend based on the linear mixed effect model. (Upper left) Change from the pretransplant Bsl in mRSS reported at timepoints after autologous HSCT. (Upper right) Change in FVC% at time points after autologous HSCT. Eight of 18 evaluable patients had a greater than 10% increase in predicted value from the pretransplant Bsl. (Lower left) Change in DLco% at timepoints after autologous HSCT. Seven of 18 evaluable patients had a greater than 15% increase in predicted value from the pretransplant Bsl. (Lower right) Change in HAQ-DI value (range 0–3.0) from pretransplant baseline up to 4 years after HSCT. Bsl, baseline; DLco%, diffusion lung capacity carbon monoxide corrected for hemoglobin percent predicted value; FVC%, forced vital capacity percent predicted value; HAQ-DI, Health Assessment Questionnaire Disability Index; HSCT, hematopoietic stem cell transplantation; mRSS, modified Rodnan skin score.

SSc relapse/progression. Five patients developed SSc relapse/progression after AHSCT. This included four patients that developed SSc disease relapse/progression requiring treatment with additional DMARDs (tocilizumab [#18 and #10], pulse CY [#16], and abatacept [#6]) at 8, 17, 9, and 53 months after transplant, respectively, despite compliance with MMF/MPA maintenance therapy (Figure 1). Skin tightness ($n = 2$) or decline in DLco% ($n = 2$) prompted the initiation of additional DMARDs (1 patient [#18] had skin worsening and DLco% decrease at month 8). One patient (#10) switched from MMF to tocilizumab at month 17 because of stable skin tightness symptoms. The addition of tocilizumab met the protocol definition for relapse/progression. Treatment with a new DMARD improved the disease status for all four patients. Two patients (#5 and #13) received weekly methotrexate for treatment of inflammatory arthritis, starting at 2 and 4 years, respectively, after transplant. As described above, one patient not taking MMF maintenance had SSc relapse, did not start DMARD, and died at month 40.

Additional DMARD- and event-free survival (DEFS).

For the entire cohort, the DEFS was 55% (95% CI 31.3%–73.5%) and 48% (95% CI 24.6%–68.3%) at 5 and 10 years, respectively (Figure 2C). DEFS excluded the protocol-prescribed MMF maintenance ($n = 13$) and weekly methotrexate ($n = 2$) given for arthritis. Four (80%) of the five patients who did not receive posttransplant MMF/MPA did not experience disease relapse/progression (mean follow-up 7.3 years). Nine (69%) of the 13 patients who took MMF/MPA maintenance therapy did not experience relapse/progression (mean follow-up 8.7 years) (Figure 1).

Impact of pretransplant SRC with impaired renal function. Among the five patients with a pretransplant history of SRC (Table 1 and Figure 1), 4 patients (#7, #9, #14, and #15) were ARA+ and had the lowest quartile of eGFR pretransplant (< 65 mL/min/1.73m²). These four patients developed AKI with evidence of SRC early after transplant and then had TRM or sustained organ injury. All other 16 patients had baseline eGFR ≥ 75 mL/min/1.73m², and none of these 16 patients experienced a sustained organ injury event/death early after transplant.

Impact of ARA+ and scl-70 (ATA+) autoantibody.

There were nine ARA+ patients (45%) at study entry (Table 1 and Figure 1). This included the four patients with a pretransplant history of SRC and eGFR < 65 mL/min/1.73m². Among these nine patients, two died of TRM, two met an early EFS endpoint (prolonged organ failure), and three experienced SSc relapse requiring initiation of DMARDs at 8, 9, and 17 months, respectively, after transplant (all patients described above). In contrast, among the 11 ARA-negative patients, as described above, one died with scleroderma relapse at 40 months, one had disease progression at 53 months successfully treated with abatacept, and one died of AML at 8 years. The 5-year point estimate of EFS for ARA+

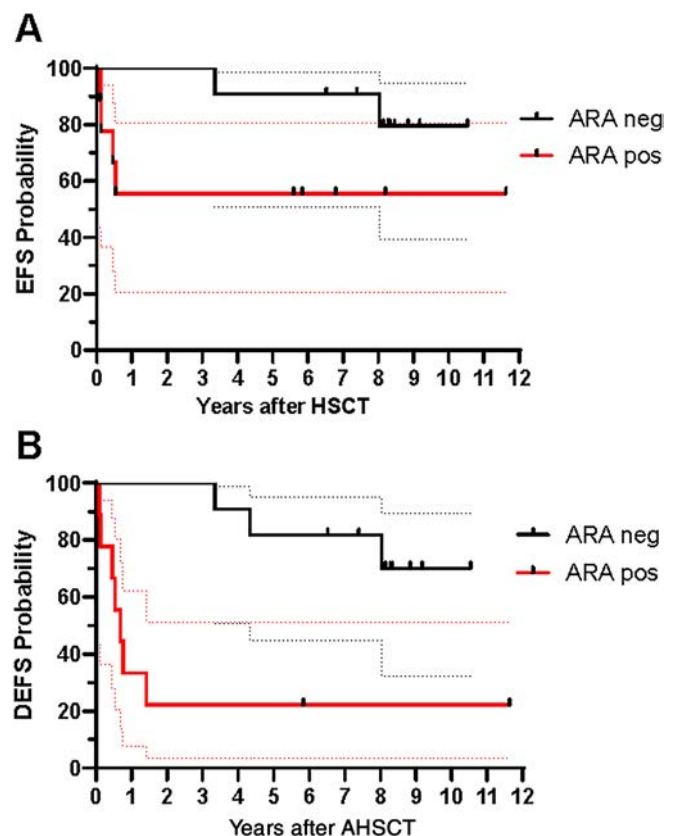


Figure 4. Kaplan-Meier survival of patients based on ARA status (neg or pos) before HSCT. (A) EFS of ARA-neg ($n = 11$) and ARA-pos ($n = 9$) patients (difference not significant). (B) - DEFS of ARA-neg and ARA-pos patients. Black lines indicate ARA neg, and red lines indicate ARA pos. Tick marks show the time of censorship and status at time of last contact. The dotted lines indicate the respective 95% confidence intervals. ARA, anti-RNA polymerase III autoantibody; DEFS, composite of additional disease-modifying antirheumatic drug and event-free survival; EFS, event-free survival; HSCT, hematopoietic stem cell transplantation; neg, negative; pos, positive.

and ARA-negative patients was 56% (95% CI 20.4%–80.5%) and 91% (95% CI 50.8%–98.7%), respectively (Figure 4A). The 5-year point estimate of DEFS for ARA+ and ARA-negative patients was 22% (95% CI 3.4%–51.3%) and 82% (95% CI 44.7%–98.7%), respectively (Figure 4B). The 5-year point estimate of EFS and DEFS for ATA+ (Scl-70+) patients ($n = 8$) was 87.5% (95% CI 38.7%–98.1%) and 75% (95% CI 31.5%–93%), respectively.

Of the four patients who became ARA seronegative after transplant, one (#10) received a DMARD (tocilizumab) at month 17, and all four eventually had sustained improvements in skin scores and lung function. One patient (#19) who remained ARA seropositive after transplant had a very favorable clinical response to transplant.

DISCUSSION

This single-arm, multicenter study confirmed the efficacy of nonmyeloablative CY200/ATG conditioning and autologous

PBSC transplantation with posttransplant MMF for patients with severe dcSSc. Similar to the ASTIS trial, which used CY200/ATG conditioning, TRM was 10%.⁷ With 20 patients in this trial, the median follow-up was 7.5 years; the 5-year OS and EFS of 85% and 75%, respectively, were numerically similar to the results observed in the ASTIS trial (81% and 78%, respectively).⁷ Because there was detailed clinical information available for each patient in this trial, we identified potential disease-associated factors that may contribute to an adverse outcome after HSCT. A history of SRC and decreased eGFR were factors that appeared to lead to early posttransplant events, including death or prolonged organ injury. In addition, a high proportion of ARA+ patients reached endpoints of death, organ injury, or disease progression after HSCT. Previous trials identified cardiac involvement of SSc and pulmonary arterial hypertension as risk factors for early adverse outcome.^{7,12} Because patients with these risk factors were excluded in this trial, we have identified additional disease factors potentially associated with adverse outcome when using CY200/ATG conditioning.

DcSSc with ARA+ autoantibody is associated with more extensive skin disease, renal crisis, and pulmonary hypertension compared with other SSc-associated autoantibodies.^{13–16} Compared with the general SSc population, there was a high proportion of ARA+ patients in this trial.^{13–16} ARA+ SSc is associated with SRC, and patients with SRC frequently develop chronic kidney disease (CKD), with impaired eGFR that does not necessarily recover.¹⁷ For this trial, no dose adjustment of CY in the setting of stage 2/3a CKD was made, and this factor very likely contributed to the observed early TRM and CY-associated toxicity. A key observation is that CY200/ATG conditioning may be too toxic for patients with dcSSc with reduced eGFR. This observation may be relevant for explaining the 0% early TRM observed in the SCOT trial, which limited the conditioning regimen total CY dose to 120 mg/kg and enrolled patients with better renal function.⁸ Recent studies have shown increased potential for CY-induced toxicity in patients with even mildly impaired renal function.¹⁸ The exact recommended lower limit of eGFR eligible for CY200/ATG is uncertain because of the limited number of patients studied but may be in the range of <65 to 75 mL/min/1.73m². For patients with SSc with reduced eGFR, CY dose adjustment should be explored in future clinical trials. No methylprednisolone dose adjustment was made for ARA+ patients. Moderate- to high-dose methylprednisolone has been associated with SRC in patients with early SSc who are ARA+.^{19,20} Although prophylactic lisinopril was given to reduce the risk of SRC after AHSCT, this did not appear to prevent SRC progression in these patients, highlighting that this population should be carefully considered for HSCT.

The relatively low DEFS among ARA+ patients is a new and potentially important finding. Patients who are ARA+ may have a more aggressive SSc disease course.^{13–16} Furthermore, compared with the SCOT trial TBI/CY/ATG conditioning, we speculate that the nonmyeloablative CY200/ATG conditioning may be

insufficient to completely eradicate the underlying autoimmune pathology in some patients with dcSSc. For patients who were ATA+ (Scl-70+), the 5-year EFS and DEFS were favorable, 87.5% and 75%, respectively. The patients with ARA+ had worse outcomes, but the data were confounded by the presence of pretransplant SRC and decreased eGFR (in four of nine ARA+ patients). The incidence of SSc relapse after AHSCT was not significantly different between the ATA+ versus ARA+ groups, but the number of evaluable patients was low. Future studies should compare the transplant outcome of ARA+ patients versus ATA+ patients with SSc.

Eight patients (40%) required ICU treatment early after transplant. This reflected the toxicity of the high-dose CY in patients with SSc in this trial. Other myeloablative conditioning regimens appear to be associated with less toxicity, such as the SCOT trial TBI/CY/ATG regimen.⁸ It is likely that the disease-related factors of recent SRC and decreased eGFR (stage 2/3a CKD) contributed to the adverse events after CY200/ATG. With a limited number of enrolled patients, we were unable to identify other variables, such as age or prior treatment, as significant risk factors for adverse outcomes. For those patients with follow-up data, there were significant improvements in mRSS, FVC%, DLco%, and the Health Assessment Questionnaire Disability Index. These findings are consistent with published AHSCT data^{7,8} and compare favorably to nontransplant treatment outcomes.²¹

Thirteen patients were compliant with MMF maintenance therapy for a ≥9-month duration. No significant adverse events were reported among the patients taking MMF maintenance other than two mild URI cases. Overall, MMF maintenance after transplant was well tolerated and appeared safe. Two retrospective, nonrandomized, SSc transplant registry studies suggested that CD34+ selection was associated with a better response to HSCT therapy; however, patients who received unmanipulated grafts in those trials did not receive MMF maintenance.^{22,23} Future randomized trials are needed to definitively assess the impact of MMF maintenance versus CD34+ selection on posttransplant disease relapse.

TBI-based conditioning has been associated with a risk of posttransplant secondary malignancies.^{24,25} One reason for avoiding TBI in this trial was to assess if there was a reduced incidence of MDS/AML using the CY200/ATG regimen. There was one patient (5%) who developed secondary MDS/AML at 6.2 years after HSCT. This is consistent with the 6% incidence of secondary MDS after TBI/CY/ATG conditioning in the SCOT trial.⁸ The patient with posttransplant MDS in our study was older and received pretransplant CY. CY is an alkylating agent with a known risk for development of secondary malignancies.^{25,26} The risk of secondary malignancy after AHSCT is low but non-negligible. Further studies are needed to compare the difference in secondary malignancy incidence between TBI- and CY-based conditioning regimens.

It was noteworthy that a minority of patients (38%) who were seropositive for SSc-associated autoantibodies at pretransplant

evaluation became seronegative after transplant. It took 1 to 4 years for these patients to become seronegative, but a clinically favorable response to transplant did not require conversion to seronegativity. Future studies are needed to assess if conversion to autoantibody seronegative status is related to more durable clinical responses.

The limitations of this study include the limited number of patients, the single-arm trial design, inadequate representation from underrepresented populations, and the incomplete adherence to MMF/MPA maintenance therapy, which may result in overestimation of the significance of study findings. The study was not designed to detect differences between groups.

In summary, this study suggests that nonmyeloablative CY200/ATG (without TBI) conditioning is an effective AHSCT regimen for many patients with dcSSc. Importantly, we identified a factor for adverse outcome after transplant: decreased pretransplant eGFR (approximately <65 to $75 \text{ mL/min/1.73m}^2$), which occurred in patients with a history of SRC with ARA+ dcSSc. For patients with reduced eGFR, we advise avoiding AHSCT using CY200/ATG conditioning and consider an alternative regimen such as TBI/CY/ATG (SCOT trial⁸) or a clinical trial with dose-reduced CY. For patients without these factors (no prior SRC and normal eGFR), the CY200/ATG regimen with MMF maintenance appears to be a highly effective treatment; however, there was a moderate incidence of ICU admission. We showed that MMF maintenance after AHSCT appeared safe and was well tolerated. Whether MMF maintenance therapy is an effective substitute for CD34+ selection remains unknown; however, the OS and EFS in this trial were consistent with those of the ASTIS trial that employed CD34+ selection.^{7,8} Finally, we observed a 5% incidence of secondary MDS late after transplant, highlighting the need for close follow-up monitoring of patients after transplant and consideration for more aggressive interventions early in the course of this complication.

ACKNOWLEDGMENTS

We are grateful to the patients and their families who supported them for participation in this trial. We thank the members of the data safety monitoring board: Dr Mary Ellen Csuka (Chair), Dr Steven Pavletic, Dr Richard Silver, and Dr Kathrine Guthrie. We thank the transplant and rheumatology teams at each of the participating sites and the research data coordinators. We thank Ms Bernadette McLaughlin, RN, for research coordination support for the trial. The participating paired transplant and rheumatology sites that enrolled patients for this trial included the following: Fred Hutchinson Cancer Center and University of Washington, Seattle, WA; City of Hope Comprehensive Cancer Center, Duarte, CA, and University of California Los Angeles, Los Angeles, CA; Colorado Blood Cancer Institute, Denver, CO, and University of Colorado Anschutz School of Medicine, Aurora, CO; University of Michigan, Ann Arbor, MI; Boston Medical Center and Boston University Chobanian & Avedisian School of Medicine, Boston, MA; and M. D. Anderson Cancer Center and University of Texas Houston McGovern Medical School, Houston, TX.

AUTHOR CONTRIBUTIONS







All authors contributed to at least one of the following manuscript preparation roles: conceptualization AND/OR methodology, software, investigation, formal analysis, data curation, visualization, and validation AND drafting or reviewing/editing the final draft. As corresponding author, Dr Georges confirms that all authors have provided the final approval of the version to be published, and takes responsibility for the affirmations regarding article submission (eg, not under consideration by another journal), the integrity of the data presented, and the statements regarding compliance with institutional review board/Declaration of Helsinki requirements.

REFERENCES

- Mayes MD, Lacey JV Jr, Beebe-Dimmer J, et al. Prevalence, incidence, survival, and disease characteristics of systemic sclerosis in a large US population. *Arthritis Rheum* 2003;48(8):2246–2255.
- Elhai M, Meune C, Avouac J, et al. Trends in mortality in patients with systemic sclerosis over 40 years: a systematic review and meta-analysis of cohort studies. *Rheumatology (Oxford)* 2012;51(6):1017–1026.
- Nihtyanova SI, Schreiber BE, Ong VH, et al. Prediction of pulmonary complications and long-term survival in systemic sclerosis. *Arthritis Rheumatol* 2014;66(6):1625–1635.
- Tashkin DP, Elashoff R, Clements PJ, et al; Scleroderma Lung Study Research Group. Effects of 1-year treatment with cyclophosphamide on outcomes at 2 years in scleroderma lung disease. *Am J Respir Crit Care Med* 2007;176(10):1026–1034.
- Khanna D, Denton CP, Jähreis A, et al. Safety and efficacy of subcutaneous tocilizumab in adults with systemic sclerosis (faSScinate): a phase 2, randomised, controlled trial. *Lancet* 2016;387(10038):2630–2640.
- Tashkin DP, Roth MD, Clements PJ, et al; Scleroderma Lung Study II Investigators. Mycophenolate mofetil versus oral cyclophosphamide in scleroderma-related interstitial lung disease (SLS II): a randomised controlled, double-blind, parallel group trial. *Lancet Respir Med* 2016;4(9):708–719.
- van Laar JM, Farge D, Sont JK, et al; EBMT/EULAR Scleroderma Study Group. Autologous hematopoietic stem cell transplantation vs intravenous pulse cyclophosphamide in diffuse cutaneous systemic sclerosis: a randomized clinical trial. *JAMA* 2014;311(24):2490–2498.
- Sullivan KM, Goldmuntz EA, Keyes-Elstein L, et al; SCOT Study Investigators. Myeloablative autologous stem-cell transplantation for severe scleroderma. *N Engl J Med* 2018;378(1):35–47.
- van den Hoogen F, Khanna D, Fransen J, et al. 2013 classification criteria for systemic sclerosis: an American College of Rheumatology/European League Against Rheumatism collaborative initiative. *Ann Rheum Dis* 2013;72(11):1747–1755.
- Inker LA, Eneanya ND, Coresh J, et al; Chronic Kidney Disease Epidemiology Collaboration. New creatinine and cystatin C-based equations to estimate GFR without race. *N Engl J Med* 2021;385(19):1737–1749.
- Cornell RF, Hari P, Drobyski WR. Engraftment syndrome after autologous stem cell transplantation: an update unifying the definition and management approach. *Biol Blood Marrow Transplant* 2015;21(12):2061–2068.
- Farge D, Burt RK, Oliveira MC, et al. Cardiopulmonary assessment of patients with systemic sclerosis for hematopoietic stem cell transplantation: recommendations from the European Society for Blood and Marrow Transplantation Autoimmune Diseases Working Party and collaborating partners. *Bone Marrow Transplant* 2017;52(11):1495–1503.

13. Nihtyanova SI, Denton CP. Autoantibodies as predictive tools in systemic sclerosis. *Nat Rev Rheumatol* 2010;6(2):112–116.
14. Nihtyanova SI, Schreiber BE, Ong VH, et al. Prediction of pulmonary complications and long-term survival in systemic sclerosis. *Arthritis Rheumatol* 2014;66(6):1625–1635.
15. Motegi S, Toki S, Yamada K, et al. Demographic and clinical features of systemic sclerosis patients with anti-RNA polymerase III antibodies. *J Dermatol* 2015;42(2):189–192.
16. Hoffmann-Vold AM, Midtvedt Ø, Tennøe AH, et al. Cardiopulmonary disease development in anti-RNA polymerase III positive systemic sclerosis; comparative analyses from an unselected, prospective patient cohort. *J Rheumatol* 2017;44(4):459–465.
17. Iliopoulos G, Daoussis D. Renal dysfunction in systemic sclerosis beyond scleroderma renal crisis. *Rheumatol Int* 2021;41(7):1203–1208.
18. Jaber MM, Takahashi T, Kirstein MN, et al. Influence of renal function on phosphoramidate mustard exposure: a nonlinear mixed-effects analysis. *J Clin Pharmacol* 2023;63(1):135–142.
19. Penn H, Howie AJ, Kingdon EJ, et al. Scleroderma renal crisis: patient characteristics and long-term outcomes. *QJM* 2007;100(8):485–494.
20. Guillevin L, Bérezné A, Seror R, et al. Scleroderma renal crisis: a retrospective multicentre study on 91 patients and 427 controls. *Rheumatology (Oxford)* 2012;51(3):460–467.
21. Gregory K, Hansen D, Penglase R, et al. Outcomes of patients with diffuse systemic sclerosis eligible for autologous stem cell transplantation treated with conventional therapy. *Arthritis Rheumatol* 2024;76(8):1294–1302.
22. Henes J, Oliveira MC, Labopin M, et al. Autologous stem cell transplantation for progressive systemic sclerosis: a prospective non-interventional study from the European Society for Blood and Marrow Transplantation Autoimmune Disease Working Party. *Haematologica* 2021;106(2):375–383.
23. Ayano M, Tsukamoto H, Mitoma H, et al. CD34-selected versus unmanipulated autologous hematopoietic stem cell transplantation in the treatment of severe systemic sclerosis: a post hoc analysis of a phase I/II clinical trial conducted in Japan. *Arthritis Res Ther* 2019;21(1):30.
24. Rohatiner AZ, Nadler L, Davies AJ, et al. Myeloablative therapy with autologous bone marrow transplantation for follicular lymphoma at the time of second or subsequent remission: long-term follow-up. *J Clin Oncol* 2007;25(18):2554–2559.
25. Pedersen-Bjergaard J, Andersen MK, Christiansen DH. Therapy-related acute myeloid leukemia and myelodysplasia after high-dose chemotherapy and autologous stem cell transplantation. *Blood* 2000;95(11):3273–3279.
26. Akhtari M, Bhatt VR, Tandra PK, et al. Therapy-related myeloid neoplasms after autologous hematopoietic stem cell transplantation in lymphoma patients. *Cancer Biol Ther* 2013;14(12):1077–1088.

Characterization of Genetic Landscape and Novel Inflammatory Biomarkers in Patients With Adult-Onset Still Disease

Joanne Topping,¹ Leon Chang,¹ Fatima Nadat,² James A. Poulter,¹ Alice Ibbotson,¹ Samuel Lara-Reyna,¹ Christopher M. Watson,²  Clive Carter,² Linda P. Pournara,¹  Jan Zernicke,³ Rebecca L. Ross,⁴  Catherine Cargo,² Paul A. Lyons,⁵ Kenneth G. C. Smith,⁵ Francesco Del Galdo,⁴  Jürgen Rech,⁶  Bruno Fautrel,⁷ Eugen Feist,⁸ Michael F. McDermott,¹ and Sinisa Savic,⁹  on behalf of the ImmunAID Consortium

Objective. Adult-onset Still disease (AOSD) is a systemic autoinflammatory disorder (AID) of unknown etiology. Genetic studies have been limited. Here, we conducted detailed genetic and inflammatory biomarker analysis of a large cohort with AOSD to investigate the underlying pathology and identify novel targets for potential treatment.

Methods. We investigated AOSD cases ($n = 60$) for rare germline and somatic variants using whole exome sequencing with virtual gene panels. Transcriptome profiles were investigated by bulk RNA sequencing whole blood. Cytokine profiling was performed on an extended patient cohort ($n = 106$) alongside measurements of *NLRP3* inflammasome activation using a custom assay and type I interferon (IFN) score using a novel method.

Results. We observed higher than expected frequencies of rare germline variants associated with monogenic AIDs in AOSD cases (AOSD 38.4% vs healthy controls [HCs] 20.4%) and earlier onset of putative somatic variants associated with clonal hematopoiesis of indeterminate potential. Transcriptome profiling revealed a positive correlation between Still Activity Score and gene expression associated with the innate immune system. *ASC/NLRP3* specks levels and type I IFN scores were significantly elevated in AOSD cases compared with HCs ($P = 0.0001$ and 0.0015 , respectively), in addition to several cytokines: interleukin (IL)-6 ($P < 0.0001$), IL-10 ($P < 0.0075$), IL-12p70 ($P = 0.0005$), IL-18 ($P < 0.0001$), IL-23 ($P < 0.0001$), IFN- $\alpha 2$ ($P = 0.0009$), and IFN γ ($P = 0.0002$).

Conclusion. Our study shows considerable genetic complexity within AOSD and demonstrates the potential utility of the *ASC/NLRP3* specks assay for disease stratification and targeted treatment. The enriched genetic variants identified may not by themselves be sufficient to cause disease, but may contribute to a polygenic model for AOSD.

INTRODUCTION

Adult-onset Still disease (AOSD) is a systemic autoinflammatory disorders (AID) of unknown etiology. Typically presenting with

prolonged intermittent fevers, arthralgias, and evanescent rash—any system can be affected.¹ It is most often diagnosed following exclusion of infection, malignancy, or other inflammatory rheumatologic diseases, and patients must fulfill classification criteria to

The views expressed herein are those of the authors and do not necessarily represent those of the NHS, the National Institute for Health and Care Research, or the Department of Health.

Supported by the European Union's Horizon 2020 Research and Innovation Program (grant 779295; Immunome Project Consortium for Autoinflammatory Disorders [ImmunAID]). Dr Savic's work was supported by a senior fellowship from Kennedy Trust and by the National Institute for Health and Care Research Leeds Biomedical Research Centre.

¹Joanne Topping, PhD, Leon Chang, PhD, Alice Ibbotson, MSc, Samuel Lara-Reyna, PhD, Linda P. Pournara, PhD, Michael F. McDermott, FRCPI, Dmed: University of Leeds, Leeds, United Kingdom; ²Fatima Nadat, PhD, James A. Poulter, PhD, Christopher M. Watson, PhD, Clive Carter, PhD, Catherine Cargo, MD, PhD: St James's University Hospital, Leeds, United Kingdom; ³Jan Zernicke, MD: Charité Universitätsmedizin Berlin, Berlin, Germany; ⁴Rebecca L. Ross, PhD, Francesco Del Galdo, MD, PhD: University of Leeds and National Institute for Health and Care Research Leeds Biomedical Centre, Chapel Allerton Hospital, Leeds, United Kingdom; ⁵Paul A. Lyons, PhD and Kenneth G. C. Smith, MD, PhD: University of Cambridge, Cambridge, United Kingdom; ⁶Jürgen

Rech, MD: Friedrich-Alexander University Erlangen-Nürnberg and Universitätsklinikum Erlangen, Erlangen, Germany; ⁷Bruno Fautrel, MD: Sorbonne University, AP-HP, Pitié-Salpêtrière Hospital, INSERM UMR 1136, Paris, France; ⁸Eugen Feist, MD: Otto-von-Guericke-University Magdeburg, Magdeburg, Germany, and Helios Clinic, Gommern, Germany; ⁹Sinisa Savic, MD, PhD: University of Leeds, St James's University Hospital, and National Institute for Health and Care Research Leeds Biomedical Centre, Chapel Allerton Hospital, Leeds, United Kingdom.

Drs Topping and Chang contributed equally to this work.

Additional supplementary information cited in this article can be found online in the Supporting Information section (<https://acrjournals.onlinelibrary.wiley.com/doi/10.1002/art.43054>).

Author disclosures are available at <https://onlinelibrary.wiley.com/doi/10.1002/art.43054>.

Address correspondence via email to Sinisa Savic, MD, PhD, at S.Savic@leeds.ac.uk.

Submitted for publication December 10, 2023; accepted in revised form October 18, 2024.

confirm the diagnosis. The criteria by Yamaguchi et al is the most commonly used.²

AOSD can be stratified into different subtypes depending on disease course or predominant clinical features. In the chronic disease course, patients either have systemic disease characterized by high fevers, rash, and multiorgan involvement, or a predominantly articular disease manifesting with inflammatory joint problems. There is frequent overlap among these presentations.³

AOSD is presumed to have a polygenic basis, but there is genetic and clinical overlap with monogenic autoinflammatory disorders (mAIDs). A systematic review of 162 patients with AOSD and systemic-onset juvenile idiopathic arthritis (sJIA; sJIA is considered the same disease as AOSD but with childhood onset) demonstrated that 51 patients (31.4%) carried at least one genetic variant associated with specific mAIDs (predominantly hereditary fever syndromes).⁴ The link was further supported by the observation that biologic therapies targeting proinflammatory cytokines, interleukin (IL)-1 β or IL-6, both key to mAIDs pathogenesis, are highly effective in treating AOSD.^{5,6}

Recent genetic developments in AID and the observation that patients with severe or resistant AOSD respond to treatment such as JAK inhibitors (JAKi), provides insight into disease pathogenesis. For example, somatic gain-of-function (GOF) mutations in autoinflammatory genes such as *NLRP3* and *NLRP4*, which arise within bone marrow and are restricted to myeloid lineage, result in spontaneous activation of the respective inflammasomes with subsequent excessive release of IL-1 β and IL-18 and late-onset autoinflammatory disorders (AIDs).^{7,8} Such cases are phenotypically indistinguishable from those with inherited (constitutional) mutations, despite only a small proportion of myeloid cells carrying the somatic mutations. Similarly, VEXAS syndrome (vacuoles, E1 enzyme, X-linked, autoinflammatory, somatic), caused by a somatic mutation in *UBA1*, and with disease pathogenesis linked to mutated and highly inflammatory myeloid cells, has clinical features that overlap with AOSD.⁹

There is also increasing recognition of the overlap between inflammatory conditions and myelodysplasia, with around 50% of patients with myelodysplastic syndrome (MDS) having autoinflammatory complications.¹⁰ Furthermore, in the premalignant bone marrow state clonal hematopoiesis of indeterminant potential (CHIP), which often precedes MDS, certain somatic mutations in bone hematopoietic stem cells have been associated with *NLRP3* inflammasome activation, release of IL-1 β , and a general proinflammatory state.¹¹ These phenomena are more frequent in the elderly, with one case series indicating a second incidence peak of AOSD in this population,¹² although the diagnosis in some of these cases was uncertain. Finally, it is increasingly recognized that some patients with resistant disease, and disease complicated by macrophage activation syndrome, are responsive to JAKi.^{13,14} This suggests innate immune pathways beyond those involving IL-1 β and IL-6, such as type I interferon (IFN), may be relevant in AOSD.¹⁵

We investigated three cohorts of well-characterized patients with AOSD at different stages of disease progression and treatment response. We sought to determine its genetic basis and establish whether low-prevalence somatic variants in candidate genes contribute to disease pathogenesis and the activation of specific inflammatory pathways linked with AOSD pathogenesis. We used bespoke assays to detect *NLRP3* inflammasome activation and measure serological IFN signature. Finally, we compared the mutation profiles of AOSD cases with defining disease signatures and inflammatory biomarkers to determine the potential functional relevance of rare genetic variants on AOSD expression.

MATERIALS AND METHODS

Please refer to the Supplemental Materials for in-depth descriptions of experimental methodology, data acquisition, and statistical analysis. In summary, 106 patients with AOSD were recruited from three separate cohorts (AOSD#1, AOSD#2, and AOSD#3); demographics are listed in Supplementary Table 1. Whole exome sequencing (WES) was performed on DNA samples extracted from whole blood ($n = 60$ from AOSD#2 and AOSD#3, mean depth 142 \times). Genetic variants were identified using in-house bioinformatic pipelines and a custom panel of 139 genes divided into three subcategories in association with CHIP, autoinflammation, and type I interferonopathies (Supplementary Table 2). Enrichment analyses of germline variants were performed using a Fisher's exact test for each variant and the recorded prevalence in the European non-Finnish population in the Genome Aggregation Database (gnomAD) for comparison. We accepted statistical significance at a P value adjusted for multiple testing with Bonferroni correction ($P < 0.05/\text{variant count}$). Bulk RNA sequencing (RNAseq) was performed on whole blood samples from AOSD cases (AOSD#2, $n = 27$) and healthy controls (HCs) (HCs, $n = 10$). Differentially expressed genes were defined as those with a log2FoldChange greater than 1 or less than -1 and an adjusted P value < 0.001 .

Functional assessments were performed on the collective AOSD cohort (AOSD#1, AOSD#2, and AOSD#3), and results were compared with other inflammatory disease and HC cohorts. We used an in-house flow cytometry assay for quantification of antibody-secreting cell (ASC)/*NLRP3* protein specks in patient sera (Supplementary Figure 1). The inflammatory cytokine profiles were investigated using the multiplex LEGENDplex Multi-Analyte Flow Assay kit (Biolegend). The type I IFN score was investigated on patient sera using a custom Luminex Discovery Assay (biotechne, R&D systems). Full details of ImmunAID investigators are provided in the Supplementary Material.

This study was approved by the South West – Frenchay Research Ethics Committee (Research Ethics Committee reference: 20/SW/0022). Data are available upon reasonable request. Processed and raw RNAseq data is publicly available at time of

publication; Gene Expression Omnibus accession number GSE244372; BioProject PRJNA1022483.

RESULTS

Patients with AOSD, disease, and HC demographics.

Demographic data for all patients with AOSD, the disease, and HCs are shown in Supplementary Table 1. The collective AOSD cohort ($n = 106$) comprised 68 women and 38 men with a mean age of 39.0 years. No significant differences in age distribution were detected across cohorts between the men and women. The sample cohorts used to produce each data set will be specified at the start of each section.

Rare germline and somatic variants identified using virtual gene panels. We compared WES data from 60 of 106 patients with AOSD (AOSD#2 $n = 30$; AOSD#3 $n = 30$) against a similar sized cohort of unrelated HCs (HC#1 $n = 49$, sequencing metrics available in Supplementary Table 3). Germline and somatic variant analyses were performed in parallel for each individual, and variant origins were distinguished bioinformatically. We investigated the burden of rare genetic variants in gene panels related to AIDs, CHIP, and type I interferonopathies (Supplementary Table 2). The genes within each panel are mutually exclusive.

Germline variant analysis. In the AOSD cohort, we identified 93 rare ($<1\%$ population allele frequency), potentially pathogenic (combined annotation dependent depletion [CADD] score >20) heterozygous germline variants (89 missense, four nonsense) across 60 genes within our gene panels (Figure 1A; Supplementary Table 4). These variants were distributed across 49 of 60 AOSD cases. The number of variants identified was normalized to the number of genes within each panel, generating frequencies of 0.70, 0.66, and 0.50 variants per gene in the CHIP-associated, autoinflammation, and type I interferonopathy panels, respectively. The variant profiles between the AOSD cohort (93 variants) and HCs (57 variants) were mostly unique with only four variants in common. No biallelic variants were identified in any samples.

We compared cohorts AOSD#2 and AOSD#3 with HCs separately to observe differences in variant burden. Cases from AOSD#3, which are treatment-resistant, had the highest variant burden across each gene panel overall. This was most evident in the autoinflammation gene panel in which variants were twice as prevalent in AOSD cases in comparison with HCs (AOSD#3 43.4%; AOSD#2 33.3%; HCs 20.4%). Genes *ALPK1*, *PLCG2*, *TRAP1*, and *NOD2* had the highest variant frequency within this panel among AOSD cases (Figure 1B), and reoccurring variants of interest include *NOD2* c.2183C>T and *PLCG2* c.1444T>C; each were identified in three separate AOSD cases (Figure 1C).

A significant proportion of AOSD cases (31 of 60) carried multiple variants (≥ 2) and cohort AOSD#3 (30.0%, 9 of 30) had the largest proportion of cases carrying ≥ 3 variants (Figure 1D).

Approximately one-third of the HC cohort were mutation-negative within our gene panels (34.7%, 17 of 49), whereas only 26.7% (8 of 30) and 10.0% (3 of 30) were mutation-negative among AOSD#2 and AOSD#3 cases, respectively.

Variant enrichment analysis. We conducted enrichment analyses on 142 variants found uniquely to either AOSD (89 of 93 variants) or HC cases (53 of 57 variants) and accepted a statistical significance at P value $<3.52 \times 10^{-4}$ after Bonferroni correction for multiple testing. Comparing with the recorded prevalence of each variant in the European non-Finnish population of gnomAD v4.0.0 (590,031 individuals), we identified that 15 of 89 variants were significantly overrepresented within the AOSD cohort across 13 cases. Two enriched variants were found in genes from the autoinflammation panel (*ALPK1*, *PSMG2*) and the remaining 13 variants were in CHIP-associated genes (Supplementary Table 4). We identified only 3 of 53 variants enriched in HCs. Despite each cohort having similar proportions of germline variants in CHIP-associated genes (AOSD#2 63.3%; AOSD#3 73.3%; HCs 66.3%), 22.0% (13 of 59 variants) of these were enriched in AOSD cases, whereas only 4.7% (2 of 43 variants) were enriched in HCs.

All variants were cross-referenced with the Infevers database (access date February 2024), which is an established registry of genetic variants associated with mAIDs. Nine variants were previously reported in Infevers, and two variants were classified as pathogenic: *TNFRSF1A* c.242G>A (P.(C81Y)) and *RIPK1* c.1934C>T (P.(T645M)); each was identified in a separate AOSD case in the heterozygous state. The genetics of autoinflammatory conditions associated with *RIPK1* are complex. The loss-of-function variants such as T645M are inherited either as homozygous or compound heterozygous states and will cause predominantly immunodeficiency with some immunodysregulation,¹⁶ whereas GOF variants, which stop the inactivation of *RIPK1*, are highly penetrant and are associated with a purely autoinflammatory phenotype.¹⁷ In this case, we have not identified a plausible second-hit or GOF variants following manual scrutiny of the sequence data. Therefore, it is highly unlikely that the T645M variant alone is sufficient to be disease-causing, and its contribution to overall AOSD phenotype is uncertain. In contrast, the *TNFRSF1A* p.C81Y mutation is an established autosomal dominant cause of TNF receptor-associated syndrome (TRAPS), with several well-characterized cases reported in the literature.^{18,19} A full case description of this patient is provided in Supplementary Materials. Furthermore, we identified a heterozygous *MVK* c.1129G>A (P.(V377I)) variant in one AOSD case that was also classified as pathogenic on Infevers. However, because of the low CADD score (15.1) this variant was omitted from further analysis (CADD >20 threshold).

Somatic variant analysis. We applied the somatic variant caller Mutect2 to our exome data and filtered out variants under 69× total read depth—a lower threshold determined by a somatic variant validated by digital polymerase chain reaction in HCs (Supplementary Figure 2). We also filtered the remaining variants

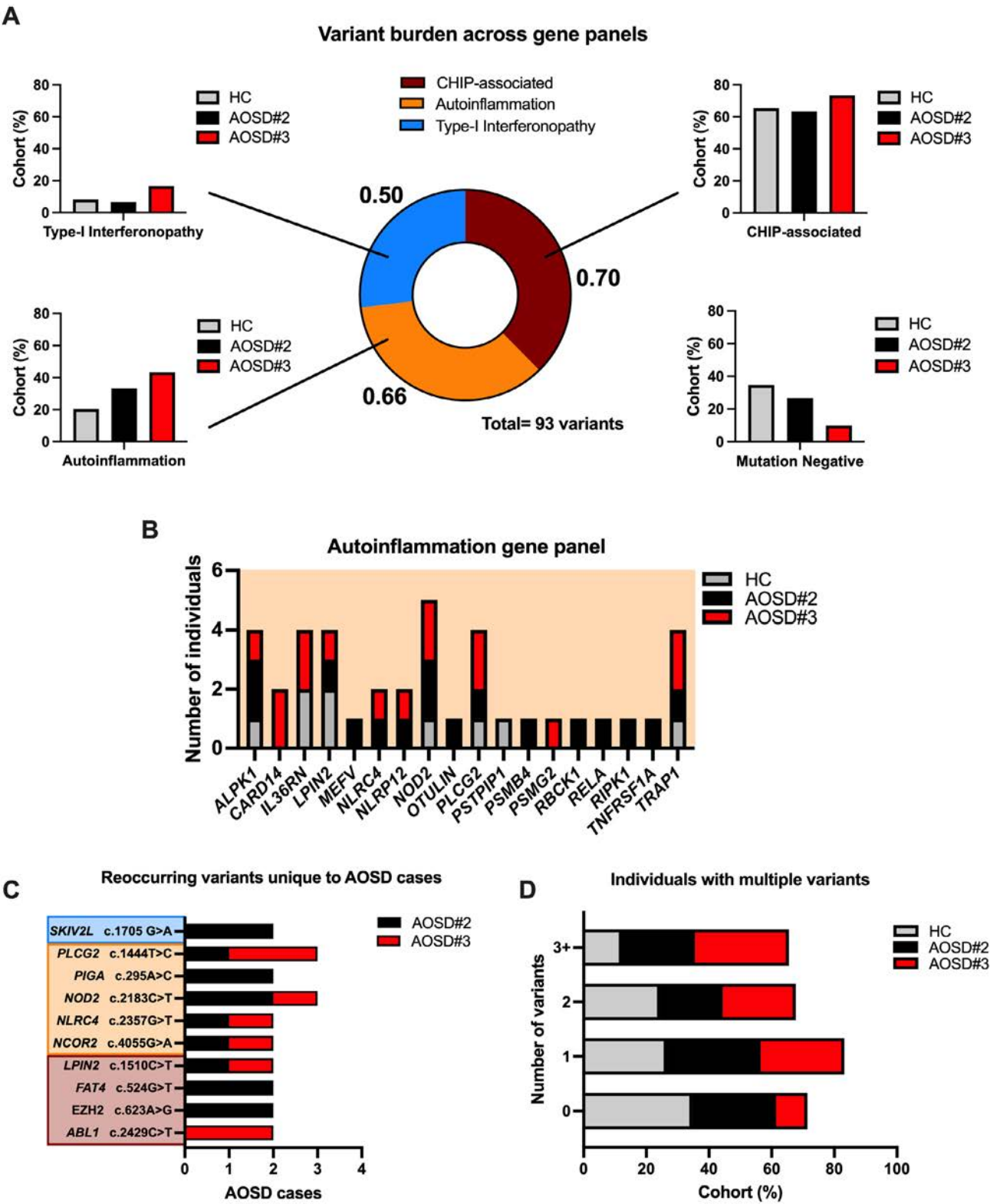


Figure 1. Rare germline variant analysis. (A) The number of variants identified in each panel (CHIP-associated, autoinflammation, and type I interferonopathy) was normalized to their corresponding gene panel size (gene count). Bar charts for each segment illustrate the proportion of AOSD and HC cohorts (%) carrying a rare germline variant in each gene panel. (B) The frequency of cases carrying rare variants across genes in the autoinflammation gene panel in each cohort. (C) Summary of the rare germline variants shared by more than one AOSD case, which are color-coded to reflect the associated gene panel: CHIP (brown), autoinflammation (orange), type I interferonopathy (blue). (D) The proportion of each cohort (%) carrying multiple variants across all gene panels. AOSD, adult-onset Still disease; CHIP, chromatin immunoprecipitation; HC, healthy control.

by CADD >20 and ≥5 variant read depth (exception allowed to variants previously confirmed as somatic in the Catalog of Somatic Mutations in Cancer [COSMIC]). This identified 18 putative somatic variants (Supplementary Table 5) across 18 of 60 AOSD cases (30.0%) and 5 variants in 5 of 49 HCs (10.2%). The burden of putative somatic variants was highest in *DNMT3A* and *FAT4* from the CHIP-associated gene panel (Figure 2A). Joint analysis with the previously discussed germline variant data identified 14 AOSD cases (23.3%) carrying a combination of at least one germline and one putative somatic variant within our targeted gene panels (Figure 2B). This combination was only found in three HC samples (6.1%) in comparison. Putative somatic variant counts were also similar between cohorts AOSD#2 (11 cases) and AOSD#3 (12 cases).

Age-related prevalence of CHIP-associated genetic variants in AOSD. The incidence of CHIP increases with age and is relatively common above 70 years old.²⁰ To establish whether the

prevalence of CHIP in AOSD is also age-dependent, putative somatic variants found in CHIP-associated genes were analyzed. To explore variant distribution with increasing age, both HC and AOSD cohorts were partitioned into three age brackets: 19 to 29, 30 to 49, and 50 to 80 years (Figure 2C). Overall, the AOSD cohort had a greater frequency of putative somatic variants associated with CHIP across all age groups in comparison to HCs, which were confined largely to the group aged 50 to 80 (Figure 2C).

Candidate gene identification following transcriptome analysis. To identify additional candidate genes of interest, we used transcriptome data generated from 27 patients with AOSD (AOSD#2) and 10 HCs (HC#2). Compared with HCs, 2,830 genes were differentially expressed in the AOSD cohort (Figure 3). Pathway and gene ontology analyses identified significant enrichment in genes associated with neutrophil

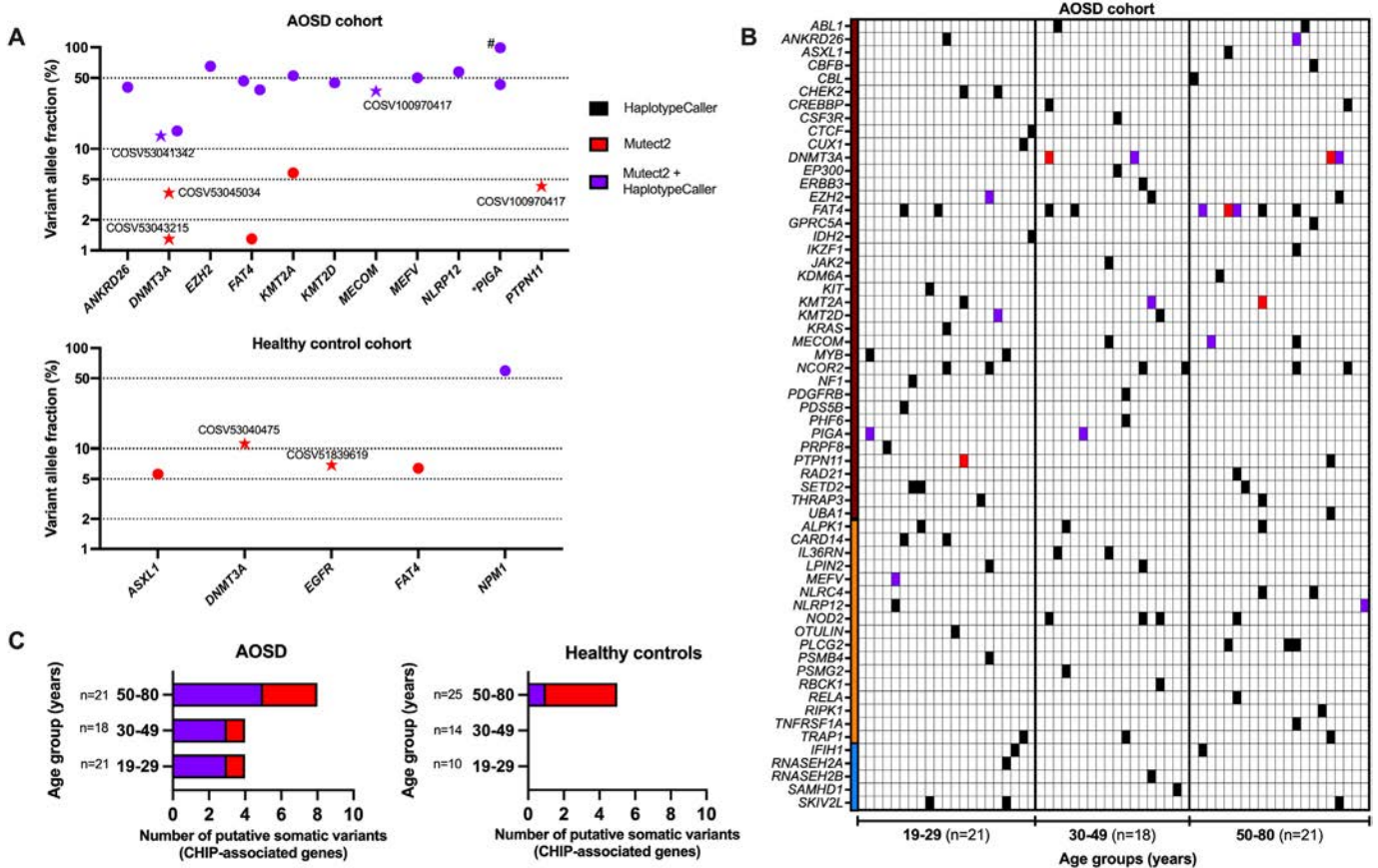


Figure 2. Somatic variant analysis in AOSD. Variants are color coded according to the variant calling tool used for identification (black: HaplotypeCaller [putative germline]; red: Mutect2 [putative somatic]; purple: found by both HaplotypeCaller and Mutect2 [uncertain origin]). (A) An overview of VAF across all putative somatic variants identified by Mutect2. Genes located on an X chromosome are highlighted *; biological males with high VAF % on these genes are annotated with #. Somatic variants previously reported in COSMIC are presented as stars annotated with their COSV numbers. (B) Mutational landscape summary of all putative somatic and germline variants identified in AOSD cases within the preselected gene panels (y-axis gene panel: CHIP = dark red; autoinflammation = orange; type I interferonopathy = blue) in age order (x-axis). (C) The distribution of putative somatic variants identified in CHIP-associated genes across each age group. AOSD, adult-onset Still disease; CHIP, clonal hematopoiesis of indeterminate potential; COSMIC, Catalog of Somatic Mutations in Cancer; COSV, genomic mutation identifier; VAF, variant allele fractions. Color figure can be viewed in the online issue, which is available at <http://onlinelibrary.wiley.com/doi/10.1002/art.43054/abstract>.

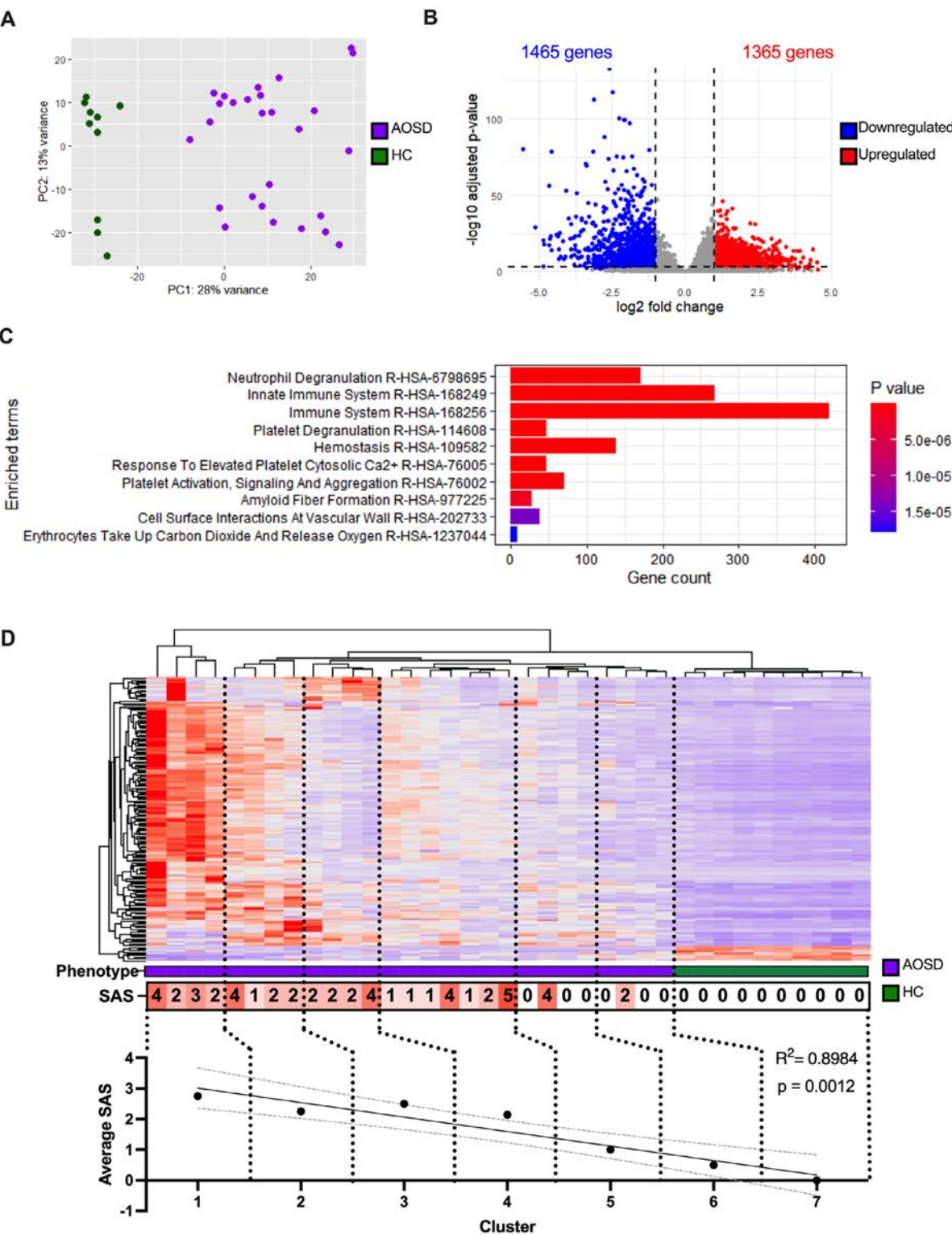


Figure 3. Transcriptome analysis of AOSD cases: (A) Principal component analysis plot illustrating the relationship between AOSD cases and HCs. (B) Volcano plot highlighting the \log_2 fold change and $-\log_{10}$ adjusted P value of 2,830 differentially expressed genes in AOSD cases. (C) Pathway enrichment analysis performed through Enrichr using terms from the Reactome pathway database, enriched pathway terms are arranged in order of P value. (D) The relative expression of 170 genes shared among the top three pathways are displayed in a heatmap. The gene expression profiles of AOSD (purple) and healthy control (green) samples are grouped into hierarchical clusters and the average SAS of each cluster was recorded. Linear regression analysis showed significant positive correlation between SAS scores and increasing gene expression. AOSD, adult-onset Still disease; HC, healthy control; SAS, Still Activity Score. Color figure can be viewed in the online issue, which is available at <http://onlinelibrary.wiley.com/doi/10.1002/art.43054/abstract>.

degranulation and the innate immune system (Figure 3C). We identified 170 genes shared between the top three ranked pathway terms, the majority of which (162 of 170 genes) had up-regulated expression in the AOSD cohort. This gene expression signature may be driven by the neutrophilia associated with active AOSD, and the variability within these pathways, observed through the heatmap, we hypothesized would reflect differences in the patient phenotype severity (Figure 3D).

To investigate this, we plotted hierarchal sample clusters of similar gene expression profile (dictated by the dendrogram) against the Still Activity Scores (SAS) of samples within each cluster (1–7). The SAS is a clinical disease activity composite score calculated using a combination of clinical presentations and laboratory findings (fever, arthralgia, neutrophilia, and ferritin levels).²¹ The highest SAS mean (2.75) was in cluster 1, which contained samples with the highest gene expression within the enriched pathways. A gradual reduction in mean SAS was observed across clusters, and linear regression analysis revealed a significant correlation ($P = 0.0012$, $R^2 = 0.898$), confirming a positive relationship between SAS and gene expression within these pathways.

We targeted these genes using our variant identification pipeline and identified an additional 87 rare germline variants across 61 of 170 genes. Only six variants were also present in the HC cohort. Enrichment analysis on the remaining 81 variants unique to AOSD identified 12 of 81 variants were significantly overrepresented across 12 of 60 (20%) AOSD cases (Supplementary Table 6).

ASC specks profiling in AOSD. The pathogenesis of AOSD has been linked to inappropriate activation of the *NLRP3* inflammasome and the release of proinflammatory cytokines.²² We have developed a novel assay to detect components of the inflammasome (the apoptosis-associated speck-like protein containing a caspase recruitment domain (ASC) and *NLRP3*, as a complex) that are released into serum following inflammasome activation and pyroptotic cell death. ASC is an adaptor protein also found in other inflammasome complexes (*NLRP1*, *NLRC4*, Pyrin, absent in melanoma 2 [AIM2], and *NLRP10*); however, because our assay detects ASC complexed with *NLRP3*, detection of these protein complexes (specks) is indicative of *NLRP3* inflammasome activation. Using this assay, we studied *NLRP3* inflammasome activation in sera from patients with AOSD and compared these data with HCs and various recognized canonical mAIDs and polygenic AIDs.

Overall, the combined AOSD cohort had significantly higher levels of ASC/*NLRP3* specks (236.5 [56.2–1,693.0] events/ μ L, median [interquartile range (IQR)]) compared with HCs ($P = 0.0001$, 48.1 [22.9–79.1] events/ μ L) and cases of familial Mediterranean fever (FMF) ($P < 0.0001$, 31.6 [15.7–73.5] events/ μ L). This was most prominent in treatment-resistant patients from cohort

AOSD#3 who also had higher ASC/*NLRP3* specks in comparison with patients with AIDs typically associated with *NLRP3* inflammasome activation, such as cryopyrin-associated periodic syndrome (CAPS) and Schnitzler syndrome (Figure 4A).

To determine if ASC/*NLRP3* specks levels might have diagnostic or prognostic value in AOSD, we compared ASC/*NLRP3* specks with C-reactive protein (CRP) levels and SAS (divided into mild [0–2, $n = 21$], moderate [3–4, $n = 35$], and severe SAS [5–7, $n = 47$]). No statistically significant correlations were identified between ASC/*NLRP3* specks and either of these variables (Figure 4B and C). Correlations between CRP and ASC specks across each condition is available in Supplementary Figure 3. We subsequently focused on patients with particularly high levels of ASC/*NLRP3* specks from the AOSD#3 cohort. These patients were treatment-resistant, predominantly diagnosed with the articular subtype of the disease, and participants in the Canakinumab for Treatment of Adult-Onset Still's Disease to Achieve Reduction of Arthritic Manifestation trial (for details, please see the Materials and Methods section). We tested samples taken before and following treatment with either canakinumab or placebo and found that ASC/*NLRP3* specks levels were significantly reduced ($P < 0.01$) following treatment with canakinumab but not placebo (Figure 4D), which suggests that this biomarker could be used to monitor treatment response to anti-IL-1 therapy.

In parallel with ASC/*NLRP3* protein specks, we measured levels of ASC (only) specks. We reasoned that this biomarker might be informative around the activation of other inflammasome complexes that use this adaptor protein. Overall, the data from ASC (only) specks closely resembled the ASC/*NLRP3* data with cases from cohort AOSD#3, having significantly greater ASC (only) specks compared with HCs and cases with other autoimmune inflammatory conditions (Supplementary Figure 4).

Interferon activity score in AOSD. Given the favorable response to JAKi observed in some patients with AOSD, we examined the role of type I IFN in disease pathogenesis using a novel assay to measure serum levels of several IFN-responsive chemokines, CCL2, CCL8, CCL19, CXCL10, and CXCL11, and combined these levels into a serological IFN score. The utility of this assay was previously demonstrated in other inflammatory diseases for which type I IFNs are thought to be important.^{23,24} Initial measurements of chemokine levels in the serum showed significantly elevated CXCL10 ($P = 0.0005$) and CXCL11 ($P < 0.0001$) levels in AOSD cases in comparison with HCs (Supplementary Figure 5). After converting raw chemokine data (CXCL10, CCL2, CCL8, CCL19, CXCL11) into a combined IFN score, we observed significantly higher type I IFN scores overall in patients with AOSD compared with HCs (4.6 [4.2–5.1] vs 4.2 [3.9–4.4], median [IQR], $P = 0.0015$) and to patients with non-type I IFN-dependent AIDs, such as FMF ($P = 0.0003$, 4.1 [3.9–4.3], median [IQR]). Within the AOSD cohort, cases from AOSD#2 had the highest type I IFN scores, which were significantly higher

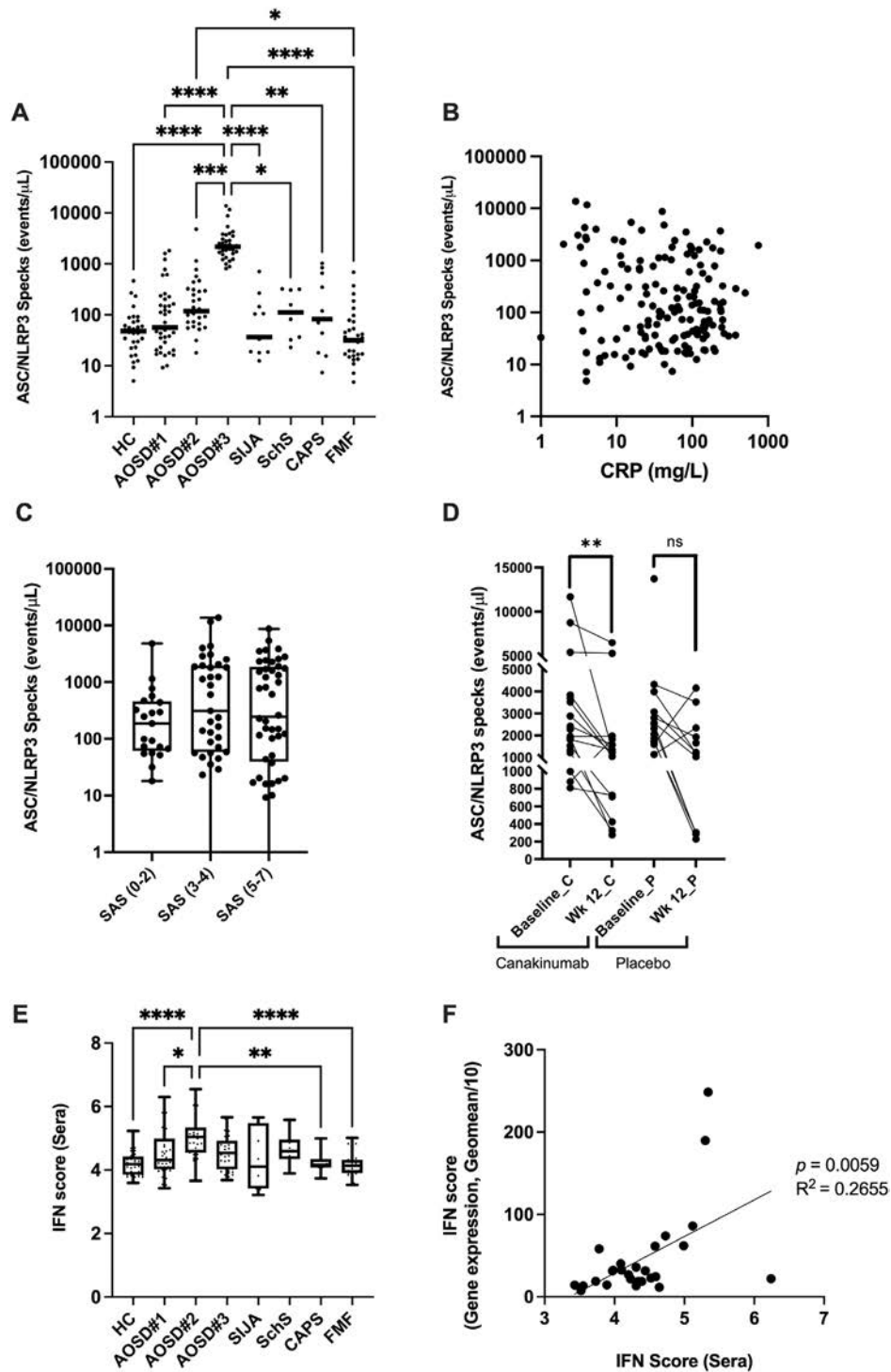


Figure 4. ASC/NLRP3 specks and IFN activity levels in AOSD and disease control cohorts: (A) ASC/NLRP3 specks in healthy controls (HC, $n = 30$) compared with AOSD cohort subsets (AOSD#1 ($n = 39$), AOSD#2 ($n = 30$) and AOSD#3 ($n = 34$), sJIA ($n = 12$), SchS ($n = 10$), CAPS ($n = 11$) and FMF ($n = 31$) cohorts. The weighted bars represent median values. (B) Scatterplot comparing ASC/NLRP3 specks to CRP (mg/L) taken from all disease cohorts. (C) ASC/NLRP3 specks comparisons within the AOSD cases, categorized by mild (0–2), moderate (3–4) and severe (5–7) Still Activity Score (SAS). (D) Change in ASC/NLRP3 specks in AOSD cases following treatment with canakinumab or placebo. (E) Boxplots comparing IFN scores (Sera) between HCs and cases from each disease cohort. (F) Comparison of IFN scores calculated from sera against IFN scores calculated from the gene expression of interferon response genes (geomeans/10), analyzed by linear regression. Statistically significant pairwise comparisons are annotated with * = $P < 0.05$; ** = $P < 0.01$; *** = $P < 0.001$; **** = $P < 0.0001$. AOSD, adult-onset Still disease; ASC, antibody-secreting cell; CAPS, cryopyrin-associated periodic syndrome; CRP, C-reactive protein; FMF, familial Mediterranean fever; HC, healthy control; IFN, interferon; SchS, Schnitzler syndrome; sJIA, systemic juvenile idiopathic arthritis.

than HCs, AOSD#1 cases, and those with CAPS and FMF (Figure 4E). We next compared our serological-based IFN score with a gene expression-based score. For each AOSD case (cohort AOSD#2), we correlated the IFN scores calculated from sera to the IFN scores calculated from whole blood gene expression (28-IFN response genes generated from RNAseq).²⁵ Linear regression analysis identified a positive correlation between both IFN score calculation methods ($P = 0.0059$, $R^2 = 0.2655$), providing validity to our novel assay (Figure 4F).

Cytokine profiling. Compared with HCs, levels of IFN- $\alpha 2$ ($P = 0.0009$), IFN- γ ($P = 0.0002$), IL-6 ($P < 0.0001$), IL-10 ($P < 0.0075$), IL-12p70 ($P = 0.0005$), IL-18 ($P < 0.0001$), and IL-23 ($P < 0.0001$) were significantly elevated in the AOSD cohort (Figure 5). IL-18 and IL-23 levels in AOSD cases were significantly elevated compared with patients with CAPS ($P = 0.0276$ and

0.0283, respectively). Interestingly, patients with AOSD (9,013 [886–18,209] pg/mL) and sJIA (15,000 [1,819–18,826] pg/mL) had similarly elevated levels of IL-18 levels, in keeping with previously published data and the recent recognition that these disorders represent the same condition, presenting at different ages.²⁶ The significantly elevated IFN- $\alpha 2$ levels observed in patients with AOSD, in combination with the elevated IFN activity scores previously described, suggest that type I IFN drive might be important in disease pathogenesis for at least some patients with AOSD.

Correlation between rare genetic variants and markers of inflammation. To investigate any additive proinflammatory effect from multiple rare variants, we examined the relationship between variant count on *ASC/NLRP3* specks and selected cytokine levels (IL-1 β , IL-6, and IL-18). A modest

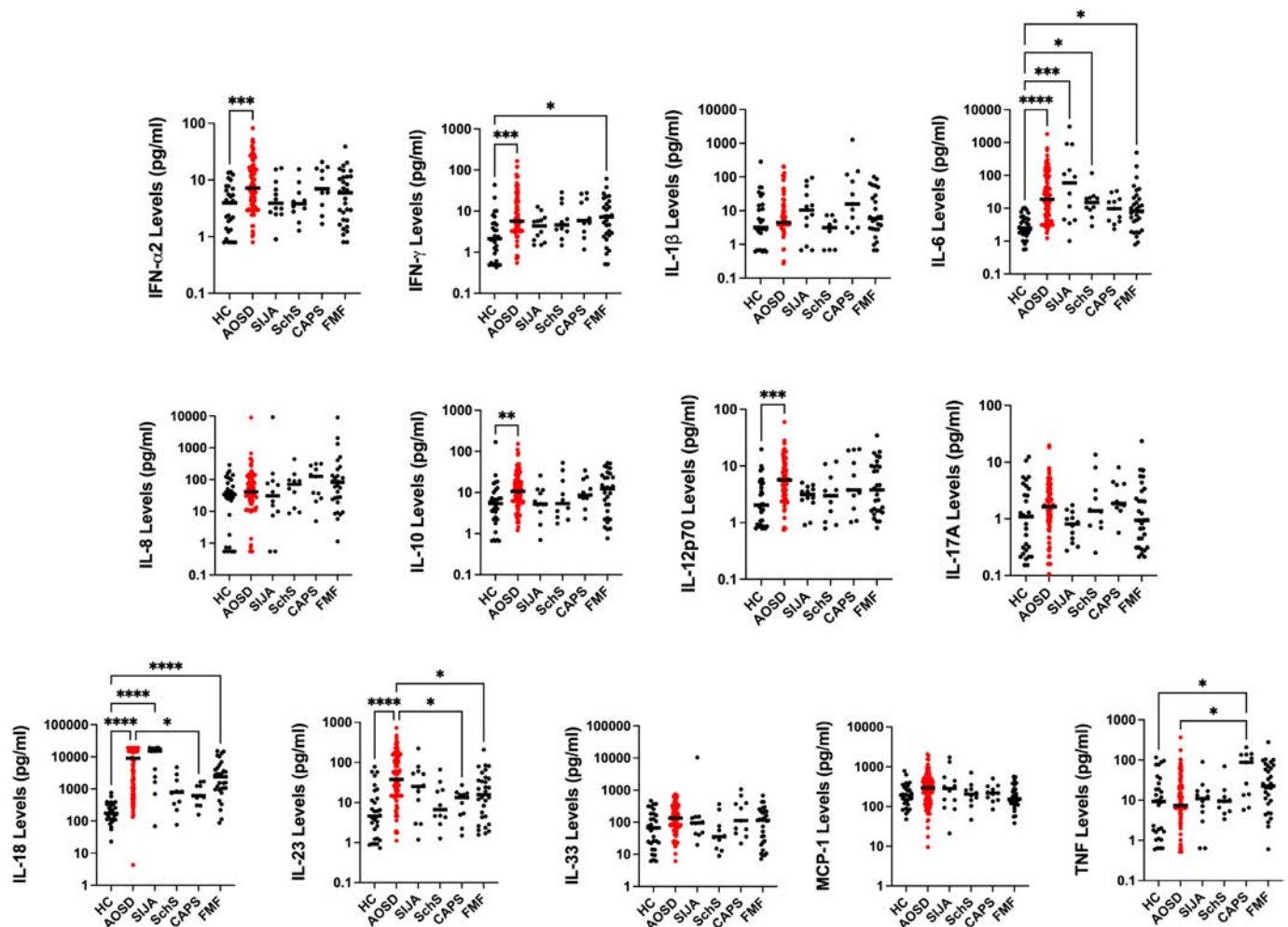


Figure 5. Cytokine profile in patients with AOSD, disease, and healthy controls: The serum cytokine levels for 13 targets are displayed on dot plots, comparing healthy controls to AOSD, sJIA, SchS, CAPS, and FMF cases. AOSD cases are highlighted in red, weighted bars represent median values, and statistically significant pairwise comparisons are annotated with asterisks. * = $P < 0.05$; ** = $P < 0.01$; *** = $P < 0.001$; **** = $P < 0.0001$. AOSD, adult-onset Still disease; CAPS, cryopyrin-associated periodic syndrome; FMF, familial Mediterranean fever; HC, healthy control; IFN, type I interferon; IL, interleukin; SchS, Schnitzler syndrome; sJIA, systemic juvenile idiopathic arthritis. Color figure can be viewed in the online issue, which is available at <http://onlinelibrary.wiley.com/doi/10.1002/art.43054/abstract>.

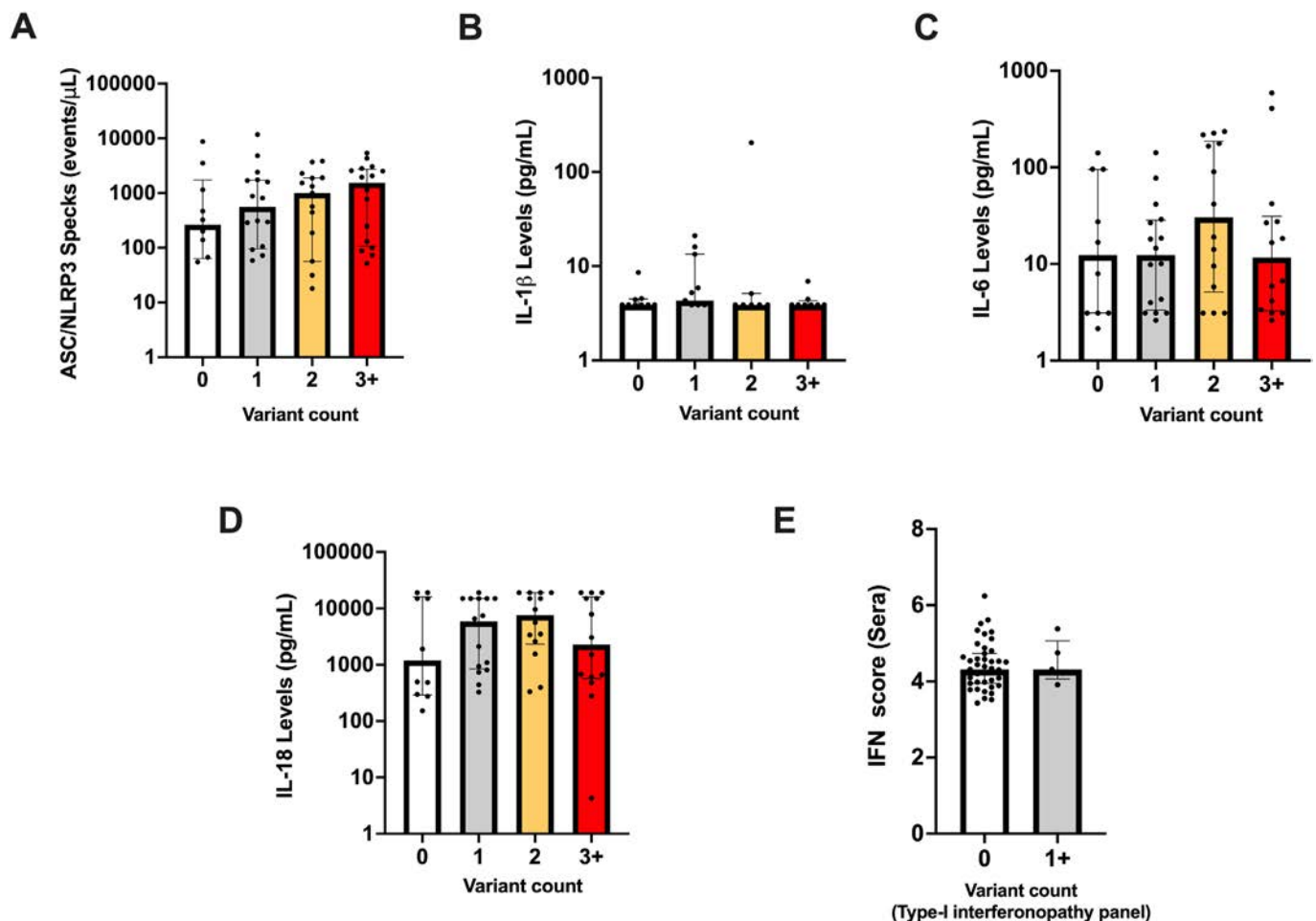


Figure 6. Correlation between rare genetic variant counts against biomarker levels: Bar charts (median, IQR) illustrating (A) ASC/NLRP3 specks; (B) IL-1 β ; (C) IL-6; and (D) IL-18 levels (pg/mL) in AOSD cases carrying 0, 1, 2, and 3+ variants (germline and/or putative somatic) within our pre-selected gene panels. (E) IFN scores in AOSD cases with and without a variant in the type I interferonopathy gene panel. AOSD, adult-onset Still disease; ASC, antibody-secreting cell; IFN, interferon; IL, interleukin; IQR, interquartile range. Color figure can be viewed in the online issue, which is available at <http://onlinelibrary.wiley.com/doi/10.1002/art.43054/abstract>.

increase in ASC/NLRP3 specks was observed with increasing variant count, but these differences were not statistically significant (Figure 6A). This might be due to a combination of insufficient sample size (mutation-negative AOSD cases) and high data variability. We further stratified this analysis for genes associated with CHIP and autoinflammation separately; once again, no significant differences were found. All the above comparisons analyses were repeated for ASC (only) specks, which produced similar results (Supplementary Figure 4). Cytokines IL-1 β , IL-6, and IL-18 levels were unaffected with increasing variant count (Figure 6B–D). We also compared type I IFN scores from AOSD cases with and without rare variants in the type I interferonopathy gene panel and found no significant IFN score increase in the mutated subset (Figure 6E).

DISCUSSION

Despite significant progress in the field of AIDs, the pathogenesis of AOSD remains largely undefined. This is a rare disease,

with clinical features overlapping with many other conditions, so it can be challenging to study. Nevertheless, there are important clues to its etiology. It is clinically similar to several mAIDs and responds to biologic therapies that target prototypic cytokines (IL-1 and IL-6) associated with innate immune system driven inflammation. These observations underpin our focus on genetic variants implicated in mAIDs and CHIP, both linked with heightened IL-1 and IL-6 levels.^{11,27–29}

Our analyses suggest a genetic correlation between AOSD and the presence of rare variants within genes associated with mAIDs and CHIP. Previous studies investigating genetic overlap between mAIDs in AOSD were limited to relatively few candidate genes, mainly those associated with hereditary fever syndromes with clinical features shared with AOSD such as TRAPS, FMF, CAPS, and mevalonate kinase deficiency.⁴ However, because some newly discovered mAIDs, such as A20 haploinsufficiency, have broad clinical manifestations, including features of sJIA and AOSD,^{30,31} we expanded our analysis to incorporate most known

mAIDs, which is currently more than 50 conditions. Furthermore, we analyzed the contribution of somatic mutations in the same genes, in recognition that such biologic mechanisms are responsible for pathogenesis of late-onset AIDs. Overall, we found that a majority of AOSD cases (51.7%) carried multiple rare germline variants in different genes of interest. Fifteen variants were found to be significantly enriched within our AOSD cohort. Putative somatic variants were also identified in 30% of AOSD cases, adding further genetic complexity.

In the autoinflammatory panel, we identified rare variants previously linked with AOSD, such as *MEFV* c.184G>T, P.(G62W)³²; however, the overall number of variants in this gene was far smaller than previously reported.⁴ We also identified several known pathogenic variants in other genes, with *TNFRSF1A* c.242G>T, P.(C81Y) being the most compelling. To date, all amino acid changes from the cysteine-81 residue have been designated as pathogenic, confirming the critical importance of cysteine at this position (Infervers). Our patient with the P.(C81Y) substitution apparently had late-onset disease presentation with symptoms at the age of 62 years. Although most patients with TRAPS develop symptoms in childhood, adult presentation has been reported.¹⁹ This is not the first time that an initial diagnosis of AOSD has later been attributed to TRAPS. A report of 20 patients with AOSD, which also identified one patient with the p.C81Y variant, suggests that prevalence of undiagnosed TRAPS might be up to 5% in unselected AOSD cohorts.³²

Other genetic variants of note include *NLRC4* c.2357G>T, P.(G786V), which was identified in two separate AOSD cases. Although not obviously disease-causing, this variant is enriched in cohorts of patients with periodic fever, aphthous stomatitis, pharyngitis, and adenitis³³ (another polygenic AID), suggesting that certain variants might contribute to several related inflammatory diseases. When examining the occurrence of somatic variants in our autoinflammatory panel, we did not find any variants in *NLRP3* or *NLRC4*, the two genes for which low-level somatic mutations have been previously described in late-onset AIDs.^{7,8,34}

Recent epidemiologic studies have linked CHIP with a broad range of chronic inflammatory diseases, including atherosclerosis, gout, and systemic sclerosis.^{35–37} To our knowledge, the prevalence of rare variants in CHIP-associated genes in patients with AOSD has not been studied. We identified several putative somatic variants within our CHIP panel, present at a greater frequency in younger AOSD age groups than expected. This observation suggests that CHIP mutations may play a role in disease pathogenesis, irrespective of age at onset. Four somatic variants were identified in *DNMT3A* (P.(G534V), P.(P700A), P.(D529N), and P.(R320*)). *DNMT3A* is frequently mutated in CHIP and has the most evidence linking to systemic inflammation.^{27,29} Unlike somatic variants, the effects of germline mutation in CHIP-associated loci are unknown, but some investigations have reported germline influence in CHIP occurrence and

progression.^{38,39} We identified 13 rare germline variants in CHIP-associated genes that were significantly enriched in our AOSD cohort, which suggests that these variants may genetically predispose individuals to disease. Further research is required to fully elucidate their impact.

With regards to germline variants, *FAT4* was the most frequently mutated gene within our preselected gene panel and is also associated with several cancers.^{40–42} *FAT4* encodes for FAT atypical cadherins 4, a membrane protein containing cadherin repeat sequences. *FAT4* mutations associated with malignancy are mainly attributed to somatic variants, whereas germline *FAT4* variants have only been associated with Hennekam syndrome and van Maldergem syndrome,^{43,44} with their contributions to autoinflammatory phenotypes unknown.

A challenge we faced in our genetic analysis was the categorization of germline and somatic variants. The recently discovered importance of somatic variants in AIDs often means that retrospective patient cohorts lack matched “normal” specimens for somatic variant analysis. We tried to overcome this problem by running Mutect2 in tumor-only mode against an in-house panel of normal created from a HC cohort; this allowed us to filter common germline variants from the population. This method is widely used but does not achieve the same sensitivity on a per-case basis with a matched normal sample. This was most problematic when somatic variants were identified with high variant allele fractions resembling a variant of germline origin. We attempted to use evidence from previous reports to raise putative somatic variants in cases of AOSD, but additional validation is required to confirm their association.

Transcriptomic analysis revealed dysregulation of gene expression in pathways associated with neutrophil activity and the innate immune system. Interestingly, elevated gene expression within these pathways was positively correlated with the SAS score, providing validity to its use as a potential biomarker for disease prognosis. Recently, whole blood transcriptomes from a similar data set were used to aid diagnosis in childhood febrile illness, which suggests both the utility and clinical applicability of this approach.⁴⁵

We performed extensive inflammatory biomarker profiling of patients with AOSD and focused on the *NLRP3* inflammasome and linking genomic data with this profile. We reasoned that the cumulative proinflammatory effect of numerous rare variants might correlate with selected biomarkers, serving as surrogate functional validation of genomic findings. We used a novel assay to show that *NLRP3* inflammasome is highly activated in AOSD, particularly in patients with resistant and articular-predominant disease. We also demonstrated that reduced levels of ASC/*NLRP3* specks correlates with treatment response in selected patients.

Previous studies demonstrated that serum ASC protein specks are a useful biomarker of inflammasome activation, in some circumstances predicting treatment response.^{46–48}

However, these assays are unable to determine the origin of ASC specks, which is a significant limitation given that this adaptor protein is involved in activation of several inflammasome complexes. We have demonstrated the different distribution of ASC/*NLRP3* and ASC (only) specks in patients with AOSD, suggesting that additional non-*NLRP3*-inflammasomes may be relevant for disease pathogenesis. We produced similar findings when we used this assay to interrogate the role of *NLRP3* inflammasome in lower-risk MDS.⁴⁹

The interplay between inflammasomes and their varying roles in pathogenesis of mAIDs has been demonstrated previously.⁵⁰ Different ASC-containing inflammasomes have also been shown to have a role in the proinflammatory character of monocytes with certain CHIP-related mutations. For example, murine monocytes with a truncating *ASXL1* mutation have increased AIM2 inflammasome activation and IL-1 β production, with inflammasome activation triggered by accumulated DNA damage.⁵¹ Our assay requires further refining to elucidate if there is contribution of different inflammasome complexes in AOSD pathogenesis or if the discrepancy between ASC (only) and ASC/*NLRP3* specks reflects the natural dissociation of the *NLRP3* component from the complexes.

We confirmed previous observations that IL-18 is significantly elevated in AOSD compared with both HCs and other AIDs. IL-18 levels might therefore be a useful diagnostic marker and contribute to a future validated and combined biochemical and clinical scoring system.^{52–54} The AOSD cohort had several other significantly elevated cytokines, most notably IL-6 (confirming its role in AOSD pathogenesis) and IFN- α 2. Together with the observation that type I IFN scores were significantly elevated in patients with AOSD compared with HCs and disease controls, the raised IFN- α 2 levels suggest that the type I IFN pathway is relevant to disease pathogenesis. This justifies the use of, particularly in treatment-resistant cases.

When we tested for correlation between various markers of inflammation and the burden of rare genetic variants in the autoinflammatory and/or CHIP gene panels, we found that the median level of ASC/*NLRP3* specks increased in patients with increasing variant count. However, this was not statistically significant, and overall, we were unable to find correlation with other inflammatory biomarkers tested. The lack of statistical significance may be due to limitations in sample size; nevertheless, this is of interest because ASC/*NLRP3* specks might be an important treatment target. Neutralization of the serum ASC/*NLRP3* specks using nanobodies has been shown to be an effective treatment strategy in several murine models of inflammatory diseases.⁵⁵

The breadth of genes affected in this cohort demonstrates considerable genetic complexity within AOSD, likely influenced by the interplay of multiple genetic components. Many enriched variants were assessed by ClinVar to be of “uncertain significance” and “conflicting interpretations of pathogenicity,” suggesting they are individually insufficient for pathogenesis,

supporting a multiple-hit model. One way in which somatic mutations can collectively lead to clinical disease was demonstrated in a case of acquired *NLRP4*-related AID, in which the concurrent *TET2* mutation allowed expansion of the hematopoietic stem cell clone carrying the *NLRP4* mutation, giving rise to the disease.⁵⁶

Future multi-omics approaches to AOSD research will help to untangle its complex pathogenesis. Although considered a distinct diagnosis, it is better seen as an umbrella term, covering overlapping pathotypes with distinct pathogenesis but common clinical manifestations. Recent work suggested patients might be subdivided into four subtypes, depending on clinical features and inflammatory biomarkers, each with different genetic backgrounds and pathologic mechanisms.⁵⁷ This detailed clinical phenotyping, combined with future OMICs studies, will facilitate improved mapping of the biologic processes underpinning AOSD and identify additional treatment targets.

AUTHOR CONTRIBUTIONS

All authors contributed to at least one of the following manuscript preparation roles: conceptualization AND/OR methodology, software, investigation, formal analysis, data curation, visualization, and validation AND drafting or reviewing/editing the final draft. As corresponding author, Dr Savic confirms that all authors have provided the final approval of the version to be published, and takes responsibility for the affirmations regarding article submission (eg, not under consideration by another journal), the integrity of the data presented, and the statements regarding compliance with institutional review board/Declaration of Helsinki requirements.






REFERENCES

- Giacomelli R, Ruscitti P, Shoenfeld Y. A comprehensive review on adult onset Still's disease. *J Autoimmun* 2018;93:24–36.
- Yamaguchi M, Ohta A, Tsunematsu T, et al. Preliminary criteria for classification of adult Still's disease. *J Rheumatol* 1992;19(3):424–430.
- Mitrovic S, Fautrel B. Clinical phenotypes of Adult-onset Still's Disease: new insights from pathophysiology and literature findings. *J Clin Med* 2021;10(12):2633.
- Li H, Abramova I, Chesoni S, et al. Molecular genetic analysis for periodic fever syndromes: a supplemental role for the diagnosis of adult-onset Still's disease. *Clin Rheumatol* 2018;37(8):2021–2026.
- Colafrancesco S, Priori R, Valesini G, et al. Response to Interleukin-1 inhibitors in 140 Italian patients with adult-onset Still's disease: a multi-centre retrospective observational study. *Front Pharmacol* 2017;8:369.
- Ortiz-Sanjuán F, Blanco R, Calvo-Rio V, et al. Efficacy of tocilizumab in conventional treatment-refractory adult-onset Still's disease: multi-center retrospective open-label study of thirty-four patients. *Arthritis Rheumatol* 2014;66(6):1659–1665.
- Rowczenio DM, Gomes SM, Aróstegui JI, et al. Late-onset cryopyrin-associated periodic syndromes caused by somatic *NLRP3* Mosaicism-UK single center experience. *Front Immunol* 2017;8:1410.
- Wang J, Ye Q, Zheng W, et al. Low-ratio somatic *NLRP4* mutation causes late-onset autoinflammatory disease. *Ann Rheum Dis* 2022;81(8):1173–1178.

9. Beck DB, Ferrada MA, Sikora KA, et al. Somatic mutations in *UBA1* and severe adult-onset autoinflammatory disease. *N Engl J Med* 2020;383(27):2628–2638.
10. Watad A, Kacar M, Bragazzi NL, et al. Somatic mutations and the risk of undifferentiated autoinflammatory disease in MDS: an under-recognized but prognostically important complication. *Front Immunol* 2021;12:610019.
11. Sano S, Oshima K, Wang Y, et al. Tet2-mediated clonal hematopoiesis accelerates heart failure through a mechanism involving the IL-1 β /*NLRP3* inflammasome. *J Am Coll Cardiol* 2018;71(8):875–886.
12. Di Cola I, Di Muzio C, Conforti A, et al. Adult-onset Still's disease with elderly onset: results from a multicentre study. *Clin Exp Rheumatol* 2022;40(8):1517–1525.
13. Hu Q, Wang M, Jia J, et al. Tofacitinib in refractory adult-onset Still's disease: 14 cases from a single centre in China. *Ann Rheum Dis* 2020;79(6):842–844.
14. Di Cola I, Ruscitti P, Giacomelli R, et al. The pathogenic role of interferons in the hyperinflammatory response on adult-onset Still's disease and Macrophage Activation Syndrome: paving the way towards new therapeutic targets. *J Clin Med* 2021;10(6):1164.
15. Ma Y, Wang M, Jia J, et al. Enhanced type I interferon signature induces neutrophil extracellular traps enriched in mitochondrial DNA in adult-onset Still's disease. *J Autoimmun* 2022;127:102793.
16. Li Y, Führer M, Bahrami E, et al. Human RIPK1 deficiency causes combined immunodeficiency and inflammatory bowel diseases. *Proc Natl Acad Sci USA* 2019;116(3):970–975.
17. Lalaoui N, Boyden SE, Oda H, et al. Mutations that prevent caspase cleavage of RIPK1 cause autoinflammatory disease. *Nature* 2020;577(7788):103–108.
18. McDermott MF, Aksentijevich I, Galon J, et al. Germline mutations in the extracellular domains of the 55 kDa TNF receptor, TNFR1, define a family of dominantly inherited autoinflammatory syndromes. *Cell* 1999;97(1):133–144.
19. Lachmann HJ, Papa R, Gerhold K, et al; Paediatric Rheumatology International Trials Organisation (PRINTO), the EUROTRAPS and the Eurofever Project. The phenotype of TNF receptor-associated autoinflammatory syndrome (TRAPS) at presentation: a series of 158 cases from the Eurofever/EUROTRAPS international registry. *Ann Rheum Dis* 2014;73(12):2160–2167.
20. Jaiswal S, Fontanillas P, Flannick J, et al. Age-related clonal hematopoiesis associated with adverse outcomes. *N Engl J Med* 2014;371(26):2488–2498.
21. Kalyoncu U, Kasifoglu T, Omma A, et al. Derivation and validation of adult Still Activity Score (SAS). *Joint Bone Spine* 2023;90(1):105499.
22. Hsieh CW, Chen YM, Lin CC, et al. Elevated expression of the *NLRP3* inflammasome and its correlation with disease activity in adult-onset Still disease. *J Rheumatol* 2017;44(8):1142–1150.
23. Saleem B, Ross RL, Bissell LA, et al. Effectiveness of SARS-CoV-2 vaccination in patients with rheumatoid arthritis (RA) on DMARDs: as determined by antibody and T cell responses. *RMD Open* 2022;8(1):e002050.
24. Di Donato S, Hughes M, Geloshi K, et al. Evidence of Type I interferon activation during vascular manifestations of systemic sclerosis. *Rheumatology (Oxford)* 2023;62(suppl 2):kead104.197.
25. Kim H, de Jesus AA, Brooks SR, et al. Development of a validated interferon score using NanoString technology. *J Interferon Cytokine Res* 2018;38(4):171–185.
26. Nirmala N, Brachat A, Feist E, et al. Gene-expression analysis of adult-onset Still's disease and systemic juvenile idiopathic arthritis is consistent with a continuum of a single disease entity. *Pediatr Rheumatol Online J* 2015;13(1):50.
27. Abplanalp WT, Cremer S, John D, et al. Clonal hematopoiesis-driver DNMT3A mutations alter immune cells in heart failure. *Circ Res* 2021;128(2):216–228.
28. Svensson EC, Madar A, Campbell CD, et al. TET2-driven clonal hematopoiesis and response to canakinumab: an exploratory analysis of the CANTOS randomized clinical trial. *JAMA Cardiol* 2022;7(5):521–528.
29. Fuster JJ, MacLauchlan S, Zuriaga MA, et al. Clonal hematopoiesis associated with TET2 deficiency accelerates atherosclerosis development in mice. *Science* 2017;355(6327):842–847.
30. Lawless D, Pathak S, Scambler TE, Ouboussad L, Anwar R, Savic S. A case of adult-onset Still's disease caused by a novel splicing mutation in *TNFAIP3* successfully treated with tocilizumab. *Front Immunol* 2018;9:1527.
31. Kadowaki S, Hashimoto K, Nishimura T, et al. Functional analysis of novel A20 variants in patients with atypical inflammatory diseases. *Arthritis Res Ther* 2021;23(1):52.
32. Sighart R, Rech J, Hueber A, et al. Evidence for genetic overlap between adult onset Still's disease and hereditary periodic fever syndromes. *Rheumatol Int* 2018;38(1):111–120.
33. Di Gioia SA, Bedoni N, von Scheven-Gête A, et al. Analysis of the genetic basis of periodic fever with aphthous stomatitis, pharyngitis, and cervical adenitis (PFAPA) syndrome. *Sci Rep* 2015;5(1):10200.
34. Ionescu D, Peñín-Franch A, Mensa-Vilaró A, et al. First description of late-onset autoinflammatory disease due to somatic *NLR4* mosaicism. *Arthritis Rheumatol* 2022;74(4):692–699.
35. Hecker JS, Hartmann L, Rivière J, et al. CHIP and hips: clonal hematopoiesis is common in patients undergoing hip arthroplasty and is associated with autoimmune disease. *Blood* 2021;138(18):1727–1732.
36. Belizaire R, Wong WJ, Robinette ML, Ebert BL. Clonal haematopoiesis and dysregulation of the immune system. *Nat Rev Immunol* 2023;23(9):595–610.
37. Ricard L, Hirsch P, Largeaud L, et al; on behalf MINHEMON (French Network of dysimmune disorders associated with hemopathies). Clonal haematopoiesis is increased in early onset in systemic sclerosis. *Rheumatology (Oxford)* 2020;59(11):3499–3504.
38. Bick AG, Weinstock JS, Nandakumar SK, et al; NHLBI Trans-Omics for Precision Medicine Consortium. Inherited causes of clonal haematopoiesis in 97,691 whole genomes. *Nature* 2020;586(7831):763–768.
39. Bick AG, Pirruccello JP, Griffin GK, et al. Genetic Interleukin 6 signaling deficiency attenuates cardiovascular risk in clonal hematopoiesis. *Circulation* 2020;141(2):124–131.
40. Furukawa T, Sakamoto H, Takeuchi S, et al. Whole exome sequencing reveals recurrent mutations in *BRCA2* and *FAT* genes in acinar cell carcinomas of the pancreas. *Sci Rep* 2015;5(1):8829.
41. Zang ZJ, Cutcutache I, Poon SL, et al. Exome sequencing of gastric adenocarcinoma identifies recurrent somatic mutations in cell adhesion and chromatin remodeling genes. *Nat Genet* 2012;44(5):570–574.
42. Herrera-Pariente C, Capó-García R, Díaz-Gay M, et al. Identification of new genes involved in germline predisposition to early-onset gastric cancer. *Int J Mol Sci* 2021;22(3):1310.
43. Cappello S, Gray MJ, Badouel C, et al. Mutations in genes encoding the cadherin receptor-ligand pair *DCHS1* and *FAT4* disrupt cerebral cortical development. *Nat Genet* 2013;45(11):1300–1308.
44. Alders M, Al-Gazali L, Cordeiro I, et al. Hennekam syndrome can be caused by *FAT4* mutations and be allelic to Van Maldergem syndrome. *Hum Genet* 2014;133(9):1161–1167.
45. Habgood-Coote D, Wilson C, Shimizu C, et al; Pediatric Emergency Medicine Kawasaki Disease Research Group (PEMKDRG); UK Kawasaki Genetics consortium; GENDRES consortium; EUCLIDS

- consortium; PERFORM consortium. Diagnosis of childhood febrile illness using a multiclass blood RNA molecular signature. *Med (N Y)* 2023;4(9):635–654.e5.
46. Rowczenio DM, Pathak S, Arostegui JI, et al. Molecular genetic investigation, clinical features, and response to treatment in 21 patients with Schnitzler syndrome. *Blood* 2018;131(9):974–981.
47. Scambler T, Jarosz-Griffiths HH, Lara-Reyna S, et al. ENaC-mediated sodium influx exacerbates *NLRP3*-dependent inflammation in cystic fibrosis. *eLife* 2019;8:e49248.
48. Basiorka AA, McGraw KL, Abbas-Aghababazadeh F, et al. Assessment of ASC specks as a putative biomarker of pyroptosis in myelodysplastic syndromes: an observational cohort study. *Lancet Haematol* 2018;5(9):e393–e402.
49. Topping J, Taylor A, Nadat F, et al; ImmunAID consortium and EU-MDS consortium. Inflammatory profile of lower risk myelodysplastic syndromes. *Br J Haematol* 2024;205(3):1044–1054.
50. Omenetti A, Carta S, Delfino L, et al. Increased *NLRP3*-dependent interleukin 1 β secretion in patients with familial Mediterranean fever: correlation with MEFV genotype. *Ann Rheum Dis* 2014;73(2):462–469.
51. Yu Z, Fidler TP, Ruan Y, et al. Genetic modification of inflammation- and clonal hematopoiesis-associated cardiovascular risk. *J Clin Invest* 2023;133(18):e168597.
52. Chen PK, Wey SJ, Chen DY. Interleukin-18: a biomarker with therapeutic potential in adult-onset Still's disease. *Expert Rev Clin Immunol* 2022;18(8):823–833.
53. Tang KT, Hsieh CW, Chen HH, et al. The effectiveness of tocilizumab in treating refractory adult-onset Still's disease with dichotomous phenotypes: IL-18 is a potential predictor of therapeutic response. *Clin Rheumatol* 2022;41(2):557–566.
54. Shiga T, Nozaki Y, Tomita D, et al. Usefulness of Interleukin-18 as a diagnostic biomarker to differentiate adult-onset Still's disease with/without macrophage activation syndrome from other secondary hemophagocytic lymphohistiocytosis in adults. *Front Immunol* 2021;12:750114.
55. Bertheloot D, Wanderley CW, Schneider AH, et al. Nanobodies dismantle post-pyrototic ASC specks and counteract inflammation in vivo. *EMBO Mol Med* 2022;14(6):e15415.
56. De Langhe E, Van Loo S, Malengier-Devlies B, et al. *TET2*-driver and *NLRC4*-passenger variants in adult-onset autoinflammation. *N Engl J Med* 2023;388(17):1626–1629.
57. Berardicurti O, Conforti A, Iacono D, et al. Dissecting the clinical heterogeneity of adult-onset Still's disease: results from a multidimensional characterization and stratification. *Rheumatology (Oxford)* 2021;60(10):4844–4849.

Clinical, Immunologic, and Genetic Characteristics in Patients With Syndrome of Undifferentiated Recurrent Fevers

Marci Macaraeg,¹  Elizabeth Baker,¹ Elizabeth Handorf,¹ Michael Matt,¹ Elizabeth K. Baker,¹ Hermine Brunner,²  Alexei A. Grom,² Michael Henrickson,²  Jennifer Huggins,² Wenying Zhang,² Pui Lee,³  Rebecca Marsh,² and Grant S. Schulert² 

Objective. Syndrome of undifferentiated recurrent fevers (SURF) is characterized by recurrent fevers and autoinflammation without a confirmed molecular diagnosis of a hereditary recurrent fever syndrome, and not fulfilling criteria for periodic fever, adenitis, pharyngitis, aphthous stomatitis syndrome (PFAPA). The goal of this study was to characterize clinical features of patients with SURF compared to patients with PFAPA and to analyze their cytokine signature, genetic variations, and responses to treatment.

Methods. We enrolled 46 patients observed at Cincinnati Children's Hospital Medical Center. Baseline data and inflammatory cytokines were collected at enrollment, and their clinical course was followed. Cytokine analysis was performed using a cytokine multiplex assay. Many patients had specific or whole exome genetic testing.

Results. The prevalence of rash and arthralgias were higher in patients with SURF compared to patients with PFAPA. Pharyngitis and adenopathy were less frequent. A subset of patients with SURF clustered together with elevated proinflammatory cytokines and more frequently required biologic therapy. Focused analysis of whole exome sequencing data revealed that variants of unknown clinical significance (VUCS) were frequently identified in genes implicated in B cell development, immunodeficiencies, and inflammatory bowel disease risk. Treatments for patients with SURF commonly included on-demand steroids, colchicine, and anti-interleukin-1 therapy.

Conclusion. Our findings suggest SURF is a heterogeneous group but has distinct clinical and immunologic features from disorders such as PFAPA. Patients have frequent VUCS, which may have relevance to disease pathogenesis. A subset of patients showed more inflammation and an increased need for biologic therapy. Further research is necessary to define whether there exist distinct SURF endotypes and to better predict treatment outcomes.

INTRODUCTION

Unexplained, recurrent fevers are a common presentation to pediatric rheumatology and cause significant burden to affected families because of days of daycare or school missed for the child and days of work missed for the parent. Recurrent fevers are often associated with signs of autoinflammation.¹

Over the past two decades, many monogenic hereditary recurrent fever syndromes (HRFs) have been identified, and

more syndromes continue to be defined. HRFs are characterized by recurrent fevers, which are associated with an exaggerated inflammatory response in the absence of high titers of autoantibodies or antigen-specific T cells, that are caused by a specific genetic pathogenic variant.^{2,3} The most common syndromes are driven by interleukin-1 (IL-1) or type I interferon.^{4,5} The HRFs in general tend to be more severe disease entities than sporadic or nonmonogenic periodic fever syndromes.

Supported by an Academic Research and Clinical award from the Cincinnati Children's Research Foundation, the Jellin Family Foundation, and the Pediatric Rheumatology Tissue Repository, a component of the Cincinnati Rheumatic Diseases Resource Center (grant P30-AR-070549).

¹Marci Macaraeg, MD, Elizabeth Baker, Elizabeth Handorf, BA, Michael Matt, MD, Elizabeth K. Baker, MD (current address: Atrium Health's Levine Children's Hospital, Charlotte, North Carolina); Cincinnati Children's Hospital Medical Center, Cincinnati, Ohio; ²Hermine Brunner, MD, Alexei A. Grom, MD, Michael Henrickson, MD, MPH, Jennifer Huggins, MD, Wenying Zhang, PhD, Rebecca Marsh, MD, Grant S. Schulert, MD, PhD: University of Cincinnati and Cincinnati Children's Hospital Medical Center, Cincinnati, Ohio, ³Pui Lee,

MD, PhD: Boston Children's Hospital and Harvard Medical School, Boston, Massachusetts.

Additional supplementary information cited in this article can be found online in the Supporting Information section (<https://acrjournals.onlinelibrary.wiley.com/doi/10.1002/art.43065>).

Author disclosures are available at <https://onlinelibrary.wiley.com/doi/10.1002/art.43065>.

Address correspondence via email to Grant S. Schulert, MD, PhD, at Grant.schulert@cchmc.org.

Submitted for publication January 22, 2024; accepted in revised form October 17, 2024.

The most common diagnosis for recurrent fevers and autoinflammation in rheumatology is periodic fever, adenitis, pharyngitis, aphthous stomatitis syndrome (PFAPA), which has significant elevation in proinflammatory cytokines during flares without a known monogenetic cause but has been found to be associated with genetic susceptibility loci in genes implicated in Behçet disease.^{6–8} There are no universally accepted classification criteria for PFAPA, but the criteria most used for diagnosis and study are the modified Marshall criteria.⁹ These criteria state that a patient must begin having regularly recurring fevers before the age of five years old; have the absence of upper respiratory infection symptoms; and have at least one of aphthous stomatitis, cervical lymphadenitis, or pharyngitis present with the febrile episodes. Additionally, cyclic neutropenia must be excluded, the patient must have completely asymptomatic periods between febrile episodes, and they must have normal growth and development.¹⁰ In 2019, Gattorno et al² used the EuroFever registry to develop and validate evidence-based classification criteria for PFAPA and HRFs. This EuroFever/Paediatric Rheumatology International Trials Organisation (PRINTO) PFAPA criteria requires seven of the following eight symptoms: presence of pharyngotonsillitis, duration of episodes three to six days, cervical lymphadenitis, and periodicity of fevers and absence of diarrhea, chest pain, skin rash, and arthritis. This criterion was found to be more accurate than the modified Marshall criteria, having a sensitivity of 97%, a specificity of 93%, and 99% accuracy.²

Historically, patients with recurrent fevers whose genetic testing was not consistent with an HRF and who did not meet criteria for PFAPA were often diagnosed with and treated for atypical PFAPA.¹ However, there is growing recognition that such patients are a distinct clinical entity, which has been termed syndrome of undefined recurrent fevers (SURF). SURF represents a disorder characterized by recurrent fever episodes and systemic autoinflammation that are self-limited but without confirmed molecular diagnosis and that do not fulfill criteria for PFAPA.¹¹ A prospective study looking at peripheral and tonsillar immune signals in patients with SURF and PFAPA showed that the immune signature of each was different enough to suggest that SURF and PFAPA were clinically distinct entities.¹² Despite this, little is known regarding the clinical, immunologic, and genetic diversity of patients with SURF, and there is no consensus on best treatment practices. The aim of this study is to better characterize patients with SURF by performing a prospective cohort study on patients with PFAPA and patients with SURF using the Cincinnati Children's Hospital Medical Center (CCHMC) Pediatric Autoinflammatory Disease Registry.

MATERIALS AND METHODS

Patients and study participants. This study was approved by the Institutional Review Board of CCHMC, and written informed consent was obtained from all patients and/or their

legal guardians. Consecutive patients presenting with symptoms consistent with autoinflammatory disease were enrolled into the pediatric autoinflammatory disease registry from the years 2018 to 2022. Study enrollment was briefly paused in 2020 because of the beginning of the COVID-19 pandemic. Baseline data were collected at enrollment for all patients, including their symptoms during episodes, family history, genetic testing, and markers of inflammation and cytokines. HRFs and PFAPA were defined using the 2019 EuroFever/PRINTO classification criteria (see Supplemental Figure 1). SURF was defined as at least three episodes in the past of stereotypical recurrent fevers, of which the episodes could not be explained by PFAPA, HRF, or any other cause. Patients were then managed and treated by their primary rheumatologist. Each treatment response was labeled as the following: complete response was defined as resolution of symptoms without the need for escalation in therapy. Partial response was defined as the abortion of an acute febrile episode with subsequent increased frequency of episodes necessitating escalation in therapy or partial resolution of symptoms during episodes. Treatment failure was defined as no change in symptoms with treatment.

Cytokine analysis. Peripheral blood samples were collected from patients at the time of enrollment, with serum and plasma aliquoted and stored at -80°C within 120 minutes of collection. Serum samples were then run using a cytokine multiplex assay to evaluate levels of interferon-inducible T cell alpha chemoattractant (ITAC), interferon- γ (IFN γ), granulocyte-macrophage colony-stimulating factor, IL-1 β , IL-10, IL-17A, IL-23, IL-8, IL-6, tumor necrosis factor α (TNF α), macrophage inflammatory protein 1 α (MIP-1 α), MIP-3 α , and MIP-1 β . One patient with a heterozygous adenosine deaminase 2 (ADA2) variant had ADA-2 levels measured at Boston Children's Hospital.¹³

Genetic analysis. We obtained results of clinically performed genetic testing for recurrent fever syndromes (single genes or panels) from the patient's medical records. For some patients, genetic testing was performed on a research basis through an exome-slice approach. The immunology exome panel, with focused analysis of 394 to 442 genes (see Supplemental Table 1) implicated in known inflammatory disorders as well as inborn errors of immunity, uses the Agilent SureSelect Clinical Research Exome V1 targeted sequence capture method or the Human Comprehensive Exome kit from Twist Bioscience to enrich for the whole exome. Variants in the panel were sliced out of the exome for analysis. The targeted regions were sequenced using Illumina HiSeq 2500 or Novaseq 6000 sequencing system with paired-end reads. Sequence reads were mapped and compared to human genome build hg19. Data quality was assessed to confirm variants had a minimum coverage of $\times 20$ for more than 95% of targets of interest. Variants within coding exons and flanking sequences were identified and evaluated

by an in-house developed bioinformatics analysis pipeline. Allele-specific analysis for the 253kb inversion as well as targeted analysis of the c.118-308 region in *UNC13D* were performed because these variants have been shown to disrupt *UNC13D* transcription in hematopoietic cells.¹⁴ The clinical significance of each variant was assessed based on the standards and guidelines for the interpretation of sequence variants, recommended by the American College of Medical Genetics and Genomics and the Association for Molecular Pathology.¹⁵ Each variant was reviewed by a clinical molecular geneticist (WZ) in the department of Human Genetics at CCHMC.

Statistical analysis. Our primary objectives were to define the clinical manifestations, treatment responses, cytokine signatures, and genetic variants of SURF. Our secondary objective was to compare clinical manifestations and cytokine signatures of patients with SURF to those in patients with PFAPA. Analysis was performed using R (R Foundation for Statistical Computing), Microsoft Office Excel, and GraphPad PRISM. Welch's *t*-tests were used to test for independence in symptoms between SURF and PFAPA. Cytokines were compared between SURF and PFAPA using Mann-Whitney U-tests. Morpheus was used to run hierarchical cluster analysis of SURF and PFAPA cytokines.

RESULTS

Clinical features of patients with SURF and PFAPA.

Between 2018 and 2022, 133 patients were enrolled into our institution's pediatric autoinflammatory disease registry with the chief complaint of recurrent fevers. Of these patients, we identified 46 who met criteria for SURF and 21 who met criteria for PFAPA (Supplemental Figure 2).

Clinical and demographic features of patients with SURF and patients with PFAPA are shown in Table 1 and Figure 1. Patients with SURF were 54% female and 46% male, whereas patients with PFAPA were 62% female and 38% male. The mean duration of febrile episodes was 6.4 days in SURF and 3.9 days in PFAPA ($P = 0.01$). The mean interval between febrile episodes in SURF was 24.4 days and 31.4 days in PFAPA ($P = 0.03$). The median age at onset was 3 years for SURF and 1.5 years for PFAPA ($P = 0.06$). The most commonly reported clinical features of patients with SURF were gastrointestinal symptoms, arthralgias, rash, and fatigue or malaise. In contrast, patients with PFAPA most commonly showed the classic features of pharyngitis, adenitis, and mouth sores. Pharyngitis and adenopathy were significantly more prominent in patients with PFAPA, with a frequency of 81% and 71%, respectively, compared to a frequency of 28% and 33% in patients with SURF ($P = 1.6 \times 10^{-5}$ and $P = 0.002$, respectively). A total of 43% of patients with SURF had rash as a part of their febrile episodes compared to zero patients with PFAPA ($P = 0.0001$). Notably, although the absence of rash is not strict exclusion criteria for PFAPA in the EuroFever/PRINTO

criteria, the presence of rash does make the diagnosis less likely. Arthralgias were found to be significantly more present in SURF compared to PFAPA, being present in 50% of patients with SURF and only 5% of patients with PFAPA ($P = 0.0001$). If we instead used the less strict Modified Marshall criteria for PFAPA, we identified 24 patients who we classified as having SURF that satisfied these criteria. However, this subgroup had distinct clinical features that more resembled SURF compared to patients with PFAPA who met both criteria, such as rash (0% vs 46%, $P = 0.0003$), arthralgias (5% vs 50%, $P = 0.0009$), and abdominal pain or anorexia (29% vs 67%, $P = 0.02$) (Supplemental Table 2, Supplemental Figure 3), supporting our use of the EuroFever criteria for the present study.

Cytokine profiles in patients with SURF and PFAPA.

To examine immunologic differences between patients with SURF and patients with PFAPA, we performed multiplex cytokine analysis using a Luminex multiplex assay. Plasma cytokines were obtained at the time of routine clinical visit, which did not correspond to fever flares, except for one patient with SURF who, although not having fevers, reported some poorly controlled symptoms.

Overall, cytokine levels between patients with SURF and patients with PFAPA were similar, with a significant difference only seen in MIP-1 β , in which the mean was 28.3 pg/mL (IQR 16.1–44.9 pg/mL) in PFAPA compared to 18.9 pg/mL (IQR 4.1–40.9 pg/mL) in SURF ($P = 0.01$). However, there was a trend in patients with SURF to have more outlier levels of proinflammatory cytokines, which was not an observation in patients with PFAPA. This was particularly pronounced for cytokines including IL-6, IL-8, TNF α , IL-23, IL-17A, and IFN γ (Figure 2). To examine whether there were different patterns of cytokine levels present between SURF and PFAPA, or within the SURF cohort, we performed hierarchical clustering on cytokine profiles (Figure 3). We identified a distinct subgroup of six patients with SURF who clustered together with elevated levels of IFN γ , IL-17A, IL-12p70, and IL-23, with lower levels of MIP-1 β compared to patients outside this cluster. These patients clustered separately from patients with PFAPA and other patients with SURF, suggesting they may have a distinct inflammatory profile. Five patients in this cluster (83%) required and were started on biologic therapy, compared to only 30% of patients who were outside this cluster ($P = 0.02$). One of these patients, although not febrile, was complaining of some poorly controlled symptoms at the time of sampling. All patients within this cluster who required biologics had rash as a part of their fever episodes. The sixth patient did not have rash as a part of their episodes and had complete response to on-demand steroids.

Treatment modalities and responses in patients with SURF and patients with PFAPA. We examined treatments administered to patients with SURF and patients with

Table 1. Demographics and clinical characteristics of fever episodes of patients diagnosed with SURF and PFAPA*

Gender	SURF (n = 46)	PFAPA (n = 21)	P value
Female, N (%)	25 (54)	13 (62)	
Male, N (%)	21 (46)	8 (38)	
Fever characteristics			
Mean duration of symptoms prior to presentation (in months)	26.1	17.8	0.3
Median duration (in months) of symptoms prior to presentation (IQR in months)	11 (6, 30)	12 (7, 24)	
Mean flare duration in days (\pm SD in days)	6.4 \pm 5.1	3.9 \pm 0.8	0.01
Mean interval between episodes (in days)	24.4 \pm 9.6	31.4 \pm 11.6	0.03
Patients with regularly occurring fevers, N (%)	26 (57)	16 (76)	
Median age of onset (IQR)	3 (1, 4)	1.5 (1, 2.5)	0.06
Clinical manifestations with fever episodes			
	SURF	PFAPA	
Pharyngitis	13 (28)	17 (81)	1.6 $\times 10^5$
Adenitis	15 (33)	15 (71)	0.002
Mouth sores	20 (43)	10 (48)	0.71
Rash ^a	20 (43)	0	0.0001
Arthralgias	23 (50)	1 (5)	0.0001
Abdominal pain or anorexia	23 (50)	6 (29)	0.10
Fatigue and malaise	19 (41)	7 (33)	0.58
Headache	7 (15)	6 (29)	0.24
Eye ^b	3 (6.5)	1 (5)	0.79
Myalgias	3 (6.5)	1 (5)	0.79
Nausea/emesis	6 (13)	1 (5)	0.48
Diarrhea	4 (9)	0	0.04
Arthritis	3 (6.5)	0	0.08

* Bolded values indicate P value <0.05 . PFAPA, periodic fever, adenitis, pharyngitis, aphthous stomatitis syndrome; SURF, syndrome of undifferentiated recurrent fevers.

^a Rashes included maculopapular, petechial, urticarial, and undefined lesions.

^b Eye findings included uveitis, conjunctivitis, periorbital edema, and eye pain.

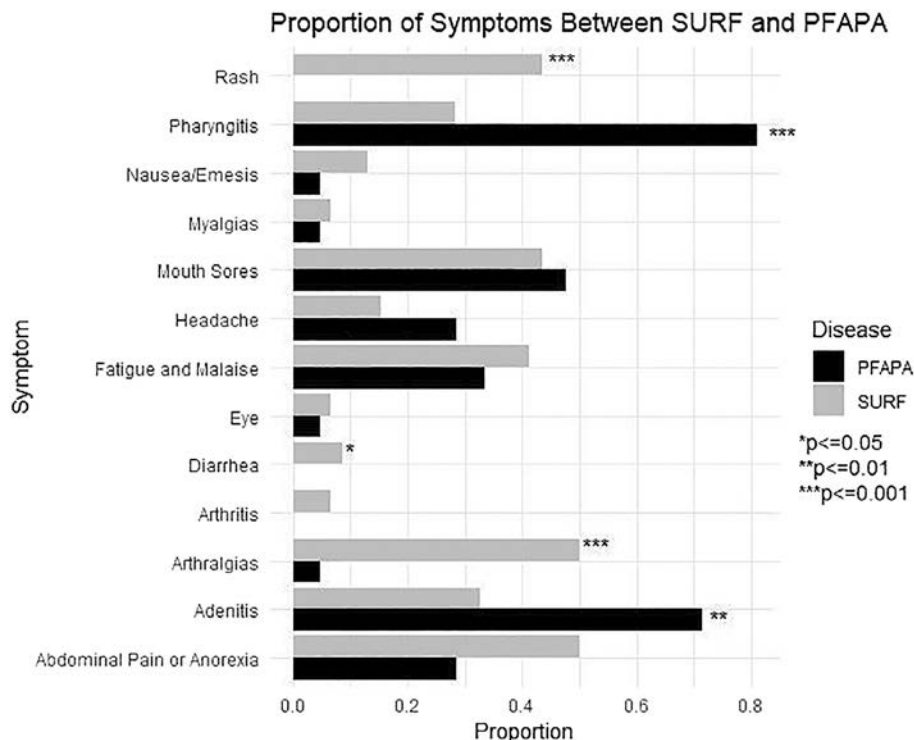


Figure 1. Proportion table of symptoms present during fever episodes in patients with SURF and patients with PFAPA. * $P \leq 0.05$, ** $P \leq 0.01$, and *** $P \leq 0.001$. PFAPA, periodic fever, adenitis, pharyngitis, aphthous stomatitis syndrome; SURF, syndrome of undifferentiated recurrent fevers.

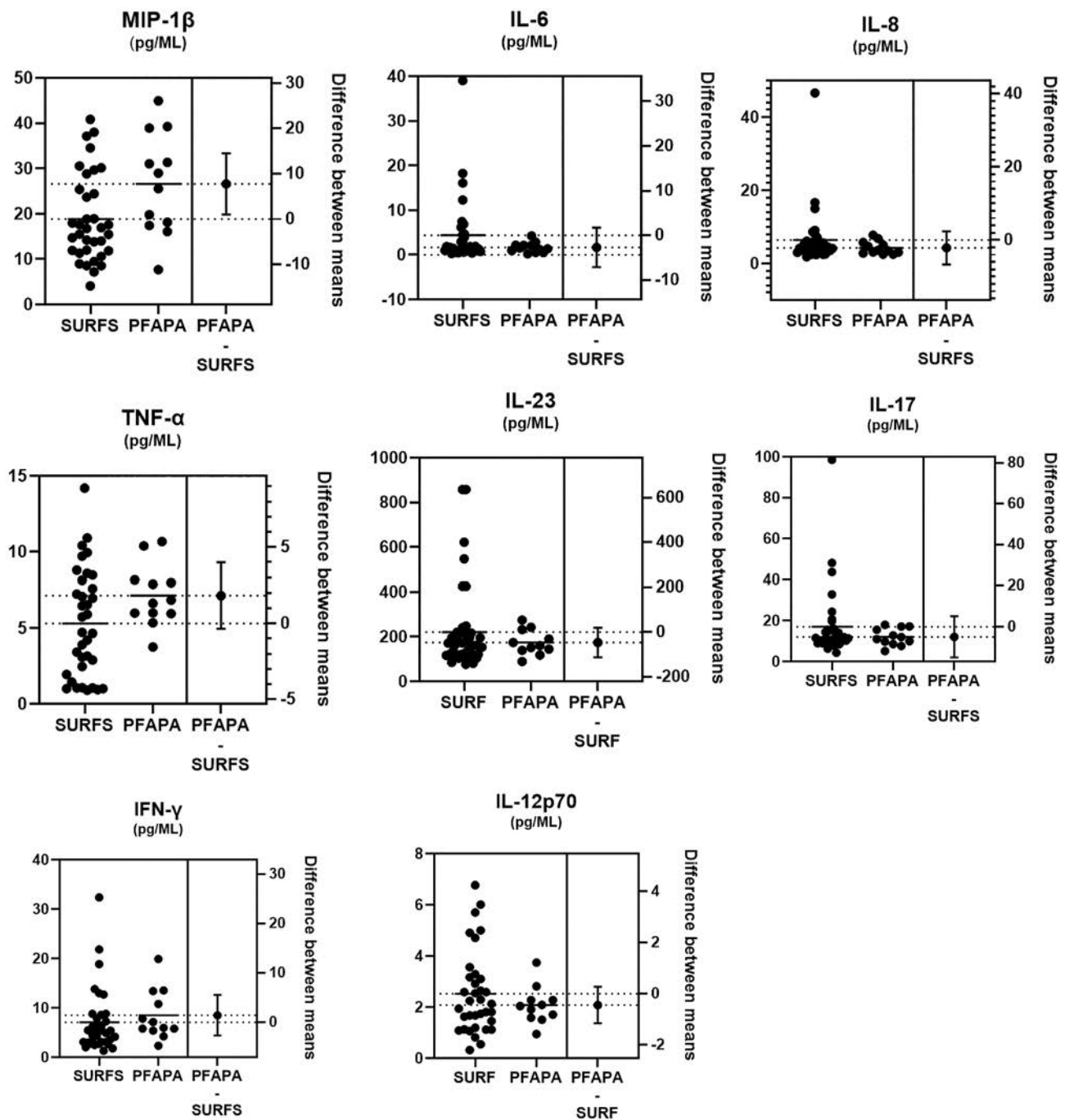


Figure 2. Estimation plots of peripheral cytokines in patients with SURF and patients with PFAPA, showing a subgroup of patients with SURF who had much higher levels compared to patients with PFAPA. In each panel, the left side shows data, and the right side shows effect size and its confidence interval. $n = 35$ for SURF and $n = 11$ for PFAPA. IFN γ , interferon- γ ; IL-6, interleukin-6; MIP-1 β , macrophage inflammatory protein 1 β ; PFAPA, periodic fever, adenitis, pharyngitis, aphthous stomatitis syndrome; SURF, syndrome of undifferentiated recurrent fevers; TNF α , tumor necrosis factor α .

PFAPA in our cohort. SURF therapies ranged from the administration of nonsteroidal anti-inflammatory drugs (NSAIDs) to the administration of biologics, which varied greatly from patients with PFAPA, who only required on-demand steroids and adenotonsillectomy (T&A) for disease control. The prescription patterns made by treating physicians between patients with

PFAPA and patients with SURF was found to be significantly different, with on-demand steroids being prescribed more in patients with PFAPA (81% vs 35%, $P = 0.006$), colchicine being prescribed more in patients with SURF (0% vs 41%, $P = 0.0003$), and anti-IL-1 therapy being prescribed more in patients with SURF (0% vs 37%, $P = 0.0006$).

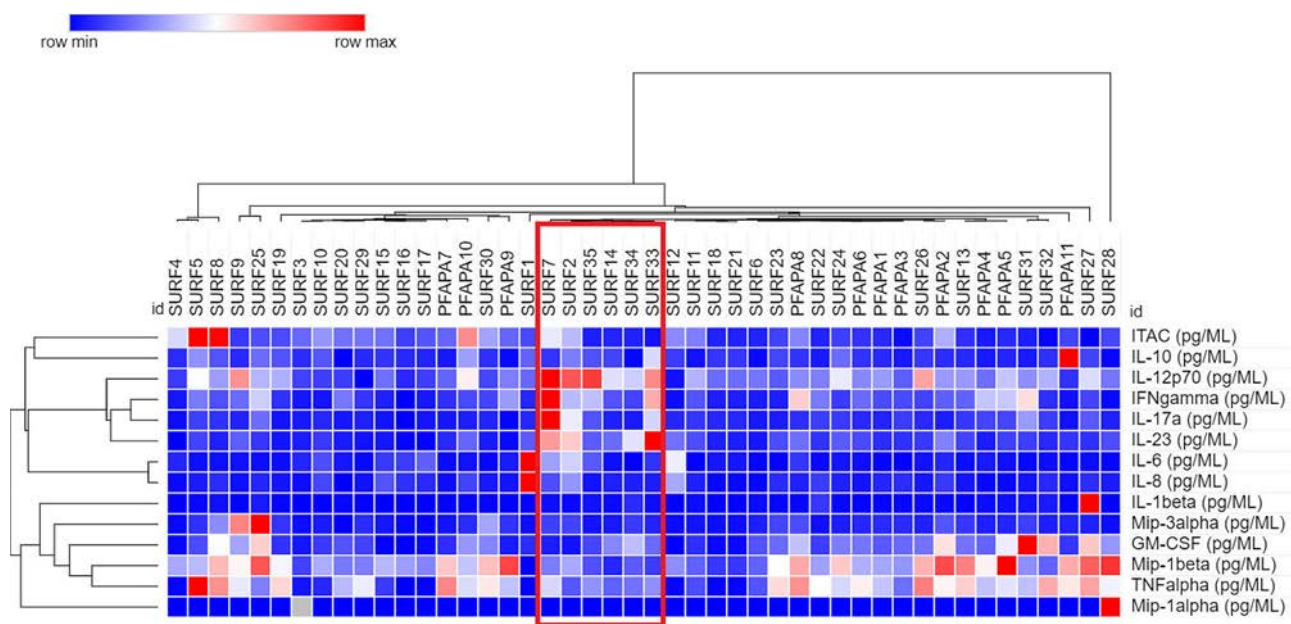


Figure 3. Hierarchical clustering of peripheral cytokines for patients with SURF and patients with PFAPA. Red box represents cluster of patients with elevated levels of IL-12p70, interferon- γ , and IL-23, in addition to lower levels of MIP-1 β . Clustering performed using Morpheus. GM-CSF, granulocyte–macrophage colony-stimulating factor; IL-1 β , interleukin-1 β ; ITAC, interferon-inducible T cell alpha chemoattractant; MIP-1 β , macrophage inflammatory protein 1 β ; PFAPA, periodic fever, adenitis, pharyngitis, aphthous stomatitis syndrome; SURF, syndrome of undifferentiated recurrent fevers; TNF α , tumor necrosis factor α .

The treatments and response rates for patients with SURF are described in Table 2. Sixteen patients received on-demand steroids. Of these, 11 patients (68.8%) had a complete response. Four patients (25%) had an incomplete response, defined as increasing fever frequency that required escalation in management or as incomplete resolution of a fever episode. One patient did not respond to steroids at all. Twelve patients underwent T&A. Of these, seven patients (58.3%) had resolution in symptoms after T&A, three patients (25%) had an incomplete response, and two patients (16.7%) had no response. For those who responded and then had a return of symptoms, or who had a partial response immediately after T&A, these patients were later treated with on-demand steroids, colchicine, or anti-IL-1 therapy and had complete responses. Of the two patients who failed T&A, both had a complete response to canakinumab. Nineteen patients were treated with daily colchicine. Of these, eight patients (42.1%) had complete response, five patients (26.3%) had an

incomplete response, five patients (26.3%) had no response and required a change in medication, and one patient had complete response but had to discontinue its use due to gastrointestinal side effects. Cimetidine was administered in four patients. One patient had complete response, one had an incomplete response, one had no response, and one had side effects that warranted discontinuation. Finally, 17 patients were initiated on anti-IL-1 biologic therapy with anakinra and/or canakinumab. Eight patients (47%) had a complete response to monotherapy, four patients (23.5%) had an incomplete response (and three of these patients went on to have a complete response to canakinumab and on-demand anakinra dual therapy), four patients (23.5%) had no response, and one patient had complete response to monotherapy but discontinued its administration due to a side effect of weight gain. Three patients who had more severe fever episodes, defined as having six or more symptoms, had complete response to colchicine or anti-IL-1 monotherapy.

Table 2. Treatment responses for patients with syndrome of undifferentiated recurrent fevers*

	On-demand steroids	T&A	Colchicine	Cimetidine	Anti-IL-1
Complete response, n (%)	11 (68.8)	7 (58.3)	8 (42.1)	1 (25)	8 (47)
Incomplete response, n (%)	4 (25)	3 (25)	5 (26.3)	1 (25)	4 (23.5) ^a
No response, n (%)	1 (6.3)	2 (1.7)	5 (26.3)	1 (25)	4 (23.5)
Did not tolerate medication, n (%)			1 (5.3)	1 (25)	1 (5.9)
Total attempted on treatment, n	16	12	19	4	17

* anti-IL-1, anti-interleukin-1; T&A, adenotonsillectomy.
^a Three of these patients went on to have good response to dual anti-IL-1 therapy with canakinumab and on-demand anakinra.

Finally, our subgroup of patients with SURF who satisfied Modified Marshall criteria showed treatment responses that were significantly different from patients meeting both PFAPA criteria but were similar to other patients with SURF (Supplemental Table 3, Supplemental Figure 4). Taken together, treatment responses were heterogeneous, and the most common biologics administered and that had the greatest success were anakinra and canakinumab. Other disease-modifying antirheumatic drugs and biologics administered to patients with SURF included methotrexate, adalimumab, tocilizumab, and rilonacept. Notably, three patients self-resolved from their fever episodes during the work-up period, or due to refusal to try recommended therapies.

Frequent variants of unknown clinical significance in patients with SURF revealed by genetic analysis.

Most of our patients with SURF had some genetic testing performed clinically to rule out monogenic HRF as a cause of disease (76%). Five patients with PFAPA (24%) had genetic testing done. Only one patient had a positive finding with a heterozygous possibly pathogenic variant in *MEFV*, but their clinical symptoms did not meet criteria for familial Mediterranean fever (FMF). Genetic testing for SURF generally consisted of single-gene testing or limited panels of more common HRFs. However, to examine whether patients with SURF carry rare genetic variants in other immune-related genes, we performed expanded genetic testing on 17 patients using an immunology exome panel. Overall, we found pathogenic or potentially deleterious genetic variants of unknown clinical significance (VUCS) in 46% of patients with SURF (Supplemental Table 1). One patient was a carrier of a single pathogenic variant in *ADA2*. Functional testing showed that they had an ADA-2 activity level of 9.0 U/L, which was consistent with carrier status.¹³ Several patients had variants in genes that are implicated in T and B cell development, granulocyte and monocyte function, inflammatory bowel disease risk, and primary immunodeficiencies. In addition, multiple novel variants were seen as well as several patients with variants in the same gene. Three patients had dedicator of cytokinesis 2 (*DOCK2*) variants. *DOCK2* is a part of the *DOCK* family of proteins and acts to regulate the development, migration, and activation of immune cells. It is expressed in lymphocytes, neutrophils, and plasma dendritic cells, and defects are associated with combined immunodeficiency and severe systemic lupus erythematosus.¹⁴ A recent study showed a patient with heterozygous *DOCK2* deficiency who exhibited decreased natural killer cell-mediated killing and, clinically, experienced recurrent episodes of hemophagocytic lymphohistiocytosis or macrophage activation syndrome (MAS).¹⁵

Our patients with heterozygous *DOCK2* mutations had an onset of symptoms at 6, 7, and 10 years old, which are older than the median age at onset of patients with SURF (3 years old).

Four patients had variants in nucleotide-binding oligomerization domain-containing protein 2 (*NOD2*), with one patient who

had two different variants in this gene. *NOD2* is in the NLRC subfamily, leads to the activation of proinflammatory transcription factors, and is associated with Blau syndrome, other autoinflammatory syndromes, and Crohn disease.^{16,17} Three variants were risk factors, one was likely benign, and one was a novel variant. All patients with *NOD2* variants experienced abdominal pain or nausea with their episodes. Two patients had variants in caspase-8 (*CASP8*), a gene that acts as a scaffold protein for TNF related apoptosis inducing ligand receptor (TRAIL-R) proinflammatory cytokines and double-stranded RNA activation of the NLRP3 inflammasome.^{18–20} Both patients with *CASP8* variants required anti-IL-1 therapy for disease control. Three patients had VUCS in *MEFV* but did not meet clinical criteria for FMF. These patients had a complete response to NSAIDs, on-demand steroids, or colchicine.

DISCUSSION

Periodic fever syndromes represent a substantial clinical problem, and many patients either do not have an identified genetic cause or satisfy criteria for well-characterized syndromes such as PFAPA, and thus best management approaches are unknown. Recently, SURF classification has emerged to describe a group of patients with recurrent fevers without a known monogenic cause and whose episodes do not fit PFAPA criteria. Here, we describe a cohort of patients with SURF who are clinically distinct from PFAPA, with heterogeneous symptoms and treatment responses, as well as a subgroup with distinctly elevated levels of peripheral cytokines including IL-12p70, IL-23, and IFN γ .

Distinguishing between PFAPA and SURF continues to be a diagnostic challenge, particularly as there is no consensus on the best diagnostic or classification criteria for PFAPA. Although many classification criteria exist, including the modified Marshall criteria,²¹ Feder and Salazar,²² Takeuchi et al,²³ and the EuroFever/PRINTO,² none of these criteria have been universally adopted. Overall, we found that SURF is a heterogeneous group of patients, with the most common symptoms including arthralgias (50%), abdominal pain (50%), oral ulcers (43%), rash (43%), and fatigue and malaise (41%). Gastrointestinal distress was common, and symptoms reported included abdominal pain, anorexia, nausea, emesis, and diarrhea. Smaller numbers of patients had headaches, myalgias, and adenitis as a part of their fever episodes. Interestingly, these findings are in agreement with some studies showing similar heterogeneity,¹² whereas the study by Sutera et al²⁴ suggested that SURF is more homogeneous. This difference in our findings may be explained by the fact that the cohort in the study by Sutera et al²⁴ was homogeneous in race and ethnicity, with 100% of the cohort being White Italian.

When distinguishing patients with SURF from patients with PFAPA, our study found rash and arthralgias were each more likely to occur in patients with SURF, whereas pharyngitis was significantly more likely to be found in patients with PFAPA. The

presence of arthralgias in these patients supports earlier findings in a cohort study on patients with SURF from the international EuroFever registry.¹¹ That same study found that fatigue, malaise, abdominal pain, myalgias, and eye manifestations were present in at least 40% of their cohort.¹¹ Our patient cohort supported that at least 40% of patients had fatigue or gastrointestinal (GI) symptoms as a part of their fever episodes. A study by De Pauli et al²⁵ found a statistically higher frequency of mouth sores, arthralgias, and abdominal pain in patients with SURF, and significantly more frequent pharyngitis in patients with PFAPA. In our study, mouth sores were present in 43% of patients with SURF and abdominal pain was seen in 50% of patients with SURF, but these findings were not significant when compared to our PFAPA cohort.

Treatment responses to on-demand steroids and T&A between patients with SURF and patients with PFAPA in our study were similar. However, no patients diagnosed with PFAPA using the EuroFever criteria required an escalation in therapy past on-demand steroids or T&A (Supplemental Table 2).

Treatment modalities for patients with SURF most commonly included NSAIDs, on-demand steroids, colchicine, T&A, and anti-IL-1 therapy.^{11,12,24–26} Marques et al²⁷ studied predictive factors for colchicine response and found that the presence of rash and a negative heterozygous *MEFV* variant were associated with increased likelihood of an incomplete response to colchicine, whereas a positive heterozygous *MEFV* VUCS was associated with a complete response. Our cohort supported this. The three patients with *MEFV* variants all had disease control with NSAIDs, on-demand steroids, or colchicine. Most patients with SURF in our cohort were first treated with typical PFAPA therapies such as on-demand steroids, colchicine, and T&A.²⁸ Treatment responses for patients with SURF were heterogeneous. For patients who did not show a complete response to traditional PFAPA therapies, escalation to biologics was common, with anti-IL-1 therapy being the most commonly used biologic. Three patients were escalated to dual anti-IL-1 therapy with scheduled canakinumab and on-demand anakinra and had a complete response. Four patients were treated unsuccessfully with IL-1 therapy. Three of the four had a later onset of symptoms, at ages 6, 9, and 16. Overall, however, for patients who responded well to anti-IL-1 monotherapy, clinical, immunologic, and genetic findings were heterogeneous. This continues to support heterogeneity within SURF and may further suggest that there are subsets of patients who do not benefit from anti-IL-1 therapy, and a subset of patients who would benefit from dual therapy.

This is the first study to our knowledge to evaluate peripheral cytokines in patients with SURF. Overall, we find that peripheral cytokines between patients with PFAPA and patients with SURF were similar, except for MIP-1 β , which was significantly higher in patients with PFAPA. We observed that patients with SURF tended to have more outliers with elevated proinflammatory cytokines, including IL-1 β , IL-6, IL-8, and IL-17A. This same

phenomenon was not seen in PFAPA (Figure 2). In addition, we identified a subset of patients with elevated levels of IL-12p70, IL-23, and IFN γ (Figure 3). Although peripheral cytokines in SURF have not been reported, the study by Luu et al¹² examined tonsils from patients with SURF after tonsillectomy and found a persistent IL-1 β and interleukin 1 receptor antagonist (IL-1RN) signature in those tonsils. They also found that the tonsils in patients with PFAPA had an increased IL-1RA expression but in association with TNF rather than¹² IL-1 β . This may suggest that localized cytokine measurement is more useful than peripheral cytokine measurement. IL-1 β is a proinflammatory cytokine that is activated after certain signals trigger the inflammasome to associate with caspase-1 leading to autoproteolysis of caspase-1, with the cleavage of pro-IL-1 β in the process.²⁹ It has a wide range of proinflammatory functions, including prostaglandin synthesis, neutrophil activation, T and B cell activation, and fibroblast activation. It also interacts with IL-12 to synergistically induce T cells to activate, proliferate, and produce IFN γ . Surprisingly, this synergistic interaction causes this cascade to occur in the absence of T cell receptor engagement.³⁰ Thus, IL-1 β could represent an important promoter of inflammation in the pathogenesis of SURF. This is supported by our cohort, in which 71% of the patients who received IL-1 inhibition had an improvement in their symptoms.

SURF can be difficult to distinguish clinically from FMF, given the high rates for GI symptoms and arthralgias associated with fever episodes in SURF. A lingering question has remained about whether SURF is a clinically distinct entity from patients with *MEFV*-negative FMF. Palmeri et al³¹ showed that they are clinically distinct by comparing pyrin inflammasome activity and IL-1 β levels in the peripheral blood of healthy controls, patients with PFAPA, patients with FMF, and patients with treated and untreated SURF.

SURF represents patients with recurrent fevers and no known single-gene cause. However, some patients with SURF may carry unrecognized causative genetic variants or have other genetic risk factors for systemic inflammation. Here, genetic VUCS were frequently found in patients with SURF. VUCSs found in our patients included genes that are implicated in B cell development, primary immunodeficiencies, granulocyte and monocyte development, and inflammatory bowel disease risk. Repeated VUCSs among patients included three patients within the gene *DOCK2*, two patients in *CASP8*, four patients in *NOD2*, and three patients in *MEFV*. Patients with a variant in *DOCK2* had an onset of symptoms at 6, 7, and 10 years old, which are older than the average age at onset of 3.5 years, and the median age at onset of 3 years for patients with SURF. Two of these variants had a Combined Annotation Dependent Depletion score greater than 20. Interestingly, *DOCK2* has a probability of being loss-of-function intolerant score of 1, which suggests intolerance to loss of function or haploinsufficiency; there is also a recent report of a patient with heterozygous *DOCK2* mutation and recurrent episodes of hyperinflammation and MAS.¹⁵ Further research is needed to evaluate the implications of heterozygous *DOCK2*

pathogenic variants. Patients with *CASP8* variants had headaches, arthralgias, and GI symptoms as a part of their episodes, and both required anti-IL-1 therapy for disease control. The four patients with variants in *NOD2* had abdominal pain or emesis as a part of their episodes. Although this study is the first report of VUCSs in patients with SURF to date, further work is needed to define potential pathogenic roles for such variation.

Our article has several important limitations. This is a relatively small, single-center cohort. In addition, the definition of PFAPA, and therefore SURF, varied among the different SURF studies, so patients with SURF in this study may have characteristics that other articles would have defined as PFAPA, making accurate comparisons between SURF groups difficult. Other limitations were that we were not able to analyze race and ethnicity data, genetics were not performed on all patients with SURF or any patients with PFAPA, cytokines were not collected during flares, and the outcome measures for treatment are imprecise. Although we were able to compare cytokine levels between patients and disease groups, Luminex does not have established normal ranges for each cytokine. These will be important limitations to address in the future.

In conclusion, SURF is a heterogeneous group of patients with recurrent fevers but without a known monogenic cause. Our findings suggest SURF has distinct clinical, treatment, and immunologic features from disorders such as PFAPA. We also find frequent VUCSs in pathways that may have relevance to disease pathogenesis, a subset of patients with SURF who stand out as having higher levels of inflammation compared to the rest of patients with SURF and all of the patients with PFAPA, and groups with distinct needs for treatments and responses to those treatments. Taken together, this raises the question of the existence of SURF endotypes, or subtypes of SURF with distinct pathophysiologic mechanisms.³² Further research is necessary to understand these SURF endotypes, what drives the disorder, and how physicians can better predict which treatment will be most successful for each patient.

AUTHOR CONTRIBUTIONS








All authors contributed to at least one of the following manuscript preparation roles: conceptualization AND/OR methodology, software, investigation, formal analysis, data curation, visualization, and validation AND drafting or reviewing/editing the final draft. As corresponding author, Dr Schultert confirms that all authors have provided the final approval of the version to be published and takes responsibility for the affirmations regarding article submission (eg, not under consideration by another journal), the integrity of the data presented, and the statements regarding compliance with institutional review board/Declaration of Helsinki requirements.

REFERENCES

- Broderick L, Hoffman HM. Pediatric recurrent fever and autoinflammation from the perspective of an allergist/immunologist. *J Allergy Clin Immunol* 2020;146(5):960–966.e2.
- Gattorno M, Hofer M, Federici S, et al; Eurofever Registry and the Paediatric Rheumatology International Trials Organisation (PRINTO). Classification criteria for autoinflammatory recurrent fevers. *Ann Rheum Dis* 2019;78(8):1025–1032.
- Manthiram K, Zhou Q, Aksentjevich I, et al. The monogenic autoinflammatory diseases define new pathways in human innate immunity and inflammation. *Nat Immunol* 2017;18(8):832–842.
- Romano M, Arici ZS, Piskin D, et al. The 2021 EULAR/American College of Rheumatology points to consider for diagnosis, management and monitoring of the interleukin-1 mediated autoinflammatory diseases: cryopyrin-associated periodic syndromes, tumour necrosis factor receptor-associated periodic syndrome, mevalonate kinase deficiency, and deficiency of the interleukin-1 receptor antagonist. *Ann Rheum Dis* 2022;81(7):907–921.
- Cetin Gedik K, Lamot L, Romano M, et al. The 2021 European Alliance of Associations for Rheumatology/American College of Rheumatology Points to Consider for Diagnosis and Management of Autoinflammatory Type I Interferonopathies: CANDLE/PRAAS, SAVI, and AGS. *Arthritis Rheumatol* 2022;74(5):735–751.
- Soon GS, Laxer RM. Approach to recurrent fever in childhood. *Can Fam Physician* 2017;63(10):756–762.
- Manthiram K, Preite S, Dedeoglu F, et al; Genomic Ascertainment Cohort. Common genetic susceptibility loci link PFAPA syndrome, Behçet's disease, and recurrent aphthous stomatitis. *Proc Natl Acad Sci USA* 2020;117(25):14405–14411.
- Stojanov S, Lapidus S, Chitkara P, et al. Periodic fever, aphthous stomatitis, pharyngitis, and adenitis (PFAPA) is a disorder of innate immunity and Th1 activation responsive to IL-1 blockade. *Proc Natl Acad Sci USA* 2011;108(17):7148–7153.
- Hausmann J, Dedeoglu F, Broderick L. Periodic fever, aphthous stomatitis, pharyngitis, and adenitis syndrome and syndrome of unexplained recurrent fevers in children and adults. *J Allergy Clin Immunol Pract* 2023;11(6):1676–1687.
- Thomas KT, Feder HM, Lawton AR, et al. Periodic fever syndrome in children. *J Pediatr* 1999;135(1):15–21.
- Papa R, Penco F, Volpi S, et al. Syndrome of undifferentiated recurrent fever (SURF): an emerging group of autoinflammatory recurrent fevers. *J Clin Med* 2021;10(9):1963.
- Luu I, Nation J, Page N, et al. Undifferentiated recurrent fevers in pediatrics are clinically distinct from PFAPA syndrome but retain an IL-1 signature. *Clin Immunol* 2021;226:108697.
- Lee PY, Aksentjevich I, Zhou Q. Mechanisms of vascular inflammation in deficiency of adenosine deaminase 2 (DADA2). *Semin Immunopathol* 2022;44(3):269–280.
- Chen Y, Di M, Tang Y, et al. A narrative review: the role of DOCK2 in immune-related diseases, hematopoietic or vascular diseases and solid tumor. *Ann Blood* 2022;7:32.
- Reiff DD, Zhang M, Cron RQ. DOCK2 mutation and recurrent hemophagocytic lymphohistiocytosis. *Life (Basel)* 2023;13(2):434.
- Maekawa S, Ohto U, Shibata T, et al. Crystal structure of NOD2 and its implications in human disease. *Nat Commun* 2016;7(1):11813.
- Nomani H, Deng Z, Navetta-Modrov B, et al. Implications of combined NOD2 and other gene mutations in autoinflammatory diseases. *Front Immunol* 2023;14.
- Henry CM, Martin SJ. Caspase-8 acts in a non-enzymatic role as a scaffold for assembly of a pro-inflammatory “FADDosome” complex upon TRAIL stimulation. *Mol Cell* 2017;65(4):715–729.e5.
- Kang S, Fernandes-Alnemri T, Rogers C, et al. Caspase-8 scaffolding function and MLKL regulate NLRP3 inflammasome activation downstream of TLR3. *Nat Commun* 2015;6(1):7515.
- Fritsch M, Günther SD, Schwarzer R, et al. Caspase-8 is the molecular switch for apoptosis, necroptosis and pyroptosis. *Nature* 2019;575(7784):683–687.

21. Marshall GS, Edwards KM, Butler J, et al. Syndrome of periodic fever, pharyngitis, and aphthous stomatitis. *J Pediatr* 1987;110(1):43–46.
22. Feder H, Salazar J. A clinical review of 105 patients with PFAPA (a periodic fever syndrome). *Acta Paediatr* 2010;99(2):178–184.
23. Takeuchi Y, Shigemura T, Kobayashi N, et al. Clinical features and new diagnostic criteria for the syndrome of periodic fever, aphthous stomatitis, pharyngitis, and cervical adenitis. *Int J Rheum Dis* 2019; 22(8):1489–1497.
24. Sutera D, Bustaffa M, Papa R, et al. Clinical characterization, long-term follow-up, and response to treatment of patients with syndrome of undifferentiated recurrent fever (SURF). *Semin Arthritis Rheum* 2022;55:152024.
25. De Pauli S, Lega S, Pastore S, et al. Neither hereditary periodic fever nor periodic fever, aphthae, pharyngitis, adenitis: undifferentiated periodic fever in a tertiary pediatric center. *World J Clin Pediatr* 2018;7(1):49–55.
26. Ter Haar NM, Eijkelboom C, Cantarini L, et al; Eurofever registry and the Pediatric Rheumatology International Trial Organization (PRINTO). Clinical characteristics and genetic analyses of 187 patients with undefined autoinflammatory diseases. *Ann Rheum Dis* 2019; 78(10):1405–1411.
27. Marques MC, Egeli BH, Wobma H, et al. Features predicting colchicine efficacy in treatment of children with undefined systemic autoinflammatory disease: a retrospective cohort study. *Eur J Rheumatol* 2022;9(3):116–121.
28. Amarilio G, Rothman D, Manthiram K, et al. Consensus treatment plans for periodic fever, aphthous stomatitis, pharyngitis and adenitis syndrome (PFAPA): a framework to evaluate treatment responses from the childhood arthritis and rheumatology research alliance (CARRA) PFAPA work group. *Pediatr Rheumatol Online J* 2020; 18(1):31.
29. Vijayaraj SL, Feltham R, Rashidi M, et al. The ubiquitylation of IL-1 β limits its cleavage by caspase-1 and targets it for proteasomal degradation. *Nat Commun* 2021;12(1):2713.
30. Tominaga K, Yoshimoto T, Torigoe K, et al. IL-12 synergizes with IL-18 or IL-1 β for IFN- γ production from human T cells. *Int Immunol* 2000;12(2):151–160.
31. Palmeri S, Penco F, Bertoni A, et al. Pyrin inflammasome activation defines colchicine-responsive SURF patients from FMF and other recurrent fevers. *J Clin Immunol* 2024;44(2):49.
32. Khurana Hershey GK, Sherenian MG, Mersha TB. Precision Medicine. *Allergy Essentials* 2022:25–39.

Evaluating Renal Disease in Pediatric-Onset Antineutrophil Cytoplasmic Antibody–Associated Vasculitis: Disease Course, Outcomes, and Predictors of Outcome

Kirandeep K. Toor,¹ Audrea Chen,²  David A. Cabral,¹ Cherry Mammen,¹ Else S. Bosman,³ Ye Shen,⁴ Jeffrey N. Bone,⁴ Damien Noone,² Eslam Al-Abadi,⁵ Susanne Benseler,⁶ Roberta Berard,⁷  Marek Bohm,⁸ Sirirat Charuvaniij,⁹ Kathryn Cook,¹⁰ Paul Dancey,¹¹ Samundeeswari Deepak,¹² Ciaran Duffy,¹³ Barbara Eberhard,¹⁴ Melissa Elder,¹⁵ Dirk Foell,¹⁶  Dana Gerstbacher,¹⁷ Merav Heshin-Bekenstein,¹⁸  Adam Huber,¹⁹ Karen E. James,²⁰ Susan Kim,²¹  Marisa Klein-Gitelman,²² Neil Martin,²³ Flora McErlane,²⁴ L. Nandini Moorthy,²⁵ Charlotte Myrup,²⁶ Phil Riley,²⁷ Susan Sheno,²⁸  Vidya Sivaraman,²⁹ Tamara Tanner,³⁰ Stacey Tarvin,³¹ Linda Wagner-Weiner,³² Rae S. M. Yeung,² Kelly L. Brown,¹  and Kimberly A. Morishita,¹
on behalf of the PedVas Investigators Network

Objective. We aimed to study the disease course, outcomes, and predictors of outcome in pediatric-onset antineutrophil cytoplasmic antibody (ANCA)–associated vasculitis (AAV) affecting the kidneys.

Methods. Patients eligible for this study had a diagnosis of granulomatosis with polyangiitis (GPA), microscopic polyangiitis, or ANCA-positive pauci-immune glomerulonephritis, were 18 years or younger at diagnosis, had renal disease defined by biopsy or dialysis dependence, and had clinical data at diagnosis and at either 12 or 24 months. Ambispective data from A Registry for Children with Vasculitis/Pediatric Vasculitis Initiative Registry was used. The primary outcome was inactive renal disease (pediatric vasculitis activity score = 0 or 1) at 12 months. Secondary outcomes included rates of improved renal function and damage within 24 months. Renal function, defined by estimated glomerular filtration rate, was categorized into Kidney Disease Improving Global Outcomes (KDIGO) stages at diagnosis and tested as a predictor of outcome using a proportional-odds logistic regression model.

Results. A total of 145 patients were included: 68% were female, and 78% had GPA. At 12 months, 83% of patients achieved inactive renal disease; however, 42% had evidence of permanent renal damage. Compared with patients with normal renal function at diagnosis, patients with moderate to severely reduced renal function, or kidney failure at diagnosis, had an odds ratio of 8.62 ($P = 0.002$; 95% confidence interval [CI] 2.31–32.1) and 26.3 ($P < 0.001$; 95% CI 6.32–109), respectively, for being in a non-normal KDIGO category at 12 months.

Conclusion. The majority of patients with pediatric AAV achieve inactive renal disease by 12 months; however, almost half have evidence of damage. Renal function at diagnosis is a strong predictor of renal function at 12 months.

INTRODUCTION

Pediatric-onset antineutrophil cytoplasmic antibody (ANCA)–associated vasculitis (AAV) is a rare, relapsing, organ or life-threatening systemic disease, characterized by inflammation

and damage to small and medium blood vessels.¹ AAV involves the presence of circulating autoantibodies, specifically ANCA, that are typically directed against myeloperoxidase (MPO) or proteinase 3 (PR3).² AAV is a group of vasculitides comprised of, in order of frequency, granulomatosis with polyangiitis (GPA), microscopic

Author Toor's work was supported by a Centre for Blood Research graduate award and Women+ and Children's Health Sciences Graduate Program child health award supporting diversity. Author Cabral's work was supported by the Canadian Institutes of Health Research (grant TR2-119188) and by the Arthritis Society Canada through the Ross Petty Arthritis Society Chair. Dr Brown's work was supported by the Canadian Institutes of Health Research (grant PJT-180302) and by a BC Children's Hospital Salary Award and a Michael Smith Foundation for Health Research Scholar Award. Dr Morishita's work was supported by the BC Children's Hospital Research Institute Seed Grant and by the Childhood Arthritis and Rheumatology Research Alliance

(CARRA) Small Grant through the ongoing Arthritis Foundation financial support of CARRA.

¹Kirandeep K. Toor, BSc, David A. Cabral, MBBS, Cherry Mammen, MD, MHSc, Kelly L. Brown, PhD, Kimberly A. Morishita, MD, MHSc: University of British Columbia and BC Children's Hospital and BC Children's Hospital Research Institute, Vancouver, British Columbia, Canada; ²Audrea Chen, MD, Damien Noone, MB, BCH, BAO, Rae S. M. Yeung, MD, PhD: The Hospital for Sick Children, University of Toronto, Toronto, Ontario, Canada; ³Else S. Bosman, PhD: University of British Columbia, Vancouver, British Columbia, Canada; ⁴Ye Shen, MPH, Jeffrey N. Bone, MSc: BC Children's Hospital Research

polyangiitis (MPA), and eosinophilic GPA. Damage to the blood vessels in these diseases cause downstream involvement of major organ systems, including the kidneys, heart, and lungs. Due to disease rarity, most knowledge about pediatric AAV is extrapolated from adult studies.^{3,4} Although “adult-derived” treatment approaches have substantially decreased mortality rates in children with AAV, concerns remain around the toxicity risks unique to children and the need for more pediatric-specific data.^{5,6} Renal disease is the most common manifestation of pediatric AAV and is the focus of this study.⁷

Our previous research demonstrated that, compared with adult-onset AAV, pediatric-onset AAV is more likely to be severe and have major organ dysfunction, including high rates of significantly reduced renal function at diagnosis.⁷ In a sample of 105 patients with AAV, 78% presented with renal disease, 16% were requiring dialysis, and 5% had kidney failure (KF).⁷ It is particularly concerning that many children have evidence of early renal damage by 12 months, despite aggressive treatment. There remains an imperative to distinguish patients who may need aggressive treatment from the patients who can be treated with less toxic therapy due to mild disease or because renal damage has become irreversible, and additional treatment will not result in any functional renal recovery. Previous adult AAV studies have examined predictors of renal outcomes and have found that estimated glomerular filtration rate (eGFR) and dialysis dependence are predictors of disease relapse, KF, and even death.^{8,9}

This study used data from A Registry for Children with Vasculitis (ARChive) and the Pediatric Vasculitis Initiative (PedVas). The aims of the study are to (1) elucidate renal disease course and outcomes within the first 24 months of disease and (2) evaluate the use of eGFR at diagnosis to predict renal outcome at 12 months.

MATERIAL AND METHODS

Participants. Patients eligible for this study were aged 18 years or younger at the time of a physician diagnosis of GPA,

MPA, or ANCA-positive immune glomerulonephritis (GN); had complete clinical data at the time of diagnosis (TOD) and follow-up at 12 months, 24 months, or both; and had renal disease defined as biopsy-confirmed GN or dialysis dependence at TOD. TOD refers to the date in which the patient was given the diagnosis of GPA, MPA, or ANCA-positive GN. All eligible patients were formally classified as follows: for a GPA diagnosis, patients met the EULAR/Paediatric Rheumatology International Trials Organization/Paediatric Rheumatology European Society classification criteria for GPA.^{10,11} For MPA, the diagnosis was based on a pediatric-modified algorithm¹² of the European Medicines Agency.¹³ Patients were excluded if they did not meet a diagnosis based on the described classification criteria. The protocol for this study was approved by the Children’s and Women’s Research Ethics Board of the University of British Columbia (H12-00894) and the respective ethics committees at participating sites. Written informed consent was obtained from parents, and informed consent or assent was obtained from patients for participation in the study.

Data collection. This study used data from ARChive (A Registry of Childhood Vasculitis), a web-based registry established in 2007 to collect TOD data from children and adolescents with primary chronic vasculitis.¹² Patients eligible for inclusion in ARChive were diagnosed after January 2004 and before data extraction in January 2023. In January 2013, as part of the PedVas, the registry was expanded to collect data beyond TOD to include postinduction (4–6 months after diagnosis), 12-months postdiagnosis, 24-months postdiagnosis, and flare visit data. Twenty-seven international sites recruited patients for this study, the majority of which were located in Canada, the United States, and the United Kingdom. Data collected include demographics, diagnosis, imaging, clinical manifestations, investigations, ANCA status, histopathology, medications, disease activity, and damage assessments. Patient ethnicity was determined from self-reported parental ethnicity from a fixed set of categories.

Institute, Vancouver, British Columbia, Canada; ⁵Eslam Al-Abadi, MBBS: Birmingham Children’s Hospital NHS Foundation Trust, Birmingham, United Kingdom; ⁶Susanne Benseler, MD, PhD: Alberta Children’s Hospital, Calgary, Alberta, Canada; ⁷Roberta Berard, MD, MSc: London Health Sciences Centre, London, Ontario, Canada; ⁸Marek Bohm, MD: Leeds Children’s Hospital, Leeds, United Kingdom; ⁹Sirirat Charuvanjij, MD: Siriraj Hospital, Bangkok, Thailand; ¹⁰Kathryn Cook, DO: Akron Children’s Hospital, Akron, Ohio; ¹¹Paul Dancey, MD: Janeway Children’s Health and Rehabilitation Centre, St. John’s, Newfoundland and Labrador, Canada; ¹²Samundeeswari Deepak, MBBS: Nottingham Children’s Hospital, Nottingham, United Kingdom; ¹³Ciaran Duffy, MBChB, MSc: Children’s Hospital of Eastern Ontario, Ottawa, Ontario, Canada; ¹⁴Barbara Eberhard, MBBS, MSc: Cohen Children’s Medical Center, Queens, New York; ¹⁵Melissa Elder, MD, PhD: University of Florida, Gainesville; ¹⁶Dirk Foell, MD: University Children’s Hospital Munster, Munster, Germany; ¹⁷Dana Gerstbacher, MD: Children’s Hospital at Stanford, Palo Alto, California; ¹⁸Merav Heshin-Bekenstein, MD: Dana Children’s Hospital of Tel Aviv Medical Center, Tel Aviv University, Tel Aviv, Israel; ¹⁹Adam Huber, MD, MSc: IWK Health Centre, Halifax, Nova Scotia, Canada; ²⁰Karen E. James, MD: Primary Children’s Medical Center, University of Utah, Salt Lake City; ²¹Susan Kim, MD, MMSc: Benioff Children’s Hospital, University of California, San Francisco; ²²Marisa Klein-Gitelman, MD, MPH: Ann & Robert H. Lurie Children’s

Hospital of Chicago, Chicago, Illinois; ²³Neil Martin, MRCPCH: Royal Hospital for Children, Glasgow, United Kingdom; ²⁴Flora McLane, MBChB: Great North Children’s Hospital, Newcastle, United Kingdom; ²⁵L. Nandini Moorthy, MD, MS: Rutgers-Robert Wood Johnson Medical School, New Brunswick, New Jersey; ²⁶Charlotte Myrup, MD, PhD: Rigshospitalet, Copenhagen, Denmark; ²⁷Phil Riley, MBChB: Royal Manchester Children’s Hospital, Manchester, United Kingdom; ²⁸Susan Sheno, MBBS, MS: Seattle Children’s Hospital and Research Center, University of Washington, Seattle; ²⁹Vidya Sivaraman, MD: Nationwide Children’s Hospital, Columbus, Ohio; ³⁰Tamara Tanner, MD: Children’s Hospital at Montefiore, Bronx, New York; ³¹Stacey Tarvin, MD, MS: Riley Children’s Hospital, Indianapolis, Indiana; ³²Linda Wagner-Weiner, MD, MS: The University of Chicago Comer Children’s Hospital, Chicago, Illinois.

Additional supplementary information cited in this article can be found online in the Supporting Information section (<http://onlinelibrary.wiley.com/doi/10.1002/art.43071>).

Author disclosures and graphical abstract are available at <https://onlinelibrary.wiley.com/doi/10.1002/art.43071>.

Address correspondence via email to Kimberly A. Morishita, MD, MHSc, at kmorishita@cw.bc.ca.

Submitted for publication May 4, 2024; accepted in revised form October 23, 2024.

Enzyme-linked immunosorbent assay ($n = 140$ cases) or immunofluorescence ($n = 4$ cases) was used to determine seropositivity for ANCA and specificity for PR3 or MPO. The study data were collected and managed in REDCap electronic data capture tool¹⁴ and hosted by servers of the University of British Columbia.

Definitions of renal-specific disease states. Disease activity was assessed using the pediatric vasculitis activity score (PVAS, total score range 0–63), which is a validated clinical scoring tool used for the systematic assessment of overall and organ-specific disease activity.¹⁵ Renal-specific disease activity was scored using the renal subcomponent of PVAS (renal PVAS score, range 0–12) and includes the following components: hypertension (systolic blood pressure >95th percentile based on age and height), proteinuria (>0.3 grams from 24-hr urine collection or spot urine protein-to-creatinine ratio >20 mg/mol), hematuria (≥ 5 red blood cells per high power field or red cell casts from urinalysis or urine microscopy), eGFR 50–80 mL/min/1.73m², eGFR 15–49 mL/min/1.73m², eGFR <15 mL/min/1.73m², and rise in creatinine >10% or GFR reduction >25% from baseline; Supplementary Table 1). Inactive renal disease was defined as renal PVAS = 0 or 1, regardless of medications.

Disease damage was assessed using a pediatric version of the vasculitis damage index (pVDI, range 0–72), a systematic assessment of individual organ systems in which damage is recorded when abnormal features and function persist for 3 months or more.^{16,17} As damage is considered to be irreversible, once scored items are captured in the pVDI, they are carried forward to all subsequent visits. Renal-specific damage was defined as a renal subcomponent pVDI score of one or more and includes the following components: blood pressure >95th percentile or requiring antihypertensives, proteinuria, eGFR 15 to 60 mL/min/1.73m², and end-stage renal disease (Supplementary Table 2).

Renal function was reflected by the eGFR, which was calculated from serum creatinine values and individual height according to the bedside Schwartz formula.¹⁸ Using the eGFR, renal function was categorized according to the Kidney Disease Improving Global Outcomes (KDIGO) classification¹⁹ as normal (eGFR >90 mL/min/1.73m², category 1), mildly reduced (MildR, eGFR 60–89 mL/min/1.73m², category 2), mild to moderately reduced (Mild-ModR, eGFR 45–59 mL/min/1.73m², category 3a), moderately to severely reduced (Mod-SevR, eGFR 30–44 mL/min/1.73m², category 3b), severely reduced (SevR, eGFR 15–29 mL/min/1.73m², category 4), and KF (eGFR <15 mL/min/1.73m², category 5) (Supplementary Table 3). For patients that underwent a renal transplant, we used their pretransplant eGFR values for analyses at subsequent follow-up time periods.

Renal outcome assessments. The primary outcome was inactive renal disease at 12 months. Secondary outcomes included inactive renal disease at 24 months, renal damage at

12 and 24 months, and changes in renal disease activity across 24 months. Renal disease course was defined by eGFR trajectories and changes in eGFR KDIGO stages from TOD to 12 or 24 months. An exploratory analysis was conducted evaluating potential predictors of renal function at 12 and 24 months.

Statistical analysis. Descriptive statistics were used to summarize baseline characteristics and to report rates of eGFR across 24 months. A proportional-odds logistic regression model was used to assess the association between eGFR at diagnosis and eGFR at 12 months. The model was adjusted for the following covariates: diagnosis (GPA or MPA), ANCA status, disease activity (total and renal PVAS at diagnosis), and induction treatment medication. These variables were selected a priori as potential factors that would associate with baseline and follow-up eGFR. A linear regression model was conducted on a subset of patients with eGFR values at diagnosis and 12 months. To determine a “threshold” value at which the outcome (renal function at 12 months) is likely to be significantly reduced (Mod-SevR or worse), a cut point analysis was conducted using R package cutpoint.²⁰ This analysis maximized the sum of sensitivity and specificity to determine an optimal cut point, which was then plotted on a receiver operating characteristic curve to visualize the trade-off between sensitivity and specificity. A linear mixed-effects model investigated longitudinal changes in PVAS scores at diagnosis, 12-months postdiagnosis, and 24-months postdiagnosis, with time point as the fixed effect and patient as the random effect. All estimates are presented with 95% confidence intervals (CIs) with interpretation based on size of estimates and range of uncertainty. Analyses were conducted using R (R Core Team 2024), and figures were created using GraphPad Prism version 9.0 statistical software (GraphPad Software). The data that support the findings of this study are available from the corresponding author upon reasonable request.

Patient and public involvement. Although patients were not involved in setting the research question, their involvement in contributing their clinical data played a crucial role. The outcomes and findings from our research will be disseminated to patients and their families through local, national, and international channels, ensuring there is widespread communication of our findings.

RESULTS

Baseline characteristics. A total of 145 patients with pediatric-onset AAV (68% female patients) with renal disease were eligible for inclusion in this study; among these, complete follow-up clinical data at 12- and 24-months postdiagnosis was available for 143 and 79 patients, respectively. Baseline characteristics are shown in Table 1. At diagnosis, patients were formally classified as GPA (78%) or MPA (22%) and had a median age of 13.8 years (interquartile range [IQR] 10.7–15.7 years). All patients with a physician diagnosis of ANCA-positive immune GN met the classification for GPA or MPA. ANCA against PR3 or MPO was

Table 1. Baseline characteristics of n = 145 patients*

Characteristics	n = 145
Age at diagnosis, median (IQR), years	13.8 (10.7–15.7)
Sex, female patients, n (%)	98 (68)
Ethnicity, White, n (%)	64 (55)
Diagnosis, n (%)	
Granulomatosis with polyangiitis	113 (78)
Microscopic polyangiitis	32 (22)
ANCA antigen positivity, n (%) of tests done ^a	
PR3	71 (49)
MPO	67 (47)
Both	4 (3)
Negative	2 (1)
Medications, n (%)	
Cyclophosphamide	101 (70)
Rituximab	19 (13)
Cyclophosphamide + rituximab	13 (9)
Renal characteristics, n (%)	
Hematuria	132 (91)
Proteinuria	131 (90)
Hypertension	41 (28)
eGFR/KDIGO, n (%)	
Normal (>90)	42 (29)
Mildly reduced (60–89)	13 (9)
Mild to moderately reduced (45–59)	12 (8)
Moderately to severely reduced (30–44)	33 (23)
Severely reduced (15–29)	21 (15)
Kidney failure (<15)	24 (17)
Dialysis, n (%)	36 (25)
Disease activity (renal PVAS), median (IQR)	12 (10–12)

* Unless indicated otherwise, values refer to the absolute number (%) of patients in each given category. Hematuria ≥ red blood cell per high power field or red cell casts; proteinuria >0.3g/24 hr or >20 mg/mmol Cr; and hypertension >95th percentile.

ANCA, antineutrophil cytoplasmic antibody; eGFR, estimated glomerular filtration rate; IQR, interquartile range; KDIGO, Kidney Disease Improving Global Outcomes; MPO, myeloperoxidase; PR3, proteinase 3; PVAS, pediatric vasculitis activity score.

^a Two patients were classified based on immunofluorescence detection of c-ANCA (likely PR3-ANCA).

detected in 49% and 47% of cases, respectively. Patients received glucocorticoid treatment, along with cyclophosphamide (70%), rituximab (13%), or both (9%), as part of their induction treatment. A comprehensive table detailing the treatments received at diagnosis, categorized by the level of kidney (dys)function, is provided in Supplementary Table 4. Extrarenal manifestations of disease at TOD were indicated by the presence of one or more scored items in organ-specific domains of PVAS: constitutional (75%), ear, nose, and throat (43%), respiratory (41%), cutaneous (35%), mucous membranes and/or eyes (33%), abdominal (26%), nervous system (12%), or cardiovascular (2%) (Figure 1A). Patients with 24-month follow-up data were comparable with respect to demographics and renal characteristics to patients without 24-month follow-up data (Supplementary Table 5). There were no deaths reported during the study period.

Outcomes. Despite high renal disease activity at diagnosis, most patients with AAV attain inactive renal disease within two years of diagnosis; however, a significant proportion have evidence of permanent renal damage.

At diagnosis, 99% of patients had active renal disease (renal PVAS ≥2). The majority (92%; 133 of 145) had highly active disease as indicated by a renal PVAS score of 10 (n = 53) or 12 (n = 80, the maximum allowable score for renal PVAS); the median renal PVAS was 12 (IQR 10–12). At 12-months postdiagnosis, 118 of 143 patients with available data (83%) had inactive renal disease (PVAS = 0 or 1). By 24-months postdiagnosis, 98% of patients (85 of 87 with available data) had inactive renal disease. Comparing changes in renal PVAS across 24 months using a linear mixed-effects model, renal disease activity decreased by 12 months (Mean Difference [MD] = −9.75; 95% CI −10.16 to −9.34) and 24 months (MD = −10.57; 95% CI −11.05 to −10.09) (Figure 1B).

Renal damage within two years of diagnosis was assessed in patients with a completed index of renal damage (renal pVDI) at 12 months (n = 129) and/or 24 months (n = 60). Despite the attainment of inactive disease in the majority of patients, more than one-third had a renal pVDI ≥1 (indicative of damage) at 12 months (42%) and 24 months (35%). The renal damage items scored at 12 months were as follows: reduced eGFR of 15 to 60 mL/min/1.73m² (31%), KF by eGFR <15mL/min/1.73m² (21%), and hypertension more than 95th percentile or taking anti-hypertensives (15%).

Renal disease course. To assess the course of renal function from diagnosis, we investigated eGFR trajectory over the first 12 to 24 months of disease. At diagnosis, renal function based on eGFR varied: 29% of patients had a normal eGFR, 9% had MildR, 8% had Mild-ModR, 23% had Mod-SevR, 14% had SevR, and 17% were in KF. Twenty-five percent of patients were on dialysis at diagnosis. At 24-months postdiagnosis, the proportion of patients with a normal eGFR (32%) was similar to that observed at TOD (29%) (Figure 2). The percentage of patients with MildR eGFR increased from 9% at TOD to 37% at 24 months. The percentage of patients with the most compromised renal function (Mod-SevR, SevR, and KF) was 54% at diagnosis versus 31% at 12 months and 24% at 24 months.

Next, we observed eGFR trajectories across 12 and 24 months for patients at the “extremes” of renal function at diagnosis, namely patients presenting with an eGFR indicative of normal function (n = 42; eGFR >90 mL/min/1.73m²) versus KF (n = 23; eGFR <15 mL/min/1.73m²) (Figure 3). Among the 42 patients that had normal renal function at diagnosis, 33 had 12-months follow-up, and 17 of these patients had 24-months follow-up. Eighteen patients (53%) retained normal renal function (normal eGFR), whereas 14 patients (41%) had mild worsening (mild eGFR) by the time of their last follow-up (12 months or 24 months). Renal function in only two patients deteriorated to levels indicative of moderate to SevR function or KF (Mod-SevR or KF eGFR). Among the 23 patients that were in KF at diagnosis, 74% were still in KF or were transplanted (n = 6) by 12 months, and none achieved a normal eGFR without a renal transplant.

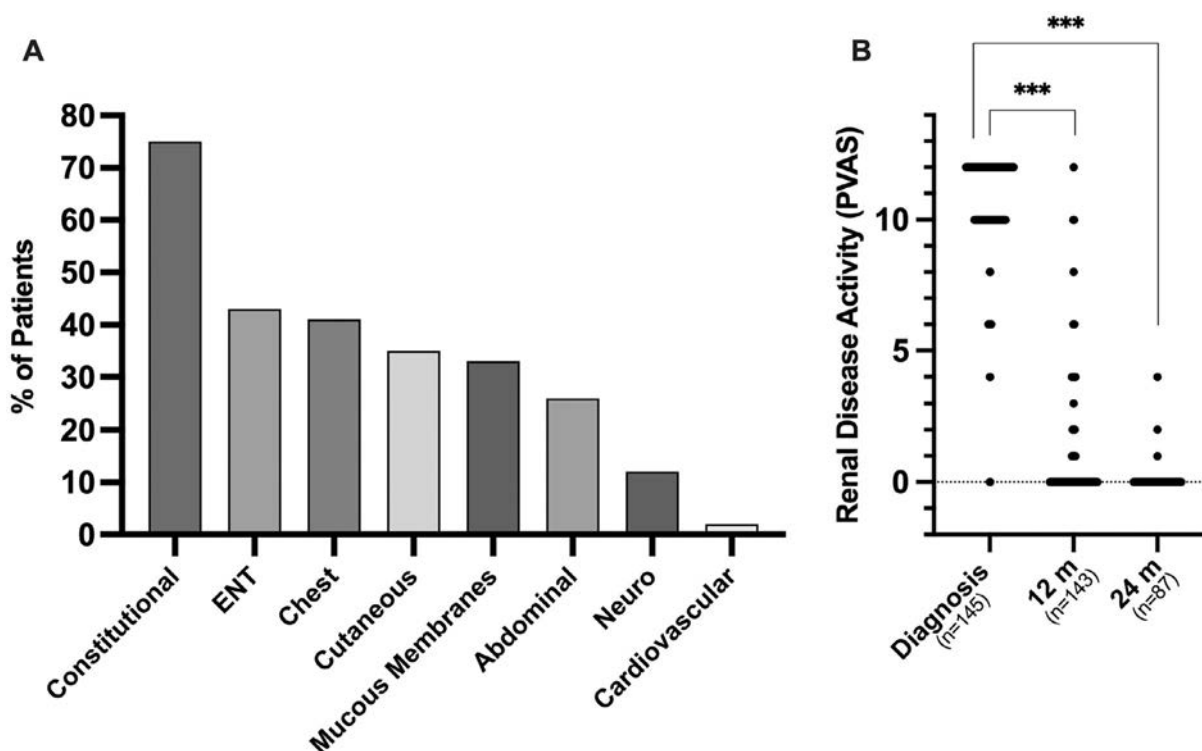


Figure 1. Extrarenal manifestations at diagnosis and renal disease activity in the first 24 months in pediatric AAV. (A) Percentage of pediatric-onset AAV cases (y-axis) with organ-specific system involvement (x-axis) at the time of diagnosis. (B) Renal PVAS (y-axis) in patients at TOD (n = 145), 12-month follow-up (n = 143), and 24-month follow-up (n = 87). Each dot represents a single patient. The width of the line indicates the number of patients with the same value. Inactive renal disease indicated by renal PVAS = 0 or 1, regardless of glucocorticoid dosage. Active renal disease is indicated by PVAS ≥ 2. *** $P < 0.001$. AAV, antineutrophil cytoplasmic antibody-associated vasculitis; ENT, ear nose and throat; PVAS, pediatric vasculitis activity score; TOD, time of diagnosis.

Predictive utility of eGFR at diagnosis. There was a clear linear relationship between baseline KDIGO category and 12-month KDIGO category. The odds of having impaired renal function (non-normal KDIGO category) at 12 months were 4.77

(odds ratio [OR] 4.77; $P = 0.005$; 95% CI 1.60–14.2), 8.62 (OR 8.62; $P = 0.002$; 95% CI 2.31–32.1), and 26.3 (OR 26.3; $P < 0.001$; 95% CI 6.32–109) times higher in patients with moderate, SevR, or KF at baseline compared with those with normal

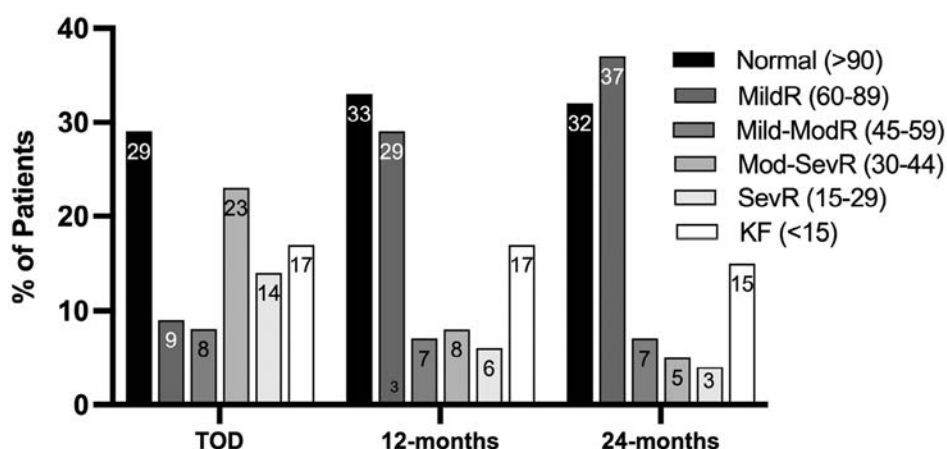


Figure 2. eGFR at diagnosis, 12 months, and 24 months in pediatric AAV. Percentage of patients with pediatric-onset AAV (%) (y-axis) with eGFR values corresponding to KDIGO category of renal function (see legend; eGFR values in brackets with units mL/min/1.73m²) at (x-axis) diagnosis (n = 145), 12 months (n = 143), and 24 months (n = 79). AAV, antineutrophil cytoplasmic antibody-associated vasculitis; eGFR, estimated glomerular filtration rate; KDIGO, Kidney Disease Improving Global Outcomes; KF, kidney failure; MildR, mildly reduced; Mild-ModR, mild to moderately reduced; Mod-SevR, moderately to severely reduced; SevR, severely reduced; TOD, time of diagnosis.

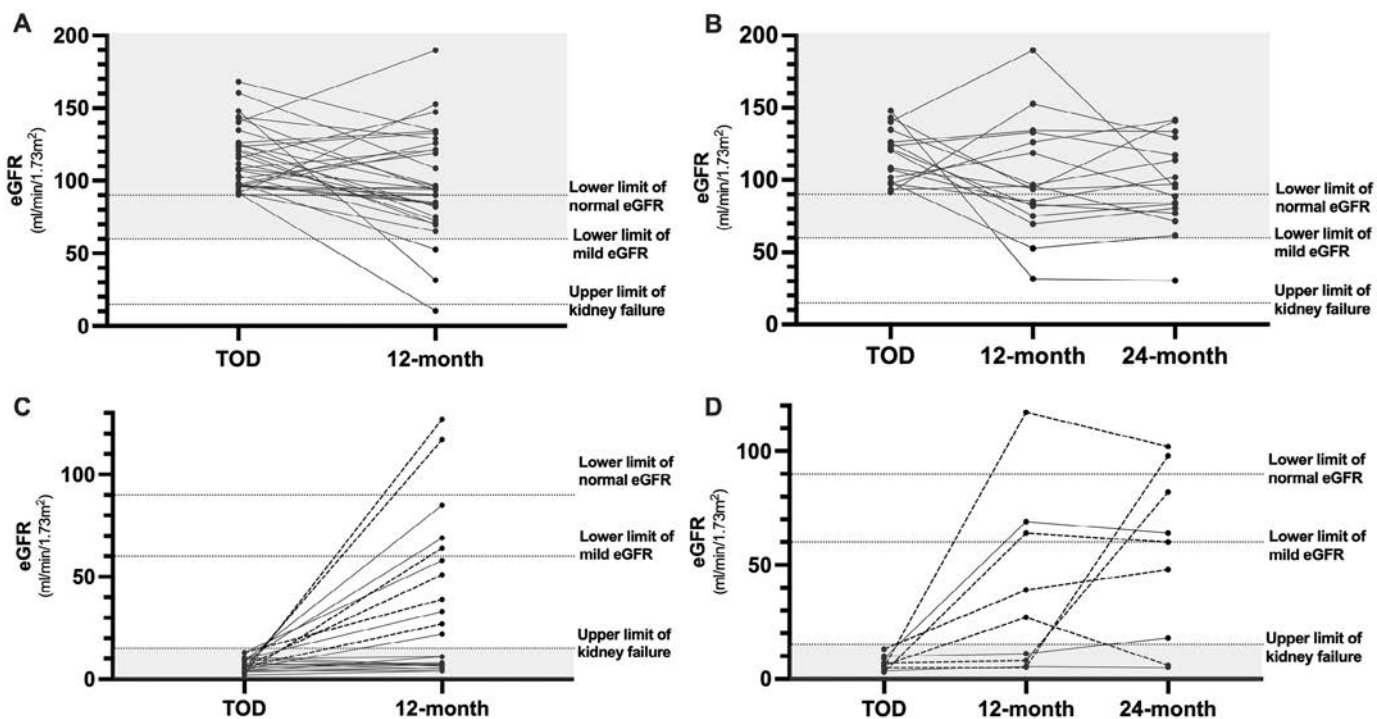


Figure 3. eGFR in pediatric AAV at diagnosis, 12-month follow-up, and 24-month follow-up for patients with “extreme” renal function (normal versus kidney failure) at diagnosis. (A–D) eGFR (y-axis; mL/min/1.73m²) with (A–B) “normal” renal function (eGFR > 90) at diagnosis followed across (A) 12 months (n = 33) and (B) 24 months (n = 17) and (C–D) kidney failure (eGFR < 15) at diagnosis followed across (C) 12 months (n = 23, including renal transplant shown by dashed line; n = 6) and (D) 24 months (n = 9, including renal transplant shown by dashed line; n = 6). Upper dotted line represents the lower limit of normal eGFR (eGFR = 90); middle dotted line represents the lower limit of MildR eGFR (eGFR = 60); and lower dotted line represents the upper limit of kidney failure (eGFR = 15). AAV, antineutrophil cytoplasmic antibody–associated vasculitis; eGFR, estimated glomerular filtration rate; MildR, mildly reduced; TOD, time of diagnosis.

baseline renal function, respectively (Table 2). Of note, for both the MildR and Mild-ModR KDIGO categories, there was no increased odds of having impaired renal function at 12 months. Based on these data, we then explored an optimal cut point eGFR value at diagnosis to help alert the clinician to which patients would be at risk of moderate to severe renal dysfunction at 12 months based on their eGFR at diagnosis. The analysis showed that an eGFR of 38 mL/min/1.73m² (95% CI 21–41) maximized the sum of

sensitivity and specificity. For this cut point, the sensitivity was 74%, and the specificity was 89%. Additionally, the area under the curve was calculated to be 0.84 (95% CI 0.76–0.92), indicating good discriminative ability. Further, 31 of 51 patients (61%) who were diagnosed below the cut point continued to have, at 12 months, renal dysfunction in the Mod-SevR range or worse, whereas the majority of patients (95%) that were above this cut point value (Mod-SevR or more mild renal dysfunction) at diagnosis remained in the same category or showed improvement by 12 months (Figure 4).

Table 2. KDIGO category at diagnosis as a predictor of worse KDIGO category at 12-month follow-up*

KDIGO Diagnosis	OR	95% CI	P value
Normal	-	-	-
MildR	1.36	0.31–5.87	0.680
Mild-ModR	1.02	0.24–4.36	0.981
Mod-SevR	4.77	1.60–14.2	0.005
SevR	8.62	2.31–32.1	0.002
KF	26.3	6.32–109	<0.001

* Adjusted for diagnosis (granulomatosis with polyangiitis or microscopic polyangiitis), antineutrophil cytoplasmic antibody (specificity for proteinase 3 or myeloperoxidase), pediatric vasculitis activity score at baseline, and induction treatment.
CI, confidence interval; KDIGO, Kidney Disease Improving Global Outcomes; KF, kidney failure; MildR, mildly reduced; Mild-ModR, mildly or moderately reduced; Mod-SevR, moderately or severely reduced; OR, odds ratio; SevR, severely reduced.

DISCUSSION

In this study of pediatric-onset AAV with renal disease, the majority of patients had a diagnosis of GPA and were predominantly female, White, and had a median age at diagnosis of 13.8 years, consistent with our previous outcome study (n = 105 patients) and other pediatric AAV studies.^{7,21} Using TOD and 12- and/or 24-month follow-up data from this cohort, we described the renal disease course, outcomes, and use of eGFR at diagnosis to predict 12-month renal outcomes.

Our study showed that although the majority of pediatric patients presented with very high renal disease activity at

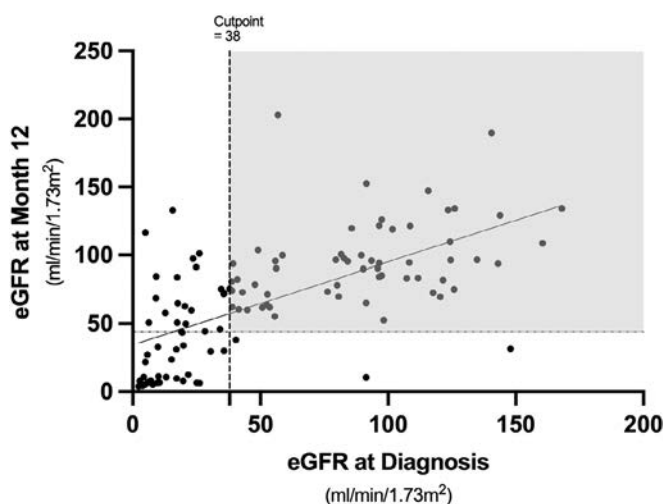


Figure 4. eGFR in pediatric ANCA-associated vasculitis at diagnosis and 12 months. eGFR values at diagnosis (x-axis; mL/min/1.73m²) against eGFR values at 12-month follow-up (y-axis; mL/min/1.73 m²) in patients with pediatric ANCA-associated vasculitis (n = 113). The vertical dotted line at the x-axis represents the cut point eGFR value of 38. The horizontal line on the y-axis represents the eGFR value of 44.0, the upper limit of the moderately reduced renal function (KDIGO category). ANCA, antineutrophil cytoplasmic antibody; eGFR, estimated glomerular filtration rate; KDIGO, Kidney Disease Improving Global Outcomes.

diagnosis, the majority achieved inactive renal disease (PVAS = 0 or 1) 12 or 24 months after diagnosis. However, despite improvement in renal disease activity, two-thirds of patients had reduced renal function (eGFR <90 mL/min/1.73m²) at 12 and 24 months, and more than one-third had evidence of permanent renal damage. A previous study of AAV in adults showed the most frequently recorded damage items at 6-months follow-up and long-term follow-up (up to 7 years) consisted of renal items, including eGFR <50 mL/min and hypertension.⁴ Comparatively, our study found that the most common renal damage items in our cohort consisted of eGFR 15 to 60 mL/min/1.73m², KF by eGFR <15 mL/min/1.73m², and hypertension >95th percentile and/or taking antihypertensives. This highlights that renal damage is also a common occurrence in pediatric individuals with AAV but is potentially a greater burden in children who have long lives ahead of them compared with adults who are usually diagnosed at over 50 years of age.

There is evidence that adult patients with chronic kidney disease (CKD) stages 4 and 5 (equivalent to KDIGO categories 4 and 5) and a lower “baseline” eGFR are at a higher risk for KF and need for renal replacement therapy.^{22,23} Although a few studies on adult-onset AAV describe low baseline eGFR as a predictor of renal survival and mortality,^{24,25} very few studies have examined this in pediatric-onset AAV.^{26,27} A single-center study (n = 48) by Yang et al suggested that a baseline eGFR <60 mL/min/1.73m² is an independent predictor of nonremission and poor long-term renal outcomes.²⁷ Another study suggested

that eGFR <19.42 mL/min/1.73m² is an independent risk factor for KF in children with AAV.²⁶ In a study involving 53 patients, several variables including baseline serum creatine and eGFR were associated with an increased risk of developing KF or progressing to CKD stages 3 to 5; however, a multivariable analysis revealed that none of these variables were independent predictors.²⁸ We demonstrated that eGFR at diagnosis is a strong predictor of eGFR at 12-months follow-up. Patients who have a normal eGFR at diagnosis are likely to maintain normal or MildR renal function. In contrast, patients who present with KF at diagnosis are unlikely to experience any substantive improvement in function and go on to need renal replacement therapy in the form of dialysis or a renal transplant.

Moreover, our study identified an eGFR cut point threshold of 38 mL/min/1.73m², below which patients exhibited a higher likelihood of having significant (Mod-SevR, SevR, or KF) renal dysfunction by 12 months. Patients with an eGFR above this threshold at diagnosis exhibited either stabilization or improvement in renal function by 12 months. This observed finding is of interest and deserves further prospective study. We acknowledge that a single eGFR value as a threshold value may be artificial given the limitations and accepted margins of error in reporting eGFR; however, the concept of having a “threshold” range or category of eGFR that has predictive use may be of significant value as a clinical tool. Validation of such a threshold could have significant clinical implications by informing prognosis and improving our ability to counsel patients at diagnosis; for patients below this threshold, the prognosis might be more guarded for renal recovery versus a more optimistic outlook for those above the threshold.

Patients in this study generally received standard therapy with either cyclophosphamide or rituximab, both in combination with glucocorticoids in varied regimens. Whether patients with very mild disease or very severe (with irreversible damage) disease at diagnosis could have been treated with lower doses or a reduced duration of these aggressive immunosuppressants remains unclear but of significant interest.²⁹ The goal remains to consider limiting glucocorticoids for patients that do not require it or will not benefit from such treatment, such as those that are on trajectory for poor renal outcomes regardless of treatment.

Currently, kidney biopsies play an important role in aiding prognostication around the TOD; however, their use is impacted by sampling limitations and challenges of conducting the procedure repeatedly or at diagnosis when the patient may be facing other critical health challenges. A previous study by Noone et al highlighted the clinical use of the Berden histopathological classification system, particularly for focal and sclerotic features on biopsy.^{30,31} The results showed that two years after diagnosis, patients with sclerotic features (n = 5) all progressed to end-stage renal disease compared with none of the patients with focal disease (n = 13). Due to small sample size, however, the “less-extreme” biopsy types (mixed and crescentic categories) had to

be combined and could not be analyzed as individual groups. This system offers important prognostic information in pediatric-onset ANCA GN; however, its use for discriminating outcomes in less-extreme biopsy cases remains unclear.³¹ Ultimately, the optimal predictor of longer-term renal function may need to use both biopsy and GFR data.

Our study has several strengths. It represents the largest study of renal outcomes in pediatric AAV to date. It provides new insight into renal disease trajectory and prognosis and improves our understanding of anticipated outcomes. Such knowledge was not possible to obtain with previous, much smaller cohorts. It is also the first study to evaluate the predictive value of GFR in a multicenter, international cohort with systematically collected prospective data in such patients. Additionally, the use of validated (ie, PVAS) or recommended (ie, pVDI) clinical scoring tools enabled outcome assessments that can be compared with adult cohorts or, more importantly, provide a benchmark for future pediatric cohorts.

Our study acknowledges certain limitations. We used GFR instead of measured GFR because this was the only feasible method for estimating renal function in the context of real-world registry data collection. Although this is a well-accepted method for estimating GFR, we recognize there are instances when it may be less representative of actual renal function. In addition, GFR at diagnosis was calculated based on the serum creatinine value entered at or near the TOD. Creatinine values at the TOD are constantly changing, and it is possible that the most representative value was not necessarily entered. Formal training in scoring the PVAS or pVDI was not required of the multiple site investigators, but they were provided a comprehensive manual for the PVAS and pVDI. Additionally, within the registry, there are multiple check points and prompts that assist the investigator in determining whether a sign or symptom should be scored as active vasculitis (PVAS) versus damage (pVDI). Some items within the PVAS and pVDI are challenging to attribute solely to active vasculitis or damage, respectively. For example, when hypertension is scored as part of PVAS or pVDI, it should not be due to glucocorticoids, other medications, fluid overload, or white coat hypertension; however, this may be difficult to differentiate clinically, and it is up to the investigator to make those judgments. These challenges are inherent to the scoring tools themselves and are not limitations to this study specifically. With respect to follow-up, there was a lack of completed 24-month data, preventing a comprehensive analysis from being conducted at this time point. There was variability in follow-up time points, with the 12-month follow-up ranging from 11 months to 15 months, which is the result of pragmatic registry data collection timing that coincided with the timing of routine clinical care closest to 12 or 24 months. At the time of establishment of the clinical registry in 2007, gender assessment from patients was not included. Although the registry has recently been modified to prospectively include gender information, this is currently available for very few patients. Sex is an important variable that has been considered in our project when describing

demographic characteristics, and this consideration is important given that in children, vasculitis affects girls more often than boys, with the opposite seen in adult-onset disease.³² Lastly, despite our diverse cohort, we acknowledge our sample may not be representative of all populations. Additionally, PedVas centers tend to be larger tertiary or quaternary centers, resulting in a cohort that is potentially more severe; however, patients with renal disease would generally require care at such centers, so it is felt that very few patients with renal vasculitis would be observed solely at a small center.

The results of this study highlight the high rate of significant renal disease in pediatric AAV and how renal function at diagnosis is a strong predictor of renal function at 12 months. The identification of a cut point threshold eGFR value has potential as a predictive clinical tool that is easy to use and understand for both clinicians and patients. Early identification of patients at highest risk for poor renal outcome may enable earlier intervention with renoprotective measures, such as controlling hypertension, treating proteinuria, managing weight, and minimizing other potential insults to the kidney. The elucidation of AAV-associated renal disease trajectories builds upon our understanding of renal disease course and will contribute to improved pediatric-specific counseling around anticipated disease course and outcome. Further research that compares the predictive use of eGFR versus other predictors such as biopsy classification, or the combination of such predictors, will ideally result in improved prognostication and ability to tailor treatment that maximizes disease control and minimizes treatment toxicity. Providing improved, individualized insights into anticipated outcomes will ultimately allow patients and their families to be more involved in shaping and participating in their own care.

ACKNOWLEDGMENTS

The authors would like to acknowledge all participating patients and their families, without whom this study would not be possible. The authors thank the PedVas site investigators and clinical coordinators for their dedicated work.

AUTHOR CONTRIBUTIONS




All authors contributed to at least one of the following manuscript preparation roles: conceptualization AND/OR methodology, software, investigation, formal analysis, data curation, visualization, and validation AND drafting or reviewing/editing the final draft. As corresponding author, Dr Morishita confirms that all authors have provided the final approval of the version to be published and takes responsibility for the affirmations regarding article submission (eg, not under consideration by another journal), the integrity of the data presented, and the statements regarding compliance with institutional review board/Declaration of Helsinki requirements.

REFERENCES

1. Qasim A, Patel JB. ANCA Positive Vasculitis. In: StatPearls. StatPearls Publishing; 2023. <http://www.ncbi.nlm.nih.gov/books/NBK554372/>. Accessed July 6, 2023.

2. Kitching AR, Anders HJ, Basu N, et al. ANCA-associated vasculitis. *Nat Rev Dis Primers* 2020;6(1):71.
3. Miloslavsky EM, Specks U, Merkel PA, et al; Rituximab in ANCA-Associated Vasculitis-Immune Tolerance Network Research Group. Clinical outcomes of remission induction therapy for severe antineutrophil cytoplasmic antibody-associated vasculitis. *Arthritis Rheum* 2013;65(9):2441–2449.
4. Robson J, Doll H, Suppiah R, et al. Damage in the ANCA-associated vasculitides: long-term data from the European vasculitis study group (EUVAS) therapeutic trials. *Ann Rheum Dis* 2015;74(1):177–184.
5. Moorthy AV, Chesney RW, Segar WE, et al. Wegener granulomatosis in childhood: prolonged survival following cytotoxic therapy. *J Pediatr* 1977;91(4):616–618.
6. Westwell-Roper C, Lubieniecka JM, Brown KL, et al; for ARChIVE Investigators Network within the PedVas initiative. Clinical practice variation and need for pediatric-specific treatment guidelines among rheumatologists caring for children with ANCA-associated vasculitis: an international clinician survey. *Pediatr Rheumatol Online J* 2017;15(1):61.
7. Morishita KA, Moorthy LN, Lubieniecka JM, et al; ARChIVE Investigators Network within the PedVas Initiative. Early outcomes in children with antineutrophil cytoplasmic antibody-associated vasculitis. *Arthritis Rheumatol* 2017;69(7):1470–1479.
8. Slot MC, Tervaert JWC, Franssen CFM, et al. Renal survival and prognostic factors in patients with PR3-ANCA associated vasculitis with renal involvement. *Kidney Int* 2003;63(2):670–677.
9. Toraman A, Soysal Gündüz Ö. Predictors of renal and patient outcomes in anti-neutrophil cytoplasmic antibody-associated vasculitis: our single-center, tertiary care experience. *Arch Rheumatol* 2021;36(3):445–457.
10. Fries JF, Hunder GG, Bloch DA, et al. The American College of Rheumatology 1990 criteria for the classification of vasculitis. Summary. *Arthritis Rheum* 1990;33(8):1135–1136.
11. Ozen S, Pistorio A, Iusan SM, et al; Paediatric Rheumatology International Trials Organisation (PRINTO). EULAR/PRINTO/PRES criteria for Henoch-Schönlein purpura, childhood polyarteritis nodosa, childhood Wegener granulomatosis and childhood Takayasu arteritis: Ankara 2008. Part II: final classification criteria. *Ann Rheum Dis* 2010;69(5):798–806.
12. Cabral DA, Canter DL, Muscal E, et al; ARChIVE Investigators Network within the PedVas Initiative. Comparing presenting clinical features in 48 children with microscopic polyangiitis to 183 children who have granulomatosis with polyangiitis (Wegener's): an ARChIVE cohort study. *Arthritis Rheumatol* 2016;68(10):2514–2526.
13. Watts R, Lane S, Hanslik T, et al. Development and validation of a consensus methodology for the classification of the ANCA-associated vasculitides and polyarteritis nodosa for epidemiological studies. *Ann Rheum Dis* 2007;66(2):222–227.
14. Harris PA, Taylor R, Thielke R, et al. Research electronic data capture (REDCap)—a metadata-driven methodology and workflow process for providing translational research informatics support. *J Biomed Inform* 2009;42(2):377–381.
15. Dolezalova P, Price-Kuehne FE, Özen S, et al. Disease activity assessment in childhood vasculitis: development and preliminary validation of the Paediatric Vasculitis Activity Score (PVAS). *Ann Rheum Dis* 2013;72(10):1628–1633.
16. Dolezalova P, Wilkinson N, Brogan P, et al. SAT0286 Paediatric Vasculitis Damage Index: a new tool for standardised disease assessment. *Ann Rheum Dis* 2014;73(suppl 2):696–697.
17. Exley AR, Bacon PA, Luqmani RA, et al. Development and initial validation of the Vasculitis Damage Index for the standardized clinical assessment of damage in the systemic vasculitides. *Arthritis Rheum* 1997;40(2):371–380.
18. Schwartz GJ, Muñoz A, Schneider MF, et al. New equations to estimate GFR in children with CKD. *J Am Soc Nephrol* 2009;20(3):629–637.
19. Levey AS, Eckardt KU, Tsukamoto Y, et al. Definition and classification of chronic kidney disease: a position statement from Kidney Disease: Improving Global Outcomes (KDIGO). *Kidney Int* 2005;67(6):2089–2100.
20. Thiele C, Hirschfeld G. cutpointR: improved estimation and validation of optimal cutpoints in R. *J Stat Softw* 2021;98(11):1–27.
21. Iudici M, Puéchal X, Pagnoux C, et al; French Vasculitis Study Group. Brief report: childhood-onset systemic necrotizing vasculitides: long-term data from the French Vasculitis Study Group Registry. *Arthritis Rheumatol* 2015;67(7):1959–1965.
22. Kovesdy CP, Coresh J, Ballew SH, et al; CKD Prognosis Consortium. Past decline versus current eGFR and subsequent ESRD risk. *J Am Soc Nephrol* 2016;27(8):2447–2455.
23. Zsom L, Zsom M, Salim SA, et al. Estimated glomerular filtration rate in chronic kidney disease: a critical review of estimate-based predictions of individual outcomes in kidney disease. *Toxins (Basel)* 2022;14(2):127.
24. Gao R, Wu Z, Xu X, et al. Predictors of poor prognosis in ANCA-associated vasculitis (AAV): a single-center prospective study of inpatients in China. *Clin Exp Med* 2023;23(4):1331–1343.
25. Kronbichler A, Jayne DRW. ANCA renal risk score: is prediction of end-stage renal disease at baseline possible? *Kidney Int* 2018;94(6):1045–1047.
26. Tan LW, Wan JL, Zhu CH, et al. Risk factors for renal outcomes in children with antineutrophil cytoplasmic antibody-associated vasculitis: a nationwide retrospective study in China. *World J Pediatr* 2024;20(5):506–516.
27. Yang J, Yang Y, Xu Y, et al. Clinical and renal histology findings and different responses to induction treatment affecting the long-term renal outcomes of children with ANCA-associated vasculitis: a single-center cohort analysis. *Front Immunol* 2022;13:857813.
28. Calatroni M, Consonni F, Allinovi M, et al. Prognostic factors and long-term outcome with ANCA-associated kidney vasculitis in childhood. *Clin J Am Soc Nephrol* 2021;16(7):1043–1051.
29. Chen A, Mammen C, Guzman J, et al; for ARChIVE Investigators within the PedVas Initiative. Wide variation in glucocorticoid dosing in paediatric ANCA-associated vasculitis with renal disease: a paediatric vasculitis initiative study. *Clin Exp Rheumatol* 2022;40(4):841–848.
30. Berden AE, Ferrario F, Hagen EC, et al. Histopathologic classification of ANCA-associated glomerulonephritis. *J Am Soc Nephrol* 2010;21(10):1628–1636.
31. Noone DG, Twilt M, Hayes WN, et al. The new histopathologic classification of ANCA-associated GN and its association with renal outcomes in childhood. *Clin J Am Soc Nephrol* 2014;9(10):1684–1691.
32. Calatroni M, Oliva E, Gianfreda D, et al. ANCA-associated vasculitis in childhood: recent advances. *Ital J Pediatr* 2017;43(1):46.

Efficacy of a Tumor Necrosis Factor Inhibitor in Chronic Low-Back Pain With Modic Type 1 Changes: A Randomized Controlled Trial

Elisabeth Gjefsen,¹  Lars C. Bråten,² Erica Ponzi,² Magnhild H. Dagestad,³ Gunn H. Marchand,⁴ Thomas Kadar,⁵ Gunnstein Bakland,⁶ Anne J. Haugen,⁷ Fredrik Granviken,⁸ Tonje W. Flørenes,³ Nils Vetti,³ Lars Grøvle,⁷ Aksel T. Nilsen,⁶  Astrid Lunestad,⁹ Thor E. Holmgard,¹⁰ Morten Valberg,¹ Nils Bolstad,² Ansgar Espeland,³ Jens I. Brox,¹ Guro L. Goll,¹¹  Kjersti Storheim,¹² and John-Anker Zwart¹

Objective. The efficacy of tumor necrosis factor inhibitors for treating chronic low-back pain with Modic changes is uncertain. This study investigated the superiority of infliximab over placebo in patients with Modic type 1 changes.

Methods. In this multicenter, randomized, triple-blind, placebo-controlled trial, patients aged 18 to 65 years with moderate to severe chronic low-back pain and Modic type 1 changes were enrolled from five Norwegian public hospitals between January 2019 and October 2022. Participants were randomly assigned to four intravenous infusions of 5 mg/kg infliximab or placebo. The primary outcome was difference in change in the Oswestry Disability Index (ODI) score from baseline to five months. Secondary outcomes included changes in low-back pain intensity, disability, and health-related quality of life. A linear mixed model was used for efficacy analyses.

Results. A total of 128 patients (mean age 43 years, 65.6% women) participated (64 in each group). All patients who received at least one dose of the allocated infusion were included in the primary analyses. The average ODI score (\pm SD) change was $-7.0 (\pm 9.7)$ in the group who received infliximab and $-6.4 (\pm 10.4)$ in the group who received placebo. The difference in the ODI score change between the two groups was 1.3 ODI points (95% confidence interval -2.1 to 4.6 , $P = 0.45$). Analyses showed no effect of infliximab compared to placebo on secondary outcomes. Adverse event rates were similar between groups.

Conclusion. Infliximab did not demonstrate superiority over placebo in reducing pain-related disability in patients with moderate to severe chronic low-back pain with Modic type 1 changes at five months.

INTRODUCTION

Low-back pain (LBP) represents a significant public health problem, being the most prevalent musculoskeletal condition in

Western countries and the leading cause of disability worldwide.^{1,2} Given the complex nature of chronic LBP, involving biologic, psychological, and social factors,^{2,3} the guidelines recommend adopting a biopsychosocial framework for assessment

[ClinicalTrials.gov](#) identifier: NCT03704363.

EudraCT database no: 2017-004861-29.

Supported by the Norwegian National Program for Clinical Therapy Research, KLINBEFORSK (grant 2017201).

¹Elisabeth Gjefsen, MD, Morten Valberg, PhD, Jens I. Brox, MD, PhD, John-Anker Zwart, MD, PhD: Oslo University Hospital and University of Oslo, Oslo, Norway; ²Lars C. Bråten, MD, PhD, Erica Ponzi, PhD, Nils Bolstad, MD, PhD: Oslo University Hospital, Oslo, Norway; ³Magnhild H. Dagestad, MD, Tonje W. Flørenes, MD, PhD, Nils Vetti, MD, PhD, Ansgar Espeland, MD, PhD: Haukeland University Hospital and University of Bergen, Bergen, Norway; ⁴Gunn H. Marchand, MD, PhD: St Olav's Hospital, Trondheim University Hospital, Trondheim, Norway; ⁵Thomas Kadar, MD, PhD: Haukeland University Hospital, Bergen, Norway; ⁶Gunnstein Bakland, MD, PhD, Aksel T. Nilsen, MD: University Hospital of North Norway, Tromsø, Norway; ⁷Anne J. Haugen, MD, PhD, Lars Grøvle, MD, PhD: Østfold Hospital Trust, Grålum, Norway; ⁸Fredrik Granviken, PhD: St Olav's Hospital, Trondheim University Hospital and Norwegian University of Science and Technology, Trondheim, Norway; ⁹Astrid Lunestad, patient representative: Norwegian Association for Female Pelvic Joint Health, Grønland, Oslo, Norway; ¹⁰Thor E. Holmgard, patient representative: Norwegian Back Pain Association, Drammen, Norway; ¹¹Guro L. Goll,

MD, PhD: Diakonhjemmet Hospital and University of Oslo, Oslo, Norway; ¹²Kjersti Storheim, PhD: Oslo University Hospital and Oslo Metropolitan University, Oslo, Norway.

Requests to access data should be addressed to Kjersti Storheim, PhD, kjersti.storheim@ous-research.no. Deidentified individual participant data (including data dictionary) will be available to medical researchers by request in accordance with local registration and ethical approval when the article has been published until September 1, 2034. All proposals requesting data access will need to specify an analysis plan and will need approval of the scientific board before any data can be released.

Additional supplementary information cited in this article can be found online in the Supporting Information section (<http://onlinelibrary.wiley.com/doi/10.1002/art.43073>).

Author disclosures and graphical abstract are available at <https://onlinelibrary.wiley.com/doi/10.1002/art.43073>.

Address correspondence via email to Elisabeth Gjefsen, MD, at ejefsen@gmail.com.

Submitted for publication August 7, 2024; accepted in revised form November 18, 2024.

and treatment.^{3,4} Nevertheless, current management strategies provide modest relief at best,^{4–6} and the overprescription of opioid medication for chronic pain including LBP underscores the need for other safe and effective treatment options.^{7,8}

One proposed way to address the challenges of optimizing treatment for chronic LBP is by identifying subgroups of patients with it and tailoring therapies accordingly. A suggested subgroup comprises patients with Modic changes (MCs), which are magnetic resonance imaging (MRI) findings. These are characterized by signal changes in the vertebral bone marrow extending from the endplate⁹ and classified into type 1 (edema), type 2 (fatty), and type 3 (sclerotic). MCs are thought to result from disc and endplate damage, coupled with a persistent inflammatory stimulus in the adjacent vertebral body¹⁰ and associated with a nociceptive source for LBP.¹¹

Tumor necrosis factor (TNF), traditionally recognized as a proinflammatory cytokine, plays a key role in the pathogenesis of various inflammatory and autoimmune diseases.¹² TNF has also been associated with symptomatic disc degeneration and MCs, triggering the expression of other proinflammatory cytokines. In vitro studies have shown that infliximab, a TNF inhibitor, can reduce the expression of these cytokines.¹³ Furthermore, increased levels of TNF-immunoreactive cells and nerve fibers have been found in patients with colocalized MCs.¹⁴ A previous randomized controlled trial evaluating infliximab treatment in patients with sciatica suggested promising results in a subgroup of patients with MCs.¹⁵

Type 1 MCs share histopathological characteristics with bone marrow lesions found in joints of the appendicular skeleton in patients with osteoarthritis (OA).^{16,17} A recent systematic review suggested that TNF inhibitors may be effective in alleviating pain in patients with hand OA with synovitis, but the effect on knee OA is uncertain.¹⁸ There is, however, some evidence suggesting that infliximab may be more effective at relieving pain in patients with OA than other biologic agents.¹⁹ Additionally, infliximab has proven effective in reducing pain and disability in patients with spinal diseases with known pathophysiology such as axial spondyloarthritis (SpA).^{20,21} The aim of this study was to assess the efficacy of infliximab as a therapeutic intervention for chronic LBP with MC type 1.

PATIENTS AND METHODS

Trial oversight. The BackToBasic study was an investigator-initiated, randomized, triple-blind placebo-controlled, multicenter trial conducted in accordance with the Declaration of Helsinki and the International Conference on Harmonization of Good Clinical Practice and reported according to the Consolidated Standards of Reporting Trials (CONSORT) guidelines (members of the BackToBasic Study Group are listed in Appendix A). It was approved by the Regional Committee for Medical and Health Research Ethics of South East Norway

(2017/2450) and the Norwegian Medicines Agency (European Union Drug Regulating Authorities Clinical Trials [EudraCT] 2017-004861-29) before the study initiation. The Clinical Trial Unit at Oslo University Hospital was responsible for monitoring the trial, and the methods were consistent throughout the trial period. The trial protocol, a protocol article,²² and the statistical analysis plan (SAP) were published in advance and are available at [ClinicalTrials.gov](https://clinicaltrials.gov) (NCT03704363). Patient representatives were actively involved in the scientific board and contributed to all phases of the study. The Norwegian National Program for Clinical Therapy Research, KLINBEFORSK (grant 2017201), funded the trial but had no role in planning, conducting the trial, data analyses or writing the manuscript. The authors assume responsibility for the accuracy and completeness of the data and analyses, as well as for the fidelity of the trial.

Trial population. Patients were recruited from outpatient clinics at five public hospitals in Norway and provided written informed consent before inclusion. Patients aged 18 to 65 years experiencing chronic LBP for at least six months were eligible for the study. Average pain intensity score of 5 or higher on the numeric rating scales (NRSs; range 0–10) for current, worst, and usual/mean LBP, or a score of ≥ 25 on the Oswestry Disability Index (ODI) was required. Confirmation of MC type 1 in the lumbar spine (superior and/or inferior endplate, Th12–S1), obtained through a standardized study-specific MRI examination, was also an inclusion criterion. Patients with a specific spinal diagnosis including SpA, previous low back surgery unrelated to disc herniation or decompression, spine surgery within the past 12 months, regular reception of opioids (except codeine and tramadol), infections, pregnancy, diabetes, immunodeficiency, or receiving immunosuppressive medication were excluded from the study. A complete list of inclusion and exclusion criteria is provided in Supplementary Table 1.

Trial procedures. The study population was randomized 1:1 to infliximab or placebo using a computer-generated procedure. Randomization was stratified by center and previous participation in the Antibiotics in Modic Changes (AIM) study²³ and blocked within each stratum, with varying block sizes of two, four, six, and eight. To avoid bias, patients, investigators, treatment administrators, data analysts, and statisticians were blinded to treatment allocation and the details of block size and allocation sequence generation.

After randomization, patients received either 5 mg/kg infliximab or NaCl used as placebo, administered as four intravenous infusions. Unblinded study personnel prepared the study medication in identical infusion bags, labeled only with the patient number to ensure blinding. Because infliximab and NaCl have the same color and appearance, complete concealment of group allocation was possible. Blinded personnel administered the infusions on days 0, 14, 42, and 98, with no dose adjustments made. Before

each infusion, patients received premedication with 1 g paracetamol and 10 mg cetirizine to reduce the risk of side effects and to maintain blinding. Patients were allowed to continue their regular LBP therapy but advised not to initiate new treatments during the study period. All cointerventions, pharmacological and non-pharmacological, and changes in cointerventions were recorded.

Outcomes and data collection. The primary outcome of the study was the change in ODI score from baseline to five months (14). ODI is a responsive and validated patient-reported measure of pain-related disability, with scores ranging from 0 to 100 (higher scores indicating worse disability) and is recommended for LBP research.²⁴ Secondary outcomes included the change from baseline to five months in average LBP intensity measured by the NRSs (scores ranging from 0 to 10, higher scores indicating higher pain intensity), disability evaluated by the Roland–Morris Disability Questionnaire (scores ranging from 0 to 24, higher scores denoting more disability),²⁵ and health-related quality of life evaluated using the EuroQol 5-Dimension 5-Level questionnaire (scores ranging from –0.59 to 1, higher scores indicating better quality of life).²⁶

Throughout the entire study period, adverse events (AEs), serious AEs (SAEs) and serious unexpected suspected adverse reactions (SUSARs) were closely monitored. Demographic information, including sex (male or female), and vital signs were collected at baseline. Safety clinical laboratory parameters were collected at baseline and before each infusion (Supplementary Table 2). Serum infliximab and antidrug antibody levels were measured in samples drawn before each infusion using automated in-house assays,²⁷ but results were not reported to the study personnel.

Exploratory outcomes included change from baseline in leg pain intensity, change in hours with LBP, symptom-specific well-being, workplace absenteeism, cointerventions, patient's satisfaction, global perceived effect (GPE), ODI score, and LBP at nine months and assessment of blinding success. For a full list of time points for reported outcome measures see Supplementary Table 3. The study used the web-based electronic case report form software solution Viedoc (Pharma Consulting Group) to record study data. Participants completed questionnaires directly through the concomitant web-based data capture system named ViedocMe.

Statistical analyses. The null hypothesis stated that there would be no difference in the change of ODI score from baseline to five months between the groups who received infliximab versus placebo. We defined the minimal clinically important difference as a 10-point difference in change in the ODI score between the groups.^{28–31} To detect this difference, with an assumed SD of ± 18 points, adding 20% to account for dropouts, we estimated a sample size of 126 patients (63 in each group) to achieve 80% power at the 5% significance level.

The primary analysis was conducted according to the intention-to-treat principle using the full analysis set (FAS). This included all patients who were randomized to a treatment group and received at least one study treatment after randomization. We assessed the change from baseline in the ODI score using a mixed-model analysis. The treatment group, interaction of the treatment group and trial visit (one, two, three, four, five, and nine months), the study center (stratification factor used in the randomization), and the ODI score at baseline were included as fixed factors. To account for dependencies in the repeated measures, we included a patient-specific random intercept. Using this model, we estimated the average marginal change from baseline for each treatment and each trial visit. Previous AIM study participation was also used as a stratification factor in the randomization but was, in accordance with the SAP, not included in the model because <5% of patients had participated in the AIM study.²³

The primary effect estimate was the difference in the average marginal change in ODI score from baseline to five months, calculated with two-sided 95% confidence intervals (CIs). Missing data were handled by the linear mixed model, incorporating all available data from each participant having at least one follow-up measurement. Unbiased estimates of the effect are given under the “missing-at-random” assumption. Sensitivity analyses were performed using the same model for the per-protocol population (see Supplementary Methods for definition of populations), the FAS population without outliers, and in the FAS population with an infliximab serum level of >3 mg/L at five months. We also analyzed the primary outcome using rank-based methods that do not assume normality such as the Wilcoxon test.

Linear mixed models with the same adjustments and structure as for the primary outcome were used to analyze the continuous secondary and exploratory outcomes. We applied logistic regression adjusted for study site to report marginal risk differences for the change in cointerventions (yes/no) at five months and GPE dichotomized as “improved” (score 1–2) or “no change or worse” score (3–7). AEs were reported descriptively by treatment group, including the numbers of mild AEs, moderate AEs, and SAEs and their relation to study medication. We also investigated if the treatment efficacy could vary between subgroups (see Supplementary Methods for definition of subgroups).

Bang's Blinding Index was calculated for each treatment group based on patients' perceptions of their allocated treatment. The Bang's Blinding Index ranges from –1 (all patients report incorrect treatment) to 1 (all patients report correct treatment); 0 indicates random reporting of treatment group.³²

The effects are described as point estimates with corresponding 95% CIs. A two-sided P value is reported for the primary outcome, with $P < 0.05$ considered statistically significant. Because there was only one primary endpoint, no adjustment was made for multiple testing. The width of the 95% CIs for the secondary and exploratory endpoints were not adjusted for multiple testing. All analyses were conducted using R software, version 4.3.1 by statistician EP.

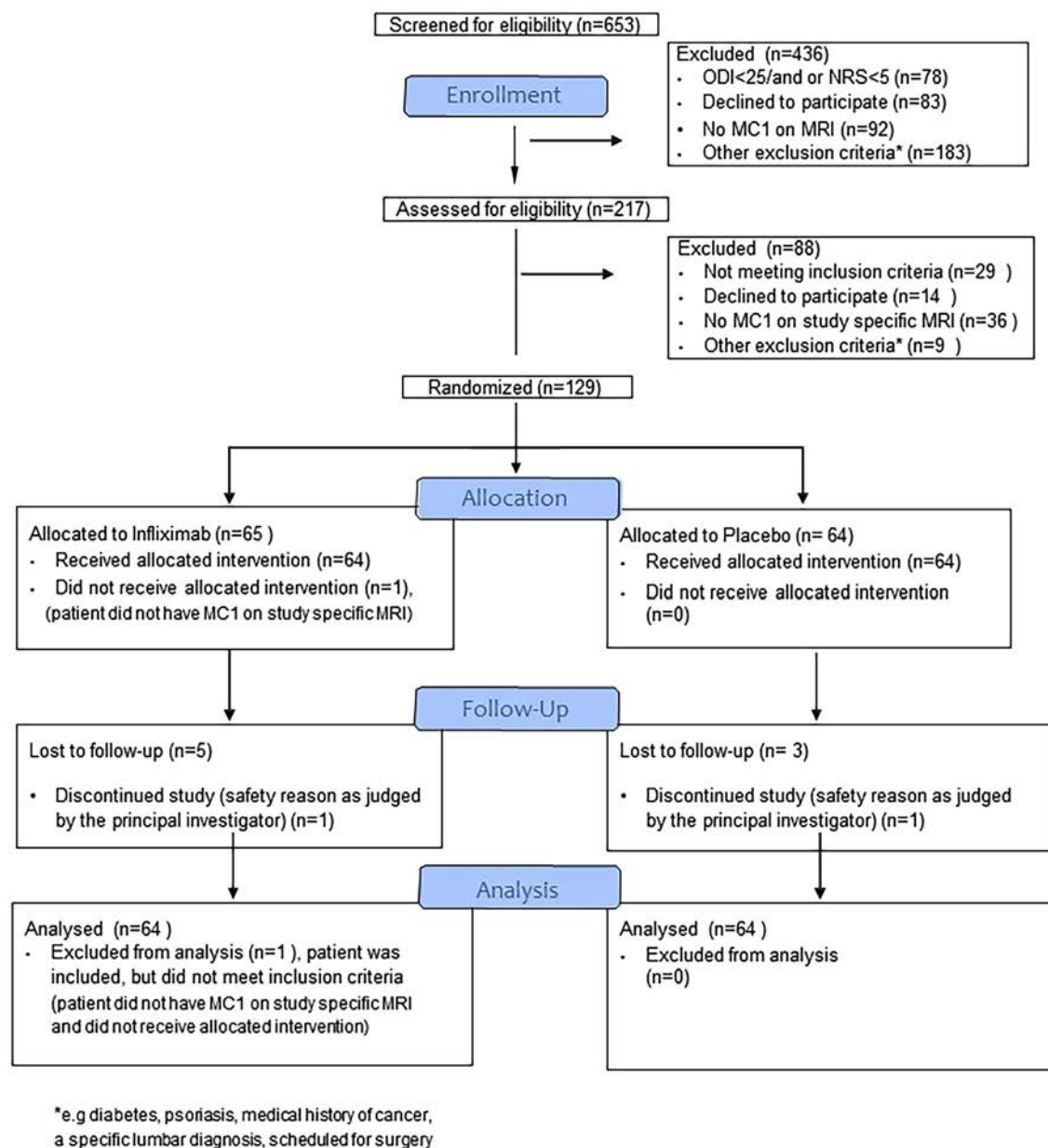


Figure 1. Flowchart showing group assignment. One patient was randomized and allocated to receive infliximab but did not fulfill inclusion criteria due to no MC1 on study-specific MRI and was excluded before receiving study medication. MC1, Modic type 1 changes; MRI, magnetic resonance imaging; NRS, numeric rating scale; ODI, Oswestry Disability Index. Color figure can be viewed in the online issue, which is available at <http://onlinelibrary.wiley.com/doi/10.1002/art.43073/abstract>.

RESULTS

Patient characteristics. Between December 12, 2018, and September 2, 2022, 653 patients were screened for eligibility (Figure 1). Of these, 129 participants were randomly assigned to a treatment group; 65 were allocated to the group who received infliximab and 64 to the group who received placebo (Figure 1). One patient from the group who received infliximab did not meet the inclusion criteria and was excluded from further participation before receiving any treatment. Table 1 and Supplementary Table 4 show the demographic and clinical characteristics of the patients at baseline. The mean age of included patients was

43.3 years, and the majority were female (65.6%). The mean ODI score at baseline was 33.5 (± 10.8). All patients who received at least one infusion were included in the primary analysis and FAS, resulting in 128 participants, 64 patients in each treatment group. At five months, 122 participants (95%; 60 in the group who received infliximab and 62 in the group who received placebo) had valid ODI scores.

Efficacy. The primary outcome showed an estimated difference of 1.3 ODI points in the average marginal change between the two groups from baseline to five months (95% CI -2.1 to

4.6, $P = 0.45$; Figure 2; Tables 2 and 3; Supplementary Figure 1). The prespecified secondary outcomes, including LBP intensity, disability, and health-related quality of life, showed no superiority of infliximab at five months. These results are summarized in Tables 2 and 3 and were further supported by sensitivity analyses (Supplementary Table 5).

Safety. A similar total number of AEs were reported in the group who received infliximab (139 of AEs by 53 patients) and the group who received placebo (138 AEs by 56 patients; Table 4). Five patients had an SAE in the group who received infliximab and two patients had an SAE in the group who

received placebo. One of the SAEs in the group who received infliximab and two in the group who received placebo were considered possibly related to the study medicine. No SUSARs were observed. Moderate AEs were more frequently reported in the group who received infliximab (by 21.9% of patients) than in the group who received placebo (12.5%). Infection was reported by 27 patients in the group who received infliximab and 31 patients in the group who received placebo (Supplementary Table 6). Three patients (one patient due to elevated transaminases and two with suspected drug-induced rash), all allocated to receive infliximab, were unblinded after reaching the five-month primary endpoint, whereas the principal investigators remained blinded.

Table 1. Baseline characteristics for each treatment group in the full analysis set*

Characteristic	Infliximab (n = 64), n (%)	Placebo (n = 64), n (%)
Age, mean (\pm SD), y	42.7 (\pm 9.1)	44 (\pm 8.9)
Female	43 (67.2)	41 (64.1)
Body mass index, mean (\pm SD), kg/m ²	24.8 (\pm 3.49)	25.1 (\pm 3.3)
Duration of symptoms, median (interquartile range), mon	36 (18.5–108)	36 (24–81.5)
ODI score, mean (\pm SD)	32.6 (\pm 11.8)	34.5 (\pm 9.6)
Comorbidity ^a		
Score 1	51	50
Score 2	11	13
Score 3	2	1
Educational level		
Primary school	3 (4.8)	2 (3.2)
Secondary education	18 (28.6)	18 (28.6)
University less than four years	18 (28.6)	23 (36.5)
University four years or more	24 (38.1)	20 (31.7)
Work status		
Working full time	35 (54.7)	37 (57.8)
Working part time	5 (7.8)	2 (3.1)
Student/other/unemployed	1 (1.6)	2 (3.2)
Partial sick leave	12 (18.8)	11 (17.2)
Complete sick leave	6 (9.4)	5 (7.8)
Disability pension	5 (7.8)	7 (10.9)
Physical workload		
Mostly sedentary	28 (48.3)	30 (50.8)
Work that requires much walking	14 (24.1)	16 (27.1)
Work that requires much walking and lifting	14 (24.1)	13 (22)
Heavy physical work	2 (3.4)	0 (0)
Light leisure time activity (three or more hours per week)	40 (66.7)	42 (66.7)
Hard leisure time activity (three or more hours per week)	14 (23)	12 (19.4)
Currently smoking	4 (6.3)	4 (6.3)
Expectation that backpain will be cured/clear improvement	41 (67.2)	47 (75.8)
Emotional distress scores ≥ 1.75 ^b	18 (29)	19 (30.6)
Fear-avoidance beliefs ^c		
FABQ physical activity, mean (\pm SD)	12.5 (\pm 4.9)	11.7 (\pm 5.7)
FABQ work, mean (\pm SD)	14.5 (\pm 11)	15.6 (\pm 10.2)
Level with Modic type 1 changes		
L1/L2	1 (1.6)	0 (0)
L2/L3	2 (3.1)	7 (10.9)
L3/L4	6 (9.4)	4 (6.3)
L4/L5	19 (29.7)	23 (35)
L5/S1	44 (68.8)	40 (62.5)

* Values are mean (\pm SD) or median (interquartile range) for continuous variables and number (percentage) of patients for categorical variables. FABQpa, physical activity subscore; FABQpw, work subscore; ODI, Oswestry Disability Index.

^a The Functional Comorbidity Index score increased by 1 for each of the 18 diagnoses associated with decreased physical function.

^b Emotional distress (25-item Hopkins Symptom Checklist) scores ≥ 1.75 show an association with a psychiatric diagnosis.

^c Fear-Avoidance Beliefs Questionnaire higher scores indicate more fear-avoidance beliefs.

Exploratory outcomes. There were no clinically relevant differences between treatment groups at five or nine months in patient-reported outcome measures (Tables 2 and 3). The difference in ODI score widens at nine months (Figure 2; Table 2), but the estimated difference of 4.2 ODI points (95% CI 0.8–7.6) in the average marginal change between the two groups is not significant. Subgroup analyses showed no difference in the treatment effect at five months across different subgroups (Supplementary Table 7). The success of blinding was assessed using Bang's Blinding Index, the score of which was -0.2 (95% CI -0.3 to 0.04) in the group who received infliximab and 0.5 (95% CI 0.3 – 0.6) in the group who received placebo at five months. Other predefined exploratory outcomes were reported descriptively (Supplementary Tables 8–10).

DISCUSSION

The BackToBasic study is the first trial to investigate the efficacy of intravenous TNF inhibitors as a treatment for chronic LBP with MCs type 1. In this randomized, triple-blind placebo-controlled multicenter trial, we found that infliximab was not superior to placebo in reducing pain-related disability at five months in patients with moderate to severe chronic LBP with MCs type 1. Sensitivity analyses and secondary outcomes supported the

primary efficacy outcome and supported the robustness of the primary result.

The incidence of reported moderate AEs was higher in the group who received infliximab, but both SAEs and overall number of AEs were similar between the treatment groups. Furthermore, no SUSARs were reported, indicating a favorable safety profile for this population. Infection, a commonly observed side effect of infliximab, was reported with similar frequency in both treatment groups.

The selected dose regimen for infliximab was consistent with the approved dose for ankylosing spondylitis. Moreover, sensitivity analysis did not show superiority of infliximab compared to placebo when serum infliximab concentrations were considered adequate (>3 mg/L). Additionally, the treatment effect was neither modified by duration of symptoms nor by the other predefined subgroups. These findings, although exploratory, consistently support the lack of efficacy.

We cannot be certain we chose the optimal time point for evaluating treatment effect. The exploratory analysis at nine months revealed a trend toward a small effect, but the effect was not clinically relevant, and no finding suggested an effect at any other time point. According to Bang's Blinding Index, most participants in the group who received infliximab were unaware of their treatment assignment, indicating successful blinding. In contrast, the index score in the group who received placebo

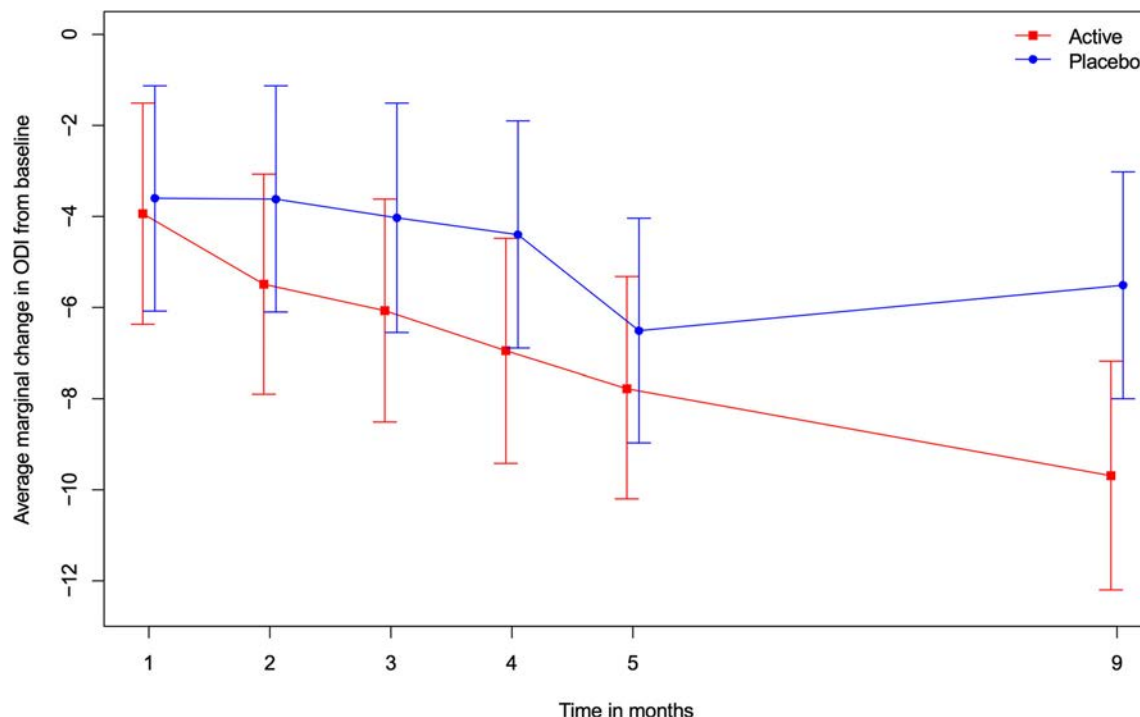


Figure 2. Estimated marginal change in ODI from baseline for treatment groups over time. Infliximab was not superior to placebo in reducing pain-related disability at five months in patients with chronic low-back pain and Modic changes type 1 (estimated difference of 1.3 ODI points in the average marginal change between the two groups from baseline to five months [95% confidence interval -2.1 to 4.6 , $P = 0.45$]). ODI, Oswestry Disability Index.

Table 2. Change from baseline in outcomes by treatment group with the estimated between-group average marginal effect*

Outcome	Infliximab, baseline values and marginal means	Placebo, baseline values and marginal means	Estimated average difference in change from baseline
Primary outcome at five months by ODI, difference (95% CI)	-7.8 (-10.2 to -5.3)	-6.5 (-9.0 to -4.0)	1.3 (-2.1 to 4.6), $P = 0.45$
Secondary outcomes			
LBP intensity measured by NRS			
Baseline, mean (\pm SD)	6.3 (\pm 1.4)	6.5 (\pm 1.2)	-
Change at five months, difference (95% CI)	-1.4 (-1.8 to -1.0)	-1.6 (-2.0 to -1.2)	-0.2 (-0.8 to 0.3)
Disability measured by RMDQ			
Baseline, mean (\pm SD)	13.2 (\pm 4.0)	13.1 (\pm 3.2)	-
Change at five months, difference (95% CI)	-3.1 (-4.3 to -1.9)	-2.4 (-3.5 to -1.2)	0.7 (-0.8 to 2.3)
Quality of life measured by EQ5D-5L			
Baseline, mean (\pm SD)	0.5 (\pm 0.2)	0.5 (\pm 0.2)	-
Change at five months, difference (95% CI)	0.1 (0.1-0.2)	0.09 (0.04-0.1)	-0.01 (-0.1 to 0.1)
Exploratory outcomes			
Leg pain intensity measured by NRS			
Baseline, mean (\pm SD)	2.9 (\pm 3.0)	2.9 (\pm 2.6)	-
Change at five months, difference (95% CI)	-0.4 (-1.0 to 0.2)	-0.4 (-1.0 to 0.2)	-0.02 (-0.8 to 0.8)
Change at nine months, difference (95% CI)	-0.8 (-1.5 to -0.2)	-0.4 (-1.0 to 0.3)	0.5 (-0.4 to 1.3)
LBP intensity measured by NRS at nine months, difference (95% CI)	-2.1 (-2.5 to -1.6)	-1.6 (-2.0 to -1.2)	0.4 (-0.1 to 1.0)
Days with sick leave			
Baseline, mean (\pm SD)	5.5 (\pm 8.1)	7.3 (\pm 9.4)	-
Change at five months, difference (95% CI)	-1.2 (-3.0 to 0.7)	-0.6 (-2.3 to 1.2)	0.6 (-1.9 to 3.1)
Disability measured by ODI at nine months, difference (95% CI)	-9.7 (-12.2 to -7.2)	-5.5 (-8.0 to -3.0)	4.2 (0.8-7.6)

* The ODI scores from 0 to 100; higher scores indicate more disability. The RMDQ scores from 0 to 24 ($n = 123$); higher scores indicate more disability. The EQ5D-5L scores from -0.59 to 1 ($n = 119$); higher scores indicate better quality of life. The NRS ranges from 0 to 10 (higher scores indicate worse pain; $n = 125$ for leg pain; $n = 123$ for LBP), calculated as the mean of three NRSs: the current LBP, the worst LBP within the last two weeks, and the usual/mean LBP within the last two weeks. For the primary analysis and the continuous secondary and exploratory outcomes, we used a linear mixed model. All reported changes at five and nine months are as compared to baseline. The estimated average difference in change between the treatment groups is the difference in the marginal averages of change from the linear mixed model (ie, the treatment effect). A positive value favors the infliximab group. CI, confidence interval; EQ5D-5L, EuroQol 5-Dimension 5-Level; LBP, low-back pain; NRS, numeric rating scale; ODI, Oswestry Disability Index; RMDQ, Roland-Morris Disability Questionnaire.

was 0.5, suggesting that a higher proportion of participants in this group were able to guess their assigned treatment, which may bias results and contribute to a reduced placebo effect in the group who received placebo.

MCs have gained attention due to their association with LBP,³³⁻³⁵ although the association has been debated.³⁶⁻³⁸ Therapeutic interventions aiming to target the proposed underlying infectious, autoimmune, or mechanical causes have been proposed.^{10,11} This study shows no effect of a TNF inhibitor. A former study reported efficacy of three months' antibiotic treatment in patients with chronic LBP and MCs when compared to placebo.³⁹ Our study group was, however, unable to replicate these findings in the AIM study.²³ In addition, trials investigating the use of bone active agents suggest some short-term benefits, but their long-term efficacy remains uncertain.^{40,41} A review of nonsurgical interventions concluded that there is currently no evidence to support specific nonsurgical treatments for patients with chronic LBP and MCs.⁴² Although infliximab is proven effective for most patients with SpA, biologic disease-modifying antirheumatic drugs have been considered a promising therapeutic approach also for patients with OA. However, high-quality trials have not

demonstrated a significant benefit over placebo, including TNF inhibitors,⁴³ reflecting different underlying etiologies. MCs share characteristics with bone marrow lesions found in the osteoarthritic knee joint. Our results are in line with the results seen in patients with OA and may indicate that TNF do not play a key role as a mediator of back pain with MCs.

Our study has several strengths that contribute to the validity of our findings. We used a randomized triple-blind design and validated outcome measures, and the study had little missing data, with only six patients (4.6% of the FAS) having missing ODI score at five months. Given the low amount of missing data and use of the linear mixed model, no other imputation method was used. Additionally, our sample provided adequate power, with a lower SD than anticipated (SD ± 10 vs assumed ± 18 in the power calculation),²² giving us an even higher power to detect differences and leading to a more precise estimate of treatment effect.

A limitation is that the strict inclusion and exclusion criteria we used limit the generalizability of results to broader populations of patients with LBP and MCs. For harms, our results do not apply to a population with diseases for whom infliximab is currently indicated. Further, there might be adverse reactions due to infliximab

Table 3. Differences between treatment groups in perceived effect and co-interventions at 5 months*

	Infliximab, numbers (%)	Placebo, numbers (%)	Estimated average risk difference (95% CI)
Global perceived effect: not improved (number above 2)			
5 months	44 (76%)	50 (82%)	0.05 (−0.1 to 0.2)
Co-interventions			
Change since last visit at 5 months	13 (20%)	12 (19%)	−0.01 (−0.2 to 0.1)

* Global perceived effect scored on a 7 – point Likert scale index, where 1 = ‘completely fine’, 2 = ‘much better’, 3 = ‘a little better’, 4 = ‘no change’, 5 = ‘a little worse’, 6 = ‘much worse’ or 7 = ‘worse than ever’. NA = not applicable. The change in co-interventions at 5 months is analyzed with logistic regression, the global perceived effect was dichotomized as improved (score 1–2) or no change or worse (score 3–7) and analyzed with a logistic model.

Table 4. Summary of AEs and SAEs*

AEs with relation to study medication	Infliximab (n = 64), [n events] n (%)	Placebo (n = 64), [n events] n (%)
AEs	[57] 32 (50)	[54] 32 (50)
Any AEs	32 (50)	32 (50)
One AE	18 (28.1)	19 (29.7)
Two AEs	7 (10.9)	10 (15.6)
Three or more AEs	7 (10.9)	3 (4.7)
SAEs	[1] 1 (1.6)	[2] 2 (3.1)
Any SAEs	1 (1.6)	2 (3.1)
Mild AEs	[40] 24 (37.5)	[45] 29 (45.3)
Moderate AEs	[16] 14 (21.9)	[8] 8 (12.5)
Severe AEs	[1] 1 (1.6)	[1] 1 (1.6)
AEs, not related to study medication		
AEs	[139] 52 (81.2)	[138] 56 (87.5)
SAEs	[5] 5 (7.8)	[2] 2 (3.1)

* AE, adverse event; SAE, serious AE.

that manifest after more than nine months’ follow-up or rare adverse reactions not captured in this study. In conclusion, the BackToBasic study showed that the TNF inhibitor infliximab was not superior to placebo in reducing pain-related disability at five months in patients with moderate to severe chronic LBP with MCs type 1.

ACKNOWLEDGMENTS

We thank the Norwegian National Program for Clinical Therapy Research, KLINBEFORSK, for funding the trial, and all patients who participated in the BackToBasic trial. We thank David J. Warren for assay development and the staff at the Department of Medical Biochemistry for analyses of infliximab and anti-infliximab levels.

AUTHOR CONTRIBUTIONS

All authors contributed to at least one of the following manuscript preparation roles: conceptualization AND/OR methodology, software,

investigation, formal analysis, data curation, visualization, and validation AND drafting or reviewing/editing the final draft. As corresponding author, Dr Gjefsen confirms that all authors have provided the final approval of the version to be published and takes responsibility for the affirmations regarding article submission (eg, not under consideration by another journal), the integrity of the data presented, and the statements regarding compliance with institutional review board/Declaration of Helsinki requirements.

REFERENCES

- GBD 2017 Disease and Injury Incidence and Prevalence Collaborators. Global, regional, and national incidence, prevalence, and years lived with disability for 354 diseases and injuries for 195 countries and territories, 1990–2017: a systematic analysis for the Global Burden of Disease Study 2017. *Lancet* 2018;392(10159):1789–1858.
- Hartvigsen J, Hancock MJ, Kongsted A, et al. What low back pain is and why we need to pay attention. *Lancet* 2018;391(10137):2356–2367.
- Knezevic NN, Candido KD, Vlaeyen JWS, et al. Low back pain. *Lancet* 2021;398(10294):78–92.
- Foster NE, Anema JR, Cherkin D, et al. Prevention and treatment of low back pain: evidence, challenges, and promising directions. *Lancet* 2018;391(10137):2368–2383.
- Maher C, Underwood M, Buchbinder R. Non-specific low back pain. *Lancet* 2017;389(10070):736–747.
- Pincus T, Kent P, Bronfort G, et al. Twenty-five years with the biopsychosocial model of low back pain—is it time to celebrate? A report from the twelfth international forum for primary care research on low back pain. *Spine (Phila Pa 1976)* 2013;38(24):2118–2123.
- Chou R, Turner JA, Devine EB, et al. The effectiveness and risks of long-term opioid therapy for chronic pain: a systematic review for a National Institutes of Health Pathways to Prevention Workshop. *Ann Intern Med* 2015;162(4):276–286.
- Jones CMP, Day RO, Koes BW, et al. Opioid analgesia for acute low back pain and neck pain (the OPAL trial): a randomised placebo-controlled trial. *Lancet* 2023;402(10398):304–312.
- Modic MT, Steinberg PM, Ross JS, et al. Degenerative disk disease: assessment of changes in vertebral body marrow with MR imaging. *Radiology* 1988;166(1 Pt 1):193–199.
- Dudli S, Fields AJ, Samartzis D, et al. Pathobiology of Modic changes. *Eur Spine J* 2016;25(11):3723–3734.
- Han CS, Hancock MJ, Sharma S, et al. Low back pain of disc, sacroiliac joint, or facet joint origin: a diagnostic accuracy systematic review. *EClinicalMedicine* 2023;59:101960.
- Kalliolias GD, Ivashkiv LB. TNF biology, pathogenic mechanisms and emerging therapeutic strategies. *Nat Rev Rheumatol* 2016;12(1):49–62.
- Walter BA, Purmessur D, Likhithpanichkul M, et al. Inflammatory kinetics and efficacy of anti-inflammatory treatments on human nucleus pulposus cells. *Spine (Phila Pa 1976)* 2015;40(13):955–963.
- Ohtori S, Inoue G, Ito T, et al. Tumor necrosis factor-immunoreactive cells and PGP 9.5-immunoreactive nerve fibers in vertebral endplates of patients with discogenic low back pain and Modic type 1 or type 2 changes on MRI. *Spine (Phila Pa 1976)* 2006;31(9):1026–1031.
- Korhonen T, Karppinen J, Paimela L, et al. The treatment of disc-herniation-induced sciatica with infliximab: one-year follow-up results of FIRST II, a randomized controlled trial. *Spine (Phila Pa 1976)* 2006;31(24):2759–2766.
- Dudli S, Ballatori A, Bay-Jensen AC, et al. Serum biomarkers for connective tissue and basement membrane remodeling are associated

- with vertebral endplate bone marrow lesions as seen on MRI (Modic changes). *Int J Mol Sci* 2020;21(11):3791.
17. Bowen A, Shamritsky D, Santana J, et al. Animal models of bone marrow lesions in osteoarthritis. *JBM Plus* 2022;6(3):e10609.
 18. Zhu R, Fang H, Wang J, et al. Inflammation as a therapeutic target for osteoarthritis: a literature review of clinical trials. *Clin Rheumatol* 2024; 43(8):2417–2433.
 19. Li Y, Mai Y, Cao P, et al. Relative efficacy and safety of anti-inflammatory biologic agents for osteoarthritis: a conventional and network meta-analysis. *J Clin Med* 2022;11(14):3958.
 20. Sieper J, Poddubnyy D. Axial spondyloarthritis. *Lancet* 2017; 390(10089):73–84.
 21. Danve A, Deodhar A. Treatment of axial spondyloarthritis: an update. *Nat Rev Rheumatol* 2022;18(4):205–216.
 22. Gjeffsen E, Bråten LCH, Goll GL, et al. The effect of infliximab in patients with chronic low back pain and Modic changes (the BackTo-Basic study): study protocol of a randomized, double blind, placebo-controlled, multicenter trial. *BMC Musculoskelet Disord* 2020; 21(1):698.
 23. Bråten LCH, Rolfsen MP, Espeland A, et al. Efficacy of antibiotic treatment in patients with chronic low back pain and Modic changes (the AIM study): double blind, randomised, placebo controlled, multicentre trial. *BMJ* 2019;367:5654.
 24. Chiarotto A, Boers M, Deyo RA, et al. Core outcome measurement instruments for clinical trials in nonspecific low back pain. *Pain* 2018; 159(3):481–495.
 25. Roland M, Fairbank J. The Roland-Morris Disability Questionnaire and the Oswestry Disability Questionnaire. *Spine (Phila Pa 1976)* 2000; 25(24):3115–3124.
 26. EuroQol Group. EuroQol—a new facility for the measurement of health-related quality of life. *Health Policy* 1990;16(3):199–208.
 27. Jørgensen KK, Olsen IC, Goll GL, et al. Switching from originator infliximab to biosimilar CT-P13 compared with maintained treatment with originator infliximab (NOR-SWITCH): a 52-week, randomised, double-blind, non-inferiority trial. *Lancet* 2017;389(10086):2304–2316.
 28. Ivar Brox J, Sørensen R, Friis A, et al. Randomized clinical trial of lumbar instrumented fusion and cognitive intervention and exercises in patients with chronic low back pain and disc degeneration. *Spine* 2003;28(17):1913–1921.
 29. Ostelo RW, Deyo RA, Stratford P, et al. Interpreting change scores for pain and functional status in low back pain: towards international consensus regarding minimal important change. *Spine (Phila Pa 1976)* 2008;33(1):90–94.
 30. Hägg O, Fritzell P, Nordwall A; Swedish Lumbar Spine Study Group. The clinical importance of changes in outcome scores after treatment for chronic low back pain. *Eur Spine J* 2003;12(1):12–20.
 31. Ostelo RWJG, de Vet HCW. Clinically important outcomes in low back pain. *Best Pract Res Clin Rheumatol* 2005;19(4):593–607.
 32. Bang H, Ni L, Davis CE. Assessment of blinding in clinical trials. *Control Clin Trials* 2004;25(2):143–156.
 33. Määtä JH, Wadge S, MacGregor A, et al. ISSLS Prize winner: vertebral endplate (Modic) change is an independent risk factor for episodes of severe and disabling low back pain. *Spine (Phila Pa 1976)* 2015;40(15):1187–1193.
 34. Teraguchi M, Yoshimura N, Hashizume H, et al. The association of combination of disc degeneration, end plate signal change, and Schmorl node with low back pain in a large population study: the Wakayama Spine Study. *Spine J* 2015;15(4):622–628.
 35. Kjaer P, Leboeuf-Yde C, Korsholm L, et al. Magnetic resonance imaging and low back pain in adults: a diagnostic imaging study of 40-year-old men and women. *Spine (Phila Pa 1976)* 2005;30(10): 1173–1180.
 36. Brinjikji W, Diehn FE, Jarvik JG, et al. MRI findings of disc degeneration are more prevalent in adults with low back pain than in asymptomatic controls: a systematic review and meta-analysis. *AJNR Am J Neuroradiol* 2015;36(12):2394–2399.
 37. Määtä JH, Karppinen J, Paananen M, et al. Refined phenotyping of modic changes. *Medicine (Baltimore)* 2016;95(22):e3495.
 38. Herlin C, Kjaer P, Espeland A, et al. Modic changes-their associations with low back pain and activity limitation: a systematic literature review and meta-analysis. *PLoS One* 2018;13(8):e0200677.
 39. Albert HB, Sørensen JS, Christensen BS, et al. Antibiotic treatment in patients with chronic low back pain and vertebral bone edema (Modic type 1 changes): a double-blind randomized clinical controlled trial of efficacy. *Eur Spine J* 2013;22(4):697–707.
 40. Cai G, Laslett LL, Aitken D, et al. Effect of zoledronic acid and denosumab in patients with low back pain and Modic change: a proof-of-principle trial. *J Bone Miner Res* 2018;33(5):773–782.
 41. Koivisto K, Kyllönen E, Haapea M, et al. Efficacy of zoledronic acid for chronic low back pain associated with Modic changes in magnetic resonance imaging. *BMC Musculoskelet Disord* 2014; 15(1):64.
 42. Mu X, Peng W, Ou Y, et al. Non-surgical therapy for the treatment of chronic low back pain in patients with Modic changes: a systematic review of the literature. *Heliyon* 2022;8:e09658.
 43. Persson MSM, Sarmanova A, Doherty M, et al. Conventional and biologic disease-modifying anti-rheumatic drugs for osteoarthritis: a meta-analysis of randomized controlled trials. *Rheumatology (Oxford)* 2018;57(10):1830–1837.

APPENDIX A: BACKTOBASIC STUDY GROUP

Members of the BackToBasic Study Group are as follows: Inger-Lise Knudsen, University Hospital of North Norway, Tromsø, Norway; Britt E. Lurud and Hege Andresen, Trondheim University Hospital, Trondheim, Norway; Jan S. Skouen, and Siv K. Claussen, Haukeland University Hospital, Bergen, Norway; Monica Wigemyr, Elina Schistad, Kaja Selmer, Benedicte A. Lie, and Maria Dehli Vigeland, Oslo University Hospital, Oslo, Norway; Knut M. Huneide and Veronica Sørensen, Østfold Hospital Trust, Grålum, Norway; Espen Haavardsholm, and Tore Kvien, Diakonhjemmet Hospital, Oslo, Norway; and Anne Froholdt, Vestre Viken Hospital Trust Drammen, Drammen, Norway.

LETTER

DOI 10.1002/art.43045

An investigation of the relationship between weight management and gout: insights from the THIN database study and recommendations for improvement. Comment on the article by Wei et al

To the Editor:

We read with interest the article by Wei J et al¹ in *Arthritis & Rheumatology*, which used data from The Health Improvement Network (THIN) of UK general practitioners and aimed to investigate the relationship between the speed of weight loss and gout among individuals with overweight and obesity within one year of initiating antiobesity medications. Its strengths lie in its large sample size and design methodology that mimics that of a randomized controlled trial while opening up new avenues for exploring the interconnections between metabolic and inflammatory diseases. Nevertheless, we believe some issues warrant further exploration.

First, the study relied on electronic health records (EHRs), which may be subject to recording bias. The study showed that 25.9% of the participants did not measure their weight after using orlistat but used their baseline weight as a proxy, which may have introduced bias. Therefore, we suggest that database designers improve data collection methods, such as using electronic devices such as smart bracelets to regularly monitor patients' weight and lifestyle information to improve the accuracy and reliability of relevant data. Supplementary surveys are also used to collect relevant information missing from EHR forms, such as dietary patterns and exercise habits, so that researchers can better control for these potential confounders. Additionally, the lack of hospitalization data in the THIN database may have resulted in some patients experiencing recurrent gouty attacks not being included by the authors, thus compromising an accurate assessment of the risk of gouty attacks. Therefore, we suggest that the author team collaborate with more health care organizations to obtain more complete hospitalization data to reduce the inaccuracy of the assessment of gouty attack risk due to missing data.

Second, the absence of routine blood uric acid measurements in the target population resulted in missing baseline values for 93.9% and 47.5% of the participants in the risk assessment of gouty attacks and recurrences, which may limit the researchers' in-depth study and further substantiation of the biologic mechanisms linking weight loss to the risk of gouty attacks or recurrent gouty attacks. This suggests that database designers should consider improving the routineness of blood uric acid measurements²

to ensure that more participants can have blood uric acid measurements at baseline and follow-up; the author team could also explore the use of other alternative indicators or biomarkers to indirectly reflect the correlation between blood uric acid levels and gout to compensate for the lack of data on blood uric acid measurements.

Finally, although the identification of gouty episodes in this study was performed based on specific codes and prescription records, the presence of misclassification could potentially bias the correlation results toward invalidation. Therefore, we suggest that the author team combine clinical symptoms, signs, and other aspects of information to make a comprehensive judgment³ and to improve the accuracy of disease identification and also refer to more objective testing indicators, such as changes in blood uric acid levels, to assist in the judgment of gouty attacks.

In conclusion, we are very grateful to Wei and colleagues for their important contribution. This study provides a new perspective on the multifaceted nature of obesity management. Future studies should aim to fully characterize potential confounding factors, fully assess the sustainability of their impact on relevant outcomes and any potential adverse events associated with medications, replicate these findings in long-term follow-up and larger and more diverse populations, and explore in depth the underlying molecular biologic mechanisms of these findings.

Supported by the National Natural Science Foundation of China (81803019), the Sichuan Science and Technology Program (2022YFS0625), and the strategic cooperation project of science and technology between Luzhou People's Government and Southwest Medical University (2023LZXNYDJ010).

Author disclosures are available at <https://onlinelibrary.wiley.com/doi/10.1002/art.43045>.

Ling Zhang, BMed
Department of Pharmacy,
The Affiliated Hospital, School of Pharmacy
Southwest Medical University
Luzhou, China
Jun Li, MMed 
ljadoctor@swmu.edu.cn
Department of Traditional Chinese Medicine,
The Affiliated Hospital
Southwest Medical University
Luzhou, China
Yaling Li, MD
lylapothecary@swmu.edu.cn
Department of Pharmacy,
The Affiliated Hospital, School of Pharmacy
Southwest Medical University
Luzhou, China

1. Wei J, Wang Y, Dalbeth N, et al. Weight loss after initiating anti-obesity medications and gout among overweight and obesity individuals: a population-based cohort study. *Arthritis Rheumatol* 2025;77(3): 335–345.
2. Zhang Y, Yu H, Chai S, et al. Noninvasive and individual-centered monitoring of uric acid for precaution of hyperuricemia via optical supramolecular sensing. *Adv Sci (Weinh)* 2022;9(18):e2104463.
3. Dalbeth N, Gosling AL, Gaffo A, et al. Gout. *Lancet* 2021;397(10287): 1843–1855.

DOI 10.1002/art.43043

Reply

To the Editor:

We appreciate Dr Zhang and colleagues' interest in our published article, "Weight Loss After Receiving Anti-Obesity Medications and Gout Among Individuals with Overweight and Obese: A Population-Based Cohort Study."¹ They raised issues regarding the nature of the electronic health records (EHRs) database and the accuracy of gout identification.

First, Zhang et al expressed concerns about missing data and suggested conducting supplementary surveys to collect additional information from participants. However, such surveys are logistically impractical because of their high cost and anticipated nonresponse rate, which would likely introduce even more missing values. We acknowledged the issue of missing data in the EHR database and conducted sensitivity analyses to address this limitation, ensuring a balanced interpretation of our results.

Second, regarding the accuracy of gout identification, our study used diagnostic codes and prescription records from The Health Improvement Network database, which is a widely accepted and validated method for identifying gout in epidemiologic research.^{2,3}

Our study provides empirical evidence of dose–response associations between weight loss after initiating orlistat within one year and a lower risk of incident and recurrent gout flares. If future studies validate our findings, this could guide the development of well-defined preventive strategies to reduce the impact of gout.

Author disclosures are available at <https://onlinelibrary.wiley.com/doi/10.1002/art.43043>.

Jie Wei, PhD 
 Department of Orthopaedics
 Xiangya Hospital, Central South University
 Changsha, China
 Hunan Key Laboratory of Joint Degeneration and Injury
 Changsha, China
 Key Laboratory of Aging-related Bone and Joint Diseases
 Prevention and Treatment
 Ministry of Education, Xiangya Hospital, Central South
 University
 Changsha, China
 Department of Epidemiology and Health Statistics
 Xiangya School of Public Health, Central South University
 Changsha, China

Yilun Wang, MD, PhD
 Department of Orthopaedics
 Xiangya Hospital, Central South University
 Changsha, China
 Hunan Key Laboratory of Joint Degeneration and Injury
 Changsha, China
 Key Laboratory of Aging-related Bone and Joint Diseases
 Prevention and Treatment
 Ministry of Education, Xiangya Hospital, Central South
 University
 Changsha, China
 Chao Zeng, MD, PhD
 Guanghua Lei, MD, PhD 
 Department of Orthopaedics
 Xiangya Hospital, Central South University
 Changsha, China
 Hunan Key Laboratory of Joint Degeneration and Injury
 Changsha, China
 Key Laboratory of Aging-related Bone and Joint Diseases
 Prevention and Treatment
 Ministry of Education, Xiangya Hospital, Central South
 University
 Changsha, China
 National Clinical Research Center for Geriatric Disorders
 Xiangya Hospital, Central South University
 Changsha, China
 Yuqing Zhang, DSc 
yzhang108@mgh.harvard.edu
 Division of Rheumatology, Allergy, and Immunology
 Department of Medicine, Massachusetts General Hospital,
 Harvard Medical School
 Boston, USA
 The Mongan Institute
 Massachusetts General Hospital,
 Harvard Medical School
 Boston, USA

1. Wei J, Wang Y, Dalbeth N, et al. Weight loss after initiating anti-obesity medications and gout among overweight and obesity individuals: a population-based cohort study. *Arthritis Rheumatol* 2025;77(3): 335–345.
2. Cipolletta E, Tata LJ, Nakafero G, et al. Association between gout flare and subsequent cardiovascular events among patients with gout. *JAMA* 2022;328(5):440–450.
3. Zhang Y, Peloquin CE, Dubreuil M, et al. Sleep apnea and the risk of incident gout: a population-based, body mass index-matched cohort study. *Arthritis Rheumatol* 2015;67(12):3298–3302.

DOI 10.1002/art.43047

Correspondence to the risk of lung cancer in rheumatoid arthritis and rheumatoid arthritis-associated interstitial lung disease: comment on the article by Brooks et al

To the Editor:

We read with great interest the recent retrospective cohort study by Brooks et al, which identified an elevated risk of lung cancer in patients with rheumatoid arthritis (RA) and RA-related interstitial lung disease (RA-ILD).¹ This important study underscores the need for considering patients with both RA and

RA-ILD as high-risk groups for lung cancer screening, with valuable implications for clinical practice and future research. We would like to offer several suggestions to further strengthen the study's findings.

Firstly, a meta-analysis has demonstrated that a history of emphysema (relative risk [RR] 2.44; 95% confidence interval [CI] 1.64–3.62), chronic bronchitis (RR 1.47; 95% CI 1.29–1.68), tuberculosis (RR 1.48; 95% CI 1.17–1.87), and pneumonia (RR 1.57; 95% CI 1.22–2.01) significantly increases the risk of lung cancer.² To minimize confounding bias, it would be prudent to adjust for these conditions as covariates in the study design.

Secondly, the potential influence of occupational carcinogen exposure warrants consideration. Prior studies have shown that exposure to asbestos, crystalline silica, and certain metals substantially increases lung cancer risk.³ Including detailed data on occupational exposures could reduce residual confounding in this study.

Thirdly, another methodologic concern is that the study excluded lung cancer diagnoses only up to the cohort entry date, without accounting for a sufficient latency period for cancer development. This may introduce detection and reverse causality biases. Incorporating a latency period of at least six months to one year as part of a sensitivity analysis could help mitigate these biases and yield a more robust assessment of lung cancer risk.

Finally, although the authors acknowledge the predominance of male participants (88%) as a limitation, we believe the study could benefit from further exploration of sex differences. Given the higher prevalence of RA and lung cancer in women,^{4,5} a subgroup analysis by sex may provide additional insights into risk stratification and screening strategies for lung cancer in RA and RA-ILD populations. We believe incorporating these considerations would reduce potential bias and strengthen the study's results.

Author disclosures are available at <https://onlinelibrary.wiley.com/doi/10.1002/art.43047>.

Tsai Yi Hung, MD 
Chen Dong, MD
Chung Shan Medical University
Taichung, Taiwan
Brian Shiian Chen, MD
Chung Shan Medical University
and Chung Shan Medical University Hospital
Taichung, Taiwan
James Cheng Chung Wei, MD, PhD 
jccwei@gmail.com
Chung Shan Medical University Hospital,
Chung Shan Medical University
and China Medical University
Taichung, Taiwan

2. Brenner DR, Boffetta P, Duell EJ, et al. Previous lung diseases and lung cancer risk: a pooled analysis from the International Lung Cancer Consortium. *Am J Epidemiol* 2012;176(7):573–585.
3. Olsson A, Bouaoun L, Schuz J, et al. Lung cancer risks associated with occupational exposure to pairs of five lung carcinogens: results from a pooled analysis of case-control studies (SYNERGY). *Environ Health Perspect* 2024;132(1):17005.
4. Favalli EG, Biggoggero M, Crotti C, et al. Sex and management of rheumatoid arthritis. *Clin Rev Allergy Immunol* 2019;56(3):333–345.
5. Stapelfeld C, Dammann C, Maser E. Sex-specificity in lung cancer risk. *Int J Cancer* 2020;146(9):2376–2382.

DOI 10.1002/art.43055

Environmental risk factors should not be overlooked: comment on the article by Brooks et al

To the Editor:

By analyzing data from the Veterans Health Administration, Brooks et al have observed in their article “The Risk of Lung Cancer in Rheumatoid Arthritis and Rheumatoid Arthritis–Associated Interstitial Lung Disease” that male seropositive rheumatoid arthritis (RA) is associated with a significantly increased risk of lung cancer, with RA-associated interstitial lung disease (RA-ILD) presenting a particularly high risk. It was proposed that the inflammatory process associated with RA may underlie this finding.¹

A study demonstrated a mechanism by which cadmium and carbon black induced idiopathic pulmonary fibrosis (IPF) via citrullination of vimentin, which acted as a ligand for Toll-like receptor 4 receptors on fibroblasts to induce fibrotic lung disease,² clearly linking IPF to the pathogenesis of RA.³ Furthermore, Brooks et al comment that IPF is associated with an increased risk of lung cancer. However, a multitude of data would suggest that occupational exposures to vapors, gases, dusts, and fumes (VGDF) significantly increase the risk of IPF development, with one in four cases of IPF attributable to these exposures. It has been suggested that male RA is an occupational disease with an excess of exposures to VGDF,⁴ and these exposures are very similar to the exposures associated with the increased risk of IPF.⁵

Specific examples of dust exposures and IPF development are apparent for various lung carcinogens, including metal and silica dust.⁵ We suggest that exposure to VGDF increases the risk of lung cancer in IPF, and this is likely to be the case with RA-ILD. Exposures to VGDF increase the risk of emphysema,⁶ an independent risk factor for lung cancer. For example, in squamous cell carcinoma, there is up to a five times increased risk of lung cancer in smokers with airflow obstruction compared to smokers with normal lung function.⁷ In conclusion, it cannot be assumed that RA-derived inflammation is the sole cause for the excess risk of cancer described in RA and RA-ILD because they share common environmental risk factors with lung cancer.


1. Brooks RT, Luedders B, Wheeler A, et al. The risk of lung cancer in rheumatoid arthritis and rheumatoid arthritis–associated interstitial lung disease. *Arthritis Rheumatol* 2024;76(12):1730–1738.

Author disclosures are available at <https://onlinelibrary.wiley.com/doi/10.1002/art.43055>.

Andreea Lazarut-Nistor, MD 

a.lazarut-nistor@nhs.net

*Targu Mures Emergency Clinical County Hospital
Targu Mures, Romania
and The Knowledge Spa, Royal Cornwall Hospitals NHS Trust
Truro, United Kingdom*

David G. Hutchinson, MRCP, MD 

*The Knowledge Spa, Royal Cornwall Hospitals NHS Trust
and Truro Health Park, Royal Cornwall Hospital Trust
Truro, United Kingdom*

1. Brooks RT, Luedders B, Wheeler A, et al. The risk of lung cancer in rheumatoid arthritis and rheumatoid arthritis-associated interstitial lung disease. *Arthritis Rheumatol* 2024;76(12):1730–1738.
2. Li FJ, Surolia R, Li H, et al. Citrullinated vimentin mediates development and progression of lung fibrosis. *Sci Transl Med* 2021;13(585): eaba2927.
3. Ytterberg AJ, Joshua V, Reynisdottir G, et al. Shared immunological targets in the lungs and joints of patients with rheumatoid arthritis: identification and validation. *Ann Rheum Dis* 2015;74(9):1772–1777.
4. Murphy D, Hutchinson D. Is male rheumatoid arthritis an occupational disease? A review. *Open Rheumatol J* 2017;11:88–105.
5. Gandhi S, Tonelli R, Murray M, et al. Environmental causes of idiopathic pulmonary fibrosis. *Int J Mol Sci* 2023;24(22):16481.
6. Blanc PD, Eisner MD, Earnest G, et al. Further exploration of the links between occupational exposure and chronic obstructive pulmonary disease. *J Occup Environ Med* 2009;51(7):804–810.
7. Durham AL, Adcock IM. The relationship between COPD and lung cancer. *Lung Cancer* 2015;90(2):121–127.

DOI 10.1002/art.43048

Reply

To the Editor:


We thank Hung et al as well as Lazarut-Nistor and Hutchinson for their interest in our article. Although adjustment for other lung diseases may seem to reduce confounding, this may introduce overadjustment bias. Rheumatoid arthritis (RA)-associated interstitial lung disease (RA-ILD) often co-occurs with other lung diseases, such as emphysema. Furthermore, in large administrative data sets, there may be misclassification of these different lung diseases, with patients with RA-ILD having diagnostic codes for these other lung diseases, particularly during the initial evaluation period. We agree that accounting for additional occupational exposures would be valuable, but these were not available for our study. It is also critical to note that environmental exposures and inflammation in RA and RA-ILD are not mutually exclusive concepts. It is well established that environmental exposures induce RA-related autoimmunity and inflammation. Thus, environmental exposures and inflammation are intertwined concepts that reside on a shared causal pathway. The presented survival curves show a persistently elevated lung cancer and lung cancer death risk throughout the entirety

of follow-up. Furthermore, nearly two-thirds of patients with RA-ILD had a chest computed tomography scan before the study index date. Together, these findings provide reassurance that latent lung cancers are not simply being detected more frequently in RA or RA-ILD. Although we agree that evaluation of sex-specific risks of lung cancer in RA and RA-ILD would be of interest, we were not powered to do such analyses in this cohort. We encourage future studies in this area.

Bryant R. England, MD, PhD 


bryant.england@unmc.edu

*VA Nebraska-Western Iowa Health Care System
and University of Nebraska Medical Center
Omaha, NE*

Rebecca T. Brooks, MD 

Mayo Clinic

Rochester, MN

Ted R. Mikuls, MD, MSPH 

*VA Nebraska-Western Iowa Health Care System
and University of Nebraska Medical Center
Omaha, NE*

DOI 10.1002/art.43061

The effect of air pollution and genetic susceptibility on systemic lupus erythematosus: comment on the article by Xing et al

To the Editor:

The link between air pollution and autoimmune diseases is gaining attention in the current field of environmental health research. A recent study based on data from the UK Biobank examined the relationship between long-term exposure to air pollution and the risk of developing systemic lupus erythematosus (SLE). The study found that long-term exposure to air pollution was significantly associated with the development of SLE, providing new insights into the role of environmental factors in the pathogenesis of SLE. The findings highlight the need for stricter air quality standards to reduce potential health risks.¹ In addition, the study lays the groundwork for further research into the relationship between air pollution and other autoimmune diseases and calls for more interdisciplinary research to understand the complex pathomechanisms. Although this study makes an important contribution to understanding the role of environmental factors in the development of SLE, other methodologic limitations not mentioned in the text need to be carefully considered when interpreting the results.

First, regarding the exclusion criteria mentioned in the text, the authors set them mainly on the basis of missing data. However, available Mendelian randomization studies and evidence-based medicine suggest that endometriosis, allergic rhinitis, atopic dermatitis, periodontitis, and celiac disease are clear risk factors for SLE.^{2,3} Early antibody testing and screening of these patients may help prevent the onset and progression of SLE. Individuals with these comorbidities should therefore be excluded from the

study. Second, important dietary information was omitted despite the presence of necessary covariates. For example, previous studies have suggested that dietary factors may play a key role in the pathogenesis of SLE⁴: consumption of black tea and coffee has been associated with the development of SLE⁵; intake of the trace elements iron, selenium, and vitamin D may be protective factors for SLE³; and animal studies have also shown that increased salt intake can promote SLE autoimmunity by promoting the expansion and function of follicular helper T cells in mice.⁶ Third, the study focused on the specific pollutants 2.5-micrometer particulate matter (PM_{2.5}), 10-micrometer particulate matter (PM₁₀), nitrogen dioxide, and nitric oxide metabolites but did not adequately consider other pollutants that may affect the risk of SLE, such as volatile organic compounds and ozone. Furthermore, air pollution does not occur in isolation. The lack of analysis of joint effects between pollutants may limit the ability to fully understand the environmental context of SLE pathogenesis. Finally, we suggest that subgroup analyses of the different types of covariates be performed to reveal the association between air pollutants and SLE in populations with different characteristics. Furthermore, because the authors emphasize the existence of a joint role of genetic risk and air pollution in SLE, it could also be investigated whether the different covariates also interact in this association.

Supported by the Government Subsidizes Clinical Medical Excellence Program (ZF2023166, ZF2024157).

Na Wang and Shugang Liu equally contributed to the study.

Author disclosures are available at <https://onlinelibrary.wiley.com/doi/10.1002/art.43061>.

Na Wang, MD
Hu Chen, MM
*Hebei University of Chinese Medicine
and Hebei Province Academy of Chinese Medicine Sciences
Hebei, China*
Shugang Liu, MM
*The Fourth Hospital of Hebei Medical University
Hebei, China*

1. Xing M, Ma Y, Cui F, et al. Air pollution, genetic susceptibility, and risk of incident systemic lupus erythematosus: a prospective cohort study. *Arthritis Rheumatol* 2024;76(10):1530–1537.
2. Xiao XY, Chen Q, Shi YZ, et al. Risk factors of systemic lupus erythematosus: an overview of systematic reviews and Mendelian randomization studies. *Adv Rheumatol* 2023;63(1):42.
3. Gergianaki I, Bortoluzzi A, Bertias G. Update on the epidemiology, risk factors, and disease outcomes of systemic lupus erythematosus. *Best Pract Res Clin Rheumatol* 2018;32(2):188–205.
4. Mu Q, Zhang H, Luo XM. SLE: another autoimmune disorder influenced by microbes and diet? *Front Immunol* 2015;6:608.
5. Washio M, Fujii T, Kuwana M, et al; Japan MCTD study group. Lifestyle and other related factors for the development of mixed connective tissue disease among Japanese females in comparison with systemic lupus erythematosus. *Mod Rheumatol* 2014;24(5):788–792.
6. Aparicio-Soto M, Sánchez-Hidalgo M, Alarcón-de-la-Lastra C. An update on diet and nutritional factors in systemic lupus erythematosus management. *Nutr Res Rev* 2017;30(1):118–137.